The main nonsulphide Zn deposits in Europe: Characterisation, timing and paleoclimatic control

(*I maggiori giacimenti a nonsolfuri di Zn in Europa: Caratterizzazione, timing e controllo paleoclimatico*)

old miner's village, Iglesias (Sardinia, Italy)

Tesi di Dottorato di Ricerca
Dott. Vito Coppola
Napoli, Italia
-2007-

UNIVERSITÀ DEGLI STUDI DI NAPOLI "FEDERICO II"
FACOLTÀ DI SCIENZE MM. FF. NN.

Dottorato di Ricerca in Scienze della Terra
XX CICLO

The main nonsulphide Zn deposits in Europe: Characterisation, timing and paleoclimatic control

(*I maggiori giacimenti a nonsolfuri di Zn in Europa: Caratterizzazione, timing e controllo paleoclimatico*)

Dottorando
Dott. Vito Coppola

Relatore
Prof.ssa Maria Boni

Coordinatore
Prof. Giuseppe Nardi

Anno Accademico 2006-2007

[“ *dunque per primo fu Chaos; poi*
Gaia dall’ampio petto, sede salda sempre di tutti
gli immortali, che abitano la vetta d’Olimpo innevato,...]
Esiodo, Teogonia 116-118

Questi tre anni di dottorato di ricerca sono stati per me, oltre che una possibilità di lavoro e di crescita scientifica, anche molto importanti per le cose viste, capite. Questo dottorato mi ha dato la possibilità di capire meglio quali sono i meccanismi sociali ed economici che governano tutto il mondo dell' estrazione mineraria. Ecco perché voglio anteporre una piccola riflessione al testo della tesi.

Lo sfruttamento selvaggio delle risorse naturali ha raggiunto oggi dei livelli altissimi, non tenendo assolutamente conto di quelli che sono gli equilibri ambientali che vengono in questo modo sconvolti. Ogni giorno in diverse parti del mondo, accadono incidenti ambientali che mettono a serio rischio l' ecosistema, e molti di essi sono dovuti proprio ad attività di estrazione mineraria. Spesso questo succede per mancanza di controllo da parte sia delle compagnie multinazionali che operano nel settore, che da parte degli organi pubblici. Dietro questo meccanismo è spesso nascosto uno stretto legame clientelistico tra i governi locali e le compagnie, che porta enormi vantaggi economici verso queste ultime. Infatti, un minor controllo sulla sicurezza ambientale e dei lavoratori negli impianti estrattivi, rappresentano una netta diminuzione delle spese da parte delle compagnie minerarie e di riflesso un maggiore margine di guadagno. A causa dei deboli equilibri sociali che sono presenti nei paesi poveri, spesso con governanti corrotti, la possibilità di meglio instaurare questi rapporti, fa sì che le compagnie si spostino proprio in questi luoghi per iniziare nuove attività. Qui tra gli altri vantaggi si aggiunge un minor costo della manodopera, costituita esclusivamente dalle popolazioni locali. E' spesso questo l'unico ruolo che le comunità locali rivestono in queste attività mentre, d' altro canto, non sono per niente integrate nella crescita economica dovuta ad esse (si sente spesso dire che i paesi più poveri sono anche quelli più ricchi di materie prime). Inoltre la mancanza di sicurezza sul lavoro porta a continui incidenti nelle miniere e alla relativa perdita di vite umane, ed è anche questo il caro prezzo che le comunità devono subire oltre che ad una vera e propria invasione selvaggia del loro territorio.

La cosa che ritengo maggiormente sbagliata è l'ipocrisia che sta dietro tutto questo. L'ipocrisia delle compagnie che da un lato effettuano campagne pubblicitarie sulla perfetta integrazione delle comunità locali e sul loro sviluppo e dall'altro compiono degli scempi ambientali e sociali; l'ipocrisia dei governi fantoccio dei paesi poveri, parte integrante di questo sistema balordo; l'ipocrisia di chi queste cose non le racconta; l'ipocrisia dei professionisti che per migliori offerte economiche convoglia per buona parte in questo settore; e l'ipocrisia di molti di noi che usano in modo superfluo molte delle risorse naturali senza nessun rispetto per il pianeta su cui viviamo.

Dopo tutto questo è stato comunque molto difficile per me portare a termine questo lavoro. Sono

state molte le persone che in tutto questo mi sono state vicine e che vorrei ringraziare. I miei genitori, senza i quali e senza la tranquillità che mi hanno offerto, non sarei stato sicuramente in grado di portare a termine questo percorso. I miei amici di tutti i giorni e ai momenti passati assieme. Antonio che mi ha fatto riscoprire l'amore per la montagna. Tutti i ricercatori precari delle università italiane. Tutti coloro che credono che il rispetto dell'ambiente sia fondamentale per una vita migliore per tutti. Syd Barret, Dave Gilmour, Roger Waters, Nick Mason e Richard Wright: "Our music can generate awesome nightmares or it can throw you into the most fascinating ecstacy. Usually the latter happens.". I Led Zeppelin e la loro mitica "Stairway to Heaven". Londra e ai sei mesi passati lì. Gabriel García Márquez e le sue storie fantastiche che sono state molto utili per allontanarsi dalla realtà ed entrare in un mondo diverso, più lento. Ringrazio tutti i minatori di questo mondo che tutti i giorni entrano nella Terra e ci permettono una vita più comoda, e ringrazio Gaia per tutto quello che ci offre. Me stesso, che tutto sommato ci ho messo impegno e tempo.
Vorrei infine ringraziare in modo particolare una persona speciale che mi è stata molto di aiuto in tutto questo.

Contents

Contents 1

Riassunto 6

1. Introduction 12

1.1. Introduction and aims of the thesis 12

2. Nonsulphide Zn deposits: an overview 16

2.1. History of nonsulphide Zn deposits 16

2.2. Nonsulphide Zn deposits: definition and main characteristics 18

2.3. Supergene nonsulphide Zn deposits and related dating problems 25

3. Sampling and analytical techniques 29

3.1. Sampling 29

3.2. Analytical methods 29

3.2.1. X-ray powder diffraction (XRPD) 30

3.2.2. Trasmitted and reflected light microscopy 32

3.2.3. Cold cathodoluminescence (CL) microscopy 32

3.2.4. Scanning electron microscopy (SEM) and energy dispersive X-ray detection (EDS) 33

3.2.5. Electron microprobe analysis (WDS) 34

3.2.6. Major, minor and trace element analysis (ICP-MS) 35

3.2.7. C and O stable isotopes geochemistry 36

3.2.8. Thermometric analysis of fluid inclusions 39

4. Nonsulphide Zn deposits in the Namur-Verviers Synclinorium, NE Belgium 42

4.1. Introduction 42

4.2. Geological setting of the Namur-Verviers Synclinorium 43

4.3. Ore deposits in the Liège district 46

4.3.1. Zn-Pb sulphide ores 47

4.3.2. Nonsulphide Zn ores 49
4.4. Mineralogy of the nonsulphide ores 53
4.4.1. Willemite 53
4.4.2. Smithsonite 56
4.4.3. Hemimorphite 57
4.4.4. Sauconite 57
4.4.5. Other minerals 61
4.5. Petrography and paragenesis of nonsulphide ores 63
4.6. Major and trace element geochemistry of nonsulphide ores 65
4.7. C and O isotopes geochemistry 68
4.7.1. Smithsonite and cerussite 70
4.7.2. Calcite and dolomite 70
4.8. Thermometric analysis of fluid inclusions 71
4.9. Discussion 73
4.9.1. Geological factors controlling the emplacement of Belgian nonsulphide deposits 73
4.9.2. Stable isotopes 74
4.9.2.1. Paleoclimate indications 74
4.9.2.2. Carbon sources 76
4.9.3. Origin and timing of willemite 78
4.9.4. Timing of supergene nonsulphide deposits in the Liège district, NE Belgium 80
5. Nonsulphide Zn deposits in the Upper Silesia, Southern Poland 81
5.1. Introduction 81
5.2. Geological setting of the Upper Silesia 82
5.3. Ore deposits in the Upper Silesia 88
5.3.1. Zn-Pb sulphide ores 89
5.3.2. Nonsulphide Zn ores 93

5.4. Mineralogy of nonsulphide ores 97
5.4.1. Smithsonite 100
5.4.2. Hemimorphite 102
5.4.3. Goethite 102
5.4.4. Dolomite 104
5.4.5. Other minerals 104
5.5. Petrography and paragenesis of nonsulphide ores 107
5.6. Major and trace element geochemistry of nonsulphide ores 110
5.7. C and O isotopes geochemistry 114
5.7.1. Smithsonite 115
5.7.2. Dolomite 117
5.7.3. Calcite 118
5.8. Petrographical observations on fluid inclusions 119
5.8.1. FIs in OBD 119
5.8.2. FIs in smithsonite and Fe-smithsonite 119
5.8.3. FIs in cerussite 120
5.9. Discussion 121
5.9.1. Geological factors controlling the emplacement of Polish nonsulphide deposits 121
5.9.2. Stable isotopes 122
5.9.2.1. Paleoclimate indications 122
5.9.2.2. Carbon sources 123
5.9.3. Origin of *white galman* 126
5.9.4. Timing of nonsulphide deposits in the Upper Silesia, S Poland 129
6. Nonsulphide Zn deposits in the Irish Midlands 132
6.1. Introduction 132
6.2. Geological setting of the Irish Midlands 134
6.3. Ore deposits in the Irish Midlands 136

6.3.1. Zn-Pb(-Cu) sulphide ores 137
6.3.2. Nonsulphide Zn ores 140
6.3.2.1. Silvermines deposit 140
6.3.2.2. Galmoy deposit 143
6.3.2.3. Tynagh deposit 145
6.4. Mineralogy of the nonsulphide ores 148
6.4.1. Silvermines deposit 148
6.4.2. Galmoy deposit 151
6.4.3. Tynagh deposit 153
6.4.3.1. Smithsonite 154
6.4.3.2. Hemimorphite 155
6.4.3.3. Cerussite 155
6.4.3.4. Cu-carbonates 157
6.4.3.5. Other minerals 157
6.5. Petrography and paragenesis of Zn nonsulphide ores 158
6.6. Major and trace element geochemistry of nonsulphide ores 159
6.6.1. Silvermines deposit 159
6.6.2. Galmoy deposit 160
6.6.3. Tynagh deposit 162
6.7. C and O isotope geochemistry 163
6.7.1. Smithsonite 163
6.7.2. Pb- and Cu-carbonates 166
6.8. Thermometric analysis of fluid inclusions 166
6.9. Discussion 167
6.9.1. Geological factors controlling the emplacement of Irish nonsulphide deposits 167
6.9.2. Stable isotopes 168
6.9.2.1. Paleoclimate indications 168

6.9.2.2. Carbon sources 169

6.9.3. Timing of supergene nonsulphide deposits in the Irish Midlands 172

7. Other nonsulphide Zn deposits in Europe **174**

7.1. Introduction 174

7.2. Nonsulphide ore deposits in the Iglesias district, SW Sardinia (Italy) 174

7.3. Nonsulphide ore deposits in the Alpine district (Italy, Austria and Slovenia) 176

7.4. Nonsulphide ore deposits in Greece 178

7.5. Nonsulphide ore deposits in Spain 179

8. Discussions and conclusions **181**

8.1. Foreword 181

8.2. Mineralogical, petrographic and geochemical comparison between the investigated European nonsulphide ore deposits: affinities and differences 181

8.3. Paleoweathering in Europe during Mesozoic and Tertiary and timing of nonsulphide Zn deposits 186

References **197**

Appendix 1: List of abbreviations **227**

Acknowledgements **228**

Riassunto

Negli ultimi decenni si è assistito ad un rinnovato interesse dal punto di vista sia economico che scientifico, verso i corpi minerari ad Ossidati di Zn (anche detti "nonsolfuri di Zn" o "calaminari"), un tipo di mineralizzazioni la cui coltivazione era stata abbandonata dopo gli anni '60 del secolo scorso a favore dei solfuri di Zn.

Le cause di questo rinnovato interesse sono: (a) lo sviluppo di nuove tecnologie per l'estrazione ed il trattamento di questo tipo di mineralizzazioni (estrazione con solventi, elettrolisi), che portano alla produzione di Zn-metallo ad alto tenore; (b) le più basse concentrazioni di elementi inquinanti come zolfo, cadmio e arsenico rispetto a quelle dei giacimenti a solfuri.

I giacimenti a nonsolfuri sono stati recentemente suddivisi da Hitzman et al. (2003) in:

1. supergenici: legati alla ossidazione di corpi a solfuri primari da parte di fluidi meteorici durante processi di *weathering* e/o *paleoweathering*;
2. ipogenici: legati alla circolazione di fluidi idrotermali ossidanti e senza zolfo.

I giacimenti supergenici a nonsolfuri di Zn si presentano con differenti tipologie:

1. *gossan* zinciferi che formano la parte superiore e ossidata dei corpi a solfuri primari
2. concentrazioni di minerali secondari di Zn che sostituiscono parzialmente la roccia incassante carbonatica nelle vicinanze dei corpi a solfuri primari;
3. concentrazioni detritiche derivate dai due tipi precedenti (a) e (b), depositate in una rete di cavità carsiche

I fattori che possono maggiormente influenzare l'ossidazione dei corpi a solfuri primari, la formazione dei minerali supergenici e la loro conservazione sono: (a) *uplift* tettonico e/o abbassamento del livello di falda; (b) fratturazione della roccia incassante che possa favorire la circolazione dei fluidi; (c) alte concentrazioni di solfuri di Fe nelle mineralizzazioni primarie, la cui ossidazione genera acidi per la mobilizzazione dello Zn; (d) clima caldo-umido con periodi secchi; (e) presenza di una roccia incassante carbonatica che tamponi i fluidi acidi; (f) condizioni climatico-geologiche favorevoli alla loro fossilizzazione (eventuali coperture).

I giacimenti a nonsolfuri in Europa sembrano essere tutti di chiara origine supergenica, nonostante rimangano alcuni dubbi su alcune mineralizzazioni (Belgio, Portogallo etc.). Per molti di essi, infatti, non è ancora chiara la distribuzione delle fasi mineralogiche e le loro

paragenesi, i meccanismi che portano alla precipitazione di una parte dei minerali, né tanto meno gli equilibri geochimici coinvolti. Inoltre, in molti distretti minerari mancano sia le scale cronologiche dei periodi di maggiore ossidazione supergenica, basate su variabili indipendenti, che indubbi *records* paleoclimatici: di conseguenza, in molti casi anche il *timing* delle mineralizzazioni risulta sconosciuto.

Lo scopo di questa Tesi di Dottorato è stato quello di investigare dal punto di vista mineralogico, petrografico e geochimico le mineralizzazioni di alcuni importanti distretti minerari dell'Europa centro-settentrionale, in cui i nonsolfuri di Zn sono stati oggetto di estrazione (distretto minerario di Liegi, Belgio nord-occidentale; distretto minerario della Slesia Superiore, Polonia meridionale; distretto minerario delle Midlands Irlandesi). I nostri dati sono stati successivamente comparati con quelli provenienti da altri giacimenti a nonsolfuri in Europa settentrionale e meridionale, come quelli del distretto minerario di Iglesias (Sardegna sudoccidentale, Italia). Si è cercato poi di capire quali fossero le condizioni geologiche e climatiche presenti nelle aree mineralizzate durante gli eventi di *weathering*, ed in quali periodi queste ultime hanno potuto contribuire maggiormente alla formazione dei giacimenti a nonsolfuri investigati. La formazione di giacimenti a nonsolfuri supergenici e gli eventi di *weathering* che li hanno (eventualmente) causati sono stati infine inquadrati nella evoluzione paleogeografica dell'Europa centro-settentrionale.

I giacimenti a nonsolfuri di Zn investigati sono quasi tutti contenuti in rocce carbonatiche (calcari e dolomie), così come molti altri giacimenti di questo tipo nel mondo. Questa sembra essere una peculiare caratteristica dei giacimenti a nonsolfuri supergenici: la presenza di un incassante carbonatico è infatti un elemento fondamentale per tamponare i fluidi acidi ossidanti che trasportano i metalli ed impedire la loro completa dispersione. In alcuni casi la presenza di rocce silicee è un'importante fonte di SiO_2 necessaria nella precipitazione di silicati di Zn. Tra le tipologie deposizionali menzionate da Hitzman et al. (2003), la concentrazione in cavità carsiche rappresenta quella più comunemente osservata nei distretti investigati.

Lo studio mineralogico e petrografico effettuato sui campioni provenienti dai tre distretti minerari citati ha evidenziato che l'associazione mineralogica più frequente comprende, in ordine di abbondanza, principalmente smithsonite [$ZnCO_3$], seguita da emimorfite [$Zn_4SiO_7(OH)_2 \cdot H_2O$] e da idrozincite [$Zn_5(CO_3)_2(OH)_6$], come minerali di Zn, e cerussite [$PbCO_3$] come minerale di Pb prevalente. La smithsonite è presente anche in una varietà ricca in Fe ("*monheimite*"). Ossidi e idrossidi di Fe e Mn, spesso contenenti alti valori in altri elementi metallici (Zn-Pb-Ni) sono spesso associati alle fasi mineralogiche più importanti, così come solfati di Fe e Zn. La calcite è il minerale di ganga più importante. Alcuni minerali secondari di

Cu (malachite [$Cu(OH)_2(CO_3$] e azzurrite [$Cu_3(OH)_2(CO_3)_2$]) sono stati individuati solo nei campioni provenienti dai depositi Irlandesi. Tra i resti di solfuri ancora presenti nelle mineralizzazioni ossidate, la galena [PbS] è di gran lunga più abbondante rispetto alla blenda [ZnS] ed alla pirite e/o marcasite [FeS_2]). Nei giacimenti della Slesia Superiore sono stati riconosciuti due tipi di associazioni mineralogiche ben distinte: la prima (*red galman*) consiste delle tipiche fasi mineralogiche presenti anche negli altri giacimenti supergenici, mentre la seconda, (*white galman*) è dominata da Fe-smithsonite e Zn-dolomite e si presenta come una facies laterale della mineralizzazione a solfuri primari. Un'altra eccezione alla tipica mineralogia dei giacimenti supergenici è rappresentata dalla presenza di abbondante willemite [$ZnSiO_4$] nel distretto di Liegi, in particolare nel giacimento di La Calamine. Sia la mineralizzazione a willemite nel distretto di Liegi, che la *white galman* nella Slesia Superiore potrebbero avere una diversa genesi (idrotermale?) rispetto agli altri nonsolfuri investigati. In entrambi i casi non si registra nell'associazione mineralogica la presenza di ossidi e idrossidi di Fe, i quali sono particolarmente abbondanti nei depositi a nonsolfuri supergenici.

L'esatta paragenesi dei giacimenti a nonsolfuri presenta ancora delle caratteristiche non completamente chiarite, come ad esempio le relazioni temporali tra minerali di Zn e di Pb. La smithsonite, comunque, oltre ad essere la fase mineralogica più abbondante in questo tipo di giacimenti, è anche la prima a precipitare tra i minerali supergenici. Essa sostituisce sia i minerali della roccia incassante che i solfuri primari, e precipita come cemento di brecce o in cavità. È generalmente seguita da emimorfite, idrozincite e altri minerali "esotici".

Analisi chimiche effettuate sui minerali supergenici provenienti dai tre distretti considerati, evidenziano una serie di affinità e differenze. La smithsonite contiene una variabile concentrazione di altri metalli, oltre allo Zn, nel suo reticolo cristallino (Mn, Mg, Pb, Ca). Insolitamente alte concentrazioni di Cd sono state misurate in alcune generazioni di smithsonite in tutti in distretti minerari esaminati, mentre altri elementi inquinanti sono praticamente assenti dalla struttura cristallina di questo carbonato di Zn.

Le diverse generazioni di emimorfite misurate, così come anche le willemiti del distretto minerario di Liegi, rivelano una composizione chimica stechiometrica, con basse concentrazioni (<1 wt%) di Al, Ca, Fe e occasionalmente Pb. Anche le cerussiti mostrano una composizione chimica stechiometrica, e solo raramente contengono tracce di Zn.

Uno studio degli isotopi stabili (carbonio e ossigeno) è stato effettuato su diversi carbonati di Zn, Pb e Cu (smithsonite, cerussite e azzurrite), così come sui carbonati della ganga e della roccia incassante (calcite, dolomite, aragonite) provenienti dai tre distretti minerari considerati. Questa tecnica è un mezzo potenzialmente utile a comprendere le condizioni di formazione del deposito.

In particolare, i dati sui rapporti isotopici dell'ossigeno ci danno informazioni sulle temperature alle quali si sono formate le diverse fasi mineralogiche, mentre gli isotopi del carbonio sono importanti nel capire la provenienza dei fluidi mineralizzanti. I rapporti isotopici dell'ossigeno misurati nelle smithsoniti dal distretto di Liegi risultano essere costanti, con valori di $\delta^{18}O_{VSMOW}$ compresi tra 27.1 e 30.6‰, ed un valore medio di 28.4 ± 0.8‰ (1σ, n = 23), mentre i rapporti isotopici del carbonio misurati nello stesso minerale mostrano una maggiore variabilità, con valori di $\delta^{13}C_{VPDB}$ compresi tra -11.6 e -1.6‰. Anche nelle cerussiti e nelle calciti associate alle mineralizzazioni secondarie sono stati osservate costanti composizioni isotopiche relativamente costanti dell'ossigeno e composizioni molto variabili del carbonio. Questo stesso *pattern* è stato anche osservato sia nelle smithsoniti che nelle cerussiti provenienti dalle Midlands Irlandesi. Le prime hanno valori di $\delta^{18}O_{VSMOW}$ compresi tra 28.3 e 31.5‰, mentre il $\delta^{13}C_{VPDB}$ varia tra -5.7 e -10.9‰, mentre le seconde hanno valori di $\delta^{18}O_{VSMOW}$ 17.6 e 19.6‰ e valori di $\delta^{13}C_{VPDB}$ compresi tra -16.4 a -0.1‰. I valori relativamente costanti di $\delta^{18}O$ misurati in queste fasi, implicano che sia la temperatura che la composizione isotopica del fluido meteorico erano rimaste costanti durante tutto il processo di ossidazione dei solfuri primari. D'altro canto, i variabili rapporti isotopici del carbonio evidenziati nei carbonati di Zn, Pb e Ca, indicano la presenza di una sorgente multipla di carbonio nella formazione dei minerali nel corso dell'alterazione supergenica. Tali possibili sorgenti di carbonio sono rappresentate da: 1) sorgenti arricchite in ^{13}C (CO_2 atmosferica, CO_2 dalla dissoluzione della roccia carbonatica incassante) e impoverite in ^{13}C (CO_2 organica presente nei suoli sovrastanti le mineralizzazioni).

I giacimenti della Slesia Superiore mostrano delle anomalie nel comportamento degli isotopi stabili rispetto agli altri distretti. La smithsonite contenuta nelle mineralizzazioni del tipo *red galman*, si presenta con un limitato intervallo di valori di $\delta^{13}C_{VPDB}$ (-11.4 e -10.1‰), mentre l'intervallo dei valori di $\delta^{18}O_{VSMOW}$ (26.8 ± 0.9‰) è più ampio rispetto al consueto andamento riscontrato nelle mineralizzazione supergeniche. Questo andamento potrebbe evidenziare la prevalenza di carbonio di origine organica (impoverito in ^{13}C) come fonte dei carbonati analizzati. Anche la smithsonite della *white galman* si differenzia isotopicamente dai comportamenti *standard* delle smithsoniti supergeniche. Essa mostra infatti una composizione isotopica del carbonio leggermente più variabile e positiva (-7.4 a -2.9‰ VPDB) rispetto quella della smithsonite nella *red galman*, mentre la composizione isotopica dell'ossigeno rimane costante ($\delta^{18}O_{VSMOW}$ = 27.8 ± 1.0).

Sono stati presi in considerazione, sulla base del loro significato geo-tettonico e paleoclimatico, le più importanti testimonianze degli eventi di *weathering* (lateriti, bauxiti, depositi di caolino, *grus*, paleosuoli e paleosuperfici), presenti nella parte centrale e settentrionale del continente

Europeo, che potrebbero avere relazioni temporali con i giacimenti a nonsolfuri di Zn. Lo scopo preciso di questa ricerca è stato quello di individuare: (a) i periodi durante i quali in Europa erano più intensi i processi di *weathering*, (b) le condizioni climatiche favorevoli alla formazione di molti giacimenti a nonsolfuri nei distretti minerari investigati.

Nonostante non sempre esistono datazioni precise dei profili di alterazione supergenica, in linea di massima è stato possibile individuare alcuni particolari periodi della storia geologica del continente Europeo in cui i processi di *weathering* superficiale sono stati particolarmente attivi. Infatti molti depositi lateritici e bauxitici, così come anche molte saproliti a caolinite, sembrano essere di poco precedenti, pur con alcune eccezioni, alla trasgressione del Cretacico Superiore nell'Europa Centrale. Altri depositi di caolino, anch'essi presenti nell'Europa Centrale e Settentrionale, sono stati invece assegnati ad un'epoca di formazione compresa tra il Terziario Inferiore e il Miocene. Altri profili di alterazione (alterazione chimica e meccanica incompleta), classificati come *grus*, presenti soprattutto nell'Europa Settentrionale, sembrano invece essere ancora più recenti (Plio-Pleistocene e Quaternario). Si potrebbe pertanto affermare che anche la formazione dei giacimenti a nonsolfuri di Zn supergenici in Europa sia probabilmente legata temporalmente ai citati periodi di *weathering* (pre-Cretacico Superiore e Paleogene-Miocene).

La geochimica degli isotopi stabili, tenendo conto delle composizioni isotopiche delle paleo-acque meteoriche locali, ha consentito inoltre di calcolare le temperature di precipitazione dei minerali supergenici nei vari distretti minerari e di ottenere una serie aggiuntiva di indicazioni paleoclimatiche. La maggior parte delle smithsoniti e delle cerussiti misurate hanno temperature di precipitazione comprese tra circa 10 e 20°C. Temperature leggermente inferiori sono state misurate solo nelle smithsoniti provenienti dal distretto minerario delle Midlands Irlandesi. Nel complesso, queste temperature vengono solitamente registrate in aree a clima temperato, come quello attualmente presente in Europa, dove esiste una ben distinta stagione secca. Ovviamente, considerando che la deposizione dei nonsolfuri è avvenuta in aree profonde della circolazione carsica, tali temperature avrebbero potuto essere raggiunte anche con condizioni climatiche esterne di tipo tropicale.

In conclusione, i probabili intervalli temporali in cui le mineralizzazioni a nonsolfuri si sono depositate nei tre distretti esaminati, sono:

1) distretto di Liegi: alcune parti dei corpi mineralizzati (ricche in willemite) sono coperte da arenarie continentali della Formazione di Aachen (Santoniano). Queste parti dei depositi sono perciò databili ad un'epoca pre-Cretacico Superiore e il loro *timing* potrebbe essere comparabile con l'importante fase di *weathering* che produsse molti depositi a caolino nell'Europa Centrale. Comunque, a causa del ridotto spessore della

copertura e la sua alta permeabilità, non si può escludere che l'ossidazione dei solfuri primari sia continuata anche dopo il Cretacico Superiore e durante tutto il Terziario.

2) distretto della Slesia Superiore: parte dei nonsolfuri sono coperti da sedimenti marini del Miocene. Se assumiamo un'età Cretacico Medio per la messa in posto delle mineralizzazioni primarie, è allora molto probabile che la maggior parte dei nonsolfuri in questo distretto si sia formata durante una fase di *weathering* Terziaria, la quale sembra essere stata inoltre responsabile della genesi di depositi di caolino e lateriti nichelifere nell'adiacente regione della Slesia Inferiore.
3) distretto delle Midlands Irlandesi: i depositi supergenici in questo distretto risultano in gran parte coperti da sedimenti glaciali e rivelano alcune caratteristiche mineralogiche che indicano una immaturità del processo di ossidazione. Quest'ultimo aspetto sembra essere confermato anche dalla presenza di molti depositi di *grus* (profili immaturi), in molte aree della Gran Bretagna e Irlanda. Probabilmente una prima fase di ossidazione che ha favorito la formazione di profili alterati sui corpi a solfuri primari, è avvenuta durante il Terziario Inferiore in concomitanza con la formazione di profili lateritici sviluppatesi sui basalti nella regione di Antrim (Irlanda del Nord). Contemporaneamente non si può escludere che il processo di ossidazione dei solfuri primari abbia agito in questo distretto anche successivamente, in condizioni climatiche meno estreme rispetto alle precedenti ed essere tuttora attivo.

Chapter 1: Introduction

1.1 Introduction and aims of the thesis

The aim of this Doctoral Thesis was to carry out an extensive study of several nonsulphide Zn deposits related to weathering (or paleoweathering) processes in Europe. More precisely, the deposits occurring in the Liège district (NE Belgium), Upper Silesia (S Poland) and Irish Midlands (Ireland) have been dealt in the present Ph.D and compared with other, already investigated nonsulphide deposits like those of the Iglesias district in SW Sardinia (Italy). Previous studies on these European nonsulphide deposits already exist, but many aspects regarding their formation had not been completely cleared. Indeed, at the current state of the art, in most European districts, the relationships between the nonsulphide ores and both their carbonate hosts and precursor sulphides deposits, as well as the chronological scale (calibrated with independent variables) of the crucial oxidation periods that could have originated the mineralization, are still lacking. Moreover, the distribution of the mineralogical phases in the weathering profile and the geochemical equilibria involved are also uncertain.

Therefore, the main goal of this Thesis project was not only to understand the genesis of the considered deposits, but also to draw a geological model that would have considered the multiple controls on their genesis, in order to place the formation of the most important nonsulphide Zn deposits in the geological evolution of Europe. To carry out this study, I have used a multidisciplinary approach, which combines fieldwork with mineralogy, petrography and geochemistry, preceded by a preliminary bibliographic research on the wide subject of Zn nonsulphides and paleoweathering in Europe. This work will deal initially with two key European nonsulphide Zn districts: the Belgian "*calamine*" (Dejonghe, 1998; Dejonghe & Boni, 2005; Boni et al., 2005a; Coppola et al. 2007) and the Polish "*galman*" (Zabinski, 1960; Smakowski & Strzelska-Smakowska, 2005; Kucha, 2005; Coppola et al., 2007), which have been studied entirely during my Thesis work. All the geological-geochemical-petrographic aspects of these deposits will be discussed. To this part, I will add also the studies carried out on the nonsulphides of the Irish Midlands (occurring in the Tynagh, Galmoy and Silvermines deposits), both by myself and from other researchers of the Naples group (Balassone et al. 2007). In the second part of the Thesis, I will integrate and compare the previously dealt ores with the

data existing in literature on other European nonsulphide deposits: SW Sardinia & Alpine district - Italy, Reocin, Las Cruces – Spain and Lavrion, Thassos – Greece (fig. 1.1 and tab. 1.1).

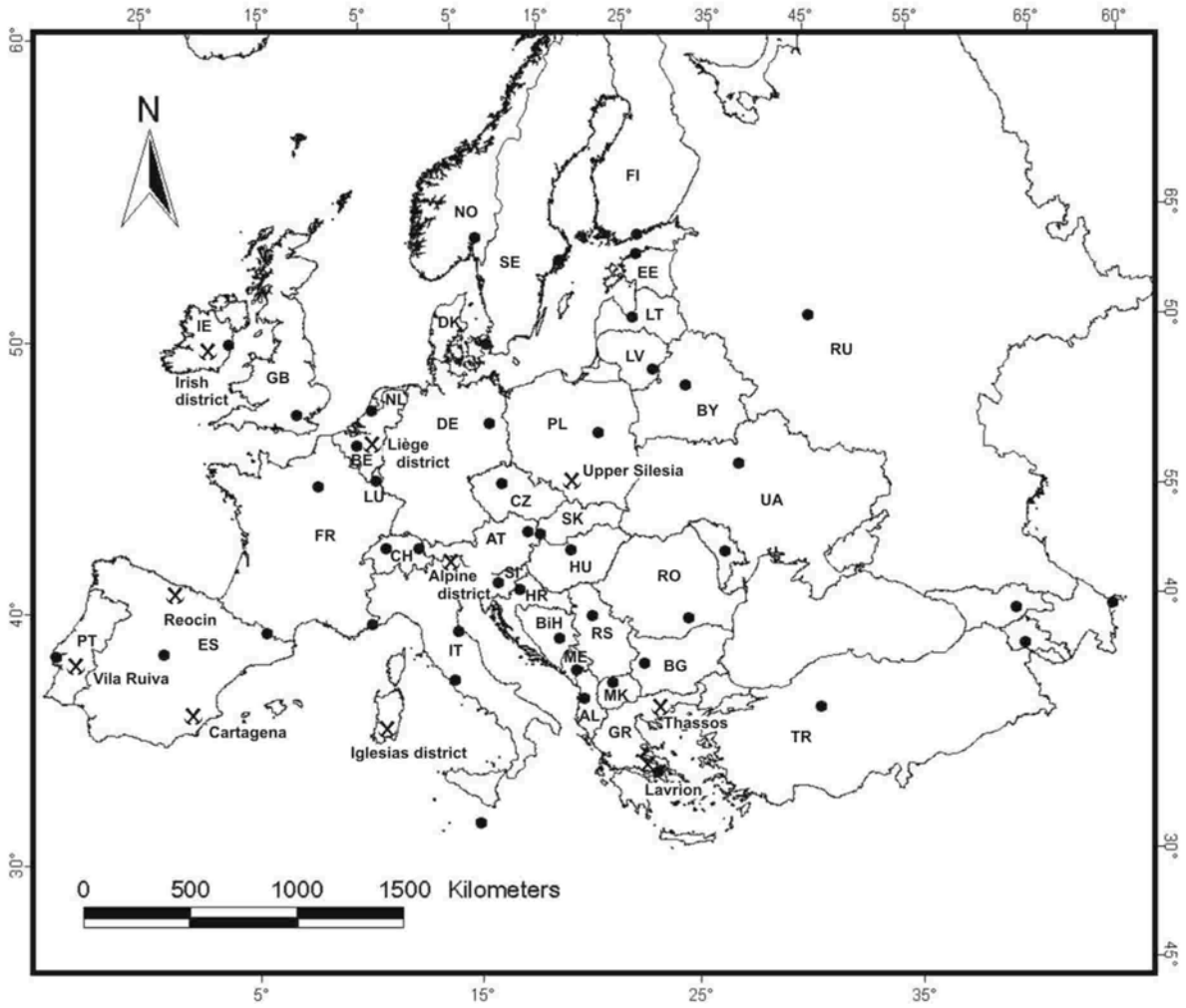

Figure 1.1: Location of the most important European Zn nonsulphide deposits (after Boni & Large 2003, modified).

An important part of this Thesis will be also the description of the paleoweathering records in Europe (paleosoils, weathered horizons and profiles, regoliths, bauxites, laterites, kaolinite deposits). In particular, the paleoweathering records in the same area or in areas adjacent to those hosting the nonsulphide Zn ores will be particularly significant. In fact, it is well known that this kind of deposits have been formed under particular climatic and geomorphological condition. Therefore the relationships between the geological conditions controlling the evolution of the weathering profiles and those responsible for the formation of nonsulphide Zn deposits, will be discussed.

Table 1.1: Main features of the most important European nonsulphide Zn deposits.

Name	Location	Age of host rock	Primary deposit type	Emplacement age of primary deposit	Supergene deposit type*	Major minerals**	Sulphide resources	Nonsulphide resources	References
Iglesias district	Sardinia, Italy	Cambrian dolomites limestones	Sedex, MVT	pre- to post-Hercynian	DR, WR, karst	sm, hem, ce	ca 150 Mt @ 2–8% Zn, 1–2% Pb (mixed res.)		Boni et al., 1996, 2003
Alpine district	Italy, Austria, Slovenia	Triassic limestones	MVT	Late Mesozoic	WR, karst	sm, hem, wulf	7 Mt	n.d Mt @ 15% Zn	Klau & Mostler, 1983; Zeeh et al., 1998; Leach et al., 2003
Liège district	Belgium	Devonian-Lower Carboniferous limestones	MVT	Mesozoic	HD?,DR, karst	will, sm, hem	1.2 Mt (conc) @ 47% Zn	1.9 Mt (conc) @ 37-43 % Zn (La Calamine)	Dejonghe et al., 1993; Dejonghe et al., 1993; Boni & Large, 2003; Coppola et al., 2007
Irish Midlands district	Ireland	Courceyan limestones	Irish type	Courceyan Arundian	karst, WR, DR	sm, hem, ce, mal, az	160 Mt @ 3-13% Zn, 0.5-6% Pb	2.2 Mt @ 10-15% Zn+Pb	Boland et al., 1992; Hitzman & Beaty, 1996; Clifford et al., 1986; Balassone et al., 2007
Reocin	Spain	Cretaceous limestones	Sedex, MVT	Cretaceous? Tertiary?	DR, WR	sm	80 Mt @ 10% Zn, 1% Pb	3 Mt @ 17-20% Zn	Large, 2001
Las Cruces	Spain	Palaeozoic sedimentary and volcanic rocks	VMS	early Carboniferous	DR, karst	chalc, dig, bor, enar	20.7 Mt @ 4.2% Zn, 2.0 % Pb, 0.8% Cu	15.5 Mt @ 6.1% Cu	Knight, 2000; Doyle et al., 2003
Beja district (Vila Ruiva, Preguica)	Portugal	Cambrian dolomites	VMS	Tertiary?	karst, DR	sm, hem		ca. 13 Mt	Vairinho & Fonseca, 1989
Lavrion and Thassos	Greece	Miocene marble	VMS, skarn	Latest Miocene?	WR, karst	sm, hem, hyz		1.1Mt (Lavrion)	Skarpelis, 2005; Boni & Large, 2003
Silesia-Krakow district	Poland	Middle Triassic limestones-dolomites	MVT	Early Cretaceous? Tertiary?	WR, DR, karst	sm, hem, Zn-do	183 Mt @ 3.8% Zn, 1.6% Pb	57Mt @ 5.6% Zn, 1.4% Pb	Zabinski, 1960; Large, 2001; Kucha, 2005

* Deposit types are referred to Hitzman's et al. (2003) classification: DR = direct replacement, WR = wall rock replacement, karst = residual and karst filling, HD = hydrothermal

** Abbreviations: az = azurite; bor = bornite; ce = cerussite; chalc = chalcocite; dig = digenite, enar = enargite, hem = hemimorphite; hyz = hydrozincite, mal = malachite; sm = smithsonite; will = willemite; wulf = wulfenite; Zn-do = zincian dolomite.

In conclusion in the present study I will report on:

a) the actual knowledge on nonsulphide Zn deposits, including the current classifications;
b) the geological-mineralogical–petrographic–geochemical characterization of the single deposits (or mineralized districts) under investigation (differences and affinities);
c) the characterization of the mineralising fluids active in most deposits (source, temperature);
d) the possible timing of the considered deposits;
e) the existing records of paleoweathering in Europe and their timing (from geologic and climatic evidences);
f) the possible correlation between the main periods of paleoweathering in Europe and the formation of the supergene nonsulphide Zn deposits.

Chapter 2: Nonsulphide Zn deposits: an overview

2.1 History of nonsulphide Zn deposits

Nonsulphide Zn deposits have represented an important source of this metal in the past. They were called "*calamine*" in French and Italian, "*galmei*" in German and "*galman*," in the Polish speaking worlds, but actually the most frequent denomination is "*Zn-oxides*" or "*Zn nonsulphides*". They consist in a mixture of Zn-carbonates and silicates with associated Pb-carbonates, Fe-Mn-(hydr)oxides and clay minerals (Boni & Large, 2005).

The exploitation of this kind of deposits goes back to Roman age, and through the Middle age, until the first twenty years of the 20th century. Zn extracted from nonsulphides was used for the production of brass, a zinc-copper ± tin alloy, mostly in Europe and Mediterranean area. The process was very easy, the oxidized mixture being heated in a crucible with copper.

At the beginning of the 19th century, a chemist from Liege, Jean-Jacques-Daniel Dony, invented the first procedure to transform calamine into malleable zinc, which was patented in 1810 under Napoleon I. It consisted in the melting of calamine concentrates in furnaces with horizontal crucibles, operating for the first time in a factory along the Saint Léonard wharf at Liège (Dejonghe & Jans, 1983). Later, the "calamine" ores were processed to produce high-grade zinc oxide in Wälz kilns (fig. 2.1), using a technology which was developed in Europe at the end of the 19th century.

Figure 2.1: Abandoned Wälz kiln in the Iglesias mining district (SW Sardinia, Italy)

After the first twenty years of 19th century this kind of deposit was practically neglected, despite a low-level exploitation lasted until the seventies in Sardinia and Poland. Sulphide ore deposits were preferred as source of Zn. This sudden change of interest has been due principally to both the difficulties in metallurgical beneficiation for the presence of Zn-oxides, silicates and clays in the mixtures, and to the discovery of new techniques for sulphides treatment (floatation and melting). Therefore, this fact led to neglect the exploration of nonsulphide deposits for the subsequent fifty years. Still now, sulphides represent the most important resource of zinc in the world.

Only in the last twenty years we could assist to a revival of both economic and scientific interest for this style of mineralisation. The principal reasons were the discovery of new hydrometallurgical acid-leaching (LTC), solvent-extraction (SX), and electro-winning (EW) technologies and the modernization of the Wälz technology for the treatment of nonsulphide zinc ores.

These techniques permit the recovering *in situ* of higher Zn grades with lower costs. This fact, associated with a higher environmental sustainability, due to the scarcity of non-economic, polluting metals (the so-called "nasties", as Cd, As), and the absence of sulphur, is the main reason which promoted the new interest of mining companies towards these ore deposits. On the other hand, the scarcity of economic by-products (Pb, Ag, Cu), compared to sulphide ores, represents a negative point. Therefore, to balance this, nonsulphide deposits will need to be larger and with higher grade with respect to sulphide deposits.

Actually Zn is still principally extracted from sulphide deposits, while nonsulphides represent only the 4.5% of world Zn production. However, on the base of economic forecasts (Teck Cominco Ltd), they will represent more than 10% of the annual total zinc production in the next decades (tab. 2.1).

Table 2.1: West world curent zinc production and projections (TeckCominco Ltd. 2006)

Type of Deposit	1996*	projection 2005-2015*
Volcanic Hosted (VMS)	30	15
Carbonate replacement/skarn (CRD)	20	25
Sedimentary-exhalative (SEDEX)	25	40
Mississippi Valley-type (MVT)	20	10
Zinc Oxides (Nonsulphides)	<5	>10

* (values in %)

Many projects are active or in development on this kind of deposits throughout the world. The individual tonnage is generally constrained from <1Mt to >100Mt, with a Zn grade ranging between 7% and 30% (Large, 2001; Hitzman et al., 2003; Reynolds et al., 2003; Boni, 2005).

Medium to large deposit projects include: Skorpion (Namibia), Mae Sod (Thailand), Lan Ping (China), Angouran (Iran), Mehdiabad (Iran), Shaimerden (Kazakhstan), Jabali (Yemen), Vazante (Brazil). Accha (Peru) and Sierra Mojada (Mexico), while there are a number of other mines producing relatively small tonnages of nonsulphide zinc ores in Vietnam, Turkey, China, Morocco, Zambia and Egypt. However, to have a complete record of the existing Zn nonsulphide ores, we should consider the high tonnages already exploited in the older deposits like those of SW Sardinia, Belgium, Ireland, Franklin/Sterling Hill (USA), Beltana-Aroona (Australia) and of Upper Silesia (Poland) (tabs. 2.2 and 2.3).

As mentioned, the economic interest has favoured also the scientific interest towards these deposits. This fact is documented by the recent publications appeared on international journals: for example the volume 98(4) 2003 Issue of Economic Geology is entirely dedicated to nonsulphide deposits, as one of the future issues of Ore Geology Review (2007-2008).

2.2 Nonsulphide Zn deposits: definition and main characteristics

Nonsulphide zinc deposits usually represent the products of oxidation of primary sulphide bodies, but a primary/hydrothermal origin cannot be excluded for some of them. Notwithstanding the many common characteristics, many different aspects regarding their mineralogy, geochemistry and emplacement process have been observed in the nonsulphide deposits throughout the world (fig. 2.2).

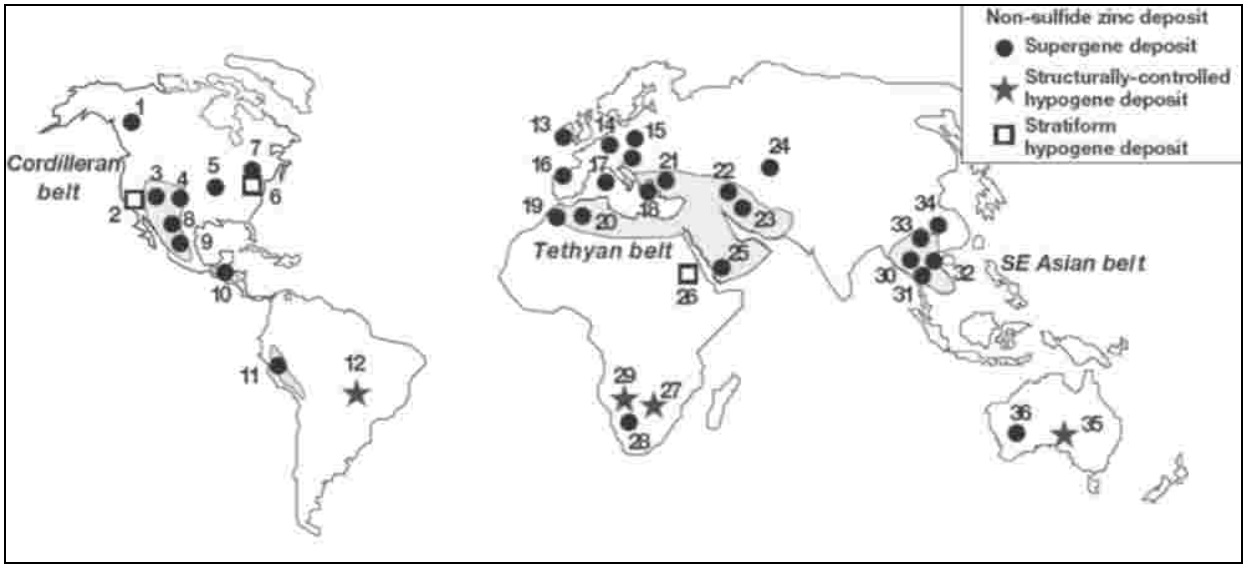

Figure 2.2: Location of the main nonsulphide Zn deposits in the world (from Hitzman et al. 2003).

Table 2.2: Main supergene nonsulphide Zn deposits in the world: primary ore, mineralogy, resources (from Hitzman et al., 2003, modified)

Name	Primary deposit type	Emplacement age primary deposit	Supergene deposit type*	Major minerals**	Sulphide resources	Mixed sulphide-nonsulphide resources	Nonsulphide resources	References
Leadville (Colorado - USA)	CRD	Tertiary	WR	sm, hem	8.1Mt @ 5.1% Zn, 4.2% Pb		8.3Mt @ 6% Zn, 2.5% Pb	Thompson & Arehart, 1990
Sierra Mojada (Mexico)	CRD	Tertiary	WR(DR)	sm, hem, sa	9Mt @ 5% Zn, 3% Pb, 500g/t Ag		> 3Mt @ 20% Zn	Titley, 1993; Metaline Mining, unpub. company report, 2000
Mapimi (Mexico)	CRD	Tertiary	DR?	sm, hem, sa			6Mt @ 15% Zn, 10% Pb, 500g/t Ag	Titley, 1993
Accha (Peru)	CRD	Tertiary	DR	sm, hem, sa			9Mt @ 9% Zn	Pasminco, unpub. company report, 2000; Hudson et al., unpub. report, 2000
Mina Grand (Peru)	MVT	Tertiary	WR?	sm			1.9Mt @ 19.3% Zn, 2.2% Pb	Solitario Resources, unpub. company report, 1998
Touissit (Morocco)	MVT	Tertiary	DR	sm, ce		70Mt @ 2.5% Zn, 7% Pb		Bouabdellah et al., 1996
Um Gheig (Egypt)	MVT	Tertiary	WR	hem, sm, gos			2Mt @ 10% Zn, 2% Pb	El Aref & Amstutuz, 1983
Zamanti (Turkey)	MVT?	Cretaceous - Tertiary	WR	sm, min			6Mt @ 26% Zn	Cerrah, pers. comm, 1999
Jabali (Yemen)	MVT	Cretaceous?	DR	sm			9.4Mt @ 10.8% Zn, 2.3% Pb, 77g/t Ag	ZincOx resources, unpub. company report, 2002
Mehdiabad (Iran)	MVT?	Tertiary?	DR, WR	sm, hem		218Mt @ 7.2% Zn, 2.3% Pb, 51g/t Ag		Union Capital Limited, unpub. company report, 2001

Table 2.2: *continue*

Irankuh (Iran)	MVT	Tertiary?	WR	sm	15Mt @ 4% Zn, 2% Pb	4Mt @ 7% Zn, 1% Pb	14Mt @ 12% Zn+Pb	Ghazba et al., 1994;
Kuh-e-Surmeh (Iran)	MVT	Tertiary?	WR	sm	2Mt @ 7% Zn, 4% Pb		0.8Mt @ 19% Zn, 7% Pb	Liaghat et al., 2000
Padaeng (Thailand)	MVT	Tertiary	WR/karst	hem, sm			5.1Mt @ 12% Zn	Reynolds et al., 2003
Long Keng (Myanmar)	MVT?	Tertiary	WR	sm			0.5Mt @ 38% Zn	Griffith, 1956
Cho Dien (Vietnam)	CRD	Triassic	karst	hem, sm, hydz	1.1Mt @ 11% Zn, 3% Pb		1.6Mt @ 15% Zn, 3% Pb	Fediuk & Kusnir, 1967
Jinding (China)	MVT	Tertiary	DR	hem, sm	90Mt @ 7.8% Zn, 1.6% Pb		50Mt @ 8% Zn, 1% Pb	Li and Kyle, 1997
Qiandong Shen Shen (China)	MVT	?	WR?	sm		9.9Mt @ 7% Zn, 1.7% Pb	1.7 Mt @ 10.5% Zn, 1.5% Pb	Page, pers. comm., 2000
Shaimerden (Kazakhstan)	Irish type/CRD	Carboniferous	DR, WR	hem, sm, sa			4.3Mt @ 20.9% Zn	Schaffalitzky et al., 2003
Skorpion (Namibia)	VMS	Neo-proterozoic	DR, WR	sm, hem, sa		60Mt @ 6-8% Zn, 1% Pb	24.6Mt @ 10.6% Zn	Corrans et al., 1993; Borg et al., 2003
Balmat (USA)	Isa/sedex	Proterozoic	WR,DR	will	40.8Mt @ 9.4% Zn		0.1 Mt @ 10-29% Zn	deLorraine, 2001
Vazante (Brasil)	Hypogene nonsulphide	Proterozoic	DR	hem, hydz, min			2.6Mt @ 13.3% Zn	Monteiro et al., 2000

* Deposit types are referred to Hitzman's et al. (2003) classification: DR = direct replacement, WR = wall rock replacement, karst = residual and karst filling.

** Abbreviations: az = azurite; ce = cerussite; hem = hemimorphite; mal = malachite; sm = smithsonite; will = willemite; wulf = wulfenite; Zn-do = zincian dolomite.

CRD = high-temperature carbonate replacement deposit; MVT = Mississippi Valley type deposit; sedex = sedimentary exhalative deposit; VMS = volcanogenic sulphide deposit.

Table 2.3: Main hypogene (hydrothermal) nonsulphide Zn deposits: host rock, mineralogy, resources (after Hitzman et al., 2003).

Name	Location	Deposit type	Age of host rock	Major minerals*	Resources	Refernces
Vazante	Brasil	Structurally controlled	Neoproterozoic	will, sph, frk	28.5Mt @ 18% Zn	F. Oliveira, pers. comm., 2001
Ariense (Masa)	Brasil	Structurally controlled	Neoproterozoic	will, sph	9.9Mt @ 18% Zn	South Atlantic resources 1999, company report
Beltana	Australia	Structurally controlled	Cambrian	will	0.86Mt @ 38% Zn	Groves et al., 2003
Aroona	Australia	Structurally controlled	Cambrian	will	0.17Mt @ 34% Zn	Groves et al., 2003
Reliance	Australia	Structurally controlled	Cambrian	will, sm	0.37Mt @ 28.8 Zn	Groves et al., 2003
Kabwe**	Zambia	Structurally controlled	Neoproterozoic	will, sph, ga	12.5Mt @ 25% Zn, 11% Pb	Kamona, 1993
Star Zinc	Zambia	Structurally controlled	Neoproterozoic	will, frk, zinc, gahn	0.2Mt @ 20% Zn	Sweeney et al., 1991
Berg Aukas**	Namibia	Structurally controlled	Neoproterozoic	will, sph, ga	3.4Mt @ 15% Zn, 4% Pb	Cairncross, 1997
Abenab West**	Namibia	Structurally controlled	Neoproterozoic	will	0.1Mt @ 25% Zn	Cairncross, 1997
Angouran	Iran	MVT	Tertiary	sm	3.2Mt @ 38% Zn, 2% Pb	Boni et al., 2007
Franklin	USA	Stratiform	Mesoproterozoic	will, frk, zinc	21.8Mt @ 19.5% Zn, 0.05% Pb	Frondel and Baum, 1974
Sterling HIll	USA	Stratiform	Mesoproterozoic	will, frk, zinc	10.9Mt @ 19% Zn	Johnson et al., 1990
Abu Samar	Sudan	Stratiform	Proterozoic	sph, wil, frk	3.6Mt @ 4.9% Zn, 0.6% Cu	El Samani et al., 1986
Desert View	USA	Stratiform	Cambrian	frk, het, wil, zinc	small	Leavens & Patton, 2000

* Abbreviations: frk = franklinite, ga = galena, gahn = gahnite, het = hetearolite, sph =sphalerite; sm = smithsonite; will = willemite; zinc = zincite

** There are some doubt on the origin of these deposits (hypogene/supergene)

The mineralogical assemblage of Zn nonsulphides include a whole series of minerals, but the main economic phases present are Zn- Pb-carbonates (smithsonite, cerussite), hydrated Zn- Pb-carbonates (hydrozincite, hydrocerussite), Zn-silicates (willemite, hemimorphite, Zn-bearing clays) and Zn- Mn-oxides (zincite, franklinite). Relicts of primary sulphides or neo-formed sulphide phases can also occur. Substantial differences are also recorded between supergene and hypogene deposits (tabs. 2.4 and 2.5). Carbonate rocks, both dolomite and limestone, are the most frequent host rocks observed, despite nonsulphides hosted in different lithologies were also recorded. These differences have rendered necessary to create a classification able to include all kinds of genetically distinct nonsulphide Zn ore deposits, often characterized by peculiar mineralogical assemblages.

Table 2.4: Most common minerals in supergene nonsulphide Zn deposits.

	Formula	Specific gravity	Moh's hardness	Class system
zinc minerals				
smithsonite	$ZnCO_3$	4.4	4.40	trigonal
hemimorphite	$Zn_4SiO_7(OH)_2 \cdot H_2O$	3.6	5.00	orthorhombic
hydrozincite	$Zn_5(CO_3)_2(OH)_6$	3.6-3.8	2-2.5	monoclin
sauconite	$Na_{0,3}Zn_3(Si,Al)_4O_{10}(OH)_2 \cdot 4H_2O$	variable, 2-3	1-2	monoclin
minrecordite	$CaZn(CO_3)_2$	3.5	3.5-4	trigonal
Zn-aragonite	$(Zn,Ca)CO_3$	3	3.5-4	orthorhombic
willemite	$ZnSiO_4$	3.9-4.2	5.50	trigonal
goslarite	$ZnSO_4 \cdot 7H_2O$	2.2	2.00	orthorhombic
loseyte	$(Mn,Zn)_7\ (CO_3)_2(OH)_{10}$	3.3	3.00	monoclin
hetaerolite	$ZnMn_2O_4$	4.6	6.00	tetragonal
idrohetarolite	$Zn_2Mn_4O_8 \cdot H_2O$	4.6	5-6	tetragonal
descloizite	$Pb(Zn,Cu)[OH \cdot VO_4]$	5.9-6.2	3.50	orthorhombic
chalcophanite	$(Zn,Fe,Mn)Mn_3O_7 \cdot 3H_2O$	3.9	2.50	trigonal
aurichalcite	$(Zn,Cu)_5[(OH)_3CO_3]$	3.5-3.6	2.00	monoclin
woodruffite	$Zn(Mn^{4+},Mn^{2+})_5 \cdot O_{10}\ 3 \cdot 1/2H_2O$	4	4.50	monoclin
tarbuttite	$Zn_2(PO_4)_2 \cdot 2H_2O$	4.2	3.5-3.7	triclin
scholzite	$CaZn_2(PO_4)_2 \cdot 2(H_2O)$	3.1	3-3.5	orthorhombic
sclarite	$(Zn, Mg, Mn^{+2})_4Zn_3[(OH)_2\ CO_3)]_2$	3.51	3-4	monoclin
lead minerals				
cerussite	$PbCO_3$	6	3.00	orthorhombic
anglesite	$PbSO_4$	6.3	3.00	orthorhombic
litharge	α-PbO	9.1	2.00	tetragonal
mimetite	$Pb_5(AsO_4,PO_4)_3Cl$	7.1	3.50	hexagonal
hydrocerussite	$Pb_3(CO_3)_2(OH)_2$	6.8	3.50	trigonal
pyromorphite	$Pb_5[Cl(PO_4)_3]$	7	4.00	hexagonal
hedyphane	$Ca_2Pb_3(AsO_4)_3Cl$	5.81	4-5	hexagonal
copper minerals				
chalcocite	CuS	5.5-5.8	2.5-3	monoclin
malachite	$Cu(OH)_2(CO_3)$	4	4.00	monoclin
azurite	$Cu_3(OH)_2(CO_3)_2$	3.8	3.5-4	monoclin
iron minerals				
goethite	FeO(OH)	4-4.4	5-5.5	orthorhombic
hematite	Fe_2O_3	5.2	5.00	trigonal

Table 2.5: Most common minerals in hypogene nonsulphide Zn deposits

	Formula	Specific gravity	Moh's hardness	Class system
willemite	$ZnSiO_4$	3.9-4.2	5.5	trigonal
zincite	(Zn,Mn)O	5.4-5.7	4-5	hexagonal
sphalerite	ZnS	3.9-4.2	3.5-4	isometric
coronadite	$Pb(Mn^{4+},Mn^{2+})_8 \cdot O_{16}$	5.44	4.5-5	monoclin
hetaerolite	$ZnMn_2O_4$	4.55	6	tetragonal
gahnite	$ZnAl_2O_4$	4-4.6	8	isometric
franklinite	$(Zn,Mn,Fe^{2+})(Fe^{3+}\ Mn^{3+})_2\ O_4$	5.1	5-5.6	isometric
galena	PbS	7.2-7.6	2.5	isometric
hedyphane	$Ca_2Pb_3(AsO_4)_3Cl$	5.81	4-5	hexagonal
hematite	Fe_2O_3	5.3	5	trigonal
Fe-dolomite	Ca(Mg,Fe))(CO3)2	3	3.5-4	trigonal
covellite	CuS	4.6	1.5-2	hexagonal

There have been so far only two classifications for this group of ore deposits. The first was compiled by Large (2001): it is based on both mineralogical characteristics and setting of the ores. Zn nonsulphide deposits are divided in three main groups:

1. "Calamine"-dominated deposits, occurring in Mississippi Valley-type and other stratiform sulphide protores in carbonate rocks. In this class of ores, nonsulphide mineralisation is related to the oxidation of primary sulphides and the preservation of the newly formed minerals is in karst-cavity in-fillings, as well as replacement aggregations;
2. Willemite-dominated deposits in late Proterozoic to early Cambrian sedimentary rocks, where the mineralisation occurs in marked fault zones. These deposits might be hydrothermal in origin, formed in low S- and high O-fugacities environment;
3. "*Gossan*"-type deposits, containing hydrated zinc silicates that were formed by residual surface oxidation *in situ* of primary sulphides and then preserved by a special set of circumstances (tectonic, climatic etc.).

According to the Large (2001) classification, the deposits of group 1 and 3 are considered supergene in origin, while nonsulphides included in group 2 could have a hydrothermal origin.

Hitzman et al. (2003) presented a lightly modified version of the classification proposed in 1962 by Heyl and Bozion. The authors made a broad distinction between supergene and hypogene nonsulphide deposits.

The supergene deposits corresponding to types 1 and 3 of Large (2001) are dominated by smithsonite, hemimorphite and hydrozincite assemblages, after Hitzman et al. (2003). Most of the exhausted and still active supergene deposits are positioned between 15° and 45° N latitude, thus pointing to specific climatic conditions. They are the result of the oxidation of primary sulphides and have been divided in (fig. 2.3):

1. Direct replacement of sulphide bodies. The Zn-oxide deposits form *gossan*s on primary sulphide bodies that are replaced *in situ*. Secondary Zn phases (smithsonite and hydrozincite) replace sphalerite, while cerussite replaces galena. The complex mineralogical assemblage can include a mixture of silicates, carbonates, and oxides (i.e. Tynagh-Ireland) (fig. 2.3a);
2. Wall-rock replacement. They form replacement bodies, dominated by smithsonite in areas adjacent to primary sulphides. The concentrations are the result of the buffering effect of carbonate host rock on acidic groundwaters containing zinc after primary sulphides oxidation. The distribution of minerals is regulated by the different mobility coefficients of the metals, and by the separation of Zn from Pb and Fe (Skorpion-Namibia, Iglesias-Sardinia) (fig. 2.3b);
3. Residual and karst-infilling deposits. This class includes reworked material forming the in-filling of karstic cavities after chemical or mechanical transport. These deposits are typical in uplifted areas under tropical climatic condition, because acidic, oxidized solutions derived from sulphides and high water availibility can increase the development of a karst network, which could represent a good receptacle for economic minerals (Cho Dien-Vietnam) (fig. 2.3c).

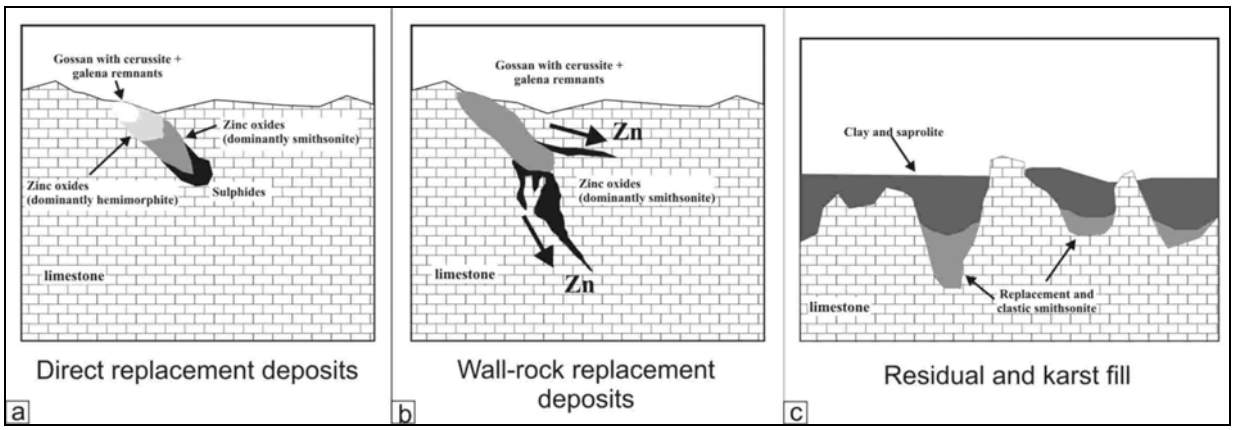

Figure 2.3: Genetic models of supergene nonsulphide Zn deposits (from Heyl & Bozion, 1962, modified).

Hypogene nonsulphide deposits form the second main group of ore in Hitzman's classification. A limited number of examples of this class, mostly located in the southern hemisphere, is actually known. They seem not to be correlated with sulphides oxidation and weathering, but commonly present some evidence of hydrothermal origin. One of the peculiar features of this group is the presence of the silicate mineral willemite locally associated with franklinite and zincite, whereas smithsonite and hemimorphite are subordinated. This class of deposits has been divided in two sub-groups:

1. Deposits related to faults in form of veins or pipes. The mineralogical assemblage includes

willemite with associated residual sphalerite, hematite and Mn-(hydr)oxides. The origin of the mineralization is probably due to mixing between an oxidized low-temperature and a reduced high-temperature (80 – 200°C) fluid, both sulfur poor (Brugger et al. 2003). Usually, in these deposits we can see an intergrowth of willemite and sphalerite, caused by changes in fluid's chemistry, also associated to its S-content. (Vazante, Brasil; Beltana-Aarona, Australia);

2. Mn-rich stratiform bodies containing franklinite, willemite, zincite and gahnite. The factors controlling the emplacement of this kind of deposits have not been fully explained (Hitzman et al., 2003; Boni, 2003; Brugger et al., 2003). Some of them could represent the metamorphic alteration of stratabound sulphide deposits (Franklin and Sterling Hill-USA; Bryson-Renfrew Region, Canada).

Both classification of Hitzman et al. (2003) and Large (2001) are currently used. But, considering the peculiar characteristics of nonsulphide Zn deposit, it is not easy to assign each of them to one of the groups and sub-groups of the mentioned classifications. Most European deposits are actually seen as typical examples of supergene weathering processes, as it will be discussed in the following chapter. For this reason, the main focus of this Thesis will be on supergene nonsulphide Zn deposits, while hypogene ones will be only considered in the European Zn districts as a rare genetic possibility.

2.3 Supergene nonsulphide Zn deposits and related dating problems

The supergene deposits, "*calamine s.l.*", represent the product of oxidation *in situ* of primary sulphide bodies and their mobilization and subsequently deposition in karstic cavities or in alteritic covers after mechanical and/or chemical transport (Coppola et al., 2007). As discussed above, the mineralogical association in supergene Zn nonsulphide deposits is dominated by smithsonite, hemimorphite and hydrozincite, with minor cerussite, Zn-smectites (sauconite), Fe-smithsonite, Zn- Pb-dolomite and Fe-Mn(hydr)oxides. As we will see below, the mineralogy of secondary deposits is influenced by both the mineralogy of the sulphide protore as well by the host rock type (limestone and/or dolomite, more rarely siliciclastic rocks).

The supergene alteration of primary Zn-Pb sulphides, and thus, the genesis of the secondary deposits, represents a peculiar case of weathering process. Therefore, the mechanisms controlling the weathering phenomena play a crucial role in the formation of nonsulphide deposits. The most important factors in the genesis of economically important supergene

deposits are:

a) the existence of a pre-existing sulphide deposit with an important content of Fe-sulphides, necessary for generating acid fluids;
b) a strong uplift tectonics and/or a constant lowering of the water table (related to local or global phenomena), to promote sulphide oxidation, and the development of karst systems;
c) climatic conditions favouring deep seasonal weathering;
d) permeable host rocks, allowing groundwater circulation;
e) the occurrence of effective traps to concentrate the newly formed minerals (often the same carbonate host rock).

However, we can easily assume that the formation of nonsulphide zinc deposits is primarily controlled by three main factors: protore composition, climate and geology (lithotype and structure) of the wall rocks. In particular, to explain the emplacement of this kind of ores, we need to combine and decode the effects of tectonics, climate and hydrogeology which contributed to the dissolution of primary sulphides together with the role of carbonate host rocks with their buffering effect and to understand the provenance and nature of the fluids which precipitated the ores. Another problem regards the temporal constrains of the oxidation processes, which generated the nonsulphide ores.

The mineralogical assemblage of the sulphide protore influences the mineralogy and the distribution of secondary deposits. In particular, the presence of Fe-sulphides in the primary deposits is conducive to the formation of he secondary concentrations because oxidative destruction of pyrite and marcasite provides low pH, and thus sulphate-bearing solutions capable of transporting metals. During the oxidation of Fe-sulphides (pyrite and marcasite) sulphuric acid is produced, while sphalerite and galena (though very susceptible to oxidation, Bladh, 1982; Boyle, 1994), produce relatively small quantities of acid sulphate-bearing solutions.

Iron sulphide-rich zinc deposits tend to produce sufficient acid during weathering, and combined with Fe^{+3} as an oxidant, completely leach zinc from the near-surface environment. Furthermore, the Fe-content in sulphide bodies might also influence the final distribution of oxidized phases (Hitzman et al., 2003). High Fe-sulphide content, for greater acid-generating capacity, might favour the formation of distal wall-rock replacement bodies, while in the case of sulphide deposits with low Fe content only replacement bodies *in situ* or replacement wall-rock bodies in the vicinity of sulphide protore can form. In extreme cases, an excessive production of sulphuric acid combined with the absence of a trap could be responsible of the dispersion for Zn-bearing fluids. Usually the trap is represented by carbonate host rock, which buffer the low pH groundwater.

The nature of primary sulphides involved in weathering processes can also influence significantly the mineralogy of secondary deposits. In fact, if nonsulphides are the oxidation product of low-temperature hydrothermal sulphides, the resulting mineralogical association tends to be relatively simple (smithsonite, hemimorphite, hydrozincite). On the contrary, the mineralogical association can be far more complex in those deposits derived from the weathering of high-temperature ores, owing to the wide range of metals occurring in this kind of primary deposit. At the same time, the composition of host rock can play a role in the final mineralogical assemblage of secondary deposits. In carbonate rocks smithsonite and hydrozincite prevail, while hemimorphite and Zn-smectite become the dominant phases in siliciclastic rocks. (Hitzman et al., 2003)

The distribution of the secondary phases is principally regulated by the different mobility coefficients of metals. Zn is more mobile in both carbonatic and siliceous environments with respect to other metals (Pb, Fe and Cu) also present in sulphide deposits. This fact favours a geochemical separation of Zn from the other metals. Lead, copper and iron remain closer to the original sulphide bodies, whereas Zn migrates out in solutions influenced by the groundwater flow gradient. Therefore Pb and Cu minerals can precipitate in the *gossan* of primary sulphide bodies, while Zn minerals (mainly smithsonite and hemimorphite) can replace dolomite and/or calcite in the host rocks, thus promoting the formation of wall-rock replacement bodies.

The most recent supergene nonsulphide deposits are located in a belt constrained between 15° and 40° latitude N (fig. 2.2). This fact could indicate that only particular climatic conditions are conducive to the development of this kind of weathering processes and to the formation of supergene nonsulphide deposits. Nonsulphide deposits located at higher latitudes are considered to be the results of paleoweathering (Hitzman et al., 2003).

Therefore, it is very important to unravel the possibly strong relationships between weathering and/or paleoweathering processes and the genesis of supergene nonsulphide Zn deposits. This is particularly true for nonsulphide deposits occurring in Europe and in the Mediterranean area, all of them considered supergene in origin. Among many other deposits, we can quote the nonsulphide Zn mineralisations occurring in: Upper Silesia - Poland, Liège district - Belgium, SW Sardinia - Italy, Alpine district - Italy, Vila Ruiva - Portugal, Reocin - Spain, Tynagh-Silvermines-Galmoy - Ireland, Laurion and Thassos – Greece, Zamanti district – Turkey, Touissit - Morocco). In spite of these deposits having been object of extensive exploitation in the past, their nature, genesis and timing are still not completely understood. Many aspects of the European and Mediterranean deposits and the factors involved, as the chemical equilibria, the control of the host rock on the mineralogical assemblage and the influence of climate and

tectonics are unclear. In particular, the periods during which the weathering processes were active in the main process of sulphide oxidation are still uncertain.

On the other side, it is well known that the weathering processes possibly causing the genesis of nonsulphide Zn ores, were also involved in the deposition of other lithotypes, as soil regoliths, laterites (including Ni-laterite), bauxites, silcretes, calcretes, kaolinite deposits etc. Their records were recognized throughout Europe, from lower (France, Italy, Greece, Spain, etc.), to higher latitudes (Ireland, Poland, Ireland, Belgium, etc.). The individuation and dating of these oxidation records could be important also to unravel the genesis and timing of Zn nonsulphide ores. However, it is well known that direct dating of the weathering records is very often a very hard task, because the weathering products are poorly age-constrained and rarely contain well-datable mineralogical phases. Current, but incomplete age information on the supergene deposits, reveal that several intense weathering periods have affected cyclically the European continent from Upper Palaeozoic to Mesozoic and until Present. Two main age intervals are considered the most favorable to provide the conditions of temperature and humidity for intense weathering: Cretaceous-Eocene and Middle Miocene (Herrington et al., 2007). Therefore my attention will be dedicated to these periods in particular and related records.

Until now, it was generally accepted that a tropical humid climate was essential to produce not only bauxites and laterites (Bàrdossy & Aleva 1990; Budel 1982), but also supergene Cu and Zn nonsulphides. Recent studies combined with paleogeographic reconstructions point out instead that in many cases an alternation between wet and dry conditions (common in savannah-type settings) is more favourable to the formation of supergene Zn ores, rather than a truly humid-tropical environment (Herrington et al., 2007). Also Reichert & Borg (2007) advocate similar climatic conditions for the formation of secondary Zn deposits in several areas of Iran.

Therefore, it seems evident that we need a better knowledge of both the climatic history in Europe during Mesozoic and Tertiary and of the paleoclimatic control on the genesis of supergene Zn nonsulphide deposits. The latter aspect will be considered in the second part of this Doctoral Thesis.

Chapter 3: Sampling and analytical techniques

3.1 Sampling

Over 150 rock and ore samples were collected in three different mining districts where nonsulphide ores have been exploited: Upper Silesia (Southern Poland), Liège district (NE Belgium) and Irish Midlands. The most important problem encountered during the sampling was not being able, in most cases, due to the closure or inaccessibility of the mines and/or to the absence of characteristic outcrops, of getting mineralized samples *in situ*. Therefore, it has been necessary to sample in the existing dumps around the old mine sites, whilst additional samples were collected from private or mine collections. For this reason, the study on the distribution of the secondary phases in the weathered profiles and on their spatial and genetic relations with the primary ores is necessarily limited. In tables 4.1, 5.1 and 6.1 is reported the detailed provenance of the samples.

In spite of the mentioned difficulties, the investigated samples cover a wide spectrum of nonsulphide minerals and their gangue, mainly consisting of Ca-carbonate crystals and concretions that were paragenetically associated or are post- nonsulphide ores. Where possible, host rock carbonate samples have been also collected, especially to compare their stable isotopic geochemistry with the values recorded by Zn and Pb carbonates.

3.2 Analytical methods

In order to carry out mineralogical and geochemical analyses, we have tried to obtain pure mineral phases by hand picking under a stereomicroscope the samples crashed beforehand, or to scrape individual crystals from the bulk sample. Then the samples were cleaned in a sonic bath for 10 minutes, to eliminate the impurities deposited on the crystal surfaces. Opportunely prepared samples were submitted to several types of mineralogical, petrographic and geochemical investigations (tab. 3.1).

Table 3.1: Methods and analytical techniques used.

methods	n of sample	
X-ray powder diffraction (XRPD)	300	single mineralogical phases, bulk rock
Trasmitted and reflected light optical (OM)	58	bulk rock
Cold Cathodoluminescence (CL)	58	bulk rock
Electron microprobe	30	smi, ce, hem, will, cc,do
Scanning electron microscope (SEM) and energy dispersive X-ray detection	50	sm, ce, hem, will, hyz, cc, do, Zn-clay, qz, mal, az, Fe-(hydr)oxides, ba, sulphide minerals
ICP-MS	17	sm, will
C and O stable isotope analyses	108	sm, ce, cc, do, az
Thermometric analyses of fluid inclusions	22	will, ce, sm, qz, do

Abbrevations: az = azurite, ba = barite, cc = calcite, ce = cerussite, do = dolomite, hem = hemimorphite, hyz = hydrozincite, qz = quartz, will = willemite.

3.2.1 X-ray powder diffraction (XRPD)

XRPD is a standard method by which crystalline phases of materials can be detected and differentiated, even in presence of a mixture of phases. Further data obtained from XRPD are for instance "crystallinity" rate of minerals and a semi-quantitative estimation of compounds in a mixture (based on peak intensity).

This technique is based on generating high-energy electrons, which bombard a Cu anode and subsequent emit X-rays. This radiation is direct on the pulverized samples, which rotate at a regular speed. When the mineral phases in the sample reach an appropriate angle, they will cause the diffraction of the X-rays according to Bragg's Law:

$$n\lambda = 2d \sin\theta$$

where n is an integer, λ is the X-ray wavelength, d is the lattice spacing and θ is the diffraction angle.

A counter transforms X-ray radiations into impulses, which are amplified and then transferred to a connected computer. The output from a diffractometer is a strip chart of the X-ray diffraction pattern where the horizontal scale is calibrated in °2θ and the vertical scale shows the intensity of the diffracted peaks. Then the peaks can be measured in terms of °2θ and automatically

converted in lattice spacing (*d*) by means of the Bragg's equation ($d = \lambda / \ 2\sin\theta$).

Minerals can be identified by comparing the obtained peaks with a set of the standard patterns compiled by the Joint Committee on Powder Diffraction Standards (JCPDS). These processes are made easier for the presence of a software interfaced with database.

X-ray powder diffraction analyses (XRPD) were carried out in two different laboratories: (1) at the Dipartimento di Scienze della Terra, Università di Napoli, Italy and (2) at the Electron Microscopy & Mineral Analysis (EMMA) Division of Mineralogy Department at the Natural History Museum of London.

At the Mineralogy Department of NHM I have used a Nonius PDS120 Powder Diffraction System with an INEL curved position sensitive detector (PSD). This detector has an output array of 4096 digital channels representing an arc of 120º 2θ and permits the simultaneous measurement of diffracted X-ray intensities at all angles of 2θ across 120º with a static beam-sample-detector geometry. A Copper $K\alpha_1$ (1.5418Å) radiation was selected from the primary beam using a germanium [111] single-crystal monochromator, and horizontal and vertical slits were used to restrict the beam to a size of 0.24 by 5.0mm respectively. Measurements were made in reflection geometry with the powder sample surface at an angle of ~5° to the incident beam. Data collection times were 10 minutes for each sample and the angular range recorded was 3º-120º 2θ. NIST silicon powder SRM640 was used as an external 2θ calibration standard and the 2θ linearization of the detector was performed using a least-squares cubic spline function. STOE Powder Diffraction system software package (in concession at Natural History Museum of London) was used for evaluation of the X-ray diffraction spectrum obtained, compared with JCPDS-ICDD international database.

Diffraction data at Dipartimento di Scienze della Terra in Naples were collected with a SEIFERT MZVI automated diffractometer (40kV, and 30mA) equipped with parallel (Soller) slit and a Na(Tl) scintillation detector and a pulse height amplifier discrimination. Copper $K\alpha_1$ (1.5418Å) radiation was selected from the primary beam using a germanium [111] single-crystal monochromator. Powder samples were deposited in the hollow (0.5mm deep) of a zero-background quartz mono-crystal plate. A long scan was performed over $3° < 2\theta < 75°$ with 0.5° 2θ/min step. Synthetic $CaCO_3$ (Mallinckrodt analytical reagent) was used as internal standard (position of the 1014 reflection for $CaCO_3$ taken as 3.035Å, JCPDS-ICDD 5-586). The XDATA program (part of the XDAL 3000 software package from Rich. Seifert & Co.) was used to evaluate the obtained profiles and to permit the comparison with JCPDS-ICDD database.

The specimens used for XRPD measures, were previously ground in a pestle in order to obtain granulometrically homogeneous powders (fraction <200μm).

Clay minerals analyses (fraction <2μm) have been performed in oriented aggregates after glycolation (EG) with several heating steps (250, 350 and 500°C).

3.2.2 Trasmitted and reflected light microscopy

54 polished thin sections were prepared from the most representative samples. Thin sections were observed under transmitted and reflected light using a Leica DMR petrological microscope located at the Electron Microscopy & Mineral Analysis (EMMA) division in the Mineralogy Department of Natural History Museum, London. Nikon cameras were used for obtaining high quality digital images of samples at the microscopic scale.

3.2.3 Cold Cathodoluminescence (CL) microscopy

Cathodoluminescence is an optical and electrical phenomenon where a beam of electrons is generated by an electron gun (e.g. cathode ray tube), then impacting on a luminescent material, causing the emission of visible light from this material. The electron bombardment of minerals causes excitement of ions, which "jump" to a state of higher energy. After a short delay time the excited ions return to their former energy state and emit a radiation. Emission in the visible spectrum is responsible for the luminescence to occur.

Cathodoluminescence in rock minerals depends on crystallographic defects and trace element concentration and distribution. In particular, some elements activate the luminescence whereas others quench it. Depending on the type of mineral and the activator/quencher quantitative ratio, different colors and/or intensity of brightness may result.

CL microscopy was carried out for all the prepared thin sections, in order to better characterize the growth features and the relations of the different mineral phases. The minerals were distinguished in extinct and luminescent. The latter were further characterized based on their CL color, intensity and zoning.

I have used CITL 8200 Mk3 Cold Cathodoluminescence instrument, coupled with an optical microscope, at the Geologisch-Paläontologisches Institut, Universität Heidelberg (Germany). The thin sections were placed on a tray controlled by X-Y manipulators in a vacuum chamber with an upper window for microscopic observation. A beam with a 23-25kV voltage and a current of 500-550μA was used. A Nikon digital camera mounted on the microscope was used to obtain high resolution images.

3.2.4 Scanning electron microscopy (SEM) and energy dispersive X-ray detection (EDS)

The scanning electron microscope (SEM) is a type of electron microscope capable of producing high-resolution images of a sample surface. This technique is based on an incident electron beam focused with magnetic lenses and accelerated by a high potential on the specimen. It is raster-scanned across the sample's surface, and results in the emission of different radiations (backscattered electrons, secondary electrons, X-rays).

Secondary electrons provides high-resolution imaging of fine surface morphology. Alternatively, backscattered electron imaging provides elemental composition variation, as well as surface topography. The efficiency of production of backscattered electrons is proportional to the sample material's mean atomic number, which results in image contrast as a function of composition, for instance material with higher atomic number appears brighter than material with lower atomic number.

X-rays, produced by ithe nteraction of the incident electron beam with the specimen, which are in function of the atomic number of element, may also be detected with SEM equipped for energy-dispersive X-ray spectroscopy (EDS). This method permits a point-to-point qualitative and quantitative chemical analysis.

The observations, as well as the qualitative and quantitative analysis were carried out using the Oxford Instrumens INCA on the JEOL 5900LV scanning electron microscope, equipped with an Energy Dispersive X-ray spectrometer. The instrument working conditions were: high vacuum, 10mm objective lens to specimen working distance, 6cm specimen to X-ray detector working distance, X-ray take-off angle to detector 40 degrees, 20kV accelerating voltage, 2nA beam current (stabilized and measured with Faraday cup). Backscattered electron images were produced. Quantitative spectra required 50 seconds acquisition time. X-ray matrix correction was carried out automatically by Oxford Instruments INCA version of the extended Pouchou and Pichoir (XPP) routine. Silicates, sulfates, sulphides, carbonates, oxides and pure elements were used as standards (tab. 3.2). Detection limits are in the order of 0.2 wt% oxide for EDX-rays. The CO_2 contents in carbonates and water content in hydrated carbonates and silicates were evaluated by stoichiometry. Analyzed samples were coated with a 15μm carbon film.

Secondary electron imaging of representative samples was produced using a Hitachi S2500 SEM at an accelerating voltage of 15kV. Before analysis, the samples were dried and stuck down onto 12mm Cambridge pin stubs using a thin smear of Araldite Precision resin, allowed to dry overnight and then coated with 20nm of gold-palladium using a Cressington HR208 sputter coater with a quartz crystal monitor to measure coating thickness.

The analyses with JEOL 5900 LV SEM and Hitachi S2500 SEM were carried out at the Electron

Microscopy & Mineral Analysis (EMMA) division of the Mineralogy Department of Natural History Museum, London.

Table 3.2: Usual standards used in quantitative analyses carried out with SEM JEOL 5900 INCA

Element	Line	Formula	Standard
Na	K_SERIES	Na_2O	Jadeite
Mg	K_SERIES	MgO	Eagle Station
Al	K_SERIES	Al_2O_3	Corundum
Si	K_SERIES	SiO_2	Eagle Station
P	K_SERIES	P_2O_5	Sc phosphate
S	K_SERIES	SO3	Pyrite
Cl	K_SERIES	NaCl	Halite
K	K_SERIES	K_2O	KBr
Ca	K_SERIES	CaO	Wollastonite
Ti	K_SERIES	TiO_2	Rutile
V	K_SERIES	V_2O_5	Vanadium
Cr	K_SERIES	Cr_2O_3	Chromium
Mn	K_SERIES	MnO	Manganese
Fe	K_SERIES	FeO	Pyrite
Co	K_SERIES	CoO	Cobalt
Ni	K_SERIES	NiO	Nickel
Cu	K_SERIES	CuO	Copper
Zn	K_SERIES	ZnO	Sphalerite
Sr	L_SERIES	SrO	Celestine
Cd	L_SERIES	CdO	Cd
Ba	L_SERIES	BaO	Frankdicksonite
Pb	M_SERIES	PbO	PbF_2

3.2.5 Electron microprobe analysis (WDS)

Electron microprobe analyses are used for high accuracy elemental characterization on the micro scale of samples for major and minor element concentrations. They can provide qualitative (identification) and quantitative (composition) analyses for the elements from Be to U. This method is based on an incident electron beam on a polished sample (stub or thin section), opportunely coated with15nm carbon, which produces an emission of X-rays. Emitted X-rays are detected by a wavelength dispersive spectrometer (WDS). From the wavelength and intensity of the lines in the X-ray spectrum, the elements present may be identified and their concentration estimated. In quantitative analyses, the intensity of X-ray lines from the specimen are compared with those from standards of known composition. The measured intensities require certain instrumental corrections.

Chemical analyses of willemite, smithsonite, hemimorphite, cerussite, calcite and dolomite were performed using a Cameca SX50 electron microprobe with a gas proportional WDS at (1) the IGAG of CNR, Rome and (2) at the Electron Microscopy & Mineral Analysis (EMMA) division

in the Mineralogy Department of Natural History Museum, London.
Instrumental conditions are 15kV, 15nA and 10μm spot size with a X-ray detector. In both cases work conditions were identical.
The data were corrected using the PAP program (Pouchou and Pichoir, 1991). Minerals and pure elements were used as standards. Detection limits are in the order of 0.01 wt%.

3.2.6 Major, minor and trace element analysis (ICP-MS)

Minor and trace elements can be incorporated in the mineral lattice as guest ions, which substitute for host ions of similar charge and radius. They may also occur interstitially between lattice planes and along crystal boundaries or occupy lattice defects or be included as solid or liquid inclusions. The entrance of an element in a lattice from its mother fluid is governed by the distribution coefficient (*k*), which describes the behavior and partitioning of elements between mineral and fluid. Therefore, an accurate estimation of the trace elements in the mineral could give information on the geochemistry of mother fluid. Due to the different modalities with which an element can be incorporated in the crystal lattice, and to the difficult estimation of the k factor in many mineralogical phases, the geochemistry of the fluids could be difficult to establish.
Many techniques are used to measure the minor and trace elements in minerals and/or mixtures. The most common is the ICP-MS (Inductively Coupled Plasma Mass Spectrometry). The ICP-MS is a type of mass spectrometry that is highly sensitive and capable of the determination of elements, whose atomic mass ranges between 7 and 250, with concentrations in the order of ppm and ppb. It is based on coupling together an inductively coupled plasma as a method of producing ions (ionization) with a mass spectrometer as a method of separating and detecting the ions.
In the present work, major, minor and trace elements in smithsonites and willemites from Belgian nonsulphides have been measured at ACME laboratories in Vancouver, Canada. Based on the different solubility of Zn-carbonates and Zn-silicates, two separate digestion procedures were used. From each pulverized willemite sample, 0.25g were added to a 10mL aliquot of the acid solution (2:2:1:1 H_2O-HF-$HClO_4$-HNO_3), heated until fuming on a hot plate and taken to dryness. A 7.5mL aliquot of 50% HCl is added to the residue and heated in a hot-water bath (~95°C) for 30 minutes. After cooling the solutions are transferred to polypropylene test-tubes and made to a 10mL volume with 5% HCl. Otherwise, an aliquot of 0.5g of each pulverized smithsonite samples reacted with a modified Aqua Regia solution of equal parts concentrated ACS grade HCl and HNO3 and de-mineralised H_2O is added to each sample of smithsonite to

leach in a hot water bath (>95°C) for 1 hour. After cooling the solution is made up to final volume with 5% HCl. Sample weight to solution volume is 1g per 20mL.
The measurements have been carried out with a Perkin Elmer Elan 6000 ICP-MS. 41 element of 1EX Group and 36 element of 1-DX Group were respectively measured in willemite and smithsonite samples. Aliquots of in-house Standard Reference Material like STD DS6 and STD DST5 were used to monitor accuracy.

3.2.7 C and O stable isotopes geochemistry

Isotopes of the same element have differences in mass and energy, which cause differences in the physical and chemical properties. In a molecule where two isotopes of the same element are present, the isotope with lighter mass is more reactive than the heavier isotope. A change in the ratio of the two isotopes during a reaction from phase A to phase B, such as the mineral precipitation, is called "fractionation". Each isotope reaction is defined by the temperature dependent fractionation coefficient α:

$$\alpha = Ra/Rb$$

where R_A and R_B are the ratios of the heavy to light isotopes in phase A and phase B respectively.
The fractionation factor (α) is correlated to absolute temperature by the following equation:

$$\ln \alpha = AT^{-2} + BT^{-1} + C$$

where A, B, C are coefficients determined experimentally and T is the absolute temperature in Kelvin.
Only a few of the lighter elements, such as Oxygen and Carbon, have isotopes with sufficient relative mass difference to cause detectable fractionation in nature. The two most abundant stable isotopes of oxygen are ^{16}O (99.757%) and ^{18}O (0.205%). The two stable isotopes of carbon are ^{12}C (98.93%) and ^{13}C (1.07%). The absolute concentration of single isotopes is difficult to measure, but on the other hand, isotopic ratio can be determined easily and accurately. Usually the $^{18}O/^{16}O$ and $^{13}C/^{12}C$ isotopic ratios of a sample (*x*) are expressed relative to a standard (*std*) of known isotopic composition. This relative difference or δ value is given by:

$$\delta^{18}O = \left[\frac{\left(\frac{^{18}\mathrm{O}}{^{16}O}\right)_x - \left(\frac{^{18}O}{^{16}O}\right)_{std}}{\left(\frac{^{18}O}{^{16}O}\right)_x} \right]$$

$$\delta^{13}C = \left[\frac{\left(\frac{^{13}C}{^{12}C}\right)_x - \left(\frac{^{13}C}{^{12}C}\right)_{std}}{\left(\frac{^{13}C}{^{12}C}\right)_x} \right]$$

This method has applications in many sectors of Earth Science. Its applications are exhaustively discussed in Faure (1986), Tucker & Wright (1990), Clauer & Chaudhuri (1992) and Hoefs (1997). Moreover, the specific application of this method to carbonates associated to hydrothermal, diagenetic and magmatic sulphide deposits has been repetitively applied and has provided data on temperature of formation, origin and evolution of metal-bearing fluids and mechanism of emplacement (Ohmoto & Rye, 1979; Field & Fifarek, 1985; Zheng & Hoefs, 1993; Schwinn et al., 2006). Only in the last decades this technique has been applied to the study of Zn nonsulphide deposits. Actually, few isotope studies have been published on carbonates from sulphide oxidation zones or hypogene nonsulphide Zn-Pb deposits (e.g. Monteiro et al., 1999; Melchiorre & Williams, 2001; Melchiorre et al., 1999, 2000; Gilg & Boni, 2004; Boni et al., 2003; Coppola et al., 2007; Gilg et al., 2007a). Direct applications to the nonsulphide ore deposits are discussed in Boni et al. (2003) for the deposits in SW Sardinia and in Coppola et al. (2007) for the Liège district.

To measure the isotopic ratios of carbonates in nonsulphide deposits, can be a powerful tool to constrain the conditions present during the emplacement of these ores. In particular, it could be useful to distinguish the ores of supergene from those of hypogene origin, to evaluate the effects of oxidative heating during sulphide oxidation, to distinguish between meteoric or sea water and their chemical-physical changes during oxidative processes, to distinguish sulphide versus wall rock replacement and, additionally, to give paleoclimatic indications. All these points and aims are potentially valid if no change in the carbon isotope composition of the carbonates occurred after their deposition due to re-equilibrium with a new fluid (closed system).

It is well known that $^{18}O/^{16}O$ ratios in the carbonate minerals are correlated with their precipitation temperatures, and are also influenced by the isotopic composition of fluid. Therefore, in every discussion about the isotopic equilibrium involved during phase

precipitations, we have to consider both these variables. Because the oxygen isotopic composition of the minerals can be used as geothermometer to determine the equilibrium temperature between fluid and mineral, this approach needs a good knowledge of the appropriate equations regulating the fluid–mineral isotopic fractionation in dependence of temperature.

While the fractionation equations between dolomite/calcite and water are known from long time, only recently these equations have been calculated for smithsonite and cerussite (fig. 3.1) (Gilg et al., 2007a), as well as for azurite (Melchiorre et al., 2000). In this work the following equations will be used:

$$10^3 \ln \alpha_{smithsonite-water} = 3.10\left(10^6/T^2\right) - 3.50 \quad \text{(Gilg et al., 2007a)}$$

$$10^3 \ln \alpha_{cerussite-water} = 2.29\left(10^6/T^2\right) - 3.56 \quad \text{(Gilg et al., 2007a)}$$

$$10^3 \ln \alpha_{dolomite-water} = 3.20\left(10^6/T^2\right) - 3.30 \quad \text{(Land, 1983)}$$

$$10^3 \ln \alpha_{calcite-water} = 2.78\left(10^6/T^2\right) - 2.89 \quad \text{(O'Neil et al., 1969)}$$

$$10^3 \ln \alpha_{azurite-water} = 2.67\left(10^6/T^2\right) + 4.75 \quad \text{(Melchiorre et al., 2000)}$$

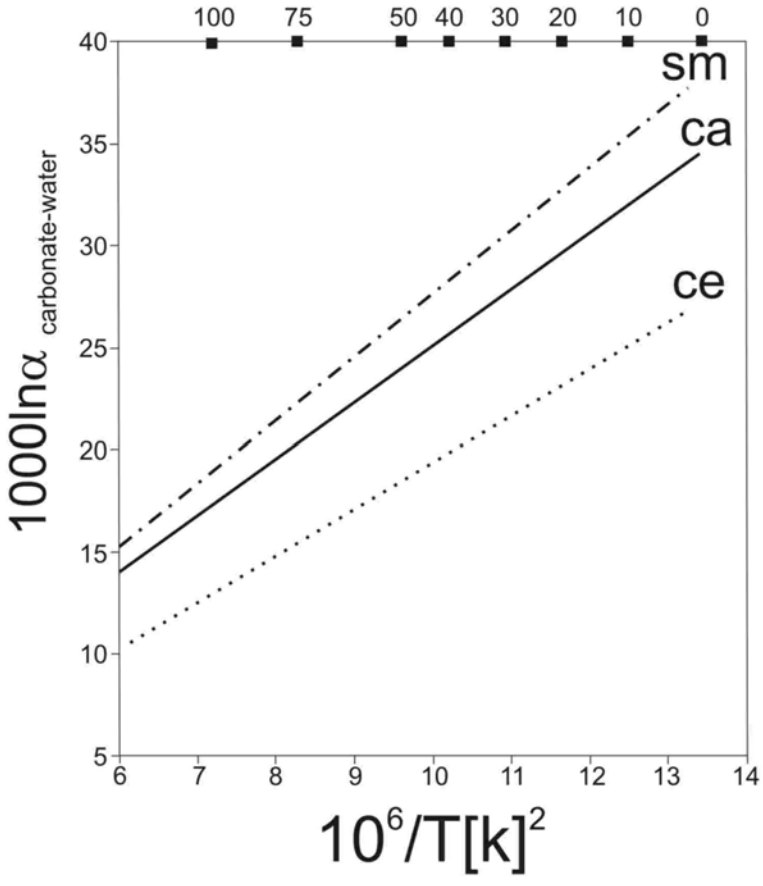

Figure 3.1: Oxygen isotope fractionation between carbonate and water based on the new equations reported in Gilg et al. (2007).

The $\delta^{13}C$ values of carbonates are strictly related to the carbon isotopic composition of CO_2 dissolved in the fluid from which the mineral precipitated. Thus, the $\delta^{13}C$ ratio can be used to individuate the carbon source/s of carbonate minerals. The carbon isotopic composition of carbonates could be an helpful tool to constrain the origin of CO_2 dissolved in the oxidized fluids, for instance atmospheric CO_2, organic CO_2 derived from decomposition of the plants in the soils or CO_2 from carbonate wall rock.

I have applied stable isotope geochemistry (Carbon and Oxygen) to several Zn, Pb and Cu carbonates (smithsonite, cerussite, azurite), as well as to gangue and host rock carbonates (calcite, dolomite, aragonite) from the three mining district examined in the present work. A number of Ca-carbonate crystals and concretions that were paragenetically associated or post-nonsulphide ores were also measured, in order to compare their stable isotopic ratios with those of the economic carbonates. The stable isotopic data on Belgian nonsulphide ores have been already published in Coppola et al. (2007).

Stable oxygen and carbon isotope ratios of 96 carbonates were determined using an automated on-line device (Finnigan Gasbench II), operated in a continuous flow mode attached to a Finnigan Deltaplus mass spectrometer at the Bayerische Staatssammlung für Paläontologie, Munich, Germany, or a Finningan DeltaS mass spectrometer at the Ruhr Universität, Bochum, Germany. The purity of handpicked samples was checked by XRD. Ancillary calcite in smithsonite-dominated samples was removed using a mild dilute hydrochloric acid treatment before isotopic analysis. All carbonate samples were reacted with anhydrous phosphoric acid at 72°C for 1.5h. Oxygen isotope analyses were corrected using the following phosphoric acid fractionation factors for calcite (1.00864, Swart et al., 1991), dolomite (1.00986, Rosenbaum & Sheppard, 1986), cerussite (1.00919, Gilg et al., 2003), smithsonite (1.00962, Gilg et al., 2003) and azurite (1.01024, Swart et al., 1991). The precision of analyses based on repeated measurements of laboratory and international standards is about 0.1‰ (1σ). The isotopic compositions are reported as δ-values in per mil. The O isotope compositions of minerals were expressed relative to the VSMOW (Vienna Standard Mean Oceanic Water) international standard and C isotope composition were expressed relative to the VPDB international standard, isotope ratio of a belemnite (*Belemnitella americana*) from the Cretaceous Pee Dee Formation of South Carolina. All the isotopic analyses have been performed by H.A. Gilg.

3.2.8 Thermometric analysis of fluid inclusions

When a crystal grows in the presence of a fluid phase, some of the fluids may be trapped as

imperfections in the growing crystal to form fluid inclusions (FIs), sealing small droplets of mother fluid. More inclusions can be also trapped in the host minerals after their formation. Different phases may be trapped in inclusions, therefore a distinction of FIs is based on number and types of phases present in the inclusions: (1) *monophase inclusion* with an homogenous fluid (liquid or vapor); (2) *two-phase inclusion*, coexistence of two different fluids (liquid and vapor) and one of them is dominant (L-rich and V-rich); (3) *multiphase inclusion* with a liquid, vapor and one or more solid phase (daughter minerals) precipitated during cooling of high-salinity inclusions; (4) *inclusion with immiscible phases*.

The most useful classification of fluid inclusions are based on genetic criteria and related to the timing of formation of inclusions relative to that of the host mineral (Roedder, 1984; Bodnar, 2003). Thus, *primary fluid inclusions* are formed during the growth of the surrounding host crystal, *secondary fluid inclusions* are inclusions formed in a later stage from a crack-healing mechanism, *pseudosecondary fluid inclusions* are trapped when fracturing occurs during crystal growth. When the petrographic relationships of inclusions with their host minerals are unclear, they are named *indeterminate fluid inclusions*. A group of fluid inclusions that were all trapped at the same time is named: Fluid Inclusion Assemblage (FIA) (Goldstein & Reynolds, 1994).

The study of FIs gives important clues for understanding the geologic and thermodynamic conditions, and the temperature, pressure, density and composition of the fluids which precipitated or re-equilibrated with the mineral phases. The techniques of FI study and their applications in Earth Sciences are exhaustively discussed in Roedder (1984), Goldstein & Reynolds (1994) and Samson et al., (2003). The principle of FI microthermometry is based on phase changes, which occur when heating and cooling FIs during experimental work. Microthermometry of FIs allows to measure some of the above cited parameters (temperature, density and composition).

The temperature at which the fluid was occluded in the host crystal is called trapping temperature (T_t) and represents the precipitation temperature of the host mineral. Fluids trapped under elevated pressure and temperature may develop a gas bubble when they approach surface conditions (*two-phase* FIs). During heating runs of these FIs the homogenization temperature (T_h), i.e. the temperature at which gas and liquid phases homogenize, can be measured. The homogenization may occur into the gas or the liquid state. However, T_h represents the minimum T_t of the FIs and gives an indication of the bulk fluid density. A pressure correction (P_c) is needed ($T_t = T_h + P_c$) because pressure acting on host mineral may be higher than vapor pressure of the fluid during formation.

When *two-phase* aqueous FIs are frozen and then heated again, phase changes occur: we can

measure the following temperatures: eutectic temperature (T_e), coexistence of liquid and ice, and final melting temperature (T_m final), at which the solid phases completely melt. In high salinity fluid inclusions (salinity > eutectic salinity) intermediate hydrated compounds may appear. In this case (T_m final), may correspond to melting of salt hydrate (T_m hy), and also intermediate peritectic temperature may be measured. T_e and T_m are features of a system, therefore they are used to identify compounds of trapped solution. Due to metastability phenomena, both T_e and T_m generally may occur at temperatures different from those in accord with theoretical values, this leading to a wrong interpretation of data. Due to the complexity of natural solutions and the paucity of PVTX data to interpret these more complex compositions, the microthermometric data are interpreted in simple system as H_2O, H_2O+NaCl, H_2O+NaCl+$CaCl_2$.

Each thermometric study on FIs must be preceded by a petrographic observation to detect the different FIAs. Moreover, the reliability of measures is based on the assumption that FI have been kept in a closed system since trapping, but external phenomena (stretching, leakage, necking-down) may have produced exchange with external environment. These inclusions have to be avoided for microthermometric measures.

10 thin sections (100-200μm) and single crystals were prepared for FIs analyses. Sample preparation was conducted with extreme care and with cold techniques in order to avoid stretching and leakage.

Microthermometric analytical measurements on fluid inclusions have been carried out at the Dipartimento di Scienze della Terra of the University of Napoli Federico II, using a Linkam TH 600 stage. The stage was calibrated using synthetic fluid inclusions (Bodnar & Sterner 1987), its precision is ± 1°C in the temperature range of interest. Samples were positioned in a chamber with an upper window, and controlled with an X-Y manipulator. Observation were carried out also with a camera on microscope and connected to a computer. Leaked inclusions were avoided for thermometric measures or discarded when leakage was produced during experiment (increase in bubble size). In order to minimize the risk of inducing stretching and/or leakage, inclusions were heated and cooled slowly (5°C/min) to further slow down (1°C/min) in the last phases of the experiment.

Chapter 4: Nonsulphide Zn deposits in the Namur-Verviers Synclinorium, NE Belgium

4.1 Introduction

Eastern Belgium, together with Upper Silesia in Poland and the Iglesias area in SW Sardinia, were the three most important mining districts in Europe for the production of the "calamine" ores. Especially the Liège district, situated in the Namur-Verviers Synclinorium (north-eastern Belgium) has represented one of the most important mining districts in the European history of metal exploitation. The metals were continuously exploited here since the Roman age, through the Middle Age and until last century. The exploited metals were Pb, Ag and finally Zn. Over 1.5Mt of zinc metal have been produced from the Belgian zinc deposits (sulphides and nonsulphides) over the last two centuries. The largest deposit, "La Calamine" ("Kelmis" in german), also named Moresnet, Altenberg, Grande Montagne and Vieille Montagne (Timmerhans, 1905), situated at ± 30km ENE of Liège, was one of the first resources of nonsulphide zinc to be developed. The production at La Calamine exceeded 600,000 tonnes of zinc metal and reached perhaps 760,000 tonnes (this uncertainty is due to the lack of production statistics before 1825). When the mine was still in operation, the concentrates were essentially made up of only Zn nonsulphide ore at 33 – 47% (tab. 1.1).

Other relatively important nonsulphides Zn resources were exploited up until the first half of the 20th century in the oxidation zones of the Fossey, Schmalgraf, Engis, Rocheux-Oneux, Theux, Welkenraedt and other smaller sulphide deposits, all concentrated in the NE of the country. At Fossey, a mine which was active until 1918, the total production of nonsulphides ranged around 485,000 tons with an ore grade of between 35 and 60% Zn. The smaller mines of Dickenbusch, Pandour, Heggelsbruck and Saint Paul were included in the Welkenraedt mining property.

The Belgian deposits, as well as most of the other European nonsulphide zinc deposits, hosted mainly in carbonate rocks and consisting largely of smithsonite-hemimorphite-hydrozincite, have been considered so far to be supergene in the sense of Hitzman et al. (2003) (Dejonghe & Boni, 2005). However, the ore exploited in the historically important "La Calamine" deposit in

Belgium, hosted in Upper Palaeozoic carbonates, contained up to 40% of the Zn silicate willemite (Dejonghe and Jans, 1983), that was discovered here by M. Levy and named after Willem I of Orange-Nassau, King of Holland (Levy, 1843). With few exceptions, the occurrence of willemite-rich ores has been recently considered (Brugger et al., 2003; Hitzman et al., 2003) as a proof of hydrothermal origin: this poses a genetic problem for the Belgian "calamines".
In this chapter I will provide a petrographical, mineralogical and geochemical characterization of the Belgian nonsulphide Zn-Pb ores, that could help in clarifying the genetical interpretation of the mineralisation process and its timing. Particular attention will be given to the discussion of the nature and possible origin of the willemite ores.
Most of the concepts treated in the following chapters are not very dissimilar from those discussed in a paper recently published by Ore Geology Reviews (Coppola et al., 2007).

4.2 Geological setting of the Namur-Verviers Synclinorium

Geology is dominated in Belgium by sedimentary rocks. Igneous rocks are very rare and of small areal extent. Three main geological units can be distinguished (fig. 4.1):

- a basement, made up of Cambrian Ordovician and Silurian rocks. The basement crops out in the Stavelot, Rocroi, Givonne, Serpont, Brabant and Condroz Massifs;
- an older cover, made up of Devonian and Carboniferous rocks. This sequence crops out in the Namur, Versiers and Neufchâteau-Eifel Synclinoria as well as in the Dinant and Ardenne Anticlinoria.
- a post-Hercynian cover, consisting of rocks whose ages range from Permian to Recent. This younger cover is found in the northern part of country (approximately to the north of the line joining Mons, Namur and Liège) and in the extreme south (Belgian Lorraine).

The Lower Palaeozoic basement underwent a first deformation during the Caledonian and was deformed again during the Hercynian orogeny, together with the post-Caledonian cover. The main Hercynian phase (Asturian phase) started at the end of the Westphalian (Upper Carboniferous) during which a large nappe, called Dinant Synclinorium (or, more generally, Ardenne Nappe), overthrust the Namur Synclinorium northward along a set of east-trending faults (fig. 4.1). These faults have different names from West to East: Midi, Eifel and Aachen.
In this area, the geological records of the period spanning from Permian to Late Cretaceous are not well documented because of the scarcity of well-preserved sections of that age. However, it is generally admitted that sub-horizontal Permian sediments were deposited and then removed by

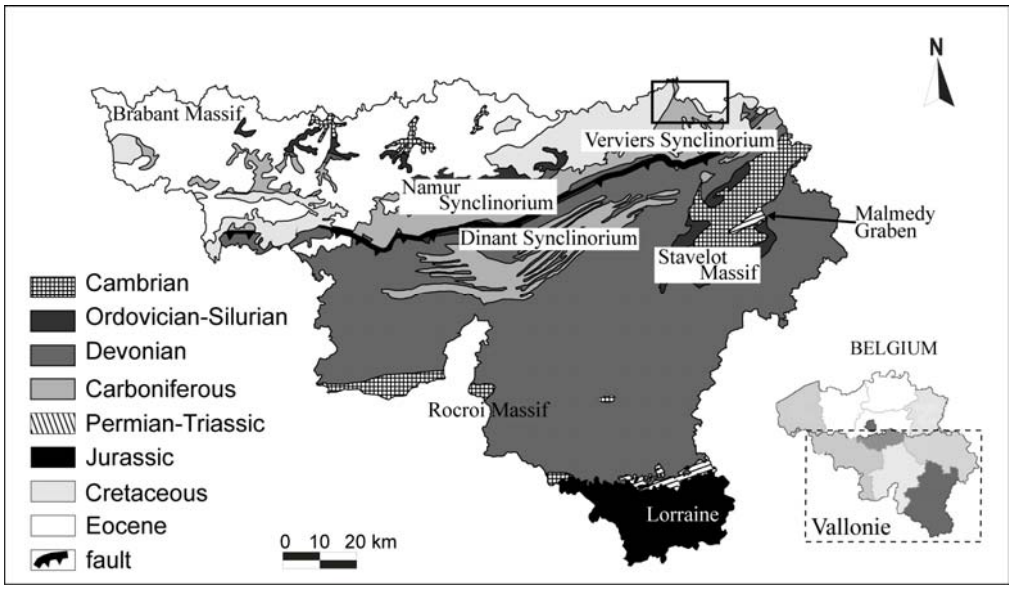

Figure 4.1: Geological sketch map of the Vallonie region in Belgium. In the square the location of the mineralized district depicted in fig. 4.2. (after Coppola et al. 2007).

erosion during later uplifts. According to Vercautere & Van den Haute (1993), on the base of apatite fission-tracks, approximately 3km of Permo-Carboniferous sediments were removed after the Middle Jurassic on the Brabant Massif. Possible relicts of Permian age may be represented by conglomerates preserved as infilling in the Malmédy Graben (fig. 4.1), though this idea has never been confirmed nor rejected (Bultynck et al., 2001). The Malmédy Formation is generally considered to represent fluvio-lacustrine deposits, whose red colour is linked to semi-arid climatic conditions during deposition.

Triassic and Jurassic sediments were either never deposited, or they were deposited only on the eastern side of the Brabant Massif, where they were completely eroded after the uplift related to the Cimmerian phase of the Alpine orogeny. Van den Haute & Vercautere (1990) and Vercautere & Van den Haute (1993) considered that ≅ 3000m of sediments, which covered the Brabant Massif, were removed after Middle Jurassic. In fact, the latter area was certainly emerged from 150 to 100Ma ago, and perhaps even since 250Ma.

The structurally complex Verviers Synclinorium (Graulich et al., 1984) is located between Liège and Aachen. This has been considered as a Hercynian fold-and-thrust unit (Hance et al., 1999), dominated by two systems of faults:

- NE-SW longitudinal faults, linked to the Hercynian overthrusting;
- NNW-SSE transverse faults, linked to the tectonic pulses responsible for the first initiation of the Rhine Graben. These faults, in which most of the primary Zn-Pb vein-type sulphide deposits occur, were reactivated on several occasions during the Mesozoic and Tertiary.

Cretaceous sediments unconformably overlie the folded Palaeozoic rocks. The Cretaceous succession starts with the deposition of the Aachen Formation (Breddin, 1932) of Santonian age (Late Cretaceous). At the base of this formation the Mospert Sands occur, followed by the Hergenrath Clays Member (Breddin et al., 1963), which consists of alternating layers of silty clays and argillaceous sands and silts, with abundant plants debris. These are overlain by the Aachen- and Hauset Sands Members (Albers, 1978), both consisting of shallow-water to continental sandstones. The Aachen Formation is then overlain by the transgressive Vaals Formation (Felder, 1975) of Campanian age, consisting of sandstone, siltstone and clay layers with glauconite. The Gulpen Formation (Upper Campanian to Mastrichtian chalk and calcarenites with chert nodules) overlies the Vaals Formation. Tertiary sediments, consisting mainly of alternating sandy and clayey units, eventually overlie the Gulpen Formation.

The uplift of the Ardenne Massif, due either to lithospheric buckling induced along the front of the developing Alpine orogeny, or driven to plume activity related to the Eifel volcanism (Demoulin, 2003), started in the Upper Oligocene and continues up to the Present. This deformation took the form of a broad bulging accompanied by block faulting along the same direction as the Rhine graben. Since Oligocene time, a maximum of 500m of uplift has occurred throughout Belgium (Demoulin, 1995). In the Ardenne region, the uplift has locally resulted in complete erosion of nearly all the Cretaceous and Tertiary cover.

If the Belgian “calamines” are, at least partly, of supergene origin (Coppola et al., 2007; Dejonghe & Boni, 2005), it become important, to consider the different paleoweathering phases (that in carbonate terrains might be associated with deep karsting), recorded in this part of Europe from the end of Hercynian orogeny throughout Mesozoic and Tertiary until Recent (Boni & Large, 2003; 2005). In fact, some of these phases could have caused the oxidation of primary sulphides in the Verviers Synclinorium and the precipitation of secondary Zn-Fe-Pb minerals in the “calamine” deposits.

Dupuis (1992), Alexandre & Thorez (1995), Demoulin (2003) and Quesnel (2003) pointed out that the Palaeozoic rocks in Belgium were affected during the Permian and Mesozoic (before the Cretaceous transgression) by deep weathering with development of paleosurfaces, as well as by multiple weathering phases during the Tertiary. Among the many paleosurfaces, three of them could be associated with especially strong oxidation phenomena: the post-Hercynian, the pre-Triassic and the pre-Santonian paleosurface.

As mentioned by Laloux et al. (2000), the top of the Palaeozoic rocks is deeply weathered (thickness reduced to 5-30m) to an alterite consisting of varicolored clays in the Verviers Synclinorium. This is overlain by Santonian sediments, which mainly correspond to the Aachen

Formation. Several studies have been performed throughout Belgium (Legrand, 1968; Dupuis, 1992; Dupuis et al., 1996) on the kaolinized post-Hercynian regoliths, developed on Palaeozoic rocks of various ages and composition and covered by Late Cretaceous sediments. In the Transinne quarry (Ardennes), where a supergene kaolinite deposit is presently exploited, this regolith on the Paleozoic surface can reach a maximum thickness of 70 m (Dupuis et al., 1996). The formation of the regolith has been dated by Yans (2003) and two distinct weathering periods have been identified: an Early Cretaceous period (126 ± 10Ma and 135 ± 15Ma, from Berriasian to Barremian) from K-Ar data on two hollandites (ideally $BaMn_8O_{16}$), and an Early Miocene (21.1 ± 0.4Ma) period from Ar-Ar and K-Ar data on cryptomelane (ideally KMn_8O_{16}). Further evidence of Early Cretaceous paleoweathering (120-130Ma) in this part of Europe comes from paleomagnetic dating of a widespread ferricrete occurrence denominated *"Borne de fer*" in Lorraine (Théveniaut et al., 2002).

After the pre-Santonian paleoweathering phases, Tertiary weathering episodes combined with karstic dissolution are recorded in several areas of Belgium, including the Verviers synclinorium. A classic example is given by halloysite accumulations occurring in the Entre-Sambre-et-Meuse and Condroz areas at the bottom of large cryptokarsts (100 to 150m deep), infilled by Oligocene marine sands and Neogene continental deposits (Dupuis, 1992; Dupuis et al., 2003).

During part of the continental periods in the Neogene (mostly Miocene), the percolation of moderately acid fluids induced karstic dissolution of the topmost limestone below the permeable sands. As a result, deep sinkholes developed under the Tertiary cover (cryptokarst or cryptolapiaz). Solutions were buffered at the limestone contact, precipitating alumina gel from which massive halloysite and associated kaolinite crystallized (Ertus et al., 1989). Pleistocene karst is recognized in Paleozoic limestones, in the region of Liege (Quinif & Vandycke 2001).

4.3 Ore deposits in the Liège district

In the Liège Zn-Pb-Ba mining district (NE Belgium) primary zinc-lead sulphides and secondary nonsulphides are the main typology of deposits present. The most productive area for both sulphide and nonsulphide Zn-Pb ores in Belgium was mainly concentrated in about 400 km^2 in the eastern part of the country (Verviers-Namur Synclinorium, Dejonghe et al., 1993). Dinant Synclinorium, in the west, and Ardenne district, in the south, represent the other two important mining area in Belgium, nevertheless here important resources of nonsulphide ore deposits have been never recorded (fig. 4.2). The total Belgian production of concentrates was about 4.1Mt

from sulphide and nonsulphide ores in the period ranging since 1837 until 1936, of which about 2Mt (~50%) came from the Verviers-Synclinorium (data from Dejonghe et al., 1993).

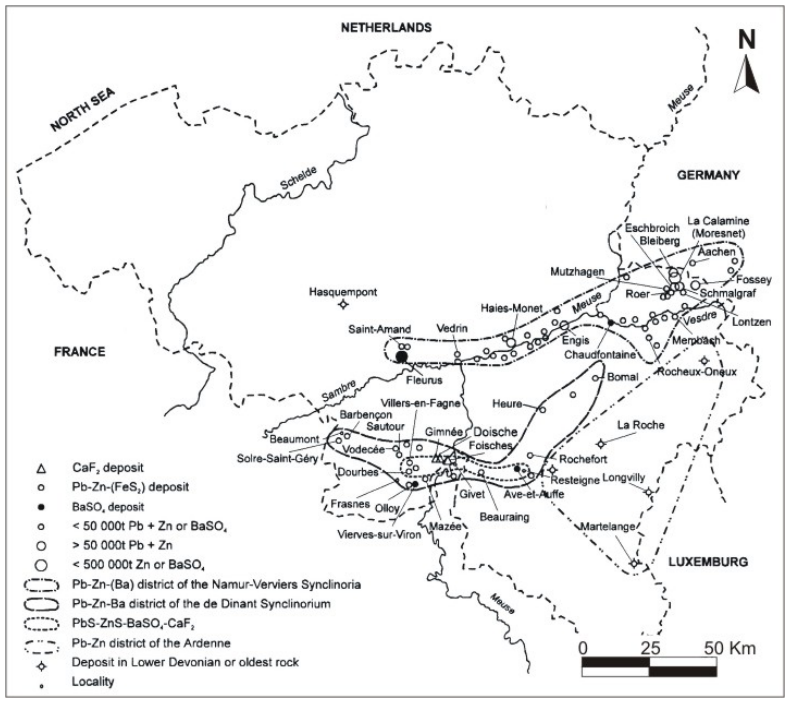

Figure 4.2: The Zn-Pb mining district of Belgium, with the location of the major ore deposits. (after Dejonghe, 1998, modified)

4.3.1 Zn-Pb sulphide ores

The exploitation of Zn-Pb deposits in Belgium dates back to prehistoric times. Its apogee was between 1850 and 1870, but the last mine was closed in 1946. During the period 1837-1945, the tonnage of exploited metals reached about 1.5Mt Pb+Zn with a Zn/Pb ratio of 8-9. A synthesis of the Belgian Zn-Pb deposits was published by Dejonghe (1998) and Dejonghe et al. (1993).

Several base metal ore deposit types may be distinguished, including syndiagenetic bodies, epigenetic vein- and connected flats (or *mantos*), and paleokarstic mineralised infilling. Sulphide mineralogy is quite simple, including sphalerite, galena, and pyrite/marcasite with collomorph structures, often brecciated. Low amounts of Ni and Co are contained in the iron sulphides (Duchesne et al., 1983). Dejonghe (1990) also found gersdorffite (NiAsS) and nickeline (NiAs) in the Bleiberg mine.

Formerly economic Zn-Pb veins occur in Devonian and Carboniferous carbonate rocks along faults, which are transverse to the Hercynian fold axes, though rare veins also occur in siliciclastic rocks of Lower Devonian age or older. The majority of the deposits, including those boasting higher tonnages, are located in the Dinantian carbonate rocks of the Namur-Verviers Synclinorium. Smaller deposits also occur in the Dinant Synclinorium, whereas Zn-Pb deposits

are rare in the Ardenne region, where they have yielded only very small tonnages (Lespineux, 1905; Dejonghe & Jans, 1983). An exception to the general carbonate host rock setting is represented by the Bleiberg lode, the easternmost of all Belgian zinc-lead deposits, which is hosted both in the Visean Limestones and in the Namurian siliciclastics.

In the adjacent ore districts of the Netherlands (Limburg province) (De Wijkerslooth, 1949) and Germany (Aachen district) (Walther, 1984, 1986), where the block-faulting effects are more evident, sulphide lodes frequently cross also the Silesian (= Namurian + Westphalian) siliciclastic rocks.

The majority of the ore traps follows an extensional post-Hercynian fault network parallel to the northern sector of the Rhine tectonic graben (Bartholomé & Gérard, 1976; Dejonghe, 1998). The tonnages of the deposits and the intensity of displacement due to the block-faulting tectonics increased, along a SW-NE trending gradient. Similar Pb-Zn orebodies occur also in the adjacent Aachen area in Germany (Gussone, 1964).

The Belgian Zn-Pb sulphide deposits located in the Namur and Verviers Synclinorium consist of post-Hercynian hydrothermal veins, connected to stratabound "flats" or "mantos" (so-called "*amas*" in French) branching of them. The flats are irregular lens-like, stratabound ore masses, located along sedimentary and/or tectonic discontinuities as well as filling dissolution cavities of variable sizes. The largest flats occur at the top of the Dinantian (Visean) limestones, directly beneath the impervious Namurian pyritiferous black shales (so-called "*ampélites*" in french). Smaller flats occur at the contact between units with different lithological composition, as at the boundary between Tournaisian dolomite and Famennian shales or sandstones. Ores from both the veins and the flats have similar characteristics and often show breccia textures. The genesis of the flats is due to solution of limestone in an evolving hydrothermal system where gas accumulated at the top of the cavities. Precipitation of sulphides took place when gas escaped (de Magnée, 1967; Bartholomé & Gérard, 1976**).** Some of the flats seem to show the form of dissolution cavities, related to subaerial paleokarstic morphology. In fact, Balcon (1981) distinguishes during the Carboniferous two periods of subaerial exposure related to emersion surfaces (intra-Visean and infra-Namurian), which could have acted also later as lithologic discontinuities for ore fluids circulation. Compared to the veins, the flats have yielded by far the largest ore tonnages.

Lead isotopic studies of the primary Belgian sulphides (Cauet & Weis, 1983 and references therein) reveal that the main source of the base metals was in Middle and Upper Devonian sedimentary rocks. Large et al. (1983) mention that the Pb-isotope data of most ore deposits hosted in the Devonian and Triassic rocks in north Eifel and north Sauerland regions in Germany

(including those of the Aachen-Stolberg district) showed the same characteristics as the Belgian ores and a linear tendency. It cannot, however, be excluded, as it was demonstrated in the case of similarly striking veins occurring in the Brilon Riff Complex in west Germany (Schriel, 1954), that several successive hydrothermal pulses could have taken place, in a period ranging from Permian to Lower Cretaceous.

Hydrothermal solutions, whose nature and origin were discussed among others by Heijlen et al. (2000, 2001), precipitated the metals in the veins at temperatures < 180°C (110°C in the Verviers Synclinorium) and pressures of 10^8 Pa (< $2x10^7$ Pa in the Verviers Synclinorium). Fluids salinities are in the range between 10 and 23 eq. wt% NaCl.

The mineralised lodes intersect the Palaeozoic rocks folded during the Hercynian orogeny but do not cross the overlying Upper Cretaceous series (Aachen Formation of Santonian age) (fig. 4.4a). Thus the timing of their emplacement is technically constrained between the end of the Hercynian orogeny (± 295Ma) and the beginning of the Upper Cretaceous (± 100Ma). After de Magnée (1967), Dejonghe (1998) and Heijlen et al. (2001), the main hydrothermal mineralising event in the Verviers district should date back to the end of the Jurassic (~150Ma). In fact, the sulphide ores of the Verviers synclinale are structurally comparable to the Zn-Pb deposits of Maubach-Mechernich in Germany, hosted in Triassic sandstones, some tens of kilometres to the southeast, and have possibly been formed at the same time. Direct sphalerite Rb-Sr dating of the Maubach deposit yielded a Middle Jurassic age of 170 ± 4Ma (Schneider et al., 1999).

4.3.2 Nonsulphide Zn ores

Nonsulphide Zn ore deposits represent the other important kind of deposits present in the Namur-Verviers Synclinorium. They are considered to be the result of paleoweathering processes, which modified primary sulphide deposits. The supergene weathering of the sulphide deposits could have taken place at several intervals between the Late Mesozoic and the present day. *Gossan*s representing the oxidation products of Zn, Fe and Pb sulphides exploited in the Belgian mineralised districts, occurred not only on top of the primary ores, but they also represent the infill of deeper karstic cavities in Paleozoic carbonates (Lespineux, 1905; Timmerhans, 1905; Dejonghe et al., 1993). Usually, oxidation of sulphides generally extends from the surface to an average of 40 to 50m in depth, though weathered profiles are also recognized at major depth. In fact, in several mines, Zn-carbonates as well as pockets of cerussite were also found irregularly enclosed in the primary sulphide bodies down to 120m in depth. The maximum reported depth of oxidation is 211m at the Schmalgraf mine.

Belgian "calamines" include different mineralogical assemblage, as a mixture of Zn-carbonate {smithsonite = $ZnCO_3$} and Zn-silicate {hemimorphite = $Zn_4(Si_2O_7)(OH)_2.H_2O$}, or the assemblage of hemimorphite, smithsonite, hydrozincite {$Zn_5(CO_3)_2$ $(OH)_6$} or willemite {Zn_2 SiO_4}, locally associated with Fe-(oxi)hydroxides and clays. Pb- and Fe- secondary minerals were always associated to the Zn ores. Belgian "calamine" ore was grey, yellow or even black in color and occurred as dense rock masses or with concretionary, foliated or stalactitic shapes (Dejonghe & Boni, 2005). The mineral aggregates were microcrystalline ("amorphous" in the old literature) or coarse-grained, but also displayed brecciated or vuggy textures. The shape of the nonsulphide concentrations ranged from bulk replacement bodies of entire blocks of the host carbonates and/or sulphides, to the concretionary infilling of isolated druses with idiomorphic smithsonite and hemimorphite crystals and cavities at different levels in the upper part of the oxidation zone.

The large La Calamine orebody was located in a narrow syncline, dipping about 15° to the SW, made up of Famennian sandstones and shales overlain by Tournaisian dolomites and dolomitic shales (Dejonghe & Jans, 1983). It formed a large lenticular pocket, located in the core of the syncline (fig. 4.3a). The economic nonsulphide concentrations overlaid the Famennian siliciclastic sediments, as well as the layer of silicified dolomite at the bottom. The deposit had the shape of a sinkhole infill, extending for a length of 450 to 500m and a width of 65 to 100m, reaching 110m in its deepest part. The orebody is located on a SW-NE thrust fault (the Schmalgraf Fault, at the front of the Donnerkaul tectonic unit) (Laloux et al., 2000; Ghysel et al., 2000). Detailed sections of La Calamine, redrawn from the old mining documents have been published in Dejonghe (1998) and Boni & Large (2003). Only traces of sulphides (galena, sphalerite, pyrite, marcasite, greenockite) occurred along the walls of the La Calamine pit (Dejonghe et al., 1983). Most of these sulphides were possibly supergene in origin. The zinciferous nonsulphides, associated with abundant Fe-(hydr)oxides, were concentrated as irregular bodies hosted in mottled Zn-clays. The ore assemblage at La Calamine ranged from dominantly Zn-carbonates at the near surface, to a mixture of Zn-carbonates and Zn-silicates with increasing depth, and a silicate assemblage (willemite and Zn-clays) below -80/85m in depth (fig. 4.3b) (Dejonghe & Boni, 2005). In the old literature (de Launay, 1913), huge willemite blocks have been often described to occur in the lowermost parts of the deposit, surrounded by Fe-hydroxides, smithsonite and hemimorphite. The latter minerals were also cementing collapse breccias containing broken willemite clasts of variable size. In the open pit a few cavities have been encountered, filled with siliciclastic sediments comparable to the Aachen Fm. sandstones (Dejonghe et al., 1993).

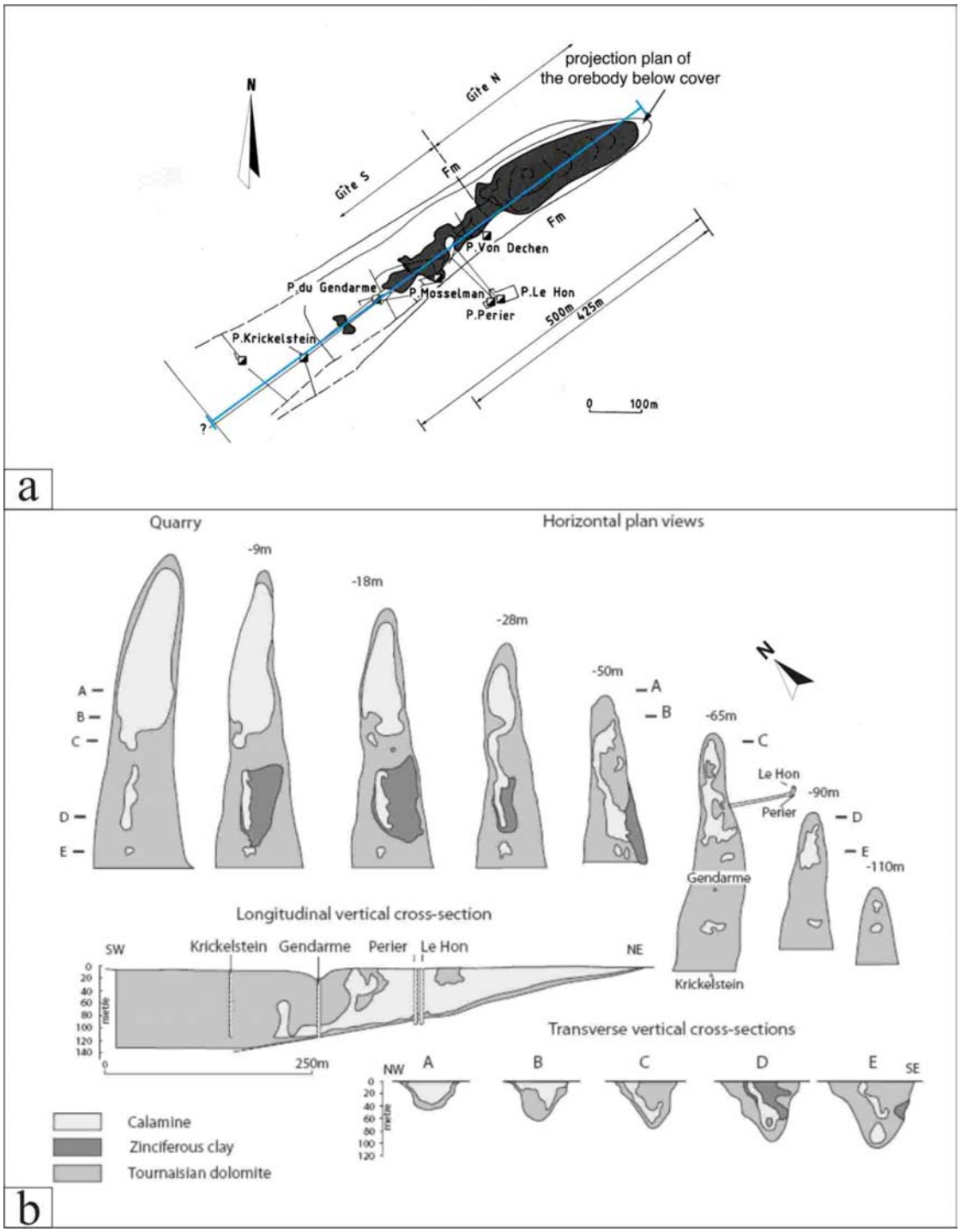

Figure 4.3: La Calamine ore deposit. a) a projection map of the La Calamine deposit below recent cover, the blue line represents approximately the longitudinal cross section shown in fig. 4.3b (after Dejonghe et al. 1993); b) cross-section and plan view of the main mining levels (with prevailing mineral content) at La Calamine (after Dejonghe & Jans, 1983, modified).

The mineralogy of the other, less important nonsulphides Zn resources at the oxidation zone of Fossey, Schmalgraf, Engis, Dickenbusch, Mützhagen, Rocheux-Oneux and Welkenraedt mines

in the NE of the country, was variable. They contained a combination of Zn-carbonates and silicates, with willemite as a common, albeit minor, component. In addition, variable amounts of Pb- and Fe-minerals were always present. At Fossey, a mine that was active until 1918, both sulphides and nonsulphide ores were exploited. In the Welkenraedt mining property the mineralisation (also comprising both sulphides and calamines) was controlled by the NW-SE oriented Welkenraedt fault and other parallel lineaments cutting NE-SW trending Hercynian structures. The calamines, including a significant amount of Pb-carbonates, could be traced to a depth of about 50m below the surface. The oxidation products and host rocks, locally comprising pockets of unweathered sulphides, are covered throughout the entire district by at least 10 m of horizontal sediments of the Aachen Formation (fig. 4.4). In the small permit of Theux, exploited until 1925, the main ore consisted of Zn and Pb-carbonates, with abundant Fe- and Mn-(hydr-) oxides (Mélon et al., 1976). Abundant hemimorphite was recorded in Theux, whereas willemite occurred only episodically.

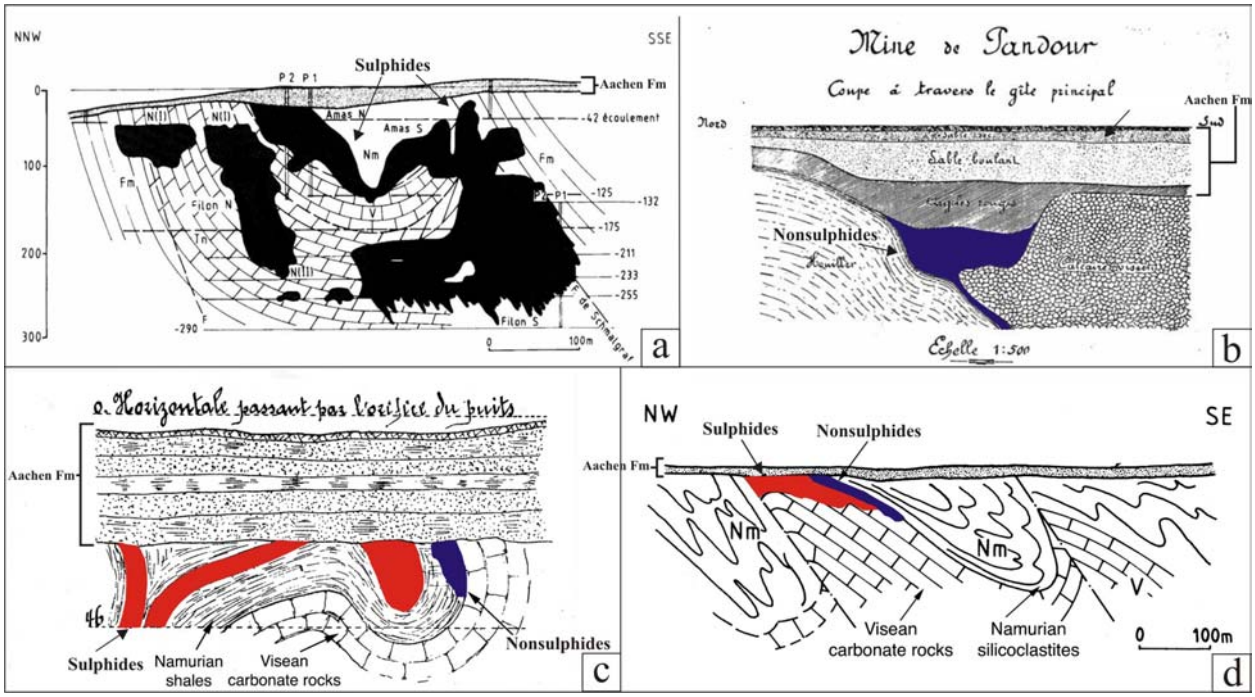

Figure 4.4: a) NNW–SSE vertical cross-section of the Schmalgraf ore deposit (from Dejonghe & Jans, 1983); b) old cross-section of Pandour mine (from Lespineux 1905, modified); c) schematic cross-section of the Mützhagen orebodies (from Lespineux 1905, modified); d) schematic cross-section of the small Dickenbusch orebody (from Dejonghe et al. 1993, modified). Note: red = sulphide orebodies, blue = nonsulphide orebodies.

4.4 Mineralogy of the nonsulphide ores

The common mineralogical phases of the nonsulphide ores in the NE Belgian mining district are smithsonite, willemite, hemimorphite and sauconite (tab. 4.1; figs. 4.5, 4.6 and 4.7). Minor hydrozincite is present, as well as remnants of primary sulphides. Calcite was often observed, both as gangue mineral, which precipitated with the primary sulphides, and as a newly formed phase associated with smithsonite. Idiomorphic quartz crystals, as well as spherules of chalcedony occur as one of the last generations, together with transparent hemimorphite laths (fig. 4.6f). Fe- and Mn-(hydr)oxides and small kaolinite agglomerates are also very common. Nonsulphide minerals from Belgium have been investigated previously by several authors (Levy, 1843; Cesàro, 1886, 1887, 1898, 1908; Servigne, 1943; Mélon et al., 1976), particular attention being devoted to willemite**.** However, with the exception of de Launay (1913), almost no paragenetic studies of the nonsulphide associations that could be applied to a genetic interpretation have been carried out.

4.4.1 Willemite

Willemite (Zn_2SiO_4) has been detected in all nonsulphide deposits in Belgium, but it was especially common at La Calamine, even if this phase was often individuated in specimens from the Welkeraedt and Fossey mines. De Launay (1913) noted the preponderance of microcrystalline willemite over smithsonite in the lower levels of the La Calamine mine. Locally, traces of incompletely replaced sulphides are intergrown with willemite (figs. 4.5b, 4.6a). Our observations, both at the stereoscopic microscope and on SEM, have shown at least two distinct forms of willemite agglomerates: a) masses of clear, idiomorphic hexagonal, mm-sized crystals with prismatic terminations (figs. 4.6b, 4.8a) (Cesàro, 1886, 1887); and b) brownish massive concretions with minute botryoidal terminations (rhombohedral) in druses and radial concretions (figs. 4.5c, 4.6c,d). Microcrystalline, massive willemite also cements a reddish-brown mottled breccia, showing evidence of mechanical reworking and chemical dissolution of a possible paleokarst infill (Fossey mine) (fig. 4.5d).

The prismatic idiomorphic hexagonal crystals can reach up to 1 mm in length (fig. 4.6b) and their terminations are well observed in open cavities. This morphology has been recorded in the specimens of La Calamine and Welkenraedt, where the crystals are often fragmented, partly dissolved on the external side and cemented by later carbonate phases (fig. 4.6e). The brownish rounded concretions, consisting of masses of elongated hexagonal crystals emanating from the

Table 4.1: XRD analyses of the samples from the Liège district (NW Belgium); mineral symbols are in order of abundance (from Coppola et al. 2007).

	Sample	Mineral(s)
LaCalamine	RN1996	sm, cc, qz
(Moresnet)	RN2005	sm, will, hem, cc,
	RN2008	hem, sm,cc,will
	RN2017	sm
	RN2044	sm, hem, cc
	RN2051	sm, hem, cc
	RN2101	sm, hem
	RN2172	sm, cc, qz
	RN2487	hem, sm, cc, qz
	RN3403	qz
	RN3834	will, sm
	RN4106	Fe-sm, qz
	RN5011	will
	RA4999	sm, cc
	RA5004	will, sph, ga, py
	RA5012	will
	RA5013	will, sa
LaCalamine	RA5014	sm, cc, qz
(Moresnet)	RA6555	hem, sm, cc, will, sa
	RA6661	will
	R2B33	qz, sm, cc
	R2B34/2624	sm, will, cc
	R2B35/3925	sm
	Museo Napoli	will
Fossey	RN2208	sm, cc, qz, Fe-sm, cl
	RN2298	hem, sm, do, Fe-sm
	RN2300	sm, will, sa
	RN2301	sm, hem
Welkenraedt	RN2220	sm
	RN2224	hem,will,sm
	RN2236	sm, cc
	RN2242	sm, cc
	RA4986	sm, cc, qz
Theux	RN2270	sm, cc

*Abbreviations: cc = calcite, cl = clay minerals, do = dolomite, ga = galena, go = goethite, hem= hemimorphite, py = pyrite, sa = sauconite, sm = smithsonite, sph = sphalerite, will = willemite

centres of numerous minute spheres, have a diameter of about 800µm. Remnants of hexagonal willemite crystals form the nucleus of the spheres (fig. 4.8c). These concretions have only been observed in specimens from La Calamine.

From the results of X-ray analysis, the cell parameters of the Belgian willemites are no perfectly in agreement with the literature data (Simonov et al., 1970; Marumo & Syono, 1971; Klaska et al., 1978; McMurdie et al., 1986). Indeed our analyses reveal higher values of crystallographic parameters. They are: *a* from 13.945(3) to 14.019(1)Å and *c* from 9.302(2) to 9.324(7)Å with a ratio *a:c* constrained from 1.497 to 1.506 (tab. 4.2). No systematic variations were observed

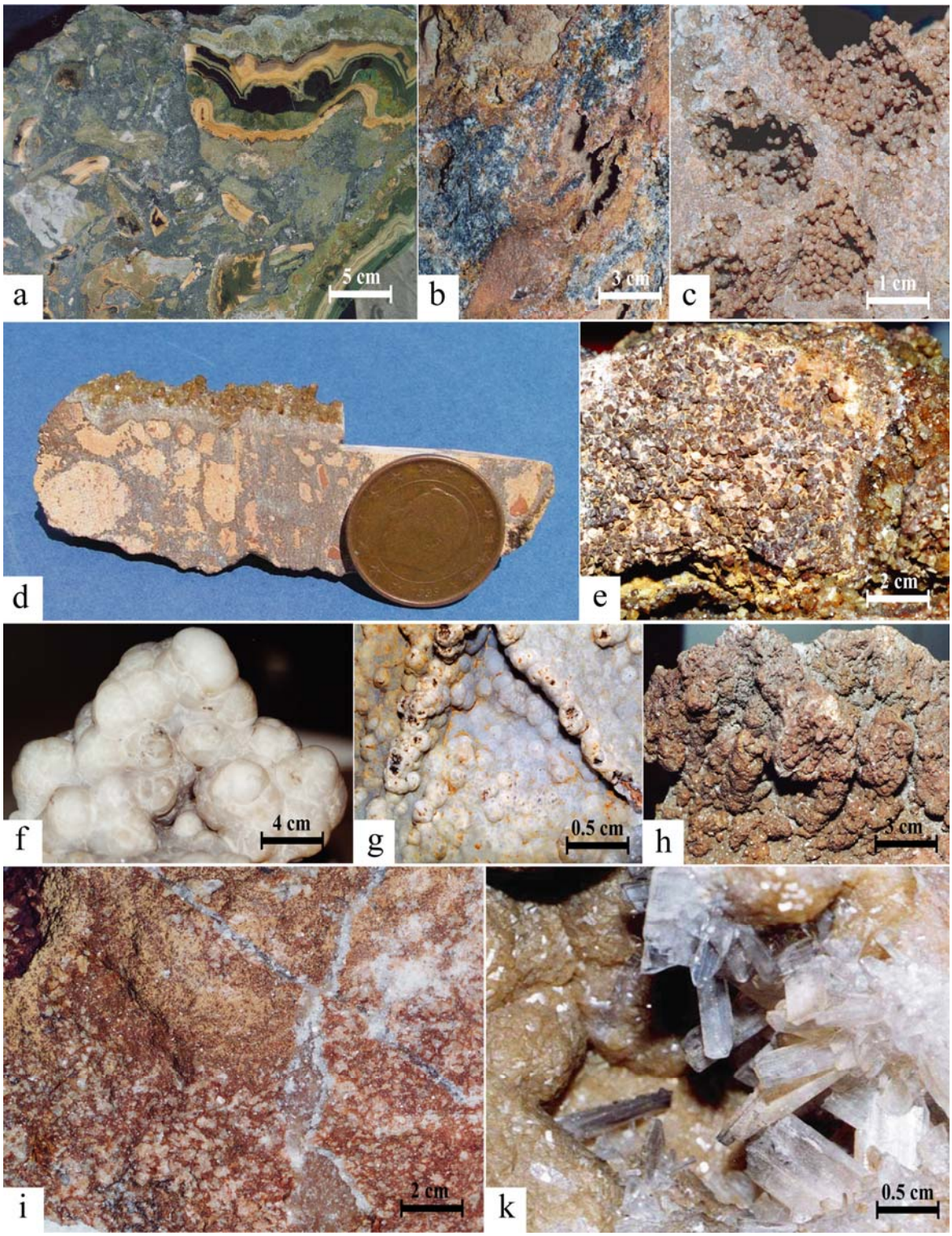

Figure 4.5: Typical ore samples from the Verviers-Synclinorium mining district. a) Primary sulphide breccia ore: zoned collomorph sphalerite fragments with minor galena are cemented by a microcrystalline sulphide assemblage, La Calamine deposit (Mineralogical Museum, La Calamine); b) sphalerite bands (dark) partly replaced by microcrystalline willemite (red-brown), La Calamine deposit (RN3861 Coll. Buttgenbach 1916); c) reddish spherical crystalline aggregates of willemite in cavity, La Calamine deposit (RN3856, Coll. Buttgenbach 1916); d) dissolution breccia, with clasts consisting of hemimorphite cemented by reddish microcrystalline willemite and late smithsonite growing on them, La Calamine deposit (RN2140); e) crust made of honey-colored rhombohedral (Type I) smithsonite crystals, Moresnet (RN3834, Coll. Buttgenbach 1916); f) mammillary microcrystalline smithsonite (Type V) concretions, Welkenraedt deposit (RN4988, Coll. Buttgenbach 1916); g) globular smithsonite (Type V) concretions, La Calamine deposit (RN2280, Coll. De Groote); h) crusts of scalenohedral smithsonite (Type VI) crystals growing on globular willemite, La Calamine deposit (RA5014, Coll. Buttgenbach 1916); i) mottled sample with hemimorphite I (pale) microclasts cemented by brownish smithsonite, La Calamine deposit (RN2051); k) hemimorphite II laths in cavity, Moresnet (RA4790) (from Coppola et al. 2007).

between the cell parameters and the different willemite morphologies.

4.4.2 Smithsonite

Smithsonite has been detected in most Belgian samples (tab. 4.1). Macroscopically, this mineral occurs in several habits. An extensive SEM study, carried out on a large number of smithsonite-bearing specimens, revealed also several types of micromorphologies. These will be compared with micromorphologies recorded in Sardinian (Boni et al., 2003) and Irish (Balassone et al. 2007; this Ph.D thesis) and with Polish (this Ph.D thesis) smithsonite. Type I smithsonite corresponds to rhombohedral, distinctly idiomorphic, and often zoned types, with the best crystals growing on external surfaces or in cavities (figs. 4.5d, e, h). Type I crystals have been observed in specimens sampled from several Belgian mines (RN2003a, RN4106, RN3834). The size of the single rhombohedra (figs. 4.7a, b) ranges from 50 to 600μm. Locally, there is evidence of superficial dissolution on the faces of the rhombohedra, and globular concretions of Fe-(hydr-) oxides occur on these surfaces.

Another, less widespread smithsonite morphological type consists of scalenohedral crystals of various colors from white to yellow, red and grey, that can reach centimetric sizes and are coated by Fe-Mn-hydroxides. Locally these grow on a microcrystalline smithsonite substrate or as infilling of vugs and fractures (fig. 4.7c). This morphology has been observed mainly in the samples from the Fossey mine (RN2301a, RN2208a), but also at La Calamine (RA5014). This type does not occur in Sardinia: it has classified as Type VI.

Concretionary, collomorph structures (figs. 4.5f, g), possibly deposited in open cavities of the vadose zone, or completely replaced internal sediments, are other types of smithsonite morphologies. In the collomorph structures, a polycrystalline aggregate of scalenohedral crystals with sizes smaller than 50μm, oriented along the crystallographic *c* axis, has been called smithsonite Type V. Locally, this type evolves in globular or mammillary forms, observed hanging in the karstic cavities of the vadose zone (similar to that found in Sardinia, Boni et al., 2003). This morphology has been observed in several samples from the Welkenraedt mining area (RN4988, RN2236a, RA4986a) and at La Calamine (RN2101, RN2280).

Fe-rich smithsonite has been identified by SEM-EDS analyses in two samples from the Fossey mine (RN2298, RN2208). It occurs as tabular aggregates with a fibrous appearance (maximum size about 400-500μm), growing between corroded hemimorphite crystals (figs. 4.7e, f). This mineral could correspond to the former so-called "*monheimite*", an intermediate member of the smithsonite-siderite series (Palache et al., 1951; Sitzia, 1965; Bak & Niec, 1978; Bak &

Zabinski, 1981). Cell parameters of this variety of smithsonite show are perfectly comparable with pure smithsonite parameters. The cell parameters of the measured smithsonites vary from *a* 4.651(1) to 4.672(6)Å and *c* between 15.024(8) and 15.175(6)Å (tab. 4.3), and are in quite good agreement with literature data (Effenberger et al., 1981; Chang et al., 1995.) There is no observed direct relationship, however, between the measured cell parameters and the crystal chemistry or morphologies of the Zn-carbonates. The Belgian "*monheimite*" is quite different from the Sardinian one, but also from similar Fe-rich smithsonites occurring in the Irish nonsulphides (Balassone et al. 2007).

4.4.3 Hemimorphite

Hemimorphite, though less important than willemite or smithsonite in the Belgian nonsulphide ores, has been identified by X-ray analysis in several specimens from all the sampled mine sites (tab. 4.1). It appears to have formed in several phases: hemimorphite I occurs in the matrix of supergene breccias (fig. 4.5i) or replaces completely the clasts cemented by a willemite matrix (fig. 4.5d); hemimorphite II forms crystals growing freely in late cavities (fig. 4.5k). Observed in the SEM, hemimorphite occurs with a typical tabular habit along the *b* axis. Hemimorphite occurrences in the late phase of nonsulphide deposits suggest a strong mobility of SiO_2 (Moore, 1972) and a lower buffering capacity of the host carbonates (Hitzman et al., 2003). The occurrence of minute spheres of chalcedony on the hemimorphite laths (fig. 4.6f) also indicates high SiO_2 activity.

The X-day diffraction data for hemimorphite reveals a slight variation of the cell parameters for the different samples (tab. 4.4). Parameter *a* is constrained from 8.345(0) to 8.400(0)Å, *b* from 10.712(6) to 10.768(7)Å and *c* from 5.081(6) to 5.136(1)Å. The values of the parameters reported in literature (McDonald et al., 1967; Cooper et al., 1981; Libowitzky et al., 1997; Boni et al., 2003) are in good agreement with the range values for the hemimorphites analysed here.

4.4.4 Sauconite

Sauconite belongs to the group of trioctahedral smectites with monoclinic symmetry $[(Na_{0,3}Zn_3(Si,Al)_4O_{10}(OH)_2 \cdot 4(H_2O)]$. Sauconite is associated with clayey bodies in most zinciferous ore deposits of Belgium. Together with hemimorphite it has been recognized as one of the components of a mixture of Zn-minerals known as "*vaneuxemite*" (Frondel, 1972). This Zn-clay was identified as "*moresnetite*" by the local miners in the Zn-deposit of Moresnet –

Table 4.2: Main d values (Å) by intensity, unit cell dimensions and volumes of selected willemite samples from the Liège district (NW Belgium)

Sample	d1(I_0)	d2(I/I_0)	d3(I/I_0)	d4(I/I_0)	d5(I/I_0)	a(Å)	±σ	c(Å)	±σ	cell vol(Å^3)	±σ	a:c
RN5011a	2.634	2.833	3.483	2.315	1.858	13.945	0.004	9.314	0.009	1568.401	1.497	1.497
RA5004a	3.490	2.838	2.636	2.319	4.036	14.007	0.012	9.302	0.026	1580.528	4.548	1.506
RA5012a	3.490	2.637	2.837	4.033	2.319	14.004	0.010	9.306	0.022	1580.522	3.837	1.505
RA5012b	3.493	2.642	2.841	4.039	2.320	14.019	0.011	9.306	0.024	1583.983	4.113	1.506
RA6661a	2.636	3.489	2.838	2.319	4.036	13.965	0.004	9.324	0.009	1574.848	1.595	1.498
RA6661b	3.493	2.640	2.841	4.039	7.029	14.013	0.011	9.307	0.024	1582.623	4.054	1.506
A5013a	3.492	2.636	4.034	7.024	2.840	14.005	0.011	9.309	0.023	1581.201	3.994	1.504
A5013b	3.492	2.637	2.839	4.037	2.319	14.001	0.011	9.306	0.023	1579.951	4.067	1.504
Museoa a	3.492	2.838	2.638	2.319	4.040	14.013	0.011	9.302	0.024	1581.826	4.125	1.507
Museo b	2.636	2.838	3.492	1.861	2.319	13.973	0.005	9.322	0.010	1576.350	1.724	1.499

Table 4.3: Main d values (Å) by intensity, unit cell dimensions and volumes of selected smithosonite samples from the Liège district (NW Belgium)

Sample	d1(I_0)	d2(I/I_0)	d3(I/I_0)	d4(I/I_0)	a(Å)	±σ	c(Å)	±σ	cell vol(Å^3)	±σ	a:c
RN1996b	2.753	1.706	3.561	2.331	4.659	0.001	15.058	0.008	283.079	0.177	0.309
RN2044c	2.751	3.560	2.330	1.948	4.662	0.031	15.043	0.024	283.102	0.500	0.310
RN2101c	2.749	1.705	3.554	2.329	4.655	0.001	15.046	0.004	282.358	0.084	0.309
RN2208a	2.751	1.705	3.558	2.111	4.655	0.002	15.051	0.012	282.504	0.248	0.309
RN2220a	2.758	1.708	3.563	1.950	4.657	0.004	15.088	0.028	283.427	0.601	0.309
RN2220b	2.754	1.708	3.562	1.951	4.665	0.006	15.060	0.463	283.810	0.952	0.310
RN2270a	2.758	3.569	1.708	2.332	4.666	0.005	15.087	0.031	284.410	0.662	0.309
RN2300a	2.744	1.702	3.550	1.943	4.651	0.002	15.025	0.012	281.413	0.226	0.310
RN4106	2.755	2.330	3.570	1.707	4.662	0.002	15.073	0.012	283.702	0.255	0.309
RA4999a	2.769	1.716	3.573	2.335	4.672	0.001	15.164	0.007	286.640	0.160	0.308
RA4999b	2.751	3.572	1.716	2.336	4.669	0.002	15.175	0.017	286.554	0.347	0.308
RN2298b*	2.774	3.581	1.786	2.342	4.663	0.015	15.069	0.093	283.689	2.098	0.309

* Fe-smithsonite

Table 4.4: Main d values (by intensity), unit cell dimensions and volumes of selected hemimorphites from the Liège district (NW Belgium).

Sample	d1(I_0)	d2(I/I_0)	d3(I/I_0)	d4(I/I_0)	d5(I/I_0)	a(Å)	±σ	b(Å)	±σ	c(Å)	±σ	cell vol($Å^3$)	±σ
RN2101a	3.105	6.606	3.291	2.402	4.189	8.369	0.004	10.739	0.006	5.118	0.004	460.060	0.386
RN2101c	6.606	3.106	3.297	2.402	5.370	8.373	0.006	10.742	0.008	5.115	0.005	460.077	0.511
RN2224a	3.105	6.603	3.293	2.199	2.402	8.367	0.005	10.736	0.006	5.119	0.004	459.789	0.422
RN2224c	6.602	3.098	3.288	2.198	2.399	8.364	0.006	10.276	0.008	5.114	0.005	458.737	0.508
RN2298a	3.117	6.672	3.306	2.409	5.406	8.418	0.011	10.811	0.015	5.133	0.009	467.126	0.998
RN2298b	6.607	3.106	3.293	2.402	2.200	8.377	0.002	10.743	0.003	5.123	0.002	461.055	0.185
RN2301b	6.609	3.107	3.299	2.200	2.402	8.373	0.006	10.750	0.008	5.128	0.005	461.515	0.050
RN2301a	6.606	3.105	3.297	2.199	2.402	8.370	0.006	10.750	0.087	5.112	0.006	460.249	0.598
RA6555b	6.619	3.106	3.296	2.402	2.200	8.373	0.005	10.744	0.007	5.124	0.004	460.898	0.474
RA6555g	6.606	3.102	3.287	2.199	2.400	8.364	0.005	10.736	0.006	5.117	0.004	459.484	0.4259

Altenberg (La Calamine) and described by Esquevin (1957) as an association of sauconite and fraipontite. In this study, sauconite was analyzed by X-ray powder diffraction on oriented samples, showing the main peak at 14.8Å [the (001) reflection]. After glycolation of oriented samples, the main peak shifted to 17.0Å. Successive heating runs at 250, 350 and 550°C, showed a constant decrease of this peak to 11Å, confirming the smectitic nature of this clay phase (fig. 4.9). Also SEM images show clearly the typical lamellar structures of this class of phyllosilicates.

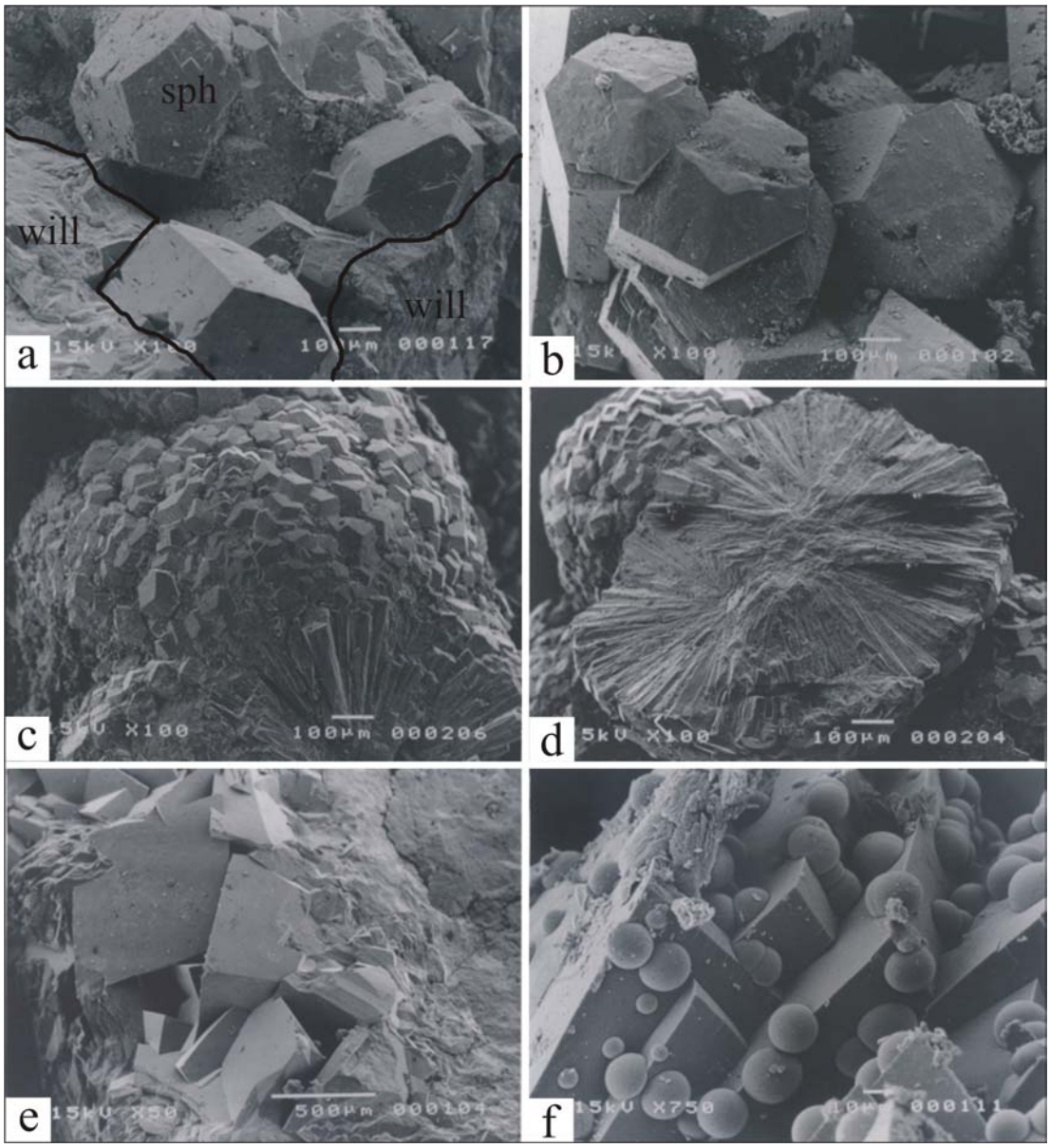

Figure 4.6: Secondary electron images of selected samples of Zn-silicates (willemite and hemimorphite) from Belgian nonsulphide deposits; a) willemite (will) replaces sphalerite (sph) crystals, La Calamine deposit (RA5004); b) hexagonal crystals of willemite in a cavity, La Calamine deposit (Museo Mineralogia Univ. Napoli); c) microcrystalline terminations of willemite spheroids in botryoidal aggregates, La Calamine deposit (A5013a); d) internal structure of the willemite aggregate 3c, La Calamine deposit; e) smithsonite Type I filling a vein in willemite, La Calamine deposit (R2B35/3925); f) aggregate of tabular hemimorphite crystals (type II), covered by opal microspheres, Fossey mine (RN2298).

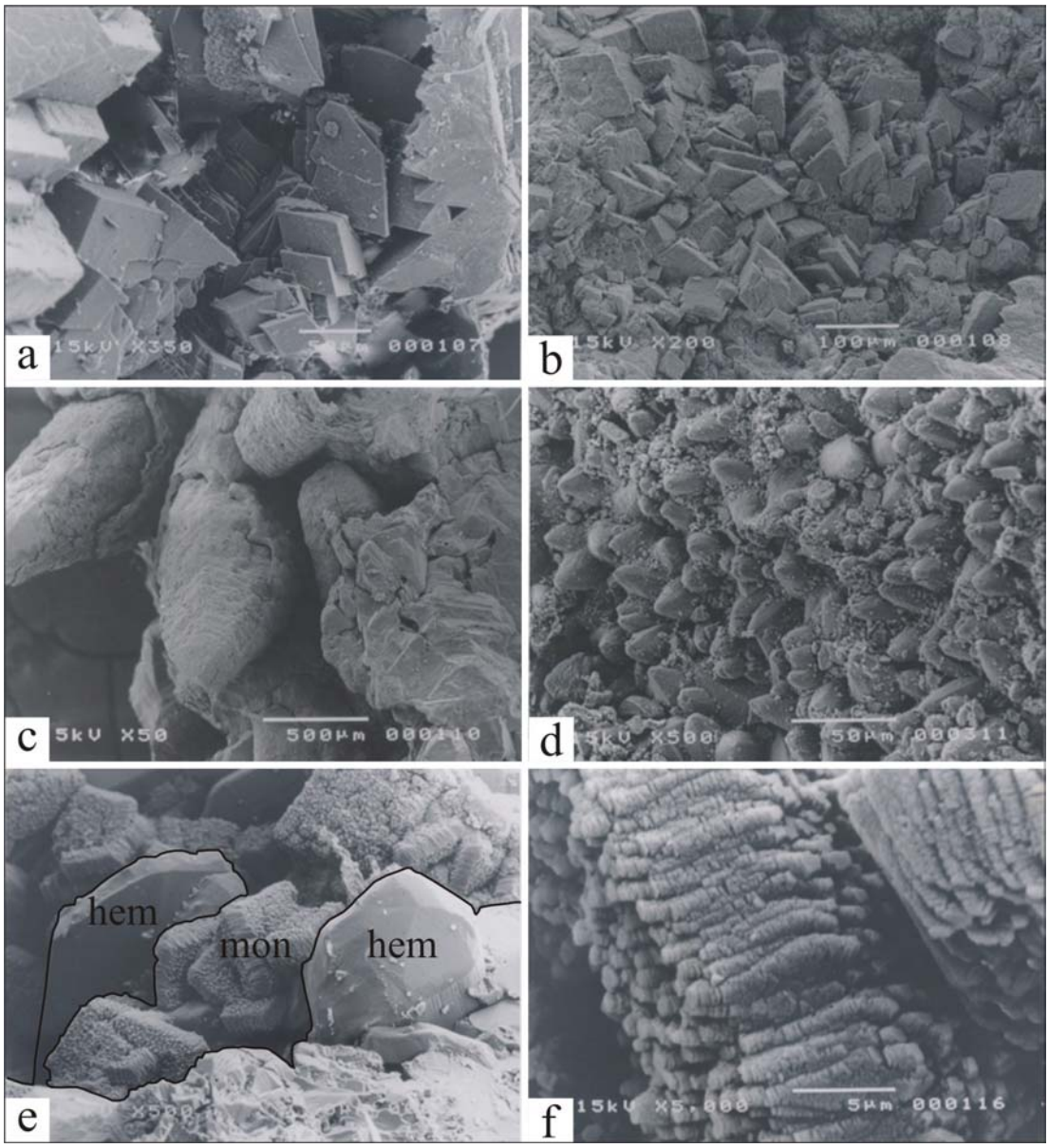

Figure 4.7: Secondary electron images of selected smithsonites from the Belgian nonsulphide deposits. a) cluster of rombohedral smithsonite (Type I) in a cavity, Fossey mine (RN2300a, Coll. Buttgenbach 1916); b) rhombohedral smithsonite (Type I) in a cavity, Moresnet (RN4106); c) scalenohedral smithsonite crystals ((Type VI)) in aggregates, Fossey mine (RN2301a, Coll. Buttgenbach 1916); d) scalenohedral terminations of pseudocolloidal "turkey fat" smithsonite (Type V), Welkenraedt deposit (RN2236a); e) Fe-smithsonite ("monheimite") Type among hemimorphite laths, Fossey mine (RN2298): f) enlargment of Fe-smithsonite crystals from (e).

4.4.5 Other minerals

Other minerals in the mining district include cerussite, anglesite, allophane, aragonite, barite, dolomite, gypsum, pyromorphite, hopeite, fraipontite, kolbeckite, siderite and kaolinite. The minerals hopeite $\{Zn_3(PO_4)_2.4H_2O\}$ (Brewster, 1822, 1824; Levy, 1843) and fraipontite $\{(Zn,Al)_3(Si,Al)_2O_5(OH)_4\}$ (Cesàro, 1886, 1887; Fransolet & Bourguignon, 1975) were described for the first time in samples from La Calamine. Additionally, several types of oxy-hydroxides are present: goethite, hetaerolite, braunite, manganite, hematite and pyrolusite.

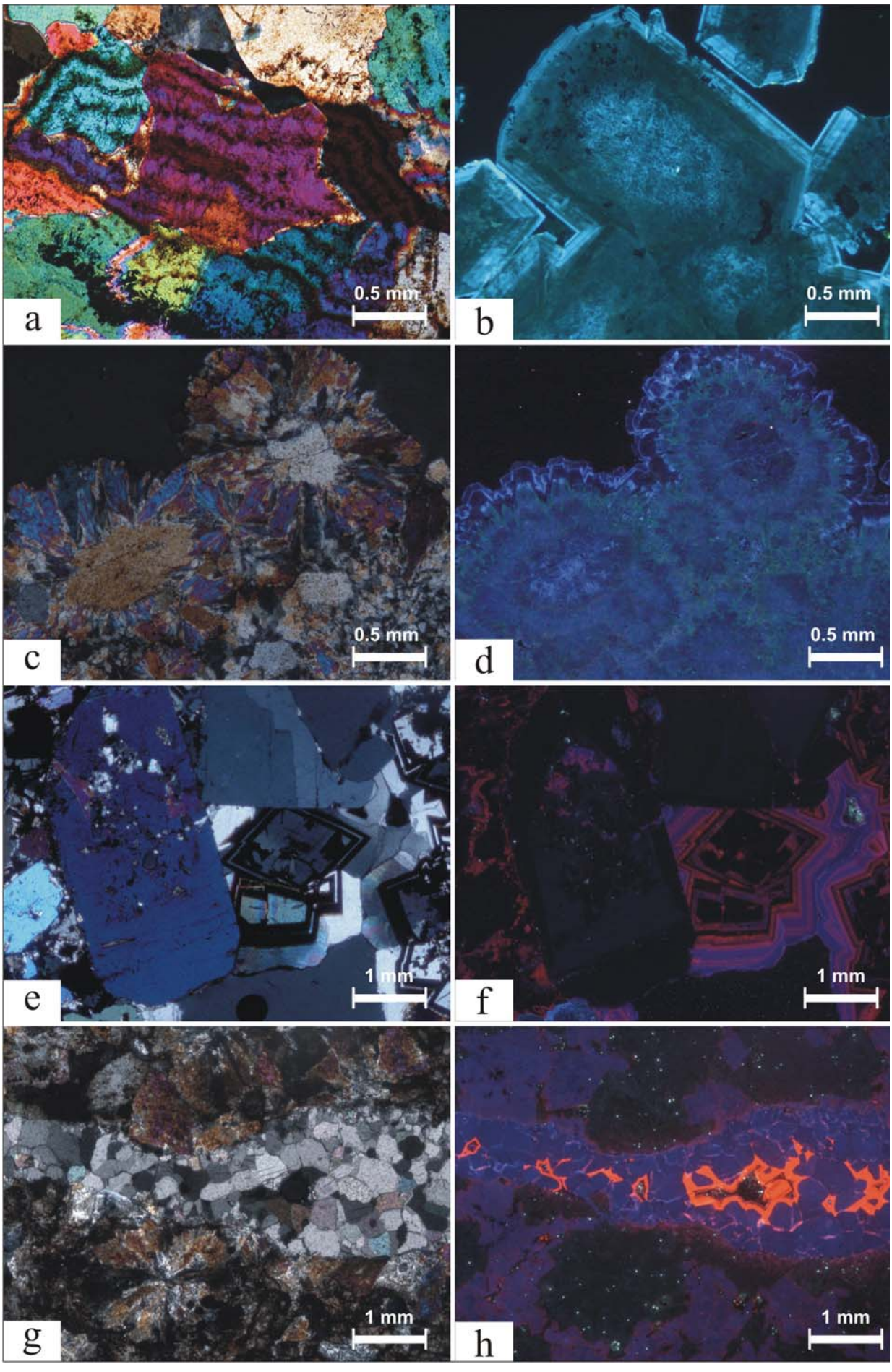
a
0.5 mm
b
0.5 mm
c
0.5 mm
d
0.5 mm
e
1 mm
f
1 mm
g
1 mm
h
1 mm

4.5 Petrography and paragenesis of nonsulphide ores

Willemite was the first mineral to be deposited within the nonsulphide assemblage. This mineral is characterized by high-order interference colours, when observed under crossed nicols. A patchwork of willemite crystals has replaced directly the collomorphic concretions of "*Schalenblende*" (fig. 4.5b, 4.8a), or crystals of sphalerite (fig. 4.6a). Sometimes are still visible the relics of sulphide structures.

As already established from the SEM analysis, two types of willemite exist: (a) idiomorphic-pseudoidiomorphic crystals with hexagonal habit and (b) botryoidal aggregates composed of acicular radiated crystals. The hexagonal crystals appear deep blue when observed using the cold CL microscope (fig. 4.8b), whereas the botryoidal concretions, although still displaying shades of blue, have a luminescence that varies in intensity from the center to the margins of the concretion (fig. 4.8d). In a few cases, a time relationship between these two willemite types could be deduced. Locally, the center of the rounded willemite concretions appears to be a fragment of one of the idiomorphic hexagonal crystals (fig. 4.8c) (e.g. RA6661 and RA6661a), whose form can be clearly recognized by CL (fig. 4.8d). This relationship indicates that the idiomorphic willemite crystals can be considered to be the precursor of the roundish concretions. In some samples from the Welkenraedt mine (RN2224), euhedral willemite is cut and locally replaced by idiomorphic rhombohedra of Fe-rich zoned smithsonite (figs. 4.8e, f), while thin and/or platy hemimorphite crystals and rare hydrozincite represent the last generation of the nonsulphide assemblage.

As mentioned above, smithsonite occurs in different generations and as aggregates with variable forms. Zn-carbonate can be present as microcrystalline sediment of subidiomorphic crystals, but it occurs also as clear rhombohedral (Type I) or scalenohedral (Type V) crystals growing in geodes or in fractures. Only the rhombohedral crystals show well-developed cleavage traces. Smithsonite can also replace earlier willemite (figs. 4.6e, 4.8g) and (locally) hemimorphite (i.e. at La Calamine). If observed under cold CL microscope, smithsonite displays a zoned luminescence, with colours varying from deep blue to deep red or orange.

It is generally regarded that red or orange luminescence colours in carbonates, including

Figure 4.8: a) Thin section image (NII) of relicts of collomorphic concretions of sphalerite completely replaced by willemite, La Calamine deposit (RN5011); b) CL image of hexagonal crystals of willemite, Moresnet (RN5004); c) thin section image (N+) of botryoidal roundish aggregates of willemite with remnant of a hexagonal crystal in the nucleus, La Calamine deposit (RA6661, Coll. Buttgenbach 1916); d) CL image of (c); e) Fe-rich zoned smithsonite replaces idiomorphic willemite in thin section (N+), Welkenraedt deposit (RN2224); f) CL image of (e), Welkenraedt deposit; g) thin section image (N+) of a microcrystalline smithsonite vein cutting willemite, La Calamine deposit (RN2051); h) CL image of (f).

smithsonite, are strongly influenced by the Mn content (as CL activator) in the carbonate lattice (Götte & Richter, 2004). From chemical analyses, both in WDS and ICP-MS, all smithsonites are enriched in Mn. As discussed above, also Fe-rich smithsonite was recognized in different samples. It represents a late phase precipited after Fe-poor smithsonite and usually presents a chemical zonation based on Fe content. This fact is confirmed by CL observation: Fe-poor smithsonite has an orange luminescence, while luminescence in Fe-rich carbonates is quenched by high iron content.

Hemimorphite I, consisting of very small, radiated crystals with lower-order interference colours, can replace the macrocrystals of willemite starting from their margins (fig. 4.5d, i). Hemimorphite in radial aggregates occurs also as vein-fillings, cutting both limestone and nonsulphide masses. It is often associated with Fe-Mn-(oxi)hydroxides, but its relationship with smithsonite are not yet clear. Although the prismatic smithsonite crystals in concretion form can often be considered as the last generation occurring in the nonsulphide deposits, there is a second apparently even younger generation of platy hemimorphite crystals (hemimorphite II) growing on them (fig. 4.5k). Sauconite and other clay minerals are interspersed with the other nonsulphide minerals, mostly with hemimorphite I. A late generation of quartz microcrystals occurs mainly as inclusions in carbonates, or crystallizes as subidiomorphic individual crystals in veins (RN3403).

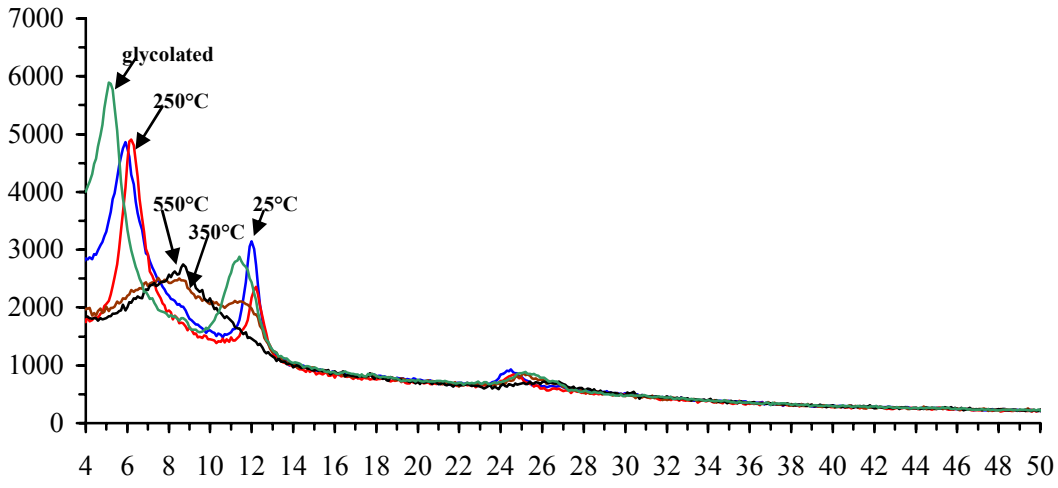

Figure 4.9: XRDP analyses of an oriented smectite (sauconite?) sample from the Belgian nonsulphide ores at 25°C, after cycles of heating at 250°, 350° and 550°C and after glycolation.

4.6 Major and trace elements geochemistry of nonsulphide ores

The nonsulphide ores in Belgium were characterized by a variably high Zn grade (>30 wt%), contained mainly in smithsonite and in the Zn-silicates willemite>hemimorphite. The Pb grade (from residual and neo-formed galena and from cerussite) was generally low (<5 wt%), this also due to the lower Pb content in the primary sulphide ore.

Hereafter will be presented the results of chemical analysis of willemite, smithsonite and hemimorphite, performed with WDS microprobe (tab. 4.5) and ICP-MS (tab. 4.6). Each single microprobe analyses reported corresponds to an average of 6 to 8 measured points.

Zn content in smithsonite is variable, ranging from 65.29 to 39.21 wt% ZnO (tab. 4.5). The higher values are recorded in exceedingly iron-rich varieties of Zn carbonate. In the latter, FeO can reach 13.96 wt% (in sample RN2008) and 14.76 wt% and 14.02 wt% (in samples RN4106 and RA4999 respectively). Fe-rich smithsonites (the so-called "*monheimites*") coexist in the same sample with Fe-poor smithsonites and are generally the final phases to be precipitated (fig. 4.10). MgO values range from 0.28 and 4.65 wt%; CaO up to 1.22 wt%, and trace amounts of Cd, Co, Cu and Ni were also detected. Both willemite and hemimorphite are nearly stoichiometric, and show only minor amounts of Fe, Mn, Ca, Co, Cu and Ni. The microprobe analyses of several Belgian hemimorphite samples reveal that they are very homogeneous (almost stoichiometric) in their composition. The only exceptions have been encountered in few samples from La Calamine, where Al^{3+} and Fe^{2+} can reach 0.025apfu and 0.145apfu respectively.

On the basis of chemical analyses performed by ICP-MS, the Zn content in smithsonite varies from 44.77 to 54.28 wt%. Among the other elements, Ca, Mn and Mg are lower than 1 wt%, and Fe is variable between 0.05 and 6.78 wt%. The average trace element composition of 11 smithsonite samples also reveals high Pb (88 to 9052ppm), variable Cu (3 to 162ppm) and Co (3 to 128ppm) contents. Ag (av. 1ppm) and As (average 10ppm) are comparably low. Ni and Cd are particularly abundant, the former ranging from 35 to 921ppm, the latter from 100 to >2000ppm. In the Fe-smithsonites, Zn is close to 27 wt%, while Fe ranges from 11.98 to 18.49 wt%. Among the smithsonites, the Fe-rich phases ("*monheimite*") could be distinguished through their high Fe content (from 10 to 18 wt%), and consequently relatively low Zn values (from 27 to 32 wt%).

Zn contents in the willemite-rich samples range from 58.87 and 63.40 wt% (tab. 4.6). Fe and Mn contents are higher in the reddish microcrystalline willemite occurring in the breccia matrix, and

Table 4.5: Microprobe analyses of selected willemites, smithsonites and hemimorphites from the Liège district (NW Belgium) pointing to compositional variations (from Coppola et al. 2007).

	willemite																			
sample	**RN3834**				**RN5011**				**RA5012**				**RA5013**				**RA6661**			
SiO_2	26.45	26.15			27.20	27.05			26.61	25.70			27.03	26.68			26.21	26.09		
ZnO	73.24	73.79			71.71	71.72			72.01	72.68			70.65	71.78			74.03	72.98		
FeO	0.05	0.03							0.09				0.48	0.18				1.18		
MnO					0.03	0.03			0.02				0.02	0.03			0.03	0.09		
CaO						0.05			0.03	0.03			0.02					0.08		
MgO						0.08							0.05				0.03			
total	99.74	99.97			98.94	98.92			98.77	98.41			98.25	98.66			100.30	100.42		

	RA6661a				**RN2300**				**smithsonite and Fe-smithsonite**										**hemimorphite**	
sample									**RN2008**				**RN3834**		**RN4106**		**RA4999**		**R2B34**			**RN2051**		
SiO_2	26.69	26.31			26.77	26.55			**ZnO**	61.70	39.21		57.62	51.99	62.20	39.48	62.80	39.60	65.29	57.21	**SiO_2**	26.44	25.92	25.99
ZnO	71.78	72.28			71.53	72.27			**FeO**	0.13	13.96		0.71	6.38	0.48	14.76	0.62	14.02		0.85	**ZnO**	68.51	69.42	69.40
FeO	0.04				0.23	0.03			**MnO**	0.03	2.93		1.54	0.41	0.03	2.42	0.25	3.79		1.51	**FeO**	0.02		
MnO		0.02							**CaO**	1.22	0.29		0.23	0.93	0.13	0.38	0.05	0.32	0.03	0.23	**CaO**		0.02	
CaO	0.06				0.05				**MgO**	0.18	4.40		4.09	3.29	0.25	3.90		4.19	0.28	4.65	**H_2O***	5.04	4.65	4.61
MgO	0.05					0.04			**CO_2***	35.19	37.40		36.73	36.20	35.16	37.21	34.72	37.30	34.42	37.12				
total	98.63	98.61			98.58	98.89			**total**	98.45	98.19		100.91	99.19	98.25	98.15	98.44	99.22	100.02	101.56	**total**	100.01	100.02	100.00

* calculated from stoichiometry

Table 4.6: ICP-MS analyses of major and trace elements in selected willemites and smithsonites from Liège district (NW Belgium) (from Coppola et al. 2007).

	Zn	Fe	Mn	Ca	Mg	Cd	S	Pb	Cu	Ag	As	Ba	Be	Co	La	Li	Ni
	%	%	%	%	%	%	%	ppm	ppm	ppm	ppm	ppm	ppm	ppm	ppm	ppm	ppm
Willemite																	
RA5012	63.40	0.37	n.d.	0.03	0.01	n.d.	0.10	1790	290	21	98	4	79	<1	0	51	7
RA6661a	61.28	0.79	0.01	0.08	0.04	n.d.	<0.10	240	5	1	91	13	35	1	10	29	73
RA5013a	61.62	0.47	n.d.	0.04	0.04	n.d.	0.30	150	<0.1	<0.1	73	17	26	1	3	19	53
RA5013b	58.87	0.84	n.d.	0.03	0.07	n.d.	<0.10	280	2	<0.1	77	12	36	3	6	31	217
Smithsonite (+ Fe-smithsonite)																	
RN2208a	54.28	0.11	0.01	0.01	0.03	0.01	<0.05	127	9	<0.1	<0.5	<1.0	n.d.	12	<1.0	n.d.	169.1
RN2008b	27.63	11.98	0.58	5.52	1.04	n.d.	<0.05	192	14	1	9	54	n.d.	21	6	n.d.	120.8
RN2017	50.70	1.65	0.10	0.14	0.25	0.03	<0.05	105.4	7	2	6	4	n.d.	11	<1.0	n.d.	220.7
RN2044b	52.66	1.27	0.04	0.22	0.15	0.03	<0.05	106	6	<0.1	4	6	n.d.	3	<1.0	n.d.	224.4
RN4106	44.77	3.57	0.67	0.33	1.36	0.01	<0.05	88	3	<0.1	6	10	n.d.	59	14	n.d.	567.2
R2B35/3925	32.10	10.68	0.44	8.50	1.27	n.d.	<0.10	210	<0.1	0	<1.0	54	14.0	16	16	15.4	297.6
RN2300b	50.63	6.78	0.08	0.15	0.13	<0.1	0.40	1410	40	2	106	16	45.0	5	25	73.7	921.2
RN2220a	48.42	1.76	0.84	0.09	0.11	0.11	0.08	9052.7	8	1	1	1	n.d.	129	1	n.d.	296.2
RN2220b	51.99	1.08	0.47	0.10	0.06	0.15	<0.05	1724.2	4	1	1	1	n.d.	71	1	n.d.	140.8
RN2236b	52.25	0.05	0.12	0.15	0.02	0.19	<0.05	422	25	0	<0.5	1	n.d.	13	2	n.d.	110.5
RN2242a	27.07	18.49	1.00	0.32	1.25	0.03	<0.05	2869.4	55	11	16	7	n.d.	120	2	n.d.	141.1
RN2270b	50.15	0.46	0.38	0.91	0.21	0.05	<0.05	3533.8	162	2	4	67	n.d.	14	48	n.d.	418.9
RA4986a	51.36	0.86	0.02	0.37	n.d.	0.50	<0.05	9792.7	9	1	52	1	n.d.	6	35	n.d.	36

*Fe-smithsonite

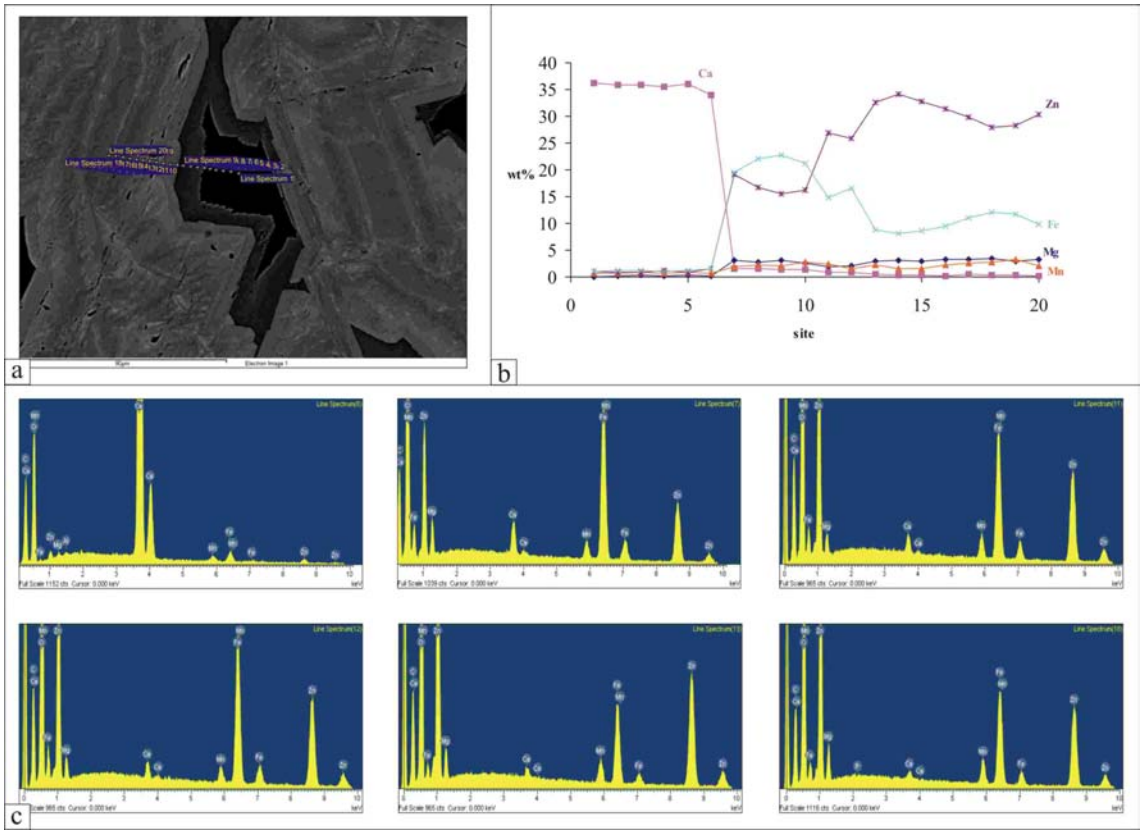

Figure 4.10: Chemical profiles carried out with a SEM JEOL 5900 INCA on smithsonite, Fe-smithsonite and calcite. a) backscattered electron image and analysed points; b) content variations of selected elements along the chemical profile illustrated in (a); c) single representative X-ray spectra of the analyzed points illustrated in (a).

much lower in the isolated crystals. This could be an evidence of Fe-Mn oxy-hydroxide impurities around the former, typical of a supergene environment. The trace element composition of willemite samples reveals again variable Cu (0 to 290ppm), Ag and Co below detection limit, Pb lower than in smithsonites (150 to 1790 pm) and higher As (73 to 98ppm). Ni has been detected (7 to 217ppm) in all the willemite specimens whereas, in contrast to smithsonites, Cd is absent.

4.7 C and O isotopes geochemistry

The results of oxygen and carbon isotope measurements on smithsonite, cerussite, calcite and two wall-rock dolomite samples from La Calamine, Welkenraedt, Fossey, Theux and Angleur mines are presented in table 4.7 and depicted in figure 4.11.

Table 4.7: Carbon and oxygen isotope data of Zn, Pb, and Ca carbonates from Liège district (NW Belgium) (from Coppola et al. 2007).

Sample	Mineral*	Description	Location	$\delta^{13}C_{V\text{-}PDB}$ (‰)	$\delta^{18}O_{V\text{-}SMOW}$ (‰)	*Ave*	$\pm\sigma$
RN1996a	sm**	clear rhombohedral crystals, outer part (Type I)	Moresnet	-9.8	28.8		
RN1996b	sm	yellowish crust, inner part (Type I)	Moresnet	-11.6	28.2		
RN2008b	sm	yellow scalenohedral crystals on RN2008c (Type VI)	Moresnet	-8.6	28.1		
RN2008c	sm	brownish massive matrix of breccia	Moresnet	-8.8	28.1		
RN2008b	sm	yellow scalenohedral crystals on RN2008c (Type VI)	Moresnet	-8.6	28.1		
RN2101c	sm	late clear crystals	Moresnet	-10.9	28.1		
RN4106	sm	reddish brown banded sediment	Moresnet	-7.4	30.6		
RN2017	sm	white crystals on globular smithsonite	La Calamine	-10.7	28.3		
RN2044c	sm	yellowish crystals	La Calamine	-1.5	28.1		
RN2051a	sm**	brownish matrix of mottled breccia and veins	La Calamine	-9.8	28.7		
RA4999a	sm**	greyish central part of concretion (Type V)	La Calamine	-6.2	28.0		
RA4999b	sm**	yellowish porous outer part of concretion (Type V)	La Calamine	-6.6	27.4		
R2B35/3925	sm	brownish massive or veins	La Calamine	-9.2	28.4		
RN2208a	sm**	yellowish clear crystals, outer part	Fossey	-11.6	28.3		
RN2208c	Fe-sm	brownish massive matrix (Fe-rich)	Fossey	-7.6	30.2		
RN2300d	sm	clear rhombohedral crystals (Type I)	Fossey	-10.2	28.6		
RN2220a	sm	black sulfide-bearing crystals, inner part	Welkenraedt	-10.1	28.9		
RN2220b	sm	yellowish clear crystals, outer part	Welkenraedt	-10.2	28.2		
RN2224b	sm	zoned Fe-rich brown rhombohedral crystals (Type I)	Welkenraedt	-8.4	29.5		
RN2236a	sm	globular greyish concretion, outer part (Iype V)	Welkenraedt	-7.1	27.2		
RN2236b	sm	brownish massive inner part (Type V)	Welkenraedt	-3.2	27.1		
RA4986a	sm	white botryoidal concretion (Type V)	Welkenraedt	-8.9	28.2		
RN2270a	sm**	white concretion, outer part (Type V)	Theux	-2.2	27.7		
RN2270b	sm	brownish, massive inner part (Type V)	Theux	-1.6	28.1	28.4	0.8
RN2487b	cc	green botryoidal crust on will.	Moresnet	-10.4	24.7		
Be4a	cc	white vitreous crystals in the oxidation zone	La Calamine	-7.4	25.7		
Be5b	cc	red vitreous crystals associated to smithsonite	La Calamine	-6.5	25.5		
Be8c	cc	red vitreous crystals associated to smithsonite	La Calamine	-6.5	25.7		
Be9b	cc	red vitreous crystals associated to smithsonite	La Calamine	-6.1	25.5	25.4	0.4
Be1a	do	black massive dolomite (wall rock)	La Calamine	2.8	16.4		
Be2b	do	black massive dolomite (wall rock)	La Calamine	2.8	19.5		
RA 7898	ce	fibrous crystals	Theux	-14.7	17.6		
RA 8497	ce	clear crystals	Theux	-15.0	17.2		
RN 2330	ce	white fibrous crystals	Theux	-14.8	16.8		
RA 8494	ce	fibrous crystals	Angleur	-15.1	18.4		
RN 2339	ce	greyish massive aggregate	Welkenraedt	-18.4	19.3	17.8	1.0

*Abbreviations: sm = smithsonite; ce = cerussite; cc = calcite; do = dolomite.

**mild acid treatment to remove calcite

4.7.1 Smithsonite and cerussite

Smithsonites exhibits a limited range of $\delta^{18}O$ values from 27.1 to 30.6‰, with an average value of 28.4 ± 0.8‰ (1σ, n = 23), with most analyses ranging between 27.0 and 29.0‰. There is no systematic difference in $\delta^{18}O$ values from different deposits or between the different morphological types. This indicates a relatively uniform isotope composition of the oxidizing water, and constant temperatures of smithsonite crystallization (Boni et al., 2003; Gilg & Boni, 2004). The oxygen isotope value of iron-rich smithsonite ("monheimite") RN2208c is higher than that of the Fe-poor smithsonites. Similarly, sample RN4106, a neoformed internal(?) sediment replaced by smithsonite, has an oxygen isotope value that is about 2‰ higher than the average of all other smithsonites. In contrast to oxygen, carbon isotope values of smithsonites, even from the same mine site, show a considerable range from -11.6 to -1.6‰. There is, however, no relationship between the stable carbon isotope composition and the crystal morphology, as it was observed for the smithsonites of the Iglesiente district, Sardinia (Boni et al., 2003). Cerussites have oxygen isotope values ranging from 16.8 to 19.3‰ with an average value of 17.8 ± 1.0‰ and carbon isotope values of -18.4 to -14.7‰. On the whole, the isotope compositions of smithsonite and cerussite from Belgium (fig. 4.11) are very similar to those from the Iglesiente district, Sardinia, which are considered as typical for supergene carbonate-hosted nonsulphide Zn-Pb deposits (Boni et al. 2003; Gilg & Boni, 2004; Gilg et al. 2007a).

4.7.2 Calcite and dolomite

Some calcite samples associated with the calamine ores were also investigated (fig. 4.11). Sample RN2487b from La Calamine consists of a yellow-orange concretion growing on late smithsonite crystals. The other calcites are reddish crystals occurring in veinlets together with nonsulphide ore minerals at the margin of the former La Calamine deposit. The $\delta^{13}C$ values of the calcites show a small range from -10.4 to -6.1‰, while the $\delta^{18}O$ values cluster around 25.5 ± 0.5‰, about 3‰ lower than those of smithsonite. The isotope values of calcite from calamine ores are again identical to those from the Iglesiente district. The $\delta^{13}C_{VPDB}$ values of two diagenetic dolomites, considered as the host rock of the La Calamine deposit, are clearly positive (2.81 and 2.75‰), while their $\delta^{18}O_{SMOW}$ values are 16.4‰ and 19.5‰, respectively. These isotopic results are broadly comparable to published data (fig. 4.11) on Dinantian dolomites from Eastern Belgium (Nielsen et al., 1994).

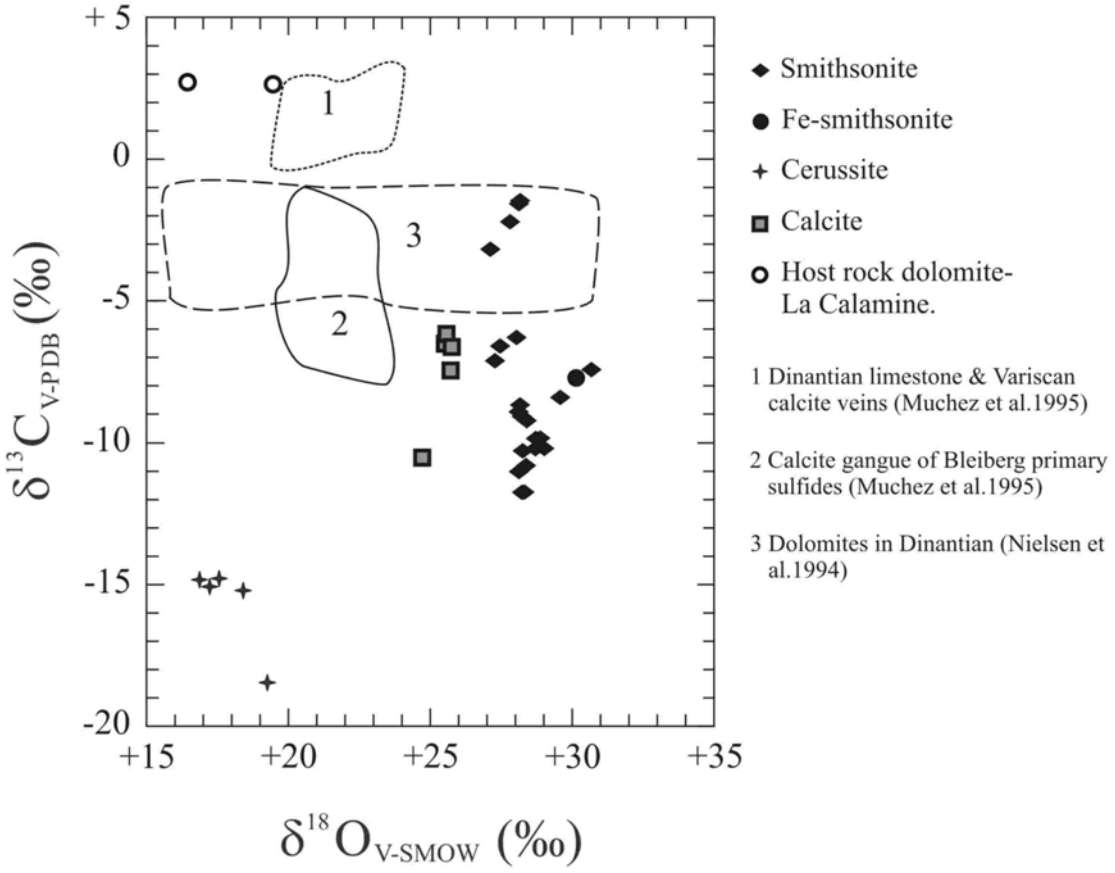

Figure 4.11: Plot of $\delta^{13}C$ vs. $\delta^{18}O$ for several types of Pb, Zn and Ca carbonates (smithsonite, cerussite and calcite, cogenetic with the former minerals) from the Belgian nonsulphide ores (from Coppola et al. 2007).

4.8 Thermometric analysis of fluid inclusions

A fluid inclusions study was carried out on transparent economic (willemite, smithsonite) and gangue (quartz) minerals of the Belgian nonsulphide ore deposits, in order to obtain dates on temperature and salinity of fluid precipitating Zn-oxides. The thermometric analyses were preceeded by a petrographic study of the fluid inclusions. This preliminary work was necessary to individuate the different Fluid Inclusion Assemblage (FIA), thus to distinguish primary and secondary fluid inclusions.

Only monophase (liquid) fluid inclusions, primary and secondary, were detected in smithsonite and in late quartz. After freezing of these monophase fluid inclusions no bubbles were generated. The dimensions of fluid inclusions are usually less than 5μm. The occurrence of only monophase

fluid inclusions points to very low formation temperatures (< 50°C) (Grooves et al., 2003), this being in agreement with a supergene origin.

As mentioned above, one of the main problems of this work was to determine the origin of the willemite (supergene or hydrothermal?). Thus, the fluid inclusion study could have helped us to clarifying the genetical interpretation of the willemite. Four samples of willemite from La Calamine and Welkenraedt mines were measured. Generally, at least two FIA were observed in the willemite crystals, representing primary and secondary inclusions. Monophase (80%) and two-phase (L+V) (20%) were observed in primary fluid inclusions in willemite. Their dimensions range from 2 to 30μm, even though small fluid inclusions are predominant. More than 60 two-phase primary and secondary fluid inclusions were measured. Widespread necking-down and leakage phenomena were detected. In the analytical procedure, those inclusions have been avoided, using as the main criteria the shape and excessive scatter of the vapor/liquid ratio (Roedder, 1984). Temperature of homogenization (T_h) (L + V → L) obtained from a set of apparently reliable primary fluid inclusions ranged from 80 to 190°C. Few eutectic points (T_e) measured during freezing of inclusions, and ranging from -18 to -29°C, indicate NaCl as the dominant salt phase present in the trapped fluid. However, we cannot exclude the presence of other components, both for the variability of the measured Te, and the chemistry of the geologic environment. On the base of the measured melting point (T_m) (constrained between 0 and -3.7°C) using the equation of Bodnar (1993) revised by Goldstein & Reynolds (1994), a salinity between 0 and 6 eq. wt% NaCl is indicated. No correlation is present between T_h and salinity of fluid inclusions.

Secondary fluid inclusions are easy to distinguish because they are aligned along fractures crossing the boundary of crystals. Most of them are monophase, with dimensions lower than 5μm, but also some two-phase inclusions were observed. Homogenisation temperatures of two-phase secondary fluid inclusions are constrained between 80 and 200°C, and their salinity, considered in the H_2O-NaCl system and relative equations (Bodnar, 1993; Goldstein & Reynolds, 1994), is less than 4 eq. wt% NaCl. Occasionally, final melting was over 0°C (max 4.7°C). The possible causes of this could be metastability phenomena, frequently recorded in low-salinity fluid inclusions, or otherwise the presence of other compounds dissolved in the fluid.

The wide range of T_h values observed in the primary fluid inclusions in willemite does not help us in clarifying the origin of willemite. This pattern may be explained with post-precipitation re-equilibration phenomena (re-equilibration can be due to variable thermal gradients, stretching or leakage). Due to the brittle nature of willemite, a mechanical and/or thermal stress could have

strongly affected the fluid inclusions and modify the liquid/vapor ratio and thus the T_h. However, the full discussion about genesis of willemite will be dealt in the next paragraph.

4.9 Discussion

4.9.1 Geological factors controlling the emplacement of Belgian nonsulphide deposits

Belgian nonsulphides present the typical characteristics of supergene deposits. They are the results of weathering *in situ* of sulphide ores, which combined the formation of surficial *gossan*s with concentrations of newly formed minerals in-filling paleokarstic cavities and replacing limestone host rocks. The formation of Belgian nonsulphide ores was favoured by tectonic uplift and consequent descent of water table, and by brittle fracture of the host rocks which enhanced the lowering of oxidation front and sulphides alteration. Erosive processes involving terrains stratigraphically overlying primary sulphide deposits could accelerate the process.

For the aims of the present work, it became important to consider the tectonic uplifts in this part of Europe from Hercynian orogeny onwards, in particular after sulphide ores emplacement (middle Jurassic) until Recent. Several uplift stages have been recorded in this part of Belgium during the Cimmerian phase of Alpine tectonics: one of the consequences was the almost complete removal of both Triassic and Jurassic sediments. During the Oligocene, a block faulting phase occurred in the Ardenne Massifs due to lithospheric buckling induced along the front of the developing Alpine orogeny, or driven by the plume activity related to the Eifel volcanism (Demoulin, 2003). However, this tectonic event probably played only a secondary role in the development of weathered profiles in mineralised carbonates.

Santonian sediments (Aachen fm.), covering nonsulphide deposits in some mines in the Liege district (fig. 4.4) could be used as a proof of a pre-Upper Cretaceous age for their oxidation. Nevertheless, we cannot exclude that nonsulphide formation was the result of multiple weathering phases during the whole Tertiary. Indeed, there are several evidences for this thesis: the modest and variable thickness (~50m) of Upper Cretaceous cover sediments, which might be in places completely absent, could allow the local percolation of meteoric waters throughout time. Moreover, several Tertiary weathering phases, producing kryptokarst networks in Paleozoic limestones, are recorded in other areas of Belgium (Dupuis, 1992; Dupuis et al., 2003). Marked fault zones in the immediate vicinity of economic bodies could have facilitated karstification processes and channelled meteoric (and/or hydrothermal?) waters after the

deposition of Santonian sediments. For example in the Welkenraedt mine a NW-SE set of faults, cutting Hercynian structures and controlling the primary mineralisation, most probably, have controlled also the emplacement of secondary phases. The same can be said for the Dickenbusch mine, where a primary sulphide body occurs laterally to a NW-SE fault and is elongated in the same direction. La Calamine deposit occurs on the SW-NE thrust (Schmalgraf fault) (fig. 4.3a), which could have played an important role for the origin of willemite mineralisation.

4.9.2 Stable Isotopes

Isotopic composition of Zn Pb and Ca carbonates is dependant from (1) temperature and (2) isotopic composition of fluids precipitating them. Therefore, stable isotopic investigation could be a helpful tool to detect the composition of oxidizing fluids and therefore the physicochemical conditions during precipitation of secondary phases.

4.9.2.1 Paleoclimate indications

Belgian smithsonite presents a constant $\delta^{18}O$ (<1%, 1σ) and a more variable $\delta^{13}C$ (fig. 4.11). The C-O patterns of smithsonite from the Liège district are almost identical to those of smithsonite in supergene nonsulphides from the Iglesiente district (SW Sardinia) (Boni et al., 2003). In particular, the $\delta^{18}O$ values measured in Belgian smithsonite (28.4‰ ± 0.8‰ VSMOW) are only 1‰ higher than in Sardinian smithsonite (Boni et al., 2003). Fe-smithsonite shows a $\delta^{18}O$ value lightly higher in respect to pure smithsonite (fig. 4.11). This difference could be caused by a different coefficient of fractionation between carbonate and water or, by a small decrease in temperature during Fe-smithsonite precipitation.

The relatively uniform values of oxygen ratio recorded in Belgian smithsonites imply a constant temperature and a constant isotopic composition of fluids during paleoweathering and precipitation of oxidized phases. Uniform values of $\delta^{18}O$ are recorded in Pb-carbonates and calcites associated.

$\delta^{18}O$ values in smithsonite (28.4‰ ± 0.8‰ VSMOW) are about 10.5‰ heavier than those of cerussite (17.8‰ VSMOW) and 3‰ heavier than calcites (25.5‰ VSMOW). These data are in agreement with theoretical (Golyshev et al., 1981; Zheng, 1999) and experimental (Melchiorre, 2001) methods predicting oxygen isotopic fractionation behaviour with changing temperature between carbonates and water. This fact could represent a further confirmation that the temperature was constant during Zn, Pb and Ca carbonate precipitations.

The knowledge of the isotopic composition ($\delta^{18}O$) of paleometeoric water and minerals can allow to calculate the temperatures of precipitation. Otherwise, assuming a temperature of precipitation based on other independent thermometric methods, we can calculate the isotopic composition of the fluids. Both these approaches are used in the present work.

Unfortunately, though the isotopic composition of paleometeoric waters during weathering phases has not been calculated for NW Belgium, we can refer to an isotopic data set from other European areas. Gilg (2000) measured the isotopic composition of paleometeoric waters in Northeastern Bavaria from Jurassic to Present, based on the isotopic compositions of kaolinite. Gilg's $\delta^{18}O$ values range from -5 to -6.5‰ VSMOW for Middle Jurassic to Cretaceous paleometeoric waters, and from -7.2 to -8.7‰ VSMOW for the period Late Oligocene – Mid-Miocene. The oxygen isotopic composition of paleometeoric water precipitating the Lower Cretaceous kaolinite at Transinne, was also calculated in -6.1‰ VSMOW by Yans (2003), on the base of an oxygen fractionation equation kaolinite-water reported in Sheppard and Gilg (1996). The isotopic composition of the fluid precipitating the Transinne kaolinite fits within the range of values established by Gilg (2000) for meteoric waters from Middle Jurassic to Cretaceous. These values are heavier than those of present meteoric waters, which range from -6.8 to -8.1‰ (Rozanski, 1993; Beyer, 1995). Therefore, an old, probably Cretaceous, age is indicated for the weathering responsible for the genesis of Belgian nonsulphides.

Considering a value of $\delta^{18}O_{VSMOW} = -6.1 \pm 0.5$‰ for the paleometeoric waters, as calculated by Yans (2003) and the smithsonite-water and cerussite-water fractionation equations of Gilg et al. (2007a), the estimated temperatures of precipitation were constrained respectively between 7°C and 19°C (av. 14°C) for smithsonite (figs. 4.12, 4.13) and between 9°C and 22°C (av. 16°C) for cerussite (fig. 4.12). These temperatures are substantially lower and probably more reliable, than the temperatures calculated for smithsonite and cerussite in Iglesiente district (SW Sardinia) and published in Boni et al. (2003) based respectively on the equations reported in Zheng (1999) and Melchiorre et al. (2001). Gilg et al. (2007a) proposed new temperatures of precipitations for these Zn and Pb carbonates from Iglesiente district, clearly lower of those proposed by Boni et al. (2003).

Using same the isotopic compositions for paleometeoric water and the fractionation equation reported in O'Neil (1969), the calcites associated to smithsonites precipitated at temperature of about 12°C (fig. 4.12).

The supergene nonsulphides in Belgium are probably the result of the same pre-Late Cretaceous paleoweathering processes that have produced the widespread kaolinized regoliths in the region (Dejonghe & Boni, 2005), associated to temperate but lightly colder climate. Indeed, the

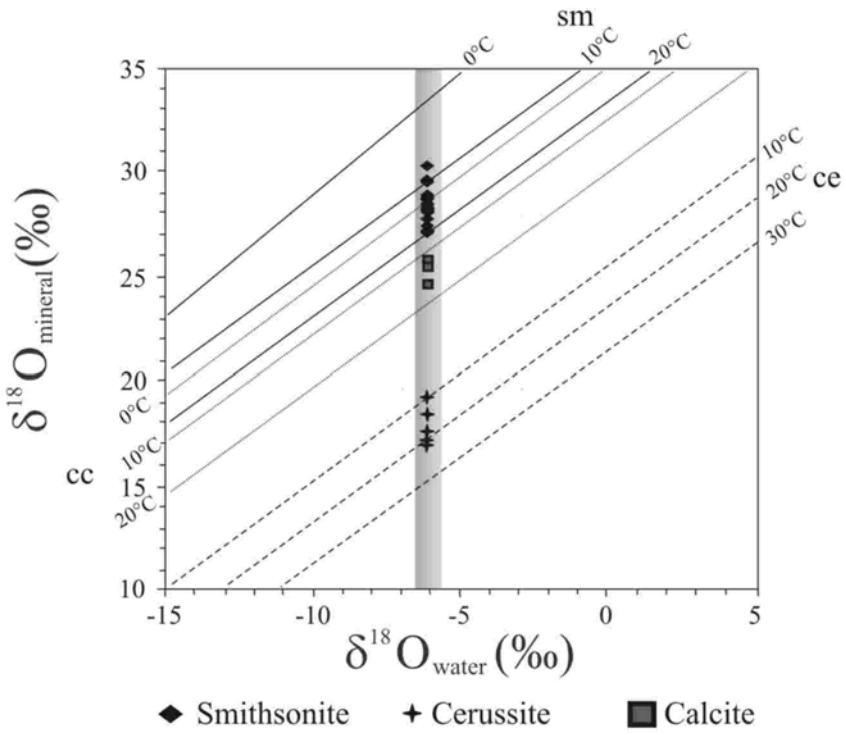

Figure 4.12: Oxygen isotope data of cerussite (ce, star), calcites (ca, circle) and smithsonites (sm, rhomb) from supergene oxidation zones in NE Belgium and estimated corresponding oxygen isotope compositions from local paleometeoric water as proposed by Yans (2003).

calculated precipitation temperature of Belgian smithsonites (8 – 19°C, av. 14°C) and cerussites (9°C – 22°C, av. 17°C) are slightly lower than the estimated temperatures for Early Cretaceous kaolinite deposit at Transinne (22°C) (Yans, 2003). Regolith deposits are usually interpreted as having formed under tropical humid climate. Nevertheless, in a few cases, the evidence seems to point out that alternances of wet-dry climate are more favourable to their formation (Harrington et al., 2007). Similar climatic conditions could also favour the formation of supergene Zn-deposits. Indeed, according to Reichert & Borg (2007), the formation of high-grade Zn-nonsulphide deposits needs at least a seasonally (hyper-) arid environment.

4.9.2.2 Carbon sources

As shown in figure 4.11 and table 4.7, the Belgian smithsonites exhibit a most variable set of C-isotopes ratios respect to cerussite. This is probably related to a more limited number of measured cerussite samples (n = 5) in respect to those of smithsonite (n = 24). A broad range of $\delta^{13}C$ measured in Zn and Pb carbonates in the Liège district indicates the presence of at least two carbon sources during oxidation process: a ^{13}C-enriched source derived from the organic matter of the overlying soils and a ^{13}C-enriched marine carbon, originated from dissolution of the

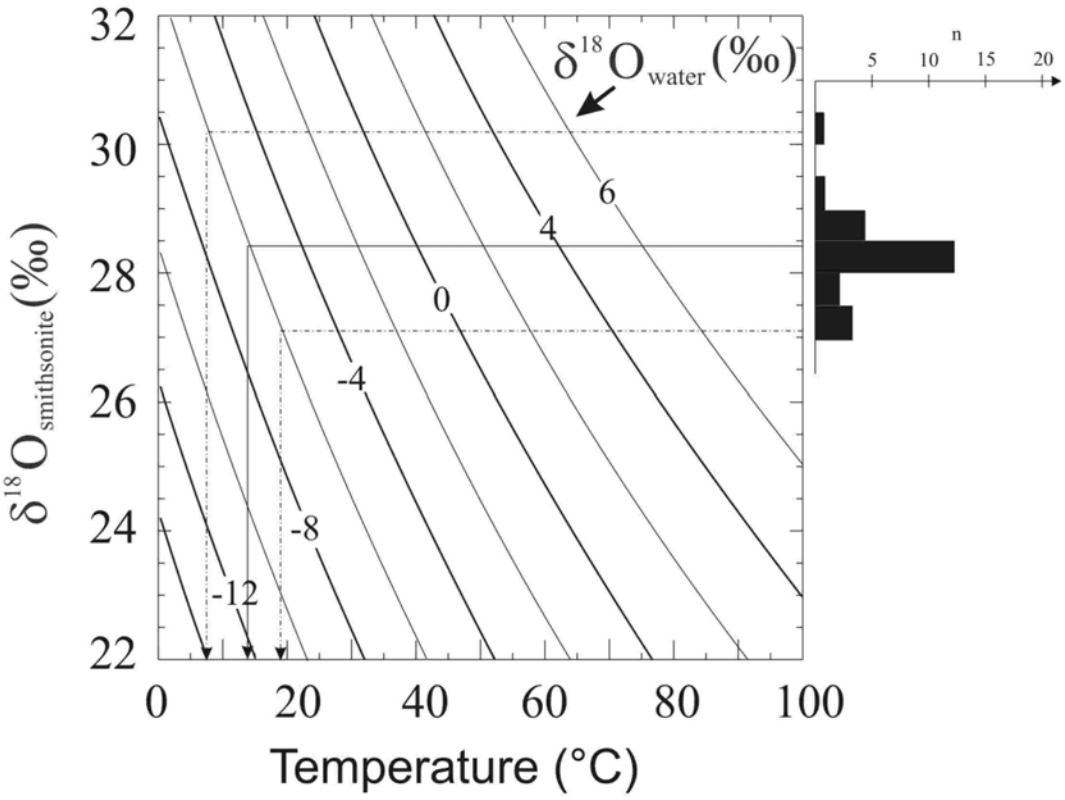

Figure 4.13: Graphic representation of oxygen isotope equilibrium curves between smithsonite and water according to Gilg et al. (2007), calculated for different $\delta^{18}O_{water}$ values as a function of temperature. The histogram to the right shows the oxygen isotope composition of smithsonites from the Liège district. Calculated temperatures for the smithsonite formation are based on the value of -6.1‰ $\delta^{18}O_{VSMOW}$ of the local paleometeoric water as proposed by Yans (2003).
Note: dashed line = max and min $\delta^{18}O_{VSMOW}$ values, continue line = average $\delta^{18}O_{VSMOW}$ value

carbonate host rocks. Smithsonites with more negative values (-11.6‰ VPDB) are similar to the isotopic composition of pedogenetic calcites formed in soils with predominant C3 plants, therefore could be related to CO_2 in the soil (Gilg et al., 2007a).

Dolomite host rock at La Calamine, with their lightly positive $\delta^{13}C$ values, could surely represent the ^{13}C-enriched source, at least in this mine. Moreover, Dinantian dolomite and Hercynian calcite veins (Muchez et al., 1994) are both characterized by high $\delta^{13}C$ values, and therefore could have contributed to the formation of secondary Zn and Pb-carbonates. Furthermore, low pH fluids, generated from Fe-sulphides oxidation, thus favouring the dissolution of dolomites and limestones hosting the nonsulphide deposits (Williams, 1990) increased Carbon availability.

Calcites associated to "calamine" show an almost similar but quite more restricted range of $\delta^{13}C$ than smithsonites. This indicates that Zn and Ca carbonates have identical coefficients of isotopic carbon fractionation (Gilg et al., 2007a): therefore they precipitated from the same carbon sources.

4.9.3 Origin and timing of willemite

The interest in this particular type of Zn-silicate ore has recently increased also elsewhere in the world, because of the high Zn grade (more than 40%) and the relatively low environmental impact during enrichment processes. Despite of this, nature and origin of willemite (hydrothermal and/or supergene) in many willemite-rich nonsulphide deposits in the world is still highly debated.

The presence of abundant willemite is usually a characteristic of hydrothermal Zn nonsulphide deposits (Hitzman et al., 2003). Nevertheless, unequivocal supergene willemite has been recognized in many deposits, as Tsumeb, Namibia (Lombaard et al., 1986; Hughes, 1987).

Recent studies (e.g., Sweeney et al., 1991; Monteiro et al., 2000; Brugger et al., 2003; Hitzman et al., 2003) have suggested that willemite formed in some nonsulphide Zn deposits of the southern hemisphere (e.g., Vazante, Beltana, Star Zinc, Berg Aukas) under hydrothermal conditions at temperatures from < 100°C up to 250°C, by mixing between a reduced, zinc-rich, sulfur-poor hydrothermal fluid with an oxidized, sulfur-poor water. This mixing is testified by the wide range of salinities measured in fluid inclusion in willemite (4-22 eq. wt% NaCl) (Hitzman et al., 2003). Furthermore, hypogene willemite mineralisation is often associated with hematite and carbonate alterations.

Few studies on the thermodynamic behaviour of willemite (Markham, 1960; Takahashi, 1960; Brugger et al., 2003) affirm that willemite is a more stable phase than hemimorphite and smithsonite with lower water activities and/or higher temperature (Ingwersen, 1990). Moreover, willemite should prevail over smithsonite in conditions of higher silica activity and lower CO_2 fugacity. At La Calamine, conditions of high silica activity in the alteration fluid may have been produced by the dolomitic wall rocks of the secondary ores that are slightly siliceous.

In conclusion, these studies indicate that willemite could precipitate throughout a wide range of environments making the explanation of its genesis more difficult.

Willemite ores in Liège district is mainly concentrated in the La Calamine deposit, but other concentrates have been abundantly described in smaller deposit, as Welkenraedt, Fossey. It is mainly present in the lower levels of mineralisation. In all the Belgian mines where willemite ores occur, they do not show the typical features of high temperature nonsulphide deposits (Hitzman et al., 2003).

At La Calamine willemite represents the first precipitated phase in the “oxidised” paragenesis: it replaces partly the primary sulphides and is commonly replaced by smithsonite and hemimorphite. Moreover the absence of an hematitization and carbonatization are contrasting with hydrothermal origin of willemite.

The majority of willemite-hosted fluid inclusions in Belgium suggest low formation temperatures and their salinities are also much lower than those reported in hypogene deposits (Hitzman et al., 2003; Gilg, pers. comm.). The presence of few two-phase inclusions with homogenization temperatures of 80 to 190°C (Boni et al., 2005a) may have been caused either by post-entrapment modifications of the fluid inclusion density related to heating or to tectonically induced deformation, or by heterogeneous entrapment of air and water within the vadose zone.

Therefore, the origin of willemite bodies, which occur in the roots of most Belgian deposits, could be related to: (1) weathering processes taking place under conditions of peculiar aridity and silica activity, (2) a low-temperature hydrothermal event briefly following sulphides emplacement.

Hovewer, the presence of moderately high (up to 50°C) temperatures of homogenization, which cannot be reached during exothermic process of sulphide oxidation, may be in accord with a low-temperature hydrothermal event.

Fluid inclusions in Belgian willemite have been recently measured with a femtosecond laser and show T_h higher than 70°C (Gilg, pers. comm.). With the same method, two sets of temperatures have been detected in the hemimorphite from the Welkenraedt deposit: FIAs Type A ranging from 20 to 27°C and ice melting temperatures of 0.0 ± 0.2°C and FIAs Type B whose T_h is constrained between 6 to 30°C with two modes around 10 and 25°C, and lower ice melting temperatures of -0.2 to -1.6°C (Gilg et al., 2007b).

Regarding the possibility of a hydrothermal genesis, the SW-NE Schmalgraf fault, located in the vicinity of the giant La Calamine deposit could have played an important role for the rise of hot, O-rich fluids necessary to willemite deposition. We mention here that a variety of active, low-temperature (<70°C) hot springs occur within the area of the Pb-Zn mineralisation, e.g. Chaudfontaine (Graulich, 1983) or throughout the Aachen district (Beyer, 1995; Herch, 2000), all located along the SE dipping Hercynian thrust zones. Their waters are mixtures of deep (>3500m), highly mineralised thermal fluids and cool meteoric waters from a shallow reservoir (Herch, 2000). The salinity of the Aachen hot spring fluids is moderately low (about 4000 ppm TDS), but their silica content is high (about 30ppm Si), and the fluids are oxidized (sulphate-dominated). Thus, similar low-temperature hot spring fluids (Si-enriched) would have been potentially capable of forming the willemite-rich deposits from their sulphide precursors. Such a scenario could also explain the mineralogical, apparently localized process, and fluid inclusion data.

4.9.4 Timing of supergene nonsulphide deposits in the Liège district, NE Belgium

Timing of nonsulphides emplacement in Belgium is far to be clarified, principally because of multiple weathering events that occurred in this part of Europe from Mesozoic through Tertiary, until Present-day. It is also unclear if the willemite-rich parts of the deposits should represent a late hydrothermal phase of the primary sulphide mineralisation or a product of oxidation of sulphides preceeding the smithsonite-hemimorphite stage.

Favourable climatic conditions (hot and humid, alternated with arid periods) for the development of weathered profiles were present in this part of Europe several times after Hercynian orogeny, Also Dupuis (1992) and Alexandre & Thorez (1995) pointed out that Palaeozoic rocks in Belgium were affected by deep weathering during Permian and Mesozoic periods before the Cretaceous transgression, as well as by multiple weathering phases during Cainozoic. In Belgium, as in many regions of Northern Europe, the geological record reveals a series of time intervals during Mesozoic and Tertiary, during which weathered profiles (locally associated to economic kaolinite deposits formed) many of which are preserved (Migoń & Lidmar-Bergström, 2001). In particular, the kaolinite deposits have been dated as Cretaceous and Palaeogene-Miocene in age (Yans, 2003).

Belgian sulphides and nonsulphides are both unconformably covered by the sediments of the Aachen Fm. (Santonian age). Therefore, it is highly probable that the principal weathering event producing the oxidation of sulphide ores preceded the Late Cretaceous transgression.

The Cimmerian uplift phase, following which a complete removal of Triassic-Jurassic sedimentary cover took place, favoured also the exposure and weathering of primary sulphides. Moreover, the prolonged Mesozoic emersion promoted the development of an extensive karstic network in carbonate rocks, which acted as a trap for secondary mineralisation.

A renewed tensional tectonic regime during Oligocene, caused uplift and block-faulting with the results of dislocating to different levels the weathered rock sections and at the same time favouring a further circulation of oxidized meteoric waters.

Chapter 5: Nonsulphide Zn deposits in the Upper Silesia, Southern Poland

5.1 Introduction

At the beginning of 19th century, Poland was leader in the world for Zn exploitation, with the 40% of Zn world production. In 1980, 220,000 tons of zinc and 50,000 tons of refined lead were produced from Zn-Pb ores in Upper Silesia (Gruszczyk & Wielgomas, 1990), both from sulphide and nonsulphide ores.

Polish nonsulphide ores are currently not exploited. For a long period of time they had no economic significance and were also considered to be a major source of environmental pollution. However, they are far from being exhausted, containing 57Mt of oxide reserves with 5.6% Zn and 1.4% Pb (Kucha, 2005). From my specific point of view, they also represent a good research theme to better understand the chemical-physical processes involved in the formation and emplacement of the nonsulphide Zn deposits in general.

The nonsulphide ("calamine") Zn mineralisation in Upper Silesia, S Poland (Krakow-Silesia mining province) are called "*galman*" in polish, which is a translation of the german name "*Galmei*". They represent the supergene oxidation products of primary sulphide, but it cannot be excluded that some of them may be hydrothermal in origin. The mineralogical composition of nonsulphide ores is not very simple; it includes smithsonite, the most common mineral, but also Fe-smithsonite (so called *monheimite*; Palache et al., 1951; Sitzia, 1965; Bak & Niec, 1978; Bak & Zabinski, 1981), hemimorphite, hydrozincite, Zn-dolomite, cerussite, goethite, anglesite, Zn and Pb hydrated sulphates, phosphates and remnants of primary sulphides (Zabinski, 1960). The *Ore-Bearing Dolomite* (OBD), which replaces Triassic carbonates, represents in >90% of the mineralized areas the prevailing host rock for the nonsulphide ores.

The mining history of Upper Silesia mining province started already in the 12th century with the extraction of "limonite" = oxidized iron and galena ores. Later (13th century) the *galman* deposits were discovered and mined until 1990, when mining activity stopped due of the exhaustion of economically worthy Zn and Pb reserves and because of strong environmental pollution. Now, the mining activity in this district is restricted only to sulphide deposits, whose estimated present reserves consist of 183Mt of sulphides with a grade of 3.8% Zn and 1.6% Pb (tab. 1.1).

Scientific research on calamine ores in Upper Silesia has been carried out intensively in the past (Zabinski, 1960; Szuwarinski, 1978; Radwanek-Bak, 1983; Osman, 1989; Smakowski & Strzelska-Smakowska, 2005). However, some of the mineralogical and geological characteristics of the calamine ores were still not fully explained, as well as their age. Indeed, there is still open uncertainity about the timing of supergene evolution or the Polish sulphide ores, about the origin of part of nonsulphide ores (hydrothermal *vs* supergene), and about the sulphides-nonsulphides relationships.

The origin of polish *galmans* could be better understood if we locate their genetic process in a wider geological setting. In particular, at least for nonsulphide ores whose origin is supergene beyond any doubt, their formation is certainly linked to one or more of the paleoweathering phases, which occurred in this part of Europe from Mesozoic onwards. A contribution to constrain the timing of the supergene deposits, could be given if we take into account the weathering phases which occurred in the Upper Silesia province from Triassic (lower temporal limit for sulphide ore emplacement) until Tertiary and Recent.

A complete mineralogical-petrographical study has contributed to explain the relationships among the different mineralogical phases, between sulphide and nonsulphide minerals and the precipitation sequences. A stable isotope (C, O) study combined with fluid inclusions microthermometry, has produced useful information about the fluids involved in the mineralizing process and about the depositional environment of the calamine deposits. These steps have been preceded by a careful bibliographic investigation of the geological setting and of paleoweathering history in the investigated area.

However, due to the closure or inaccessibility of part of the mines where nonsulphides are present and owing to the virtual absence of good mineralized outcrops, a major problem encountered during this study was not being able, sometimes, to get representative samples *in situ*. Therefore, we have been forced to sample in dumps around the old mine sites. Additional samples were collected in private or mine collections.

5.2 Geological setting of the Upper Silesia

The Krakow-Silesia district (S Poland) is located north of the front of the Carpathian overthrust (fig. 5.1), on the boundary between the Upper Silesia Coal Basin in the south, and the Krakow-Silesia Mesozoic Monocline structures to the northeast. Zn-Pb deposits (primary and secondary) in the Upper Silesia occurred in the sedimentary cover of the Caledonian Krakow-Myszków

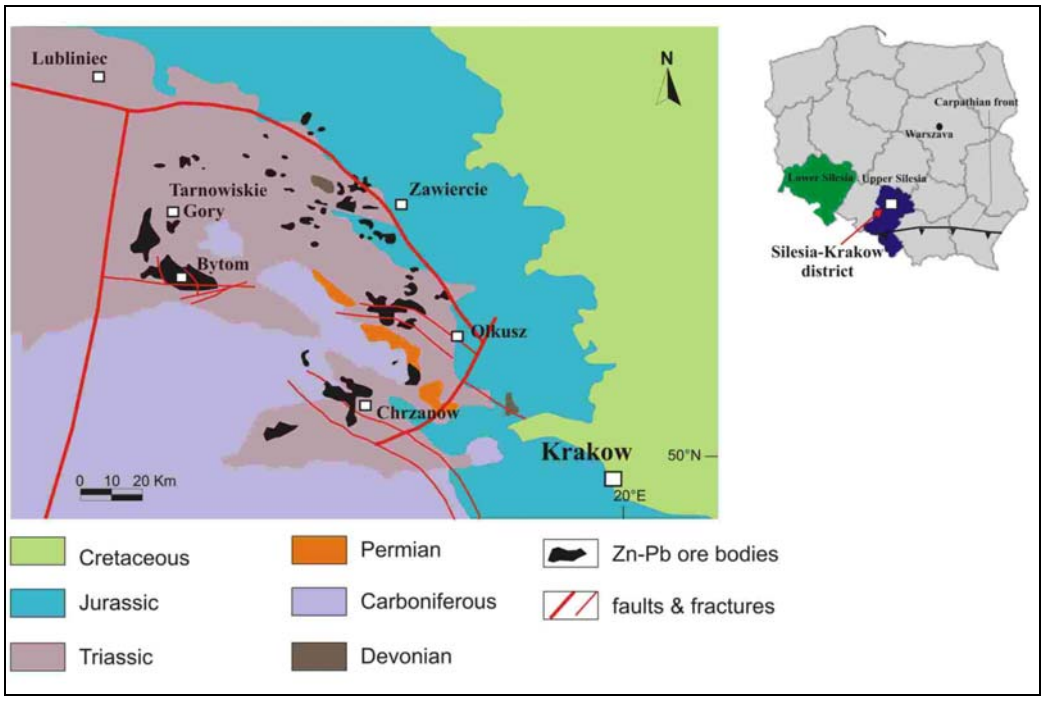

Figure 5.1: Geological map of the Upper Silesia region with location of main Zn-Pb ore deposits.

structural unit, and in the sediments of a Permian Basin, which formed on the north-eastern boundary of the Upper Silesia Coal Basin. They are almost completely hosted by carbonate rocks of Middle Triassic age (Muschelkalk) (figs 5.1 and 5.2).

The Precambrian basement in Upper Silesia was unconformably covered by a complex of Lower Paleozoic rocks, Cambrian-Silurian in age, which were intensely folded along a NNW direction during the Caledonian orogenetic phase (Eikert, 1971). The Caledonian complex is discordantly overlain by Devonian clastic sediments, as well as by Lower Carboniferous (Visean) carbonates and flysch successions (Gorecka, 1993). Namurian tuffites and Westphalian molasse sediments with coal beds represent the upper part of the Paleozoic sequence (Wodzicki, 1987; Gorecka, 1993).

The Upper Silesian Basin represents a foredeep basin of the Hercynian chain superimposed on the lithotypes of the Upper Silesia Massif, which have been subsequently deformed during the Sudetic and Austrian phases of the Hercynian orogeny (Unrug et al., 1971; Kotas, 1982). The Triassic sedimentary rocks hosting ore deposits have been deposited directly on the Palaeozoic terrains into Upper Silesia Basin, nevertheless Permian sediments may be present between them (fig. 5.2). Palaeozoic rocks actually are visible only in depressions.

The Krakow-Myszków structural unit is believed to follow the boundary between the Precambrian Upper Silesian Massif and the Early Caledonian Malopolska Massif (Kotas, 1982; Brochwicz-Lewinski et al., 1983; Bukowy, 1984). It was only marginally involved in the

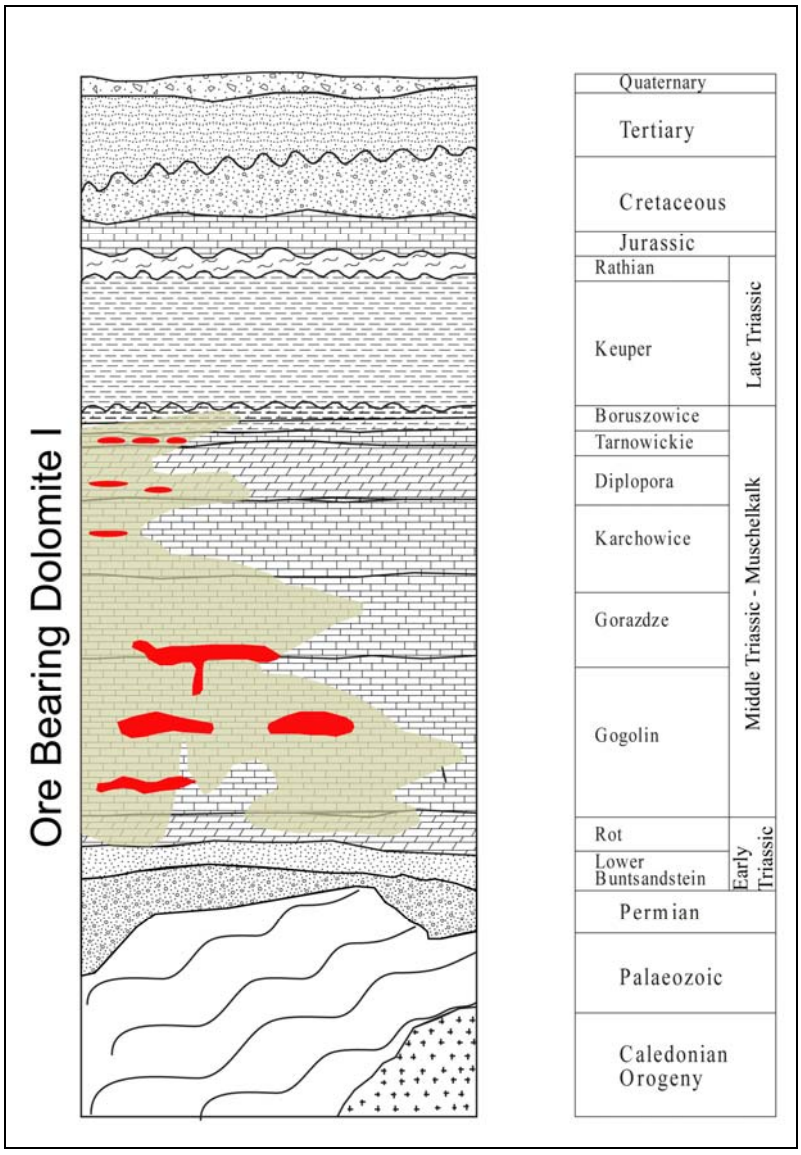

Figure 5.2: Schematic stratigraphic column of Upper Silesia and position of main Zn-Pb orebodies

Caledonian Orogeny, whereas it was uplifted during Hercynian orogeny. In its actual appearance the Krakow-Myszków structural unit represents a block-faulted, positive relief (Przenioslo, 1976; Gorecka, 1993; Unrug et al., 1999).

The Permian and Mesozoic geological evolution of the area was strongly influenced by extensional wrenching and the destabilization of the western and central European crust, related to the break-up of the Pangea super-continent (Ziegler, 1990). During this phase a shear and tensional tectonics was active in most parts of Europe, with a consequent formation of horst and graben structures (Bukowy, 1984; Kiersnowski & Maliszewska, 1985). The effect of this tectonic regime in the Upper Silesia was the formation of the Permian graben, located on the NE side of the Upper Silesia Basin. This graben is filled with continental conglomerates and sandstones, containing gypsum-rich beds (Heijlen et al, 2003).

In the Permian-Mesozoic time interval, the erosion removed part of the Paleozoic lithologies, and karst processes developed on carbonate rocks (Kurek, 1988). This denudation process continued until the Raethian, when epi-continental sediments, mainly consisting of carbonates, were deposited (Sliwinski, 1969; Wyczolkowski, 1982). The first sediments deposited on the Paleozoic rocks consist mainly of the Muschelkalk (Middle Triassic) carbonate lithologies, whose depositional environment ranges from shallow to very shallow marine, although locally well developed sandstone and argillaceous dolostone beds of the Buntsandstein Formation (Lower Triassic) were deposited directly on Paleozoic rocks (Moryc, 1971) (fig. 5.2). The Muschelkalk terrains are actually present both in the Krakow-Silesia Monocline (north-eastern part of the district) and on the Krakow-Myszków structural unit. The Muschelkalk in the studied region consists of the Gogolin, Goradze, Karchowice, Diplopora, Tarnowickie and Boruszowice members (Gruszczyk & Wielgomas, 1990; Szuwarynski, 1993; Kucha, 2003; Leach et al., 2003) (fig. 5.2), which were originally represented by limestone or early diagenetic dolomite, mainly in full (Bogacz 1975; Bogacz et al. 1972; Krzyczkowska-Everest, 1990; Gruszczyk & Wielgomas, 1990; Gorecka, 1993). The Tarnowice and Boruszowice limestone members have beenrecognized mostly in the southern Chrzanòw area (Szuwarynski, 1993). Locally the Muschelkalk is covered by non-marine claystones of the Keuper Formation (Upper Triassic); among them there is a local unconformity (Sass-Gustkiewicz et al., 1982), linked to the erosion and paleokarst processes, which affected the Muschelkalk rocks after deposition (Wilk, 1989 and references therein; Motyka, 1998). Later, a new epoch of sub-aerial exposure, paired with extensive karstification was established in the entire region during the Early and Middle Jurassic (Sass-Gustkiewicz et al., 1982, Leach et al., 2003).

Formally, in the Muschelkalk succession also the “Ore-Bearing Dolomite” (OBD), which is the prevailing host rock of the ore deposits, has been included. Two generations of Ore-Bearing Dolomite have been described (Szuwarzynski, 1978; Leach et al., 1996a, 2003. Hejilen et al., 2003): the first (named OBD I), consisting of a pre-ore burial dolomite poor in Fe and Zn replacing early diagenetic dolomite and/or limestone, is quite widespread in the whole region and represents the prevailing type. The dolomitisation process, which formed the first Ore-Bearing Dolomite occurred much earlier than ore emplacement, surely after the deposition of the Muschelkalk, and before that of the Jurassic sediments, as confirmed by field evidence already by Sass-Gustkiewicz et al. (1998). A fluid inclusion study showed that the fluids involved in the formation of the most widespread type of OBD (OBD I) had different salinity, temperature and composition with respect to the fluids depositing the sulphide ores (Kozlowski, 2001). The second one (named OBD II) is a sparry dolomite, very rich in Fe and Zn (Bak, 1986, 1993),

which forms halos usually less than several hundred meters wide around the ore bodies. However, a detailed petrographic study on these dolomite generations has never been performed by the former authors.

Also the paleomagnetic studies (Symons, 1995) on the Ore-Bearing Dolomite revealed the presence of two distinct dolomite generations, thus confirming the theory of the above mentioned authors: a first dolomite, more widespread (related to a pre-ore dolomitizing event), shows a Middle to Upper Triassic signature, while a second dolomite (a sparry one, contemporaneous or shortly preceeding sulphide ore emplacement) has a Tertiary imprint.

Sass-Gustkiewicz (1998) and Krzyczkowska-Everest (1990) have distinguished three main dolomite generations: 1) crypto-microcrystalline dolomite replacing the micritic early diagenetic dolomite and/or limestone, and forming the real host rock of the mineralisation (disseminated sulphides have been observed); 2) coarser crystalline sparry dolomite; 3) Fe-Mn sparry dolomite and ankerite (gangue minerals) in veins, paragenetically associated with sulphides. The authors have frequently observed numerous zoned crystals with cloudy centers composed by the first dolomite generation and clear rims of sparry dolomite.

After a petrographic study, Hejjlen et al. (2003) confirmed the existence of two generation of dolomite: iron-poor (dolomite generation I) and iron-rich (dolomite generation II). The iron-poor generation, replacing early diagenetic dolomites and limestones, occurs as cloudy centers of planar-S to nonplanar dolomite crystals while the iron-rich dolomite is represented by clear rims of coarser crystals, nonplanar dolomite cement or big crystals in veins and fractures. In the last case, dolomite is associated with sulphide minerals, and probably could be compared with the Fe-rich sparry dolomite reported by Krzyczkowska-Everest (1990). Under cold cathodoluminescence observation, dolomite I showed blotchy brown, brown-red to absent luminescence and dolomite II a red to bright red zoned luminescence (Heijlen et al., 2003). These authors measured the homogenisation temperatures and salinities of primary fluid inclusions in both dolomite generations: dolomite generation I had T_h constrained between 50 and 104°C and an extremely variable salinity (0-22wt% $CaCl_2$); dolomite generation II had T_h between 61 and 95°C and salinity between 20-22 wt% $CaCl_2$. However they think that most of the inclusions in the high temperature range, in both dolomite generations, may have leaked. The reason for this conclusion is derived from the different temperatures in the dolomites calculated from stable isotopes. Therefore, they consider that dolomite generation I, predating mineralisation, was precipitated at temperature of ~50°C. The Zn-Pb sulphide mineralizing process started with the recrystallization of this dolomite generation and was accompanied by the precipitation of dolomite generation II, at temperature of ~80°C.

After this brief review, it results that a relative uniformity (with some differences, though) exists among all these authors (Sass-Gustkiewicz, 1998; Krzyczkowska-Everest, 1990; Narkiewicz, 1993; Leach et al., 1996a, 1996b; Heijlen et al., 2003) about the paragenesis of the dolomites. Thus, we will use the term OBD I referred to the earlier generation, which pre-dates the main mineralizing event, and OBD II for the dolomite generation associated with sulphide ores. This late dolomite phase could represent, together with the barite- and (Fe)-smithsonite halo, a hydrothermal alteration of host rock linked to the main mineralizing event. It is characterized by higher metal content (Fe, Mn and Zn) with respect to OBD I. A distinct variety of metal-rich dolomite, mainly containing Zn percentages, has been recognized in the Chrzanòw area (Zabinski, 1986).

The distribution of OBD I is controlled by local geological characteristics: fractures, faults, bedding or stratigraphic contacts between different lithologies. OBD I was developed more or less horizontally over a large area, forming tabular bodies, which replaced partly or totally the Lower Muschekalk rocks. In fault zones OBD I is also present, forming completely discordant bodies, as in the Olkusz area. The Ore Bearing Dolomite I replaced the Goradze, Terebratula and Karchowice members and it is confined between the Lower Gogolin Beds (below) and the Diplopora Dolomite (above). The age of this main dolomitisation process is not very clear, but it has been hypothesized that it should be comprised between Triassic and Upper Jurassic (Petrascheck, 1918; Bogacz, 1975; Bogacz et al., 1972; Sass-Gustkiewicz, 1982).

The Triassic sediments are covered only locally, near Chrzanòw and in the Krakow-Silesia Monocline, from limestones and marls Upper to Middle Jurassic in age. On these terrains were deposited unconformably some hundreds of meters of Cretaceous sandstones, marking the beginning of the early phase of Alpine orogeny (Leach et al, 2003). Indeed, the Krakow-Silesia area was involved in the Alpine Orogeny, which was responsible of the actual conformation of the Carpathian chain. This orogeny started in the Middle Cretaceous and lasted until Recent. We can distinguish two important Alpine tectonic phases affecting this area (Krokowski, 1984; Gorecka, 1993): Early Alpine (Cimmerian-Laramide) and Late Alpine (Early Tertiary - Miocene).

The Early Cimmerian phase produced broad deformations of the Triassic terrains and a fault networks with minor offsets, which often represent reactivated old tectonic lines of the basement, (Gorecka, 1993). More intense faulting was ascribed to the Laramide phase, which produced an extensive network of faults and fractures and was responsible of the final structure of the Krakow-Silesia Monocline (Burzewski, 1969; Kutek et al., 1972). During the Tertiary, this area was characterized again by block faulting caused by Late Alpine tectonic phase, which resulted

in a fault network with directions striking N-S and E-W and vertical offsets around 50-70m (Gorecka, 1993; Leach et al., 1996c). These dislocations may have caused short periods of emersion, with related erosion and weathering (affecting preferentially the Triassic carbonate lithotypes), alternated to local ingressions. According to Szuwarzynski (1978) the climatic conditions in the Lower Tertiary were very favourable to erosion and dissolution, thus facilitating the removal of Mesozoic and Paleogene sequences, and creating erosion surfaces paired by a deep karst morphology. Among these weathering phases, one of the most intense has been recorded before the Middle Miocene (Tortonian) transgression (Panek et al., 1975, 1976; Sobczynski et al., 1978, Gustkiewicz et al., 1982). The effect of this karsting event was the formation of numerous sinkholes in Triassic limestone and dolostone. These sinkholes were then filled by argillaceous residues derived from dissolution of Triassic (mainly), Jurassic and presumably also Cretaceous carbonate rocks, by dolomitic sand derived from the disintegration of Ore-Bearing Dolomites, fragments of cherts, fine-grained quartz sands, calcareous tufa (Panek et al., 1975) and fragments of calamine ores (Szuwarzynski 1978). These paleo-cavities contain also galena concentrated mainly in the lower part of the sinkhole. The sinkholes are then covered by Tortonian marine clays, especially in the Charzanow Trough (Radwanski, 1968; Alexandrowicz, 1969; Szuwarzynski 1978). A discontinuous Quaternary cover is relatively widespread in the whole region (Niec, 1980; Niec et al., 1993).

5.3 Ore deposits in the Upper Silesia

The Upper Silesia mining province represents one of the districts better endowed with zinc (Zn), lead (Pb) and silver (Ag) resources in Europe. The mining go back to the beginning of the Polish Kingdom, at least to the 11th century. In the Krakow-Silesia mining province different kinds of deposits were mined. In this area four principal kind of ore deposits are present: Zn-Pb sulphides, Fe(hydr)oxides, Ag-bearing galena and last, but not least, nonsulphide ore deposits. The 19th century was a very healthy period for mining exploitation in Europe, including Poland, owing to the development of new technologies for the treatment of sulphide ores and the enrichment processes of several metals. An important increase of mining activity in Poland has been also recorded after World War II, when a evaluation of Zn-Pb deposits was made in Orzel Bialy, Marchlewski, Warinsky, Novi Dwor and Matylda mines and adjacent areas, and new mines were initiated: Boleslaw (1953), Trzebionka (1962), Olkusz (1968) and Pomorzany (1974). The annual production of Zn-Pb ores in the Krakow-Silesia district passed from about 500,000 tons

during inter-war period, up to about 5Mt in the 1980 (Gruszczyk & Wielgomas, 1990).

As discussed above, four principal types of ores are present in Krakow-Silesia district, but in accord to the purposes of this work, I will dedicate my attention particularly to Zn nonsulphide ore deposits. In order to explain their nature and genetic evolution, it is necessary to describe firstly the main characteristics of the primary Zn-Pb sulphide deposits.

5.3.1 Zn-Pb sulphide ores

Even if a detailed description of the nature of primary base metal ores in Poland is not the principal aim of this study, a short review of their setting and still debated emplacement timing, could be crucial to understand the origin and age of nonsulphide deposits.

Zn-Pb sulphide concentrations in the Upper Silesia district are located on both sides of the Permian basin, at the northeastern edge of the Upper Silesia Coal basin and above the Krakow-Myszków orogenetic zone. Mining activity started in the 12th century and it is now still active. It has been estimated that until 1994 there has been a production of about 30Mt of Zn + Pb metal (Leach et al., 2003). For the last twenty years, mine production was 4 to 5 million tonnes of ores per year, including 140-250 thousand tons of zinc and 40-90 thousand tons of lead (Gruszczyk & Wielgomas, 1990). Presently, exploitation is active in four mines, three of which located in the eastern Olkusz district (Boleslaw, Pomorzany and Olkusz) and the other more in the south, near the town of Chrzanòw (Trzebionka) (fig. 5.3a).

Sulphide ores occur mostly in the Ore Bearing Dolomite, and are related to epigenetic replacement of Muschelkalk carbonates (figs. 5.2 and 5.3b). However, small base-metal concentrations are also present in carbonate rocks ranging in age from Devonian to Upper Jurassic, as well as along Tertiary faults (Gorecka, 1993; Szuwarzynski, 1993, 1996; Leach et al., 2003).

The location and geometry of the mineralized bodies reflect the relationships between faults, carbonate dissolution and host rock permeability. Several authors (Sass-Gustkiewicz et al., 1982, 1998; Leach et al. 1992, 1996b, 1996c, 2003) have mentioned the existence of the two most important kinds of mineralisation, both emplaced in Triassic terrains: (a) replacement bodies and (b) in-filling of open-spaces occurring in fractures and breccias. However, a real distinction between the two mentioned types is often difficult, because commonly many mineralized breccias represent the result of a selective replacement of pre-ore breccia zones.

Replacement ores essentially occur as tabular and/or stratabound bodies, which locally show a thickening in correspondence with faults or dissolution cavities. The lateral extension of these

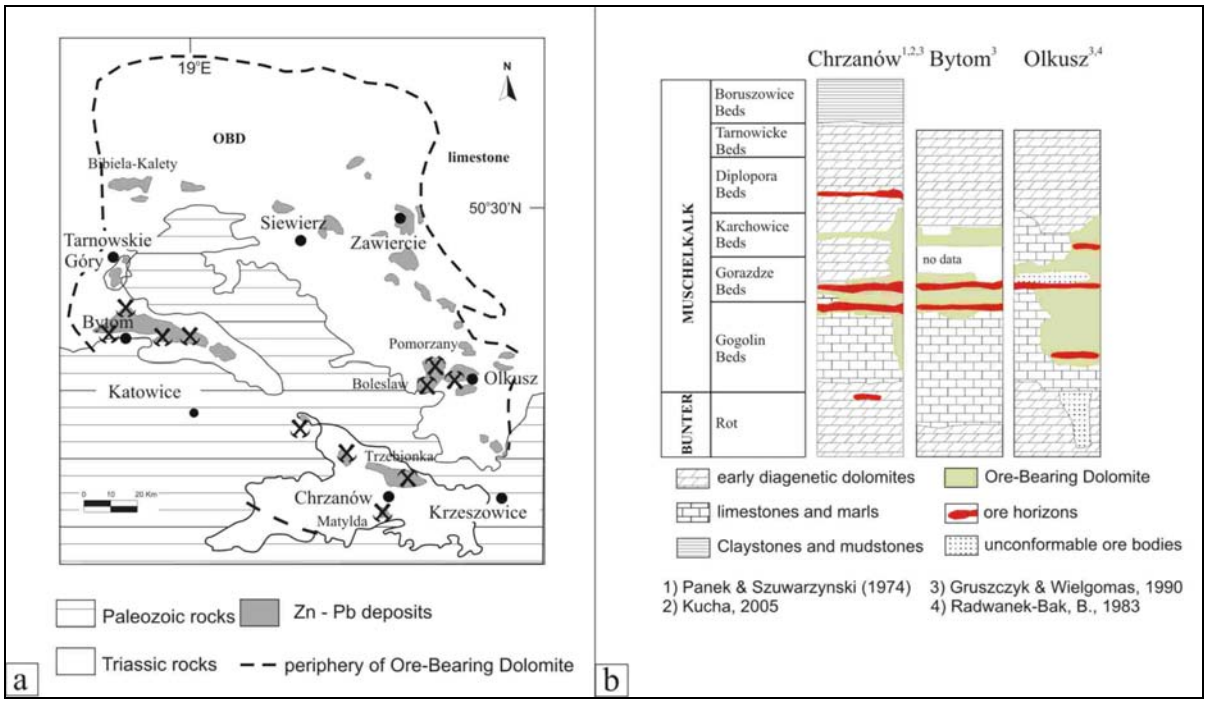

Figure 5.3: a) Schematic geological map of the Krakow-Silesia mining district. In the map are shown both exploited and undeveloped deposits. b) schematic stratigraphical columns of three important mineralized areas.

bodies can be considerable. In the Bytom area, in the western part of the mining province, three ore levels have been recognized, which extend for a few km and are 3-5 m thick (Szuwarynski, 1996). Other deposits occur as infilling of empty spaces within dissolution/collapse breccias or even as replacement of its matrix.

The mineralogical assemblage of the sulphide deposits is very simple: it includes sphalerite, galena, marcasite, and pyrite with associated sulphoarsenides and siderite-smithsonite bands (Kucha, 2005). The ores show colloform and banded textures in the breccia zones (fig. 5.5a), while in the replacement bodies the typical "rythmites" texture has been frequently observed (fig. 5.5b). For a more detailed description of the sulphide ores see Sass-Gustkiewicz et al. (1982), Sass-Gustkiewicz (1996), Gorecka (1996) and Leach at al. (1996a, 1996b).

Sulphide bodies are surrounded by a thin halo of barite + Fe-smithsonite and by a large halo of OBD II (Bak, 1993; Leach, 2003).

An epigenetic hydrothermal origin of the Silesian deposits is by now almost completely accepted, but their emplacement age is still highly controversial.

Sass-Gustkiewicz et al. (1982, 1998) mention three different types and locations of the sulphide deposits in Upper Silesia: (1) ore veins in Paleozoic and Pre-Cambrian rocks; (2) replacement- and karst-filling bodies in the Ore-Bearing Dolomite (most important), (3) galena ores in pre-Miocene sinkholes hosted in Triassic carbonate rocks (Bogacz & Sobezynski, 1972; Panek & Szuwarinski, 1975). According to the former authors, the ores in the Paleozoic rocks are related

to late Paleozoic igneous activity and pre-date Triassic. About the timing of the main mineralizing event, which caused the precipitation of most sulphides, Sass-Gustkiewicz et al. (1982, 1998) have proposed a pre-Neogene age based on the presence of altered clastic fragments of galena in pre-Miocene sinkholes (Michael, 1913; Bogazs et al., 1970; Panek & Szuwarinski, 1975), and on the observation of Zn-Pb ores displaced by Neogene faults (Sass-Gustkiewicz et al. 1982). From field evidence, they recorded that a Jurassic unconformity cuts, and therefore post-dates the OBD (no difference was made between OBD I and OBD II). Therefore they concluded that the main mineralizing event was pre-Jurassic in age.

Three distinct times were then hypothesized by Sass-Gustkiewicz et al. (1982) for the mineralizing processes: (a) the end of Paleozoic, (b) a period between the end of the Muschelkalk and the Middle Jurassic (main event), (c) Cretaceous and/or Lower Tertiary. The same authors consider that a hydrothermal ascending fluid moving from the Krakow-Myszków area, entering the Triassic acquifer along the north-eastern margin of the Upper Silesia Basin and then spreading south and southwest through the more permeable formations, was responsible for the emplacement of the most important sulphide ores. Its hydrothermal origin is confirmed by the presence of two-phase fluid inclusion (Kozlowski et al., 1995).

After Leach et al. (1992, 1996a, 1996b, 1996c, 2001), all the sulphide deposits of Upper Silesia (from the Devonian- through Mesozoic and Tertiary hosted sulphides) were formed in a single mineralizing event lasting a relative short time (~50Ma) in Lower Tertiary, as confirmed by isotopic and geochemical studies (Church et al., 1996; Leach et al., 1996a, 1996c; Viets et al., 1996). Indeed, according to these studies, the ores in both Jurassic and Triassic terrains have indistinguishable isotopic and geochemical composition. A Tertiary timing of ore emplacement is in agreement with paleomagnetic results on massive sphalerite and galena (Symons et al., 1995), which point to a Tertiary pole position. After the quoted authors, also other indications seem to confirm a Lower Tertiary age for the sulphide ores. These are: the presence of normal faults, which dislocate Upper Jurassic rocks and are cut by tabular ore bodies in the Klucze region near Olkusz (Gorecka, 1993) and the dislocation of some ore deposits by younger Alpine faults of Miocene age (Leach et al., 2003).

Another point of disagreement between the genetic concepts of Leach et al. (1996c) and Sass-Gustkiewicz et al. (1982) concerns the origin of the breccias hosting the ores. Indeed Leach et al. (1996a, 1996c), recognized different kinds of breccias hosting the sulphide minerals, considering most of them as pre-ore with only a limited amount of breccias produced during sulphides deposition. Dissolution/ collapse breccia in the Muschelkalk carbonate rocks can be related to disconformities at the top of Muschelkalk, before the deposition of Keuper and Rhaetian

sediments (Leach et al, 2003) or they could be related to a period of sub-aerial exposure and deep karsting in Middle Jurassic (Glazek, 1989). On the contrary, Sass-Gustkiewicz et al. (1982) hypothesize a coeval origin for OBD, breccia formation and the main mineralisation event (see above).

Several microthermometric study on fluid inclusions in sphalerite from the Upper Silesia district (Kozlowski, 1995; Kozlowski et al., 1996; Gorecka et al., 1996; Leach et al., 1996c) reveal salinities of the mineralizing fluid constrained between 0 and 23% eq. wt% NaCl and homogenisation temperatures (T_h) between 40 and 160°C. A pressure correction of 5-10°C has been applied, based on the estimated maximum burial depth of the deposit (500m) in the Tertiary. Both temperature and salinity show a positive correlation with depth. These considerations led Leach et al. (1996c, 2003) to establish a regional geological-hydrological model to explain the fluid flow and ore emplacement. After the latter authors, the fluids should have been moved from the Carpathian orogenic chain in a gravity-driven system or were originated from the compaction of the sediments contained in the foredeep basins of the same chain. Middle Tertiary coincides with the maximum uplift of the Carpathian chain (Burchfield, 1980) and with the higher rate of deposition in the foredeep where the Miocene molasses were accumulated. The old faults in the Krakow-Myszków zone should have provided the pathways for the ascending fluids charged with metals into the Mesozoic rocks (Leach et al., 1996c). At the local scale, the extensive horst and graben structure should represent the most important control factor for the ore emplacement. In the mineralizing process at least two different fluids were involved: saline formation brines and meteoric water, which were mixed during ore formation (Kozlowski, 1994).

On the contrary, Heijlen et al. (2003), after analysing the fluids in the inclusions from several ore and gangue minerals, concluded that these were more evolved than the brines of the Upper Silesian Coal Basin, so far considered as the source of the mineralizing fluids (Sass-Gustkiewicz et al. 1982). The fluid probably originated from seawater evaporation during Permian or Triassic and then migrated downward in the sediments, thus causing a strong fluid-rock interaction. The same authors, on the base of Rb-Sr direct dating of sphalerite, assigned a 135 ± 4Ma age to the main mineralizing phase, thus considering both the hydrothermal activity and ore deposition as caused in response of Early Cretaceous extension connected to the opening of the Northern Atlantic Ocean.

5.3.2 Nonsulphide Zn ores

Before describing in detail the nonsulphide ore deposits in Poland, we need to explain the meaning of some words of common use among the local geologists. The polish nonsulphide Zn deposits are called *Galman*, a translation of the german word *Galmei (=Calamine)*. In the polish literature we can find either *Galman* or *Galmei*. Under this name are comprised a mixture of Zn and Pb carbonates {smithsonite=$ZnCO_3$; Fe-smithsonite=$(Fe,Zn)CO_3$ (so called *monheimite*; Bak & Niec, 1978); cerussite=$PbCO_3$; Zn-dolomite, Pb-aragonite (so called *tarnowitzite*; Zabonski, 1960)}, goethite, hemimorphite {$Zn_4(Si_2O_7)(OH)_2.H_2O$}, and relicts of primary sulphides. The polish authors (Zabinski, 1960; Kucha, 2005; Smakowski & Strzelska-Smakowska, 2005) distinguish among different types of *galman* on the base of their prevailing mineralogical composition: (1) *smithsonite galmei*, dominated by smithsonite (the most common type), (2) *monheimite galmei* (ferrogalmei), described mainly from the Matylda mine, and (3) *dolomite galmei*, where Zn-dolomite is the most important economic mineralogical phase (Zabinski, 1960). These three types are assigned to the category of the *carbonate galmei*. A further subdivision has been made between a so-called *white galman*, with a low Fe^{+3} content, and the highly ferruginous *red galman,* where abundant goethite occurs. The latter can pass laterally to real "limonite" (a mixture of Fe-oxides and hydroxides) deposits. In the *white galman* the Fe-smithsonite ("monheimite") is particularly abundant. But, as we will discuss in the next chapters, the distinction between *white and red galman* has been mainly based on their differently hypothesized origin. A supergene origin is commonly accepted for *red galman,* whereas a hydrothermal origin, possibly linked to a late phase of the main sulphide mineralisation, has been advanced for the *white galman*. The opinions and the proofs reported in the geological literature on this theme are far for being exhaustive and call for further investigations. We will present our mineralogical-petrographical and geochemical data on *red* and *white galman* as a contribution to the discussion.

Nonsulphide Zn ore deposits are widespread in the Krakow-Silesia mining province. They occur in several districts (fig. 5.3a): in the Trzebinia-Kreszowice-Olkusz-Siewierz belt, in the Tarnowskie Gory (Fryderyk mine), in the Bytom trough (Nowy Dwor, Orzel Bialy, Warynski, Marchlewski, Dabrowka mines), in the Chrzanòw trough (Matylda, Galmany, Trzebionka mines) and in the Olkusz region (Boleslaw, Olkusz, Pomorzany mines). The Zn oxidized deposits occur in form of layers, nests and lenses throughout the whole thickness of the Ore-Bearing Dolomite I, from the basal contact with the Gogolin Limestone beds up to the upper contact with overlying Diplopora Dolomites. The relationships between the primary sulphides and oxidation minerals are variable depending from the different areas where the latter occur.

In the western part of the district (Tarnowiske Gory and Bytom area), there are different types of ores: "limonite"=oxidized iron ore, galena, sulphides and calamine. Precisely, galena and limonite prevail in the Tarnowiskje Gory district, while the calamine and sulphide ores are particularly abundant in the Bytom area. The latter represents the oldest mining district in the Upper Silesia. Here the mining activity started in the 12th century. From the geological point of view, the Bytom area represents a trough 14 km large and 2-4km wide, where Palaeozoic and Permo-Carboniferous rocks are covered by Triassic terrains (Gorecka, 1993). Sulphide ores are stratabound, from 2 to 2.5m thick, and located at the bottom of OBD I, precisely in the Goradze Beds (Gruszczyk & Wielgomas, 1990) (fig. 5.3b). The calamine bodies, are developed immediately over the sulphides, but also several meters above them (Smakowski, 2005), at the contact between OBD I and the Gogolin Limestone beds, as well as at different levels in the OBD.

Pomorzany, Olkusz and Boleslaw mines are located in the Olkusz area, pertaining to the Krakow-Silesia Monocline. The Pomorzany deposit consists of elongated nests and lenses few hundreds meters long and several meters thick. In this deposit the relationships between sulphides and nonsulphides are not very clear. The deposit is completely below the surface, from 200m a.s.l. to 242m a.s.l., and it is covered by Triassic claystones.

The Olkusz deposit consists mostly of nests, and, in minor abundance, of lenses and strata hosted in several horizons ranging from the Lower Gogolin Beds to the Karchowice Beds (Radwanek-Bak, 1983; Gruszczyk & Wielgomas, 1990). Remnants of sulphides in the weathered zone represent small bodies scattered in the oxidized groundmass; the contact between sulphide and nonsulphide bodies is gradational.

A peculiar geological setting occurs in the Boleslaw deposit. Here the main ores are hosted in a horst and graben structure delimited by normal faults, with direction approximately E-W, probably linked to (or reactivated by) the flexural extension during Carpathian thrust loading (Leach et al., 2003). The ores (sulphides and nonsulphides) are hosted by the Ore-Bearing Dolomite I replacing the Gogolin and Lower Muschelkalk carbonates, but smaller bodies were found also in the Röt sediments (fig. 5.4a). Other non-economic bodies have been discovered in the Lower Triassic, in Permian conglomerates and in Carboniferous sediments (Niec et al., 1993). The ore bodies located in the Muschelkalk are stratabound, few meters thick, and are developed horizontally. The bodies in the Röt form nests 30m in thickness, which occasionally reach down to the lower strata of the Gogolin Beds (Niec, 1980). Several authors have described the sulphide and nonsulphide deposit setting at Boleslaw (Radwanek-Bak, 1982, Smakowski, 2005). In the uplifted blocks (horsts) are located only the nonsulphide deposits, which can be

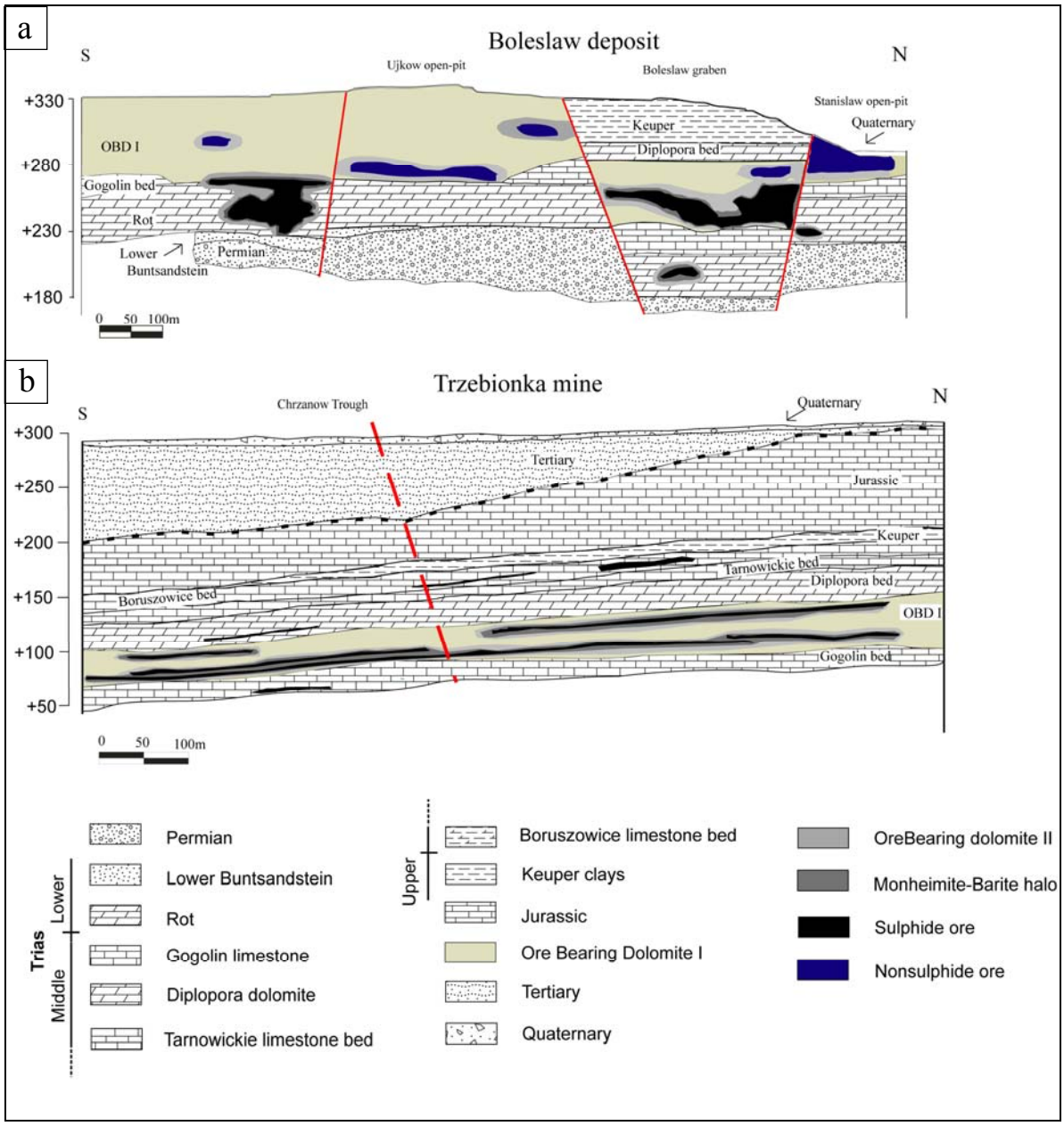

Figure 5.4: a) N-S schematic cross-section of the Boleslaw deposits; b) N-S schematic cross-section of Trzebionka mine.

seen either in outcrop or underneath a thin Quaternary cover. In the graben areas the nonsulphides are located directly under the Keuper sediments and commonly overly the primary sulphide ores. In these areas the depth of the oxidation front is not uniform, being constrained between 279m a.s.l and 313m a.s.l, and the intensity of the oxidation is variable both vertically and horizontally (Radwanek-Bak, 1982).

The Chrzanòw trough is located in the southern part of the mining district and is elongated in a NW-SE direction. It is situated at the boundary between the Krakow-Silesia monocline and the

Upper Silesian Trough. Triassic rocks are preserved solely in the synclines and are unconformably covered by Jurassic and Miocene sediments. An uninterrupted Quaternary cover is widespread in the whole area. In this district, sulphide exploitation is currently active only in the Trzebionka mine. In this mine-site, as in the other districts, the OBD I is the principal host rock for the ore. However, small base metal deposits have been recognized also in Jurassic, Tertiary and Quaternary rocks (Szuwarzynski, 1993). The sulphide ores form several elongated bodies parallel to the bedding in the Bünter and Muschelkalk dolomites, but only horizons hosted in Lower Muschelkalk strata were important from an economic point of view (Gruszczyk & Wielgomas, 1990) (fig. 5.3a). The sulphide horizons hosted in OBD I present an envelope of Zn-dolomite and Fe-dolomite at the contact with the barren host rock (Kucha, 2003; Kucha & Czajka, 1984) (fig. 5.4b). Especially in this district, banded smithsonite-siderite preceding sulphides precipitation has been recognized with fluid inclusions temperatures of 95°C. In the Trzebionka mine the ore exploited under the name of "calamines" form a non-continuous layer located immediately above the sulphide bodies; however, nests of calamine were also observed in the midst of sulphide ores (Smakowski & Strzelska-Smakowska, 2005).

In the Matylda mine the ores consisted of several horizons mainly located in the Ore-Bearing Dolomite I (Panek & Szuwarzynski 1974; Kucha, 2005). Three important mineralized horizons have been recognized in this mine: horizon III (*upper mineralized body*) hosted in Diplopora Dolomite; horizon II (*lower mineralized body*) hosted in the Goradze Beds; horizon I, positioned at the boundary between the Gogolin and Goradze Beds. The horizons II and III are constantly present in the mining district, while the horizon I occurs only in its western part. The upper level (horizon III) consisted mostly of galena whereas the lower ones had calamines prevailing. The contact between the ore horizons and dolomite host rock follows the primary stratification of the rock. In the lower horizons (II) the ore types "*white galman"* and "*red galman"* have been described by Panek & Szuwarzynski (1974).

The "*white galman"*, has been recorded not only in the Matylda mine, but also in other deposits of the mining province, as in Bytom (Zabinski, 1960, 1986; Panek & Szuwarzynski 1974; Kucha & Czajka, 1984; Kucha, 2005). After these authors, the distinction between *white* and *red galman* is based on its macroscopic appearance (lighter *vs* red colour) and on other mineralogical and geochemical characteristics. The *white galman* (quite rare) is characterized by a low Fe^{+3} content while the *red galman* is much more widespread and associated to abundant goethite. I can anticipate from my own work, that from a mineralogical point of view the *white galman* contain also abundant Fe-smithsonite and Zn-dolomite compared to *red galman*. At Matylda the *white galman* is located mostly in the outer part of the deposit or form patches in the *red galman*,

with a gradational passage between them (Smakowski & Strzelska-Smakowska, 2005).
Also in the Matylda area detrital fragments of calamine and eluvial galena have been observed in the Paleogene continental sediments filling a paleochannel feature (Szuwarzynski, 1978).
Actually, the origin of *white galman* is far to be fully explained. Therefore, in the following steps of this work, with the aid of petrographic observations and stable isotope measures, combined with a fluid inclusions study, I will try to add my contribution to the solution of this problem.
Another big issue that is still unresolved, is the timing of secondary nonsulphide ores. Indeed, it is already well known that in Upper Silesia the weathering processes on the Triassic rocks hosting the primary sulphides, have acted in several distinct periods of time, starting from Upper Mesozoic until to the Present. However, it is still unknown in which periods these processes were stronger, and particularly, when they attacked the primary sulphides, in order to cause the formation of the main bulk of the supergene nonsulphide Zn deposits. Moreover, the solution of the above-cited problems will give also an important contribution to constrain the age of the primary sulphides, in particular as far as concerns the setting of the uppermost time limit for their emplacement, a still hotly debated subject.

5.4 Mineralogy of nonsulphide ores

Polish calamines show a very ample range of texture and morphologies. They occur as earthy (figs. 5.5d, i, k) to crystalline-looking rocks (figs. 5.5c, h, l), crystal aggregates (fig. 5.5e) and concretions in cavities (figs. 5.5f, g). Breccia and replacement textures are very common.
In literature, a clear mineralogical distinction is made between the two types of Zn nonsulphide deposits present in Krakow-Silesia mining province. The *red galman* type seems to be dominated by smithsonite and goethite, and in minor abundance by hemimorphite and cerussite, while the peculiar feature of the *white galman* type is the high content of Fe-smithsonite ("monheimite"). The mineralogical assemblage of the *white galman* from the Matylda mine includes, in order of abundance: smithsonite, Zn- dolomite, Fe-smithsonite with associated galena, Mn- and Fe-hydroxides and clay minerals of the montmorillonite group (tab. 5.1) (Grszczyk et al., 1963). Quartz enrichments were often found in these levels.
After the analyses carried out in this work, the most important mineralogical phases recognized in the nonsulphide Zn deposits in the Upper Silesia are: smithsonite, Zn-dolomite, goethite and Fe- Mn-(hydr)oxides (tab. 5.1; figs. 5.5, 5.6, 5.7). Hydrozincite has been found in some samples

Table 5.1: XRD analyses of the samples from the Upper Silesia district (S Poland); mineral symbols are in order of abundance.

	Sample	Mineral(s)		Sample	Mineral(s)
Boleslaw	CV05-2	do, cc, qz, sa	Pomorzanj	CV05-24	hem, cc, do, go
	CV05-4	cc, sm, go, qz, do		CV05-25	do, qz
	CV05-6	cc, do, go, eps		CV05-53	do, qz, go, sm
	CV05-7	do, cc		CV05-80	hem, hyz, sm, sph, ce, ga
	CV05-8	cc, qz, go, hyce		CV05-83	ga, sph, qz
	CV05-9	do, sm, go	Matylda	CV05-62	sm, do, qz, sa, nk
	CV05-10	cc, sm, do, go, qz, mel, scl		CV05-63	sm, sa
	CV05-11	do, sm, go		CV05-65	Fe-sm, sa, do
	CV05-14	dol, sm, hem, go, cc		CV05-73	do, go
	CV05-15	do, sm, hem, qz, sa		CV05-74	do, go
	CV05-17	min, sm, do, go, cc, qz		CV05-75	do, go, qz
	CV05-44	dol, go		CV05-81	sm, do, qz, sa
	CV05-45	cc, sm		CV05-85	do, qz, sm, go, ang
	CV05-49	do, go, cc, qz, sm		CV05-86	sm, do, sa, go, qz
	CV05-50	do, sm, sch	Olkusz	CV05-64	do, sm, sch
	CV05-51	do, cc		CV05-66	hem, sm
	CV05-51b	do, sm, go		CV05-67	sm, go, qz, hyce
	CV05-58	dol, sm, qz, go, sph, ga		CV05-68	ce, ga
	CV05-59a	sm, dol, go, sa, qz	Bibiella	CV05-27	sm, sa
	CV05-77	cc, dol, sm, go, hyce		CV05-28	do, sm
	CV05-78	cc, do, sm, go		CV05-29	cc, do, go
	CV05-79	do, cc		CV05-30	sm
Trzebionka	CV05-18	do		CV05-32	sm, go, do, gy
	CV05-19	do, sa, go, gy		CV05-33	sm, do, hem, sa
	CV05-20	do		CV05-34	cc, do
	CV05-52	do, cc, go, hyce		CV05-35	do, cc, go
	CV05-55	cc, ar		CV05-37	go, he
	CV05-56	sm	Szczesé Boze	CV05-46	do, cc, go, qz
	CV05-57	hem	Zabinski coll.	CV05-69	cc, go
	CV05-60	cc		CV05-70	hyz, do, go, sa
	CV05-82	sm, go, sph, ga, ce, nk		CV05-71	sm, hem, ga, sph
Bytom	CVO5-54	do, nk		CV05-72	do, cc, sm, bass, gos

*Abbreviations: ang = anglesite, ar = aragonite, bass = bassanite, cc = calcite, ce = cerussite, do = dolomite, eps = epsomite, ga = galena, go = goethite, gos = goslarite, gy = gypsum, he = hematite, hem = hemimorphite, hyce = hydrocerussite, hyz = hydrozincite, mel = melanterite, min = minrecordite, nk = nantokite, py = pyrite, qz = quartz, ros = rosasite, sa = sauconite, scl = sclarite, sch = schafarzikite, sm = smithsonite, sph = sphalerite.

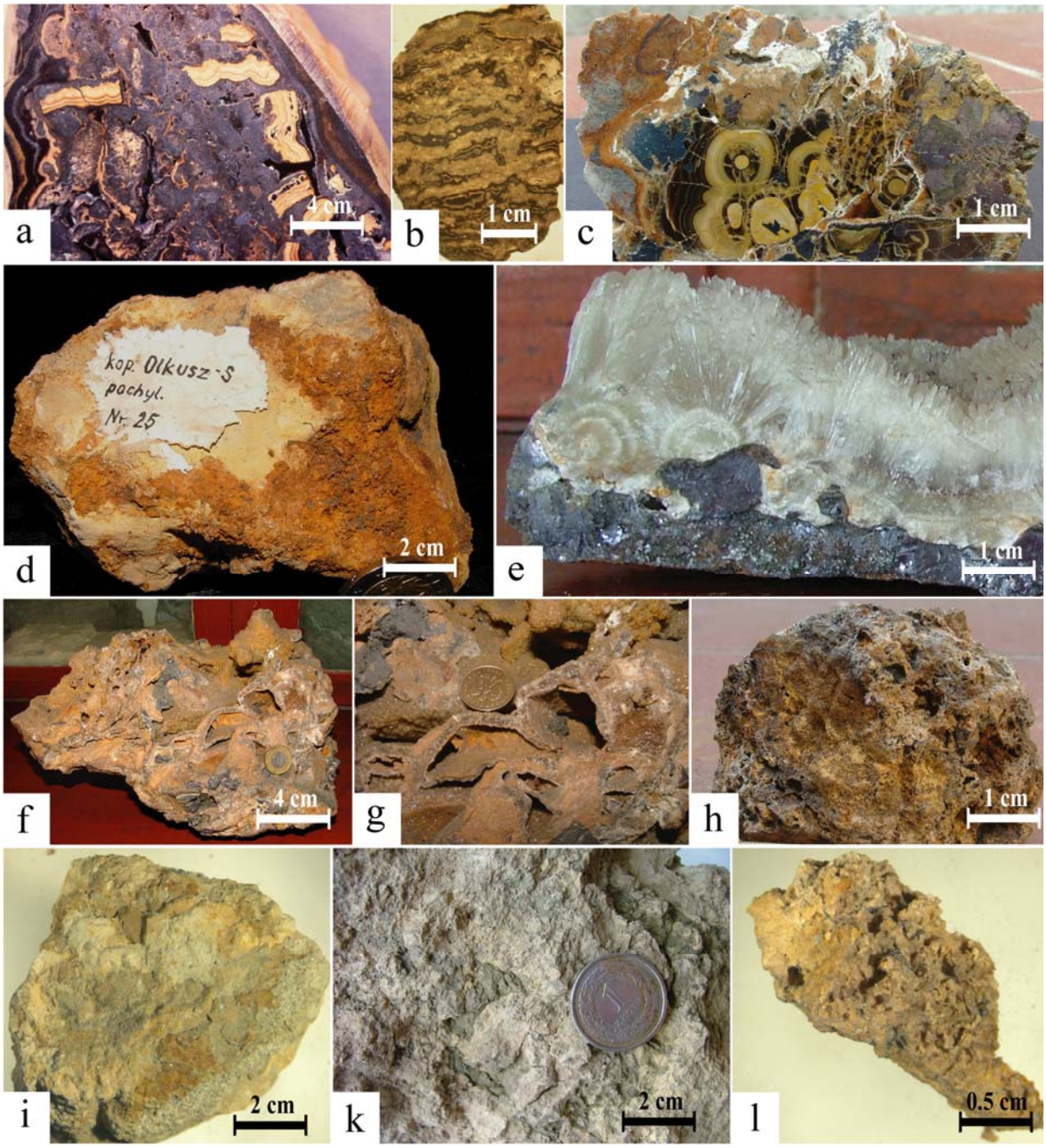

Figure 5.5: Typical ore samples from the Silesia-Krakow mining district. a) hydrothermal breccia ore wi fragments of primary sulphide minerals cemented by late marcasite and pyrite, Pomorzanj mine; b) sparry dolomi and sulphides replacing and filling the porosity of OBD I, Tzrebionka mine, c) banded colloform sphalerite partial replaced by smithsonite. Hemimorphite (orange phase) grows in fractures and hydrozincite (earthy white) in tl cavities. Pomorzany mine – 242m a.s.l. (CV05-80); d) earthy ore samples with smithsonite and goethite, Olku mine (coll. AGH University – Krakow); e) fibrous Pb-aragonite ("tarnowitzite") on massive galena, Tzrebionk mine (mine collection); f) smithsonite concretion in cavity, Tzrebionka mine (mine collection); g) enlargement of h) porous smithsonite with goethite, Bibiella dump (CV05-32); i) massive sample ore with smithsonite and F smithsonite ("monheimite"), Matylda mine (CV05-63); h) massive smithsonite and Fe-smithsonite with residual Z clays in cavity (CV05-62); k) smithsonite replacing and growing on dolomite, Olkusz mine (CV05-64).

collected in the Boleslaw open pit, where it occurs as white microcrystalline concretions and in the Pomorzany mine where this Zn hydrated carbonate form a late earthy phase in cavities (figs.

5.5c and 5.7f). Hemimorphite is present in many deposits, with the exception of the Matylda mine, replacing sphalerite (fig. 5.5c) and forming aggregates of euhedral crystals in cavities (fig. 5.7f). Cerussite and hydrocerussite are quite rare, as well as sulphide remnants. Some common and also rare sulphates represent late phases. Calcite is the principal gangue mineral**.** Spherical chalcedony concretions have been detected only in few samples from the Matylda mine (CV05-73, CV05-74, CV05-75), where they are associated to (Zn-)dolomite. Usually clay minerals (mainly smectites) accompany the oxidation products. Tarnowitzite have been detected in a single sample from Trzebionka mine (CV05-55) growing on galena (fig. 5.5e).

5.4.1 Smithsonite

Smithsonite has been detected in many specimens sampled in several districts of the mining province. It occurs in different morphologies. In the samples from the Boleslaw open-pit, smithsonite presents at least two morphologies consisting in anhedral micro-crystals replacing the dolomite host rock (OBD I – II) (type A) (fig. 5.7a) and as zoned hexagonal scalenohedral crystals replacing partially dissolved dolomite crystals (OBD III) growing in cavities (type D) (fig. 5.7a). In the first case, the dimension of the smithsonite crystals is less than 100μm, while in the second case the crystals can reach 400μm in diameter. The same morphology could be observed also in the specimens collected in the dumps around the old mining area of Bibiella, in the north-eastern part of the district, few kilometres to north of Tarnowiske Gory.

Globular concretions of Zn-carbonates, growing on and/or partly replacing several dolomite generations, were observed in few samples from the Boleslaw mine and in the Trzebionka mine (type B) (figs. 5.6e, f), as well as rhomboedral crystal in cavity have been observed in samples from Bibiella dump (type C) (fig. 5.6c). A different smithsonite morphology has been recognized in the specimens collected in the Trzebionka mine. Here the subhedral crystals of smithsonite have scalenohedral habit and seem to form concretions in the empty cavities of the OBD I. The maximum dimensions of these crystals are 700μm (type E). Smithsonite is usually associated with Fe- and Mn-(hydr)oxides. Globular concretions of smithsonite growing in open cavities have been also observed in other mines.

The cell parameters measured in these smithsonites vary from *a* 4.644(7) e 4.670(7)Å and *c* between 15.036(2) e 15.120(6)Å (tab. 5.2). The values of the parameters reported in the literature (Effenberger et al., 1981; Chang et al., 1995; Boni et al., 2003; Coppola et al., 2007) are in good agreement with the range values for the analysed polish smithsonites. We could not observe a direct relationship, however, between the measured cell parameters and the morphologies of the

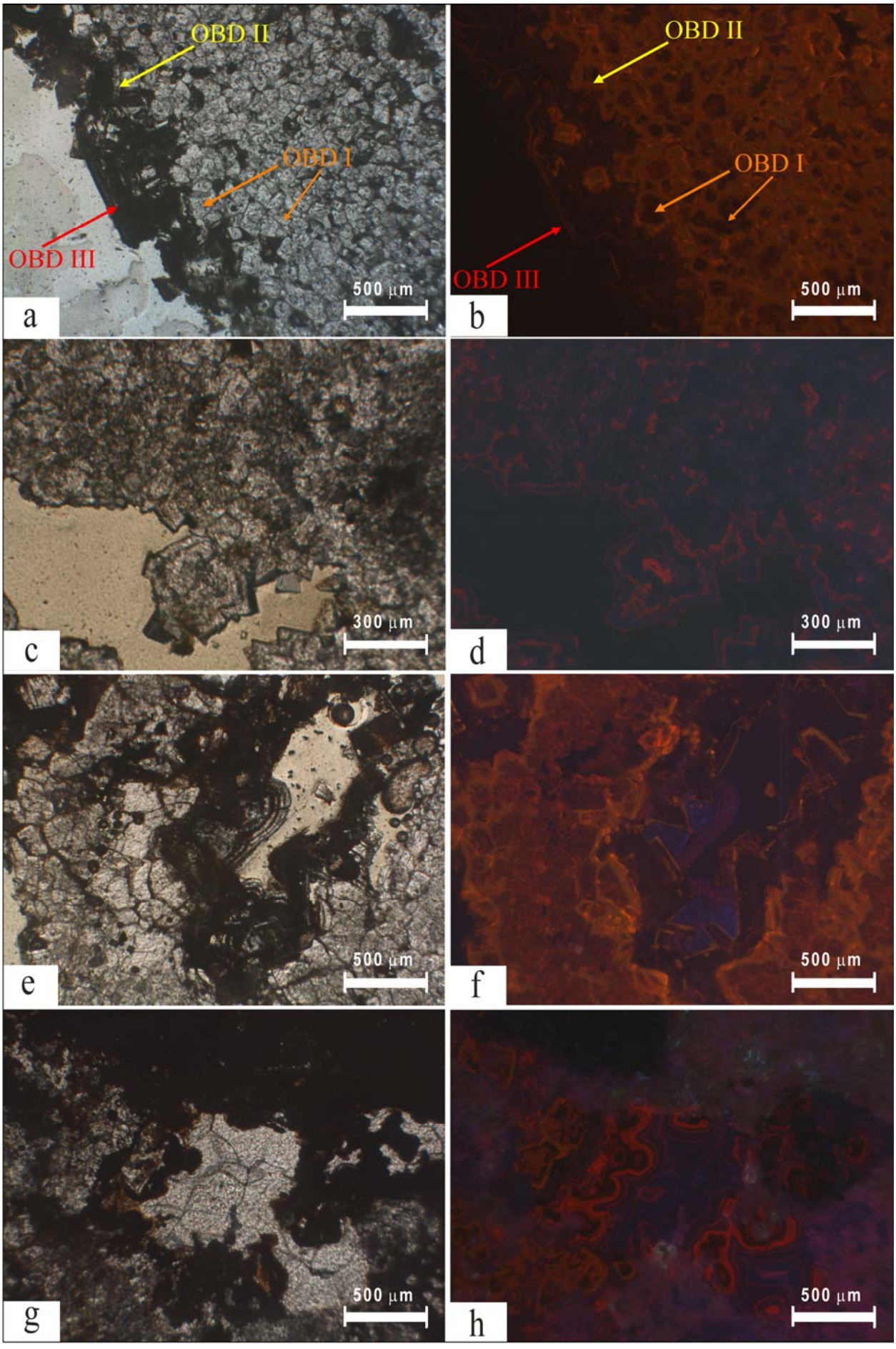
OBD II
OBD I
OBD III
500 µm
a
OBD II
OBD I
OBD III
500 µm
b
300 µm
c
300 µm
d
500 µm
e
500 µm
f
500 µm
g
500 µm
h

Zn-carbonates.

X-ray diffraction analyses revealed also the presence of Fe–smithsonite ("monheimite"), as evidenced by the value of 2.775(1)Å for the main peak in the sample CV05-65 from Matylda mine. These values were also observed in Sardinian (Aversa et al., 2002; Boni et al., 2003) and Belgian (Coppola et al., 2007) Fe-smithsonites.

5.4.2 Hemimorphite

Hemimorphite, though less abundant than smithsonite, was identified from XRD analyses in the specimens from many deposits. In all these specimens, the hemimorphite shows tabular crystals elongated along the *b* axis. In the specimens from the Boleslaw open-pit, hemimorphite forms concretions growing on rhombohedral dolomite crystals in cavities and/or on previously deposited smithsonite. The crystal sizes of hemimorphite are variable with a maximum of 400μm. In the specimens from the Pomorzany mine, hemimorphite forms orange crystals in radial aggregates. The results of the XRD analyses for hemimorphite, show most variable cell parameters, which are nevertheless in agreement with the literature data (McDonald et al., 1967; Cooper et al., 1981; Libowitzky et al., 1997; Boni et al., 2003; Coppola et al., 2007).

The values of *a* are constrained between 8.336(6) and 8.363(3)Å, of *b* between 10.699(6) and 10.953(7)Å ed of *c* between 5.105(6) e 5.123(4)Å.

5.4.3 Goethite

Diffractometric analyses revealed that goethite is omnipresent in most nonsulphide specimens from the Krakow-Silesia province. Only in few concretions of pure smithsonite and hemimorphite there is no trace of this mineral. This is in good agreement with the description made by other polish authors of the mineralogy of the nonsulphides in Upper Silesia (Zabinski, 1960; Radwanek-Bak, 1983). According to them, goethite represents one of the most important phases in the *red galman*, where iron occurs in its most oxidized form. Goethite occurs generally on the external specimen's surface.

Figure 5.6: a) thin section image (NII) of OBD III growing on OBD I (core crystals), cemented in turn by OBD II (rim crystals), Boleslaw deposit (CV05-50), b) CL image of (a): OBD I (dark red), OBD II (orange-red), OBD III (no-luminescence); c) thin section image (NII) of rhombohedral zoned crystals of smithsonite (type C) in cavity, Bibiella dump (CV05-29); d) CL image of (c); e) thin section image (NII) of late smithsonite (type B) on OBD III, Boleslaw deposit (CV05-51b); f) CL image of (e); g) thin section image (NII) of partially replaced dolomite host rock by microcrystalline smithsonite (type A) with late smithsonite sealing voids (type B); relicts of oxidized sulphides are also visible, Boleslaw deposit (CV05-58); h) CL image of (g).

Table 5.2: Main d values (Å) by intensity, unit cell dimensions and volumes of selected smithsonite from Upper Silesia district (S Poland).

Sample	d1(I_0)	d2(I/I_0)	d3(I/I_0)	d4(I/I_0)	a(Å)	±σ	c(Å)	±σ	cell vol(Å^3)	±σ
CV05-4b	2.751	3.550	1.707	2.323	4.6483	0.002	15.0767	0.010	282.1094	0.180
CV05-15c	2.754	3.562	1.708	2.329	4.6618	0.002	15.0814	0.015	283.8453	0.256
CV05-27a	2.758	3.560	1.711	2.331	4.6631	0.002	15.0999	0.015	284.3548	0.275
CV05-27b	2.757	3.561	1.710	2.332	4.6636	0.001	15.0944	0.008	284.3038	0.141
CV05-30a	2.761	3.562	1.711	2.336	4.6669	0.002	15.1103	0.015	285.0168	0.277
CV05-30b	2.759	3.563	1.712	2.332	4.6627	0.001	15.1191	0.010	284.6637	0.182
Cv05-32a	2.758	3.561	1.711	2.331	4..6634	0.002	15.1050	0.013	284.4815	0.227
CV05-32b	2.758	3.560	1.710	2.333	4.6662	0.006	15.0872	0.045	284.4842	0.798
CV05-32c	2.761	3.563	1.713	2.334	4.6686	0.002	15.1176	0.014	285.3494	0.255
CV05-33a	2.757	3.559	1.710	2.332	4.6625	0.002	15.0916	0.015	284.1181	0.226
CV05-33b	2.755	3.556	1.710	2.331	4.6595	0.002	15.0879	0.012	283.6684	0.204
CV05-50b	2.763	3.563	1.713	2.337	4.6707	0.003	15.1206	0.021	285.6683	0.376
CV05-56a	2.754	3.559	1.709	2.327	4.6580	0.002	15.0850	0.011	283.4466	0.197
CV05-56b	2.755	3.563	1.710	2.330	4.6591	0.006	15.1058	0.041	283.9687	0.740
CV05-58a	2.753	3.560	1.708	2.331	4.6619	0.001	15.0682	0.009	283.6067	0.161
CV05-59aA	2.752	3.553	1.706	2.329	4.6559	0.002	15.0559	0.010	282.6484	0.179
CV05-59aB	2.760	3.562	1.711	2.335	4.6696	0.002	15.1027	0.017	285.2014	0.292
CV05-62a	2.752	3.560	1.707	2.328	4.6594	0.002	15.0705	0.014	283.3474	0.237
CV05-64b	2.759	3.561	1.711	2.333	4.6657	0.001	15.1054	0.009	284.7702	0.165
CV05-64c	2.757	3.560	1.710	2.332	4.6639	0.001	15.0930	0.009	284.3145	0.157
CV05-67a	2.754	3.556	1.708	2.327	4.6562	0.001	15.0822	0.005	283.1757	0.095
CV05-71b	2.756	3.563	1.709	2.330	4.6627	0.001	15.0948	0.010	284.2067	0.174
CV05-72a	2.760	3.564	1.710	2.334	4.6671	0.002	15.1058	0.013	284.9537	0.242
CV05-81a	2.749	3.550	1.705	2.326	4.6544	0.003	15.0394	0.021	282.1584	0.390
CV05-85b	2.753	3.555	1.706	2.331	4.6580	0.002	15.0604	0.013	282.9899	0.226
CV05-85c	2.750	3.548	1.707	2.323	4.6542	0.007	15.0473	0.051	282.283	0.912
CV05-86a	2.752	3.552	1.706	2.328	4.6540	0.001	15.0609	0.010	282.51	0.172

The diffraction spectrum shows commonly amorphous characteristics for this mineral, testified by broad peaks and a very high background noise. Goethite replaces also the crystals of pyrite along cleavage. This aspect is particularly visible in samples from the Boleslaw mine (CV05-14).

5.4.4 Dolomite

Dolomite is a very important mineralogical phase in the Upper Silesia mineralisation. It constitutes the host rock (ODB I) of the primary sulphide ores. During our investigation, dolomite has been recognized in almost all the analyzed samples. Microscopic studies have revealed at least three different kinds of dolomite generations (fig. 5.6a). The first one represents the typical host rock (OBD I). It occurs as anhedral or subhedral crystals whose maximum dimension is about 100μm, and a hypidiotopic mosaic. The second one is observed in voids and fractures. It shows euhedral rhombohedral crystals bigger than those of the first generation (300μm), or forms the clear rim of the blotchy crystals of first generation. These two types of dolomite occur in the entire province. The last generation we could observe contains planar dolomite crystals (saddle dolomite), growing in fractures and voids especially occurring in samples from the Boleslaw mine and Bibiella dumps. Very often in the nonsulphide deposits, this kind of dolomite occurs as empty dissolved crystals. We can see only the frame ("skeleton") of the old crystals which are commonly dissolved in the core. These crystals are visible at hand-specimen scale as red rombohedral crystals. For a more detailed description of different generation of dolomite see the paragraph 5.5.

The following cell parameters were measured: *a* is constrained between 4.791(2) and 4.829(1)Å and *b* between 16.033(0) e 16.164(5)Å. Our results are in good agreement with the data reported in the literature (Hurbult, 1957; Steinfink et al., 1959; Zabinski, 1959, 1980, 1981, 1986). A variation of the major peak, up to 2.89(8)Å, is observed in the Zn-rich dolomite, as predicted by Zabinski (1959) and references therein. However, in all the considered specimens we could not observe a direct relationship between the measured cell parameters of the Mg-Ca-carbonates with the chemistry and/or crystal morphologies.

5.4.5 Other minerals

Many other neo-formed or pre-existing phases were quoted in previous mineralogical studies (Zabinski, 1960; Radwanek-Bak, 1983; Gruszczyk & Wielgomas, 1990; Smakowski & Strzelska-Smakowska, 2005). Our study has confirmed the presence of cerussite, hydrozincite,

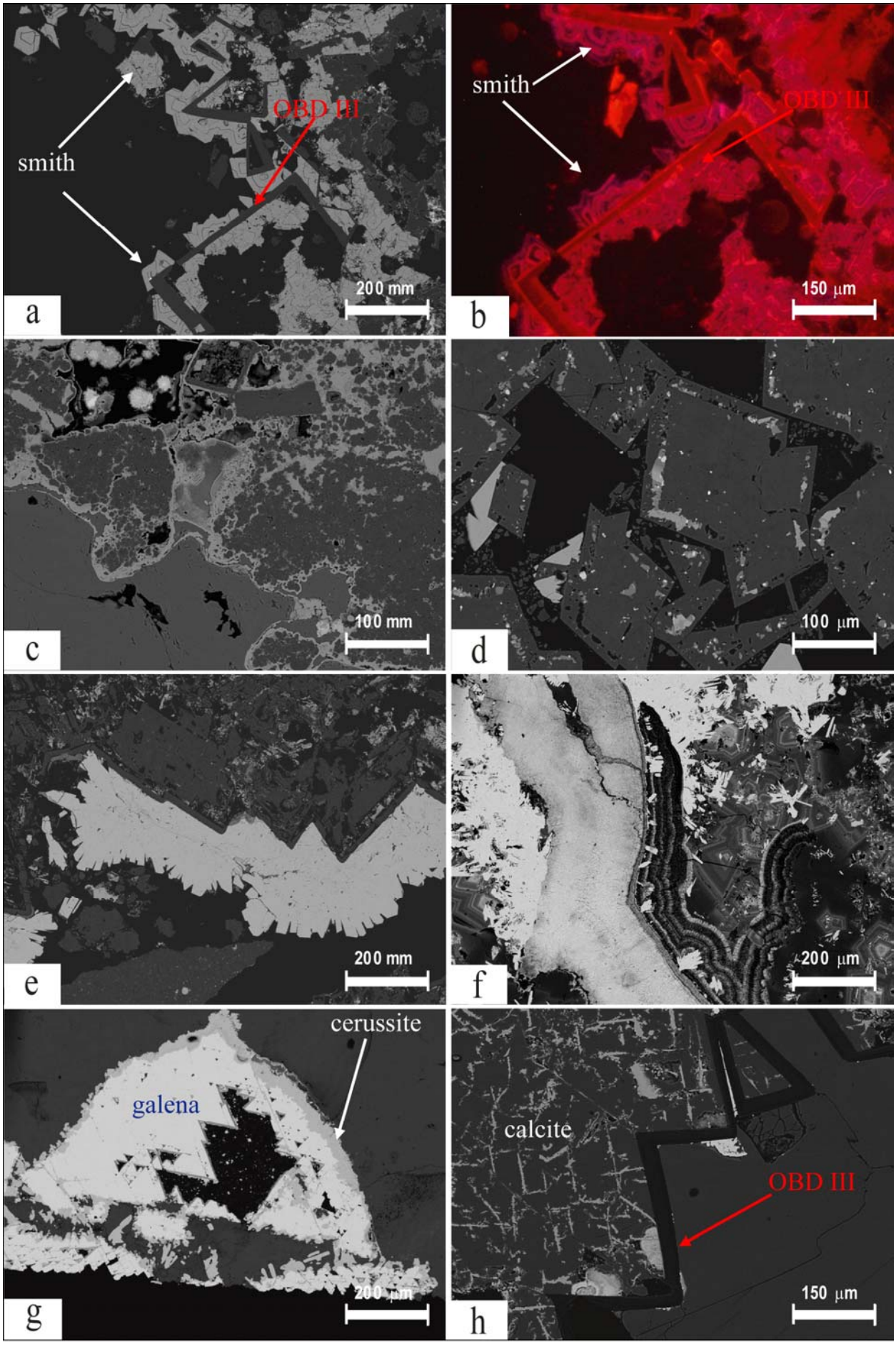
smith
OBD III
200 mm
a
smith
OBD III
150 μm
b
100 mm
c
100 μm
d
200 mm
e
200 μm
f
cerussite
galena
200 μm
g
calcite
OBD III
150 μm
h

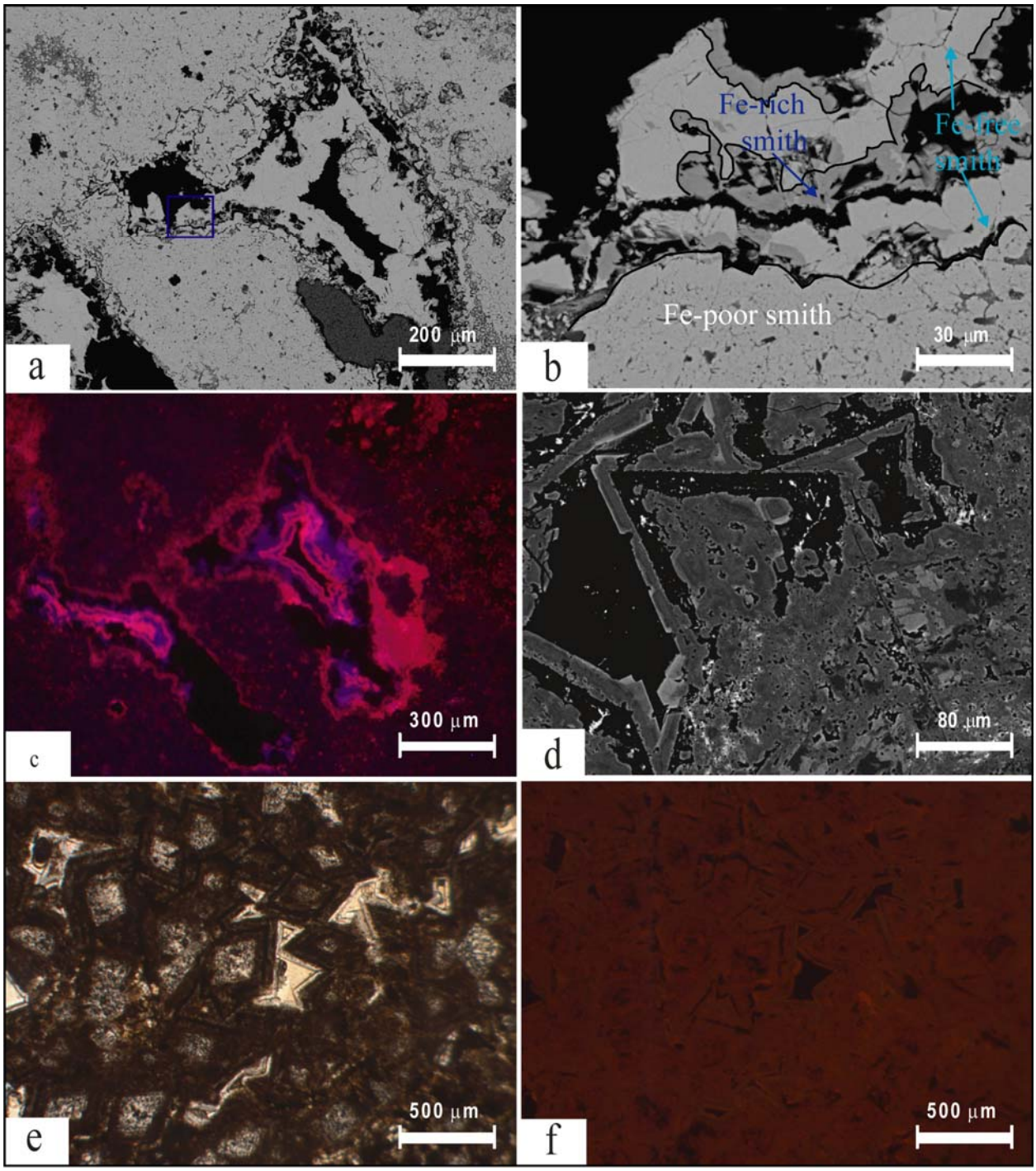

Figure 5.8: a) backscattered electron image of microcrystalline Fe(poor)-smithsonite from white galman, with late smithsonite and Fe(rich)-smithsonite in cavity, Matylda mine (CV05-86); b) enlargement of a selected area from (a) showing relationship between three different types of smithsonite, Matylda mine (CV05-86); c) CL image of (a); d) partially dissolved Zn-dolomite, Matylda mine (CV05-73); e) thin section image (NII) of different generations of Zn-dolomite, Matylda mine (CV05-73); f) CL image of (e).

Figure 5.7: a) backscattered electron image of zoned hexagonal scalenohedral crystals of smithsonite (type D) growing on the border of skeleton crystals of OBD III, Boleslaw deposit (CV05-51b); b) CL image of a selected area from (a); c) backscattered image of microcrystalline smithsonite (type A) replacing host dolomite (OBD I and II), Tzrebionka mine (CV05-10); d) backscattered electron image of inclusions of smithsonite and Fe-smithsonite in the porosity of Fe-dolomite (OBD II), Bibiella dump (CV05-28); e) aggregates of tabular crystals of hemimorphite on partially dissolved OBD III crystals, Boleslaw deposit (CV05-14); f) globular concretion of hydrozincite with small hemimorphite crystal aggregates growing on, Pomorzany mine (CV05-24); g) galena replaced by cerussite along cleavage, Pomorzany mine (CV05-80); h) late calcite filling OBD III crystals with Zn-Mn (hydr-)oxides in the cleavage fractures, Boleslaw mine (CV05-51).

Pb-aragonite ("tarnowitzite"), Zn-bearing sulphates, Zn-, Pb-, Fe- and Mn-(hydr)oxides, smectitic phyllosilicates and relics of sulphides.
Calcite has been detected in many samples from the entire mining province. It usually represents a late phase paragenetically subsequent to main nonsulphide minerals, in fractures and cavities.

5.5 Petrography and paragenesis of nonsulphide ores

Petrographic studies have revealed the mineral paragenesis of the polish calamines, thus allowing the characterization of their relative timing of precipitation in the Upper Silesia.
The Ore-bearing Dolomite represents the more common host rock for both sulphide and nonsulphide mineralisation (see above): this aspect is confirmed also by the observation of many samples in thin section.
Different generations of dolomite with different mineralogical and petrographic characteristics have been observed (fig. 5.6a, b). A first generation of dolomite occurs as a crypto-microcrystalline lithotype, with anhedral and subhedral crystals with non-planar boundaries. These crystals usually show evidence of alteration, as well as abundant Fe-oxides, especially visible in the core of dolomite crystals while the rims are oxides-free. This distinct dolomite generation can be correlated throughout the entire district. Non-planar dolomite crystals replace primary limestone and a micritic early diagenetic dolomite. This replacement is particularly clear in samples from the Boleslaw mine, where remnants of micritic early diagenetic dolomite with ghost crystals of dissolved gypsum, occur as not-replaced enclaves in the mentioned microcrystalline dolomite. Under cold cathodoluminescence microscopy, the micritic dolomite shows a homogeneous red luminescence. The contact between these two dolomite generations is sharp.
A paragenetically subsequent generation of dolomite precipitates at the border of cavities and/or fractures with euhedral and subhedral crystals with planar boundary; this dolomite can build also the clear rims around the former non-planar dolomite crystals. This late dolomite generation has higher Fe, Mn and Zn content with respect to former dolomite (see below). Cold cathodoluminescence observations emphasize the difference between these two generations of dolomites. Indeed, earlier dolomite shows dark red to absent luminescence, while later dolomite presents a red to orange-zoned luminescence. Usually, we can observe zoned rhombohedral crystals with a dark red to not-luminescent core (earlier dolomite) and variably brighter red rim (later dolomite). Fe-sulphides and galena, partially replaced by goethite and cerussite

respectively, are disseminated in both dolomite generations.

An even later dolomite grows in open fractures and cavities between both former dolomite generations. It presents big, usually saddle-shaped crystals, which can reach few millimetres in maximum length. This dolomite shows clear signs of dissolution: frequently the crystals are completely empty, leaving only the external skeleton in place. This dolomite skeleton shows dark red cathodoluminescence colors. The insoluble residuum remaining from the dissolution, mainly composed of smectites and quartz, fills locally the inner part of the crystals. Otherwise, the empty crystals can be filled by late calcite, by Fe-Mn(hydro)oxides along the cleavage, or by a carbonate phase with a high Zn and Fe content in the lattice, showing an orange luminescence. This distinct generation of dolomite dissolved in its inner part, has been observed only in the samples from the Boleslaw and Bibiella mines.

In conclusion, our OM and cathodoluminescence study has revealed a substantial agreement (with some differences) with the observations and interpretations made by Heijlen et al. (2003) on the different dolomite generations. Therefore I will use also the term OBD I for crypto-microcrystalline dolomite replacing early diagenetic dolomite and OBD II for the red-luminescing dolomite corresponding to the clear rim crystals. The latest dolomite growing in cavities probably corresponds to the saddle dolomite generation in fractures, which Heijlen et al. (2003) consider to be a special type of OBD II, also paragenetically associated with sulphides. Unfortunately, we did not record the presence of sulphides in our samples, due to the oxidation process, which involved both host rock and ore deposits. Contrary to Heijlen et al. (2003), we will use the term OBD III for this distinct type of dolomite.

A different approach has to be used for the dolomite from the horizon II of Matylda mine (sample CV05-73). Theoretically, this dolomite, associated to Fe-smithsonite, could be included in the mineralogical assemblage of the *white galman* ore, which is represented almost exclusively in this ore horizon (sulphide minerals are absent) (Kucha, 2003; Kucha, 2005). This dolomite type has been described as Zn-rich dolomite (Zabinski, 1980; 1986), as also other dolomites occurring in the mining district. However, some petrographic differences have been observed between the latter and the other metal-rich dolomites throughout the district. Several generations of dolomite have been observed in this sample, and all of them are Zn-rich (see paragraph 5.6). No evidence of micritic early diagenetic dolomite has been observed here. An early dolomite, (hydr-)oxides-free, shows planar euhedral crystals in an idiotopic mosaic (sensu Sibley & Gregg, 1987), whose single crystals size are less than 200μm, and are cemented by a later dolomite impregnated of (hydr-)oxides minerals (mainly goethite), where porosity of the bulk rock is higher. In open cavities bigger crystals are visible (up to 500-600μm), which show a

clear external rim few μm thick (fig. 5.8e). (Hydro-)oxides bands, parallel to the crystal faces, are included in the single crystals. Under cold cathodoluminescence microscopy, the earlier (hydr-)oxides-free dolomite (dull red) is less luminescent than the paragenetically successive dolomite generations (bright red). Moreover, it is impossible to distinguish the clear external band of the dolomite crystals in cavities, due to their similar luminescence with respect to dolomite impregnated with Fe-oxides (fig. 5.8f). Also this dolomite generation may show evident signs of dissolution (fig. 5.8d).

Distinct generations of smithsonite, with different morphology, have been observed in the analyzed samples; however the same generations are not always are comparable throughout the entire district. A first generation of microcrystalline smithsonite (type A) has been observed to replace both the host dolomite (OBD I and II) as well as sphalerite. The partially replaced host shows a blotchy blue and red luminescence (fig. 5.6g, h). Type A smithsonite is almost uniformly distributed in the entire mining province. Later generations of smithsonite form concretions and crystalline aggregates in open cavities and fractures in the host rock. Different morphologies occur. Concretions of smithsonite, with globular zoned crystals (type B), have been observed in cavities and fractures of many samples from the Boleslaw open pit and the Trzebionka mine (fig. 5.6e, g). They usually show a blue-red luminescence in the core of the crystals and a blue-pink zoned luminescence in the outer part (fig. 5.6f, h). Rhomboedral zoned crystals of smithsonite (type C) have been observed in voids specially in the samples from Bibiella dump (fig. 5.6c). These crystals probably represent the last generation in the paragenesis of smithsonite. The luminescence of type C smithsonite varies from a low banded blue-pink in the in the core of the crystals, to a bright red at their rims (fig. 5.6d). Zoned hexagonal scalenohedral crystals of smithsonite (type D), with a zoned blue-pink luminescence grow both on the inner and on the external border of empty saddle dolomite crystals in cavities (fig. 5.7a, b). Probably the peculiar pink luminescence of smithsonite is due to the high Mn content in the crystal lattice (Götte & Richter, 2004).

Tabular crystals of clear hemimorphite grow also on empty skeletons of dolomite crystals (Boleslaw mine) (fig. 5.7e) or on top of the smithsonites generations growing in cavities and fractures (i.e. in the Bibiella dump). Hemimorphite presents high-order interference colours when observed under crossed nichols, but it shows no luminescence under cathodic light. The paragenetical relationship between Zn and Pb secondary phases are not fully explained because of they are not in contact in the analysed samples. However, cerussite replace galena along cleavage (fig. 5.7g).

Fe-smithsonite and other carbonate phases with a high Zn-Fe content form solid inclusion

infilling porosity of a Fe-rich variety of OBD II; this was observed in several samples collected in the Bibiella dump (fig. 5.7d). In samples from the Matylda mine different generations of Fe-bearing smithsonite, chemically different (see below), have been recorded (fig. 5.8a, b, c). The first generation shows subhedral crystals in a cryptocrystalline texture, replacing dolomite host rock. It has variably blotchy red-blue to non-luminescent colours. A late generation of pure smithsonite, followed by Fe-smithsonite grows in cavities and show a zoned blue-pink luminescence.

Late calcite, surely syn- or post- nonsulphide emplacement, with orange cathodoluminescence colours, fills the voids, but it can replace the dolomitic host rock, too (fig. 5.7h).

In, conclusion we have recognized two important mineralogical assemblages: 1) smithsonite - hemimorphite dominated and 2) (Fe-)smithsonite – Zn-dolomite dominated. The first one is typical of supergene Zn nonsulphide deposits. Smithsonite is the dominant and the paragenetically earlier mineralogical phase. Nevertheless, the paragenetic relationships between smithsonite and the other supergene minerals are not fully clear. Local variation in the paragenesis has been observed: petrographical observations suggest that hemimorphite had a more limited interval of precipitation compared to smithsonite. Hydrozincite precipitated surely after all the smithsonite types. Locally it seems to have been contemporaneous with late hemimorphite.

The mineralogical assemblage occurring in the samples from the Matylda mine appears to be different from that of the supergene deposits worldwide.

5.6 Major and trace element geochemistry of nonsulphide ores

Nonsulphide ores in Upper Silesia are far more rich in Zn than in Pb. Zinc is contained mainly in smithsonite, Fe-smithsonite, Zn-dolomite and in minor abundance in hemimorphite, hydrozincite, Zn-sulphates (mainly goslarite) and in Mn (hydr-)oxides which can contain few points per cent of Zn. Lead is contained in the galena remnants and in alteration products, like cerussite and hydrocerussite.

Chemical analyses performed with WDS microprobe and EDS JEOL 5900V SEM, have established the chemical composition of the most important economic minerals of the district (smithsonite, Fe-smithsonite, cerussite, hemimorphite, metal-rich dolomite) (tab. 5.3).

metals replacing Zn in the crystalline structure of smithsonite is very low. The Mg and Ca contents, consisting of 0 - 1.42 wt% and 0.27 - 1.62 wt%, respectively, are probably reflecting

Table 5.3: Microprobe analyses of selected smithsonite, hemimorphite, cerussite and dolomite from Upper Silesia district (S Poland), pointing to compositional variations.

	smithsonite and Fe-smithsonite														
sample	**CV05-15**			**CV05-56**			**CV05-86**			**CV05-80**			**CV05-28**		
ZnO	61.34	60.18	64.41	62.31	60.68	60.77	60.47	60.83	62.07	59.10	58.07	59.28	61.53	62.56	38.02
FeO	0.56	3.15	0.35	tr		0.43	0.72	1.86	1.14	tr	tr	tr	0.85	0.28	16.50
MnO	tr		tr				tr	tr	tr	tr	tr		tr	tr	2.49
CaO	1.13	0.76	1.07	0.86	1.18	1.12	0.91	0.37	0.27	1.04	0.14	1.15	0.79	0.79	2.65
MgO	1.20	0.34	0.14	0.63	0.67	0.75	1.42	0.56	0.31	tr	0.14	0.10	0.48	0.48	2.03
CdO	tr	tr	tr	tr	0.77	0.60	tr	0.30	tr	2.84	4.19	1.87	0.17	0.12	
PbO	tr		tr	0.54	1.06	0.85	tr	tr	tr	0.95	1.11	1.36	0.66	0.66	0.17
CO_2*	35.96	35.97	36.22	35.30	35.15	35.41	36.13	36.45	36.10	34.18	34.30	34.10	35.31	35.31	35.39
total	100.19	100.40	102.19	99.64	99.51	99.93	99.65	100.37	99.89	98.11	97.95	97.86	99.79	100.20	97.25

	cerussite				hemimorphite									
sample	**CV05-56**		**CV05-80**			**CV05-14**			**CV05-24**			**CV05-27**		
ZnO	0.30	0.28	0.23	1.13	**SiO_2**	26.45	26.24	26.79	25.85	25.75	25.47	26.59	26.52	26.49
FeO	tr				**ZnO**	66.91	66.89	67.3	65.73	66.79	66.86	65.69	65.78	65.49
MnO	tr	tr			**FeO**	tr	0.09	0.20	0.13	0.10	0.12	0.014	0.019	
CaO	0.26	0.19	0.85	0.63	**CaO**	0.04	0.06	0.00	0.07	0.02	0.04	0.35	0.43	0.46
PbO	82.40	82.67	82.12	81.09	**PbO**		tr		0.07	0.09	0.07	0.46	0.28	0.35
CO_2*	16.85	16.73	17.17	17.25	**H_2O***	6.63	6.81	5.68	8.01	7.25	7.35	6.95	6.965	7.23
total	99.81	99.87	100.37	100.10	**total**	100.02	100.08	99.97	99.85	99.99	99.91	100.05	100.00	100.03

	dolomite, Fe-dolomite and Zn-dolomite														
	OBD I			**OBD II**			**OBD III**			**Fe-dol**		**Zn-dol**			
	CV05-15			**CV05-15**			**CV05-51**			**CV05-28**		**CV05-73**			
ZnO	0.27	0.1	0.69	0.44	0.85	0.17	1.27	1.65	2.54	0.03	0.042	5.47	5.39	2.01	3.56
FeO	0.65	tr	0.16	0.3	1.14	1.26	0.14	0.29	0.2	7.32	10.82	1.28	0.2	3.01	0.12
MnO	0.15	0.21	0.13	0.13	0.13	0.17	0.27	0.14	0.06	0.83	1.29	0.71	0.58	0.61	0.60
CaO	31.07	30.73	31.22	31.13	31.74	31.56	32.5	31.34	31.75	30.62	28.62	28.56	29.2	29.27	29.27
MgO	20.03	21.09	20.62	19.95	18.77	19.01	18.72	19.01	19.37	15.45	13.62	17.06	17.22	17.85	19.48
PbO							0.04		0.08				0.11	0.07	tr
CO_2*	48.05	47.48	47.9	46.93	46.75	46.61	47.01	46.62	47.72	46.04	45.06	45.32	47.4	46.14	46.96
total	100.2	99.61	100.7	98.88	99.38	98.78	99.95	99.05	101.7	100.3	99.45	98.40	100.10	98.96	99.99

the presence of dolomite remnants not completely replaced by smithsonite. Pb can reach up to 1.36 wt%. Traces of Mn, Co and Ni, both below detection limits, have been detected in all the analysed smithsonites. Cadmium is present in traces in smithsonite, but in the specimen CV05-80, where the Zn-carbonates are directly in contact with sphalerite, the Cd content is higher (up to 4.19 wt%).

The presence of Fe-rich smithsonite (earlier called "monheimite") is confirmed by combined SEM and microprobe analyses, whilst the X-ray analyses often did not reveal the presence of this phase in most specimens, because of low content of Fe-rich variety in the analysed samples. The "monheimite" is an intermediate member of the smithsonite-siderite series (Palache et al., 1951; Zabinski, 1958; Sitzia, 1965; Bak and Niec, 1978; Bak and Zabinski, 1981; Boni et al., 2003; Coppola et al., 2007). It was described in the polish Zn-Pb deposits from Zabinski (1958), Bak & Niec (1978) and Kucha (2005).

In the samples collected for this thesis, the iron-rich smithsonite variety was detected only in few specimens sampled in the mine dumps near Bibiella and in the Matylda mine. In the first case, solid inclusions of Fe-smithsonite inside former Fe-dolomite crystals contain up to 16.50 wt% of FeO. MgO, CaO and MnO contents are respectively of 2.03, 2.65 and 2.49 wt%.

In the Matylda mine, at least three generations of Fe-smithsonite, with different Fe-content, have been detected. The first generation (Fe-poor smithsonite) is the most abundant and has a cryptocrystalline lithology. It contains 0.72-1.99 wt% FeO and 60.22-60.47 wt% ZnO respectively. In the cavities of the mentioned Fe-smithsonite, grows a smithsonite with traces of FeO, then followed by another generation of Fe-rich smithsonite. The FeO and ZnO contents of the latter are constrained between 15.43-16.78 wt. FeO and 32.92-34.92 wt% ZnO respectively.

Hemimorphites are nearly stoichiometric, with the exception of the hemimorphite from the Pomorzany and Bibiella mines, where the Pb content reaches a maximum of 0.46 wt%. Only traces of Mn, Cu, Fe^{+2}, Ni and Cd have been detected in the Polish hemimorphites.

The combined SEM-WDS study has been carried out also on several specimens containing dolomite from different mines. I analyzed all the different dolomite generations (OBD I, II, III), after having distinguished them with OM and CL observations. The analyses revealed the presence of a first dolomite (OBD I) with a nearly stoichiometric composition, which only occasionally has a certain content in Zn (up to 0.69 wt% ZnO), Fe (up to 0.65 wt% FeO) and Mn (up to 0.21 wt% MnO). Traces of other metals have also been detected. This type of dolomite has been located well inside the specimens and does not present evidence of dissolution by an oxidizing fluid. This kind of dolomite has been detected in the whole district, but it has never been found in the specimens from the Matylda mine. A second type of dolomite (OBD II) with a

higher content of FeO and ZnO, has been individuated in all the mines with the exception of Matylda. In these dolomites ZnO is constrained between 0.17 and 0.85 wt% and FeO between 0.30 and 1.26 wt%. After OM study, we recognized a paragenetically subsequent dolomite generation (OBD III) with a higher Zn content (up to 2.54 wt% ZnO) with respect to OBD I and II, while Fe is moderately low (0.14 – 0.29 wt% FeO). An exceptionally Fe-rich dolomite variety was observed and measured only in the sample CV05-28 from the Bibiella dump,with a content in FeO constrained between 7.32 and 10.82 wt%, while the measured Zn content is very low (0 – 0.7 wt% ZnO). The distribution of these metals in each single crystal is random. Fe-dolomite is also characterized by high MnO values, constrained between 0.76 and 1.29 wt%. Traces of Ni, Cd, Co and Pb have been detected in this phase. This distinct type of dolomite is non-luminescent due to Fe-quenching as well as to possible self-quenching by Mn in high concentration (Machel et al., 1991). A Fe-bearing dolomite has been formerly described by Bak (1993) in the Krakow-Silesia district: Fe and Mn contents are perfectly comparable with those in our analyses but the Zn content is slightly higher (up to 2.24 wt% ZnO). Narkiewicz (1993) described the presence of Fe-dolomite only in the northernmost part of district, in the area encompassed between Bibiela-Kalety and Siewierz, and in direct neighborhood of the mineralisation in the Trzebionka and Pomorzany mines.

The dolomite from the ore horizon II of the Matylda mine (CV05-73) requires a different explanation. Nevertheless after combined OM and CL observation different dolomite morphologies of crystals (and generations) have been distinguished. The chemical analyses reveal a constant high Zn content, while Fe is randomly distributed in the crystal lattice (fig. 5.9). In this phase the Zn content ranges between 3.27 and 5.47 wt% in Zn-oxide: the highest amount detected in the dolomites of the whole district, while the Fe-oxide amount is variable between 0.12 and 3.01 wt%. This particular kind of dolomite (Zn-rich) has been named “Zincian dolomite” by Zabinski (1960, 1980, 1986). It was recognized in several mines in Upper Silesia (Zabinski, 1959; 1980, 1981, 1986; Panek & Szuwarzynski 1974; Kucha, 2005; Kucha & Czajka, 1984).

Many other authors have described the dolomites from the Zn-Pb mineralisation in Upper Silesia, due to their possible economic importance associated to its high content in base metals (Gruszczyk, 1956; Wazewska-Riesenkampf, 1959; Zabinski, 1959, 1960, 1981, 1986; Sliwinski, 1966, 1969; Smolarska,1968; Zawislak, 1971, Zawislak et al., 1970; Jasienska et al., 1972; Rosenborg et al., 1963; Przenioslo 1974; Haranczyk, 1981; Haranczyk et al., 1969; Mochanka et al, 1981; Bak, 1986, 1993; Czajka 1991; Kucha, 2005; Kucha & Czajka, 1984). From this literature it can be desumed that the zinc-oxide content of some of the analyzed Zn-dolomites

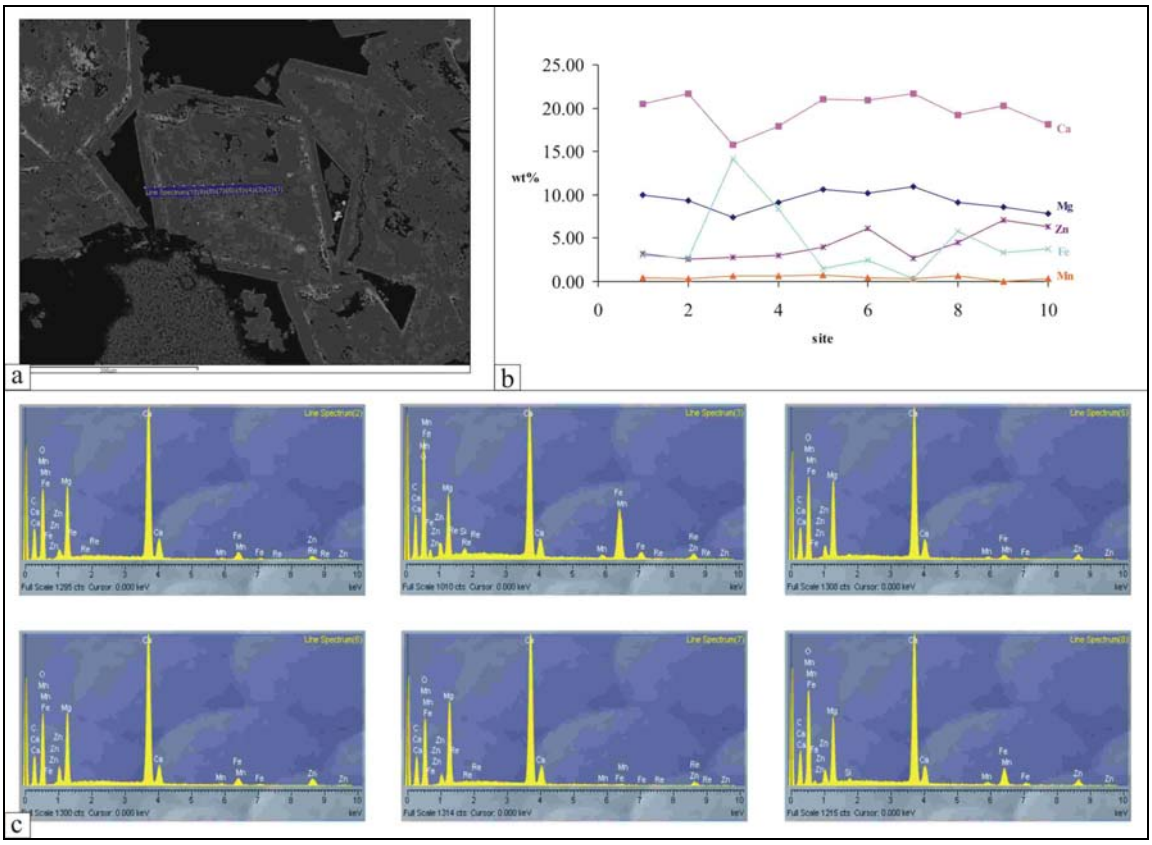

Figure 5.9: chemical profile analysed with SEM JEOL 5900 INCA on the Zn-dolomite from Matylda mine (CV05-73). a) backscattered electron image and analysed points. The clear zones are Fe-rich and the darker ones Zn-rich. b) variation in the elements contents along the chemical profile shown in (a); c) single representative X-ray spectra of the analysed points shown in (a).

can exceed 10 wt%.

The few measured cerussites have a stoichiometric composition, with a content of Zn, Ca and Fe minor than 1.0 wt%, while Ni, Cu, Cd, Co, and Mn are present only in traces.

5.7 C and O isotopes geochemistry

Stable isotopes (O-C) geochemistry was carried out on smithsonites, dolomites and calcites sampled from the different deposits investigated in the present work. The choice of specimens to which this technique has been applied, was dictated by their purity, confirmed by XRPD analysis, and by the possibility to cover an ample range of crystal morphologies. All the obtained results are presented in figure 5.10 and table 5.4.

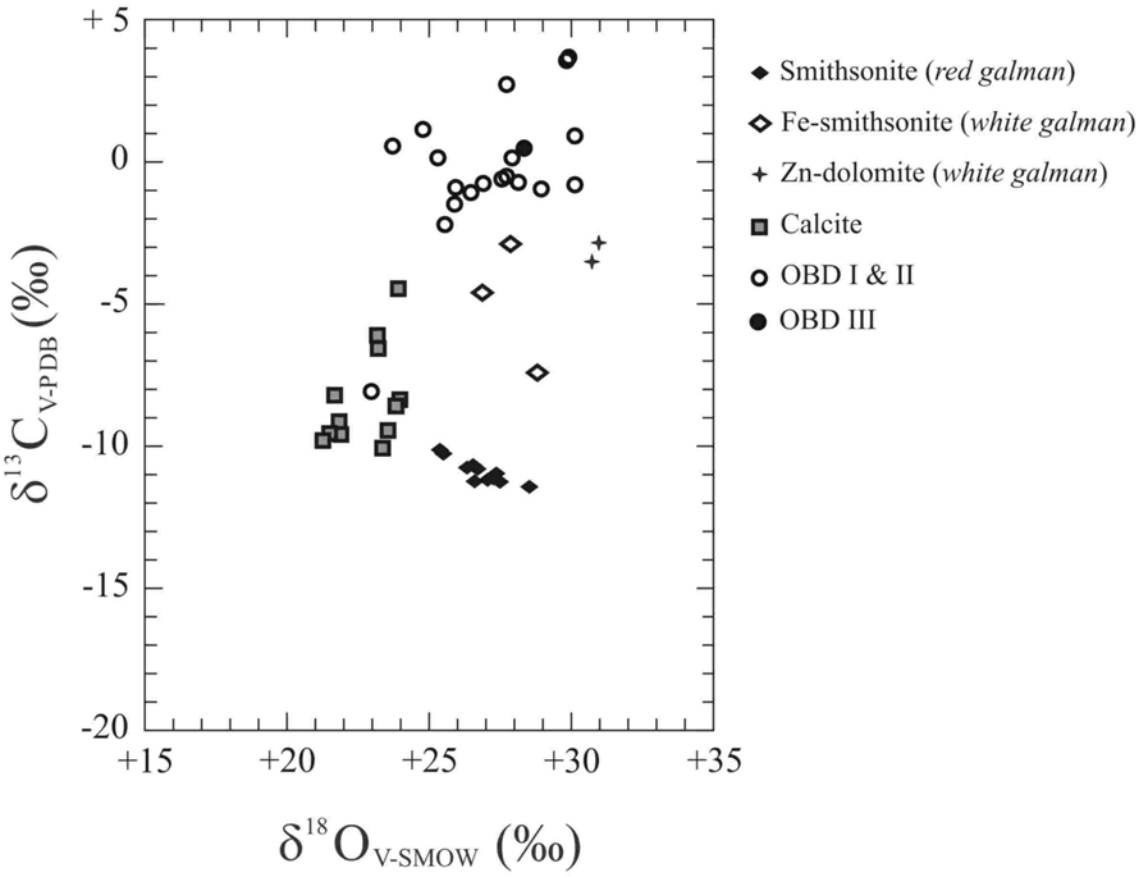

Figure 5.10: Plot of $\delta^{13}C$ *vs.* $\delta^{18}O$ for various Zn, Ca and Mg-Ca carbonates (smithsonite, supergene late calcite and dolomite host rock- OBD I, II, III-) from Polish nonsulphide ores.

5.7.1 Smithsonite

We have measured the carbon and oxygen isotopic ratios of smithsonite in *red* and *white galman* (paragraph 4.3.2). The reliability of these results is confirmed by the high number of analyzed specimens and by the heterogeneity of provenance (all the mine are represented).

Differences between these two Zn nonsulphide ore types are mirrored by the stable isotope results in the Zn-carbonates. Smithsonite from the *red galman* shows a limited range of $\delta^{13}C_{VPDB}$ values (-10.1 to -11.4‰, 1σ=0.16, n=11), and slightly variable $\delta^{18}O_{VSMOW}$ values (25.3 to 28.5‰, av. 26.8 ± 0.3‰, 1σ=0.28, n=11). The low uniform values of $\delta^{13}C_{VPDB}$ detected in the *red galman* smithsonite, are really unusual for supergene carbonate-hosted deposits (Boni et al., 2003; Coppola et al., 2007; Gilg et al., 2007a). It could mean a predominance of reduced soil-derived carbon source during the *red galman* supergene smithsonite formation. Smithsonites from *white galman* (-2.9 to -7.4‰) have more variable and positive carbon isotope values than *red galman*, but broadly similar oxygen isotope compositions (26.8 to 28.9‰ $\delta^{18}O_{VSMOW}$). The slight variation in $\delta^{18}O_{VSMOW}$ (~3‰ "*red galman* smithsonite", ~2‰ "*white galman*

Table 5.4: Carbon and oxygen isotope data of Zn, Ca and Mg-Ca carbonates from Upper Silesia district (S Poland).

Sample	Mineral*	Description	Location	$\delta^{13}C_{V\text{-}PDB}$ (‰)	$\delta^{18}O_{V\text{-}SMOW}$ (‰)	*Ave*	$\pm\sigma$
CV05-82a	sm	earthy reddish matrix	Tzrebionka	-11.4	28.5		
CV05-27b	sm	massive crystalline smithsonite	Bibiella	-10.8	26.3		
CV05-27a	sm	aggregates of brown crystals	Bibiella	-10.8	26.6		
CV05-56a	sm	crystalline concretion, outer part	Tzrebionka	-10.1	25.3		
CV05-56b	sm	crystalline concretion, inner part	Tzrebionka	-10.2	25.4		
CV05-30a	sm	rottenly crystalline smithsonite	Bibiella	-11.2	27.0		
CV05-30b	sm	massive crystalline smithsonite	Bibiella	-11.1	26.6		
CV05-32a	sm	massive crystalline smithsonite	Bibiella	-10.8	26.7		
CV05-32c	sm	rhombohedral red crystals in cavities	Bibiella	-11.1	27.3		
CV05-33a	sm	rottenly crystalline smithsonite	Bibiella	-11.0	27.4		
CV-71B	sm	globular vitreous concretion	Matylda	-11.3	27.5	26.8	0.9
CV05-64b	Fe-sm	brown crystalline aggregates (*white galman*)	Olkusz	-4.7	26.8		
CV05-63a	Fe-sm	massive crystalline smithsonite (*white galman*)	Matylda	-7.4	28.9		
CV05-85b	Fe-sm	spherical crystalline aggregates (*white galman*)	Matylda	-2.9	27.8	27.8	1.0
CV05-73a	Zn-do	white concretion in cavities	Matylda	-3.5	30.8		
CV05-73b	Zn-do	massive microcrystalline wall rock	Matylda	-2.9	31.0	30.9	0.2
CV05-50a	do	massive grey wall rock	Boleslaw	-1.4	26.0		
CV05-35a	do	microcristalline wall rock	Bibiella	0.5	23.7		
CV05-9b	do	massive grey wall rock in clasts	Boleslaw	-0.7	27.0		
CV05-51Ba	do	massive grey wall rock in clasts	Boleslaw	-0.9	26.0		
CV05-51b	do	massive grey wall rock	Boleslaw	-8.0	23.0		
CV05-44a	do	massive grey wall rock	Boleslaw	-2.3	25.5		
CV05-75a	do	microcristalline wall rock	Matylda	1.1	24.8		
CV05-79b	do	reddish rhombohedral crystals in cavities	Boleslaw	-7.9	22.9		
CV05-15a	do	massive grey wall rock in clasts	Boleslaw	-0.5	27.8		
CV05-11c	do	spherical crystalline aggregates	Boleslaw	0.3	28.0		
CV05-74b	do	massive microcrystalline wall rock	Matylda	0.2	25.3		
CV05-54b	do	massive microcrystalline wall rock	Bytom	-0.5	27.6		
CV05-25a	do	residual sediment granulometrically omogeneous	Pomorzanj	2.8	27.7		
CV05-49a	do	massive microcrystalline wall rock	Boleslaw	-1.0	26.4		
CV05-25b	do	altered red dolomite	Pomorzany	3.6	29.8		
CV05-25c	do	yellow altered dolomite in clasts	Pomorzany	3.6	29.9		
CV05-25d	do	grey dolomitic matrix	Pomorzany	-0.7	28.2		
CV05-20a	do	oxidized dolomite	Tzrebionka	-1.0	28.9		
CV05-17a	do	laminated sediment	Boleslaw	-0.8	30.1		
CV05-2a	do	massive wall rock	Boleslaw	0.9	31.1		
CV05-44b	do	reddish rhombohedral crystals in cavities	Boleslaw	0.6	28.3	27.0	2.3
CV05-68a	ce	white crystals	Olkusz	-12.8	13.8		
CV05-55b	cc	crystalline massive level	Tzrebionka	-9.6	21.9		
CV05-6a	cc	white crystals	Boleslaw	-4.4	23.9		
CV05-60a	cc	rhombohedral white crystals on sulfides	Boleslaw	-9.8	21.4		
CV05-78b	cc	globular white vitreous concretion	Boleslaw	-8.7	23.8		
CV05-55b	ar	crystalline massive level	Tzrebionka	-9.5	21.5		
CV05-77b	cc	white vitreous concretion	Boleslaw	-6.6	23.2		
CV05-45b	cc	white crystals	Boleslaw	-6.1	23.2		
CV05-34b	cc	white vitreous concretion	Boleslaw	-9.4	23.5		
CV05-8a	cc	red crystals in cavities	Boleslaw	-10.1	23.3		
CV05-51a	cc	calcite in veins	Boleslaw	-8.4	23.9		
CV05-55a	cc	fibrous white crystals	Tzrebionka	-8.2	21.7		
CV05-24a	cc	globular white vitreous concretion	Pomorzany	-9.2	21.8	22.1	2.68

*Abbreviations: cc = calcite; ce = cerussite; do = dolomite, sm = smithsonite

smithsonite") could be due to a variation of isotopic composition of the fluid and/or a fluid temperature variation during precipitation. The C-isotope variation of *white galman* smithsonites indicates a mixed contribution between carbon derived from OBD host rock and organic carbon from the soils: a range commonly reported in supergene smithsonites (Gilg et al., 2007a). This has important implications about the genesis of smithsonite in *white galman*, which will be discussed below. No correlation exists between stable isotope values and morphology or chemistry of smithsonite, as it was the case of other supergene deposits (Boni et al., 2003).

5.7.2 Dolomite

After petrographic and geochemical investigation we had distinguished at least three different dolomite generations: OBD I, II and III..We should remember that OBD I and OBD II are not necessarily the same defined by Hejilen et al. (2003). Stable isotope analyses were carried out on each of them. However, it was impossible to separate OBD I and OBD II for isotopic analysis, due to the tight intergrowths of both generations. For this reason the samples we have measured were generally mixed (OBD I + OBD II).

OBD I and II show $\delta^{13}C_{VPDB}$ values ranging from -2.25 to 3.62‰ (av. 0.17‰, $1\sigma = 1.68$) and $\delta^{18}O_{VSMOW}$ values constrained between 23.71 and 31.10‰ (av. 27.42‰, $1\sigma = 2.03$). These values are perfectly comparable with stable isotopes results on the separated and mixed samples of OBD I and II from Trzebionka and Pomorzany area obtained by Heijlen et al. (2003) (fig. 5.11) and with the values of OBD (no distinction was made between OBD I and II) from the Pomorzany area by Narkiewicz (1993). A very low value for both $\delta^{13}C$ (-8.05‰ VPDB) and $\delta^{18}O$ (22.96‰ VSMOW) has been recorded in the dolomite of sample CV05-51B (Boleslaw mine). The cause of this relatively low $\delta^{13}C$ value measured in this sample could be the presence of late meteoric calcite in micro-veins, as evidenced by SEM, and/or of $Fe(CO_3)OH$ compounds in the goethite impregnated dolomitic host rock. Both these substances formed in supergene environment show relatively negative values of $\delta^{13}C_{VPDB}$ (Cerling, 1984; Yapp, 1997) and could have contributiond to give a ^{13}C-poor imprint to the dolomite.

Carbon and oxygen isotopic composition of a single OBD III sample show values comparable with those of the previous dolomite generations.

Zn-dolomite (this term refers to high Zn content and for the moment it has not a genetic meaning) from Matylda mine (sample CV05-73) is slightly depleted in ^{13}C (-3‰ VPDB) isotope with respect to other dolomite generations. This fact may point to a major contribution of a C-reduced source during precipitation of Zn-dolomite at Matylda and may be an evidence of a

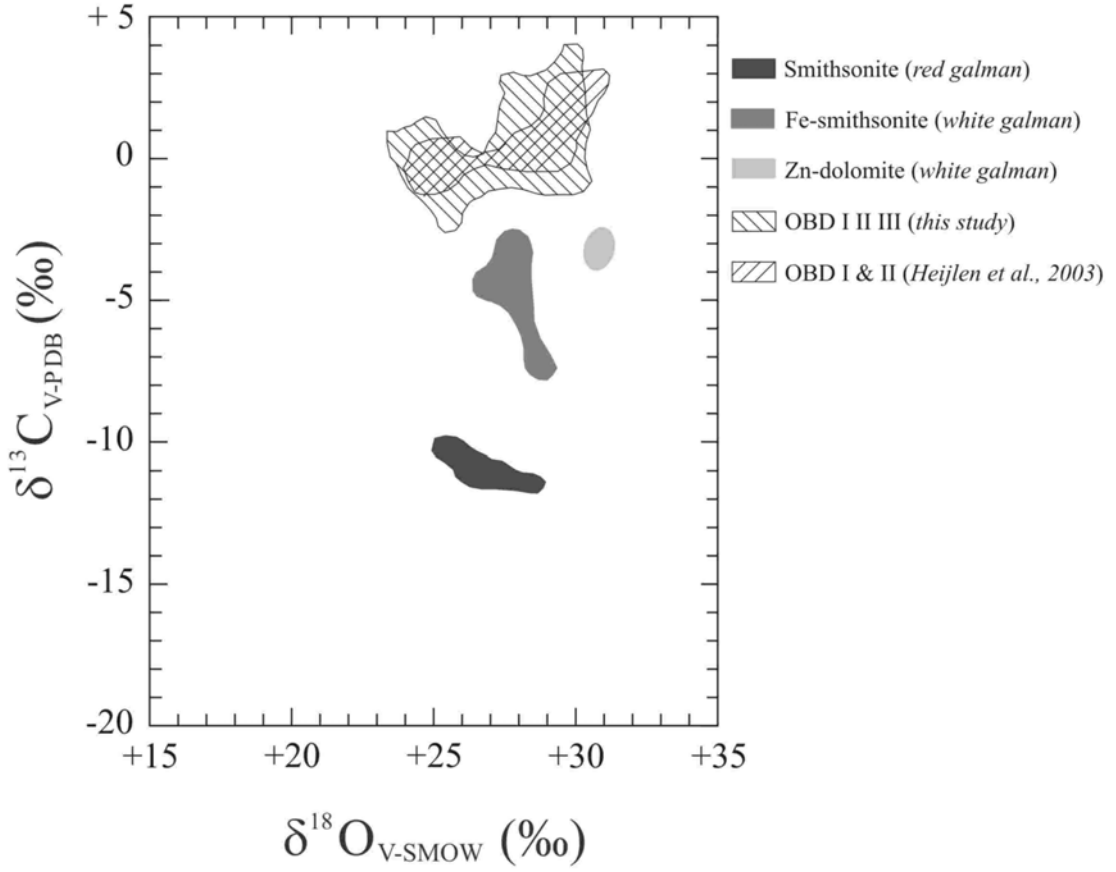

Figure 5.11: C-O isotope diagram showing the field of smithsonite in *red galman*, and the fields of Fe-smithsonite and Zn-dolomite in *white galman*. C-O isotopes fields of the different generations of OBD are shown: two different symbols characterise the values obtained in this study and those published by Heijlen et al. (2003).

different genetic mechanism compared with the genesis of the other dolomites. Also the oxygen isotope ratios of this Zn-dolomite are ~3‰ higher (30.8‰ SMOW) than in the other dolomite generations.

5.7.3 Calcite

Late calcites, syn- and post-nonsulphide ores, of supposed meteoric origin, were also measured. They show a very restricted range of $\delta^{18}O$ values between 21.3 and 23.9‰ (av. 22.8 ±1.5‰, 1σ, n=12). The values of the C-isotope ratios have an ampler spread, but all in the negative range (-4.4 to -10.1‰). Pb-aragonite (once called "tarnowitzite") from the Trzebionka mine (specimen CV05-55B) has a perfectly comparable stable isotopic composition ($\delta^{13}C_{VPDB}$ = -9.48‰ and $\delta^{18}O_{VSMOW}$ = 21.50‰) with measured meteoric calcite. The data show a predominance of the light C-source (organic matter) during the precipitation of calcite. However, the most ^{13}C-

enriched calcite (-4.44‰ VPDB) is present in sample CV05-6 from Boleslaw mine, where economic minerals are totally absent. This sample can represent calcite deposited in a barren zone, not directly interested by metal-bearing fluids.

The $\delta^{18}O$ ratios of calcites are about 4‰ lower than those of all the smithsonite generations, in accord with the theoretical model of isotope fractionation between carbonate minerals and water proposed by Zheng (1999) and modified by Gilg et al. (2007a).

5.8 Petrographical observations on fluid inclusions

A detailed petrographic study on various carbonate phases has revealed the presence of different fluid inclusion assemblages (FIAs). Fluid inclusions have been observed in the most important transparent minerals present in Polish nonsulphide ores: dolomite, smithsonite and cerussite. The thermometric experiments (freezing and heating of inclusions) have been made difficult by the presence of abundant Fe- oxides impregnating the carbonates.

5.8.1 FIs in OBD

Few fluid inclusions are present in this phase, randomly distributed in the crystals. Most of them are very small (<1μm) and only few inclusions are up to 5μm. The latter are generally monophase or empty and have irregular shape. The darkness of the crystals, the presence of oxides and the small size of the inclusions have prevented any measurement.

No suitable inclusions have been observed either in OBD II and III crystals.

5.8.2 FIs in smithsonite and Fe-smithsonite

FI observations in smithsonite have been performed on different generations. In most cases no inclusions have been identified in the smithsonite crystals. Some interesting observations were possible only on Fe-poor smithsonite (*white galman*?) from the Matylda mine and on the late smithsonite concretion occurring in the oxidation zone of the Boleslaw and Trzebionka deposits. In the first case only one FI assemblage, probably primary, has been individuated. These inclusions could be seen in three dimensions and are concentrated mainly in the crystal cores. Most of them (90%) are <1μm in length; only few of them reach up to 7μm. Isolated inclusions, of the same FI type, are present in the outer part of the crystals. Most big fluid inclusions are monophase while only the 5% of them seem to be two-phase (L+V). After heating of few two-phase inclusions up to 200°C no homogenisation was observed. This may be a clear evidence of

leaking. Some monophase inclusion have been frozen down to -80°C and heated again to promote bubble nucleation, but also in this case no change of phase was observed. Moreover, the small dimensions of most inclusions have hampered thermometric measurement. The fluid inclusions assemblage recognized in Fe-smithsonite from Matylda, show the predominance of monophase inclusions, as frequently observed in minerals precipitated at low temperature (Sabouraud et al., 1980; Goldstein, 2001).

FI study on late smithsonite has evidenced the presence of a single FIA. FIs are clearly distributed along the growing surface of the crystals and therefore they can be clearly classified as primary. The length of these inclusions is generally lower than 1μm while only 30% of the inclusions are up to 3-4μm (exclusively at Trzebionka). The shape of these fluid inclusions is variable: irregular, lobate and rounded. They are often elongated in parallel to the crystal growth plans. Most bigger inclusions are monophase (L) and only few two-phase liquid-rich inclusions have been observed. Also in this phase no thermometric measurements have been obtained.

5.8.3 FIs in cerussite

FIs observations have been carried out on cerussite crystals growing on altered primary sulphides from Olkusz deposit. Only liquid monophase fluid inclusions are present in cerussite crystals. They are divided in at least two different FIA. Inclusions clearly primary, with dimensions usually less than 1μm, and occasionally reaching 5μm, are aligned along the surfaces of single crystals. Less common small inclusions grouped in clusters crosscut growth planes. These inclusions are surely successive to the primary inclusions, but could be also pseudosecondary, sealing the fractures during crystals formation. Monophase inclusions have been repeatedly submitted to freezing and heating to promote bubble nucleation, but no change has been observed in them.

In conclusions, all the assumed primary FIAs in the “oxidized” phases are dominated by monophase liquid inclusions. Some two-phase inclusions, observed especially in the Fe-smithsonite from Matylda mine, most probably underwent leaking and/or stretching phenomena. This suggest that they have precipitated primarily from low-salinity fluids at temperatures ≤50°C (Sabouraud et al., 1980; Goldstein, 2001).

5.9 Discussion

5.9.1 Geological factors controlling the emplacement of Polish nonsulphide deposits

Literature data combined with maps and field observations at the deposit scale suggest that old re-activated faults, block-faulting, impermeable levels (as Keuper clays in this case), the presence of karst cavities filled by sulphide mineralized breccias, the porosity of host rock and the buffer role of dolomite and carbonate host rock for acidic fluids derived from oxidation of sulphides played a primary role in the nonsulphide mineralizing event.

As already mentioned in the paragraph on geological setting, we should remind that Upper Silesia was involved only marginally in the Caledonian and Hercynian orogenies, while Alpine orogeny (from Late Mesozoic onwards) influenced strongly the geological setting of this region. Especially during the Laramide phase of the former orogeny a fault network with N-S and E-W directions was produced (Gorecka, 1993: Leach et al., 1996c). This late Alpine faulting, together with the reactivation of pre-existing basement faults, enhanced the fracture permeability of the carbonate rocks, thus favouring the possible circulation of the metal-bearing fluids that deposited the primary sulphide ores and providing the pathways for their ascent (Leach et al., 1996b,1996c, 2003). According to Heijlen et al. (2003) the tensional tectonic regime established in this part of Europe during Cretaceous was the real motor for the sulphides emplacement. If the Zn-Pb primary mineralisation was emplaced during Early Cretaceous, as reported by Heijlen et al. (2003), then the uplift process and block-faulting, which affected these areas from Early Tertiary, promoted the dislocation of the lithotypes hosting primary sulphides to near-surface environment, more vulnerable to the action of meteoric waters. This process was one of the most important controlling factors for the deep oxidation of sulphides, and consequent supergene nonsulphides formation. More precisely the acting mechanisms were twofold: 1) dislocation of the blocks hosting the primary sulphide ores up to higher morphological levels, rendering them more vulnerable to weathering; 2) creation of conduits along the faults for the infiltration of meteoric fluids to facilitate the supergene alteration of sulphides.

The presence of impermeable Keuper clays on top of OBD hosting the primary deposits could have partially protected them from the circulation of oxidized meteoric water and therefore from supergene alteration. As a proof of this setting is could be reported that, especially in the Boleslaw area, supergene nonsulphides are mainly present in the horsts blocks, where the Keuper sediments are absent or have a reduced thickness. On the contrary, supergene ores occur only scarcely in the grabens, where the cover of the Keuper clays is very thick (fig. 5.4a). The situation was quite different in other areas, as in Chrzanòw region, where ore deposits (sulphides

and *white galman*) were partially protected by Jurassic sediments on top of the Ore-bearing dolomite (fig. 5.4b).

The uplift processes linked to the final stages of the Alpine orogeny also promoted the lowering of water table, thus favouring the interaction between sulphides and meteoric water in the vadose zone and the formation of a well-developed karstic network. Unfortunately, we have no data on the fluctuation of the paleo watertable through geological time. Presently, the water table in most Upper Silesia areas is relatively shallow. Before pumping began, the level of the watertable was 300 m a.s.l., (only 20m below surface) in the Pomorzany mine and about 280m a.s.l. (also 20m below surface) in the Trzebionka mine (friendly communication of the mine geologist). Therefore the nonsulphide bodies were completely immersed in the phreatic zone up to the now. These facts emphasize the concept that the weathering processes responsible for oxidation of sulphide ores and formation of supergene nonsulphides were associated with a paleowater table, much was lower than in present time.

5.9.2 Stable isotopes

5.9.2.1 Paleoclimate indications

The knowledge of oxygen isotopic composition of carbonate minerals and their mother fluids, and the use of appropriate equations of isotopic fractionation is an accurate method to obtain temperatures of precipitation, as well as to characterize the fluid type. In supergene environment, where most of polish nonsulphide ores have been formed, these temperatures are directly correlated to the atmospheric temperature and climate.

As shown in table 5.4, the O-isotopic values for smithsonite from polish *galman* have values not very different from those values measured in other supergene smithsonites around the world (Boni et al., 2003; Coppola et al., 2007; Gilg et al., 2007a).

Similar values of $\delta^{18}O$ were measured in smithsonite of both *white* (which should have a different origin) and *red galman*. However, an ampler spread (3.5‰) is recorded in the oxygen isotopic compositions of *red galman* smithsonites. This variation in the *red galman* can be related either to a change in the isotope composition of the oxidation fluid, or to a temperature variation or a combination of both. Measured values in smithsonite from *white galman* are more concentrated and point to a constant composition and temperature of the fluid during mineralizing processes.

The similar oxygen isotopic signatures recorded in these two kinds of smithsonite, does not

necessarily mean that these two types of "Zn-oxide" have been coeval. Indeed, if *red galman* formed surely after sulphides emplacement, during strong weathering events, *white galman* has been hypothesized to have been formed contemporaneous to sulphides ores, as a lateral hydrothermal product. Therefore, two mineralizing processes, each one acted by different fluids, were active in distinct geological periods, both causing the precipitation of smithsonite.

The major component of the "mother" fluid producing the supergene alteration of sulphides (and hence the *red galman*) should be of meteoric nature. Therefore, if we have indications about the isotopic composition of meteoric fluids in several epochs from Late Mesozoic till Recent, we will be able to prove the possible age of the polish supergene smithsonite ores.

On the base of most geological consideration discussed above, the Tertiary should be the most probable age for paleoweathering phenomena causing the oxidation of primary sulphides in Upper Silesia. Gilg (2003) calculated the H-O composition of paleometeoric water from three important kaolinite deposits in the near Lower Silesia, surely post Upper Cretaceous in age (most probably Tertiary), obtaining a value of $\delta^{18}O$ of about -8‰ (VSMOW). Assuming this constant oxygen isotope composition for the local Tertiary palaeometeoric waters involved in the genesis of supergene nonsulphide ores in Upper Silesia, and based on oxygen isotope composition of smithsonites, we have calculated formation temperatures of about 7 to 18°C for this minerals in Krakow-Silesia mining province (fig. 5.12, 5.13). These temperatures are in agreement with a continental near-surface environment in a temperate climate. Moreover, they are perfectly similar to those measured in Belgian smithsonite, but they are slightly lower than the temperatures measured for other supergene Zn-deposits located in southern Europe, as Iglesiente (SW Sardinia), Vila Ruiva (Portugal) and Freihung (Bavaria, Germany): 20°C ± 6 (Gilg et al., 2007a). The most probable cause of the lower temperatures should be that in Poland during the Tertiary the climate was colder in respect to other regions where supergene Zn-deposits were established.

Also the precipitation temperatures for late meteoric calcite (11 – 21°C) (fig. 5.12) are typical of a temperate climate, only slightly warmer than that occurring during the formation of nonsulphide Zn minerals. It is probable that this calcite formed in a distinct geological period with respect to the economic Zn phases.

5.9.2.2 Carbon sources

The C-isotope composition of smithsonite in *white* and *red galman* shows a substantial difference (figs. 5.10 and 5.11). *Red galman* smithsonites are ^{13}C-poor, and with uniform values

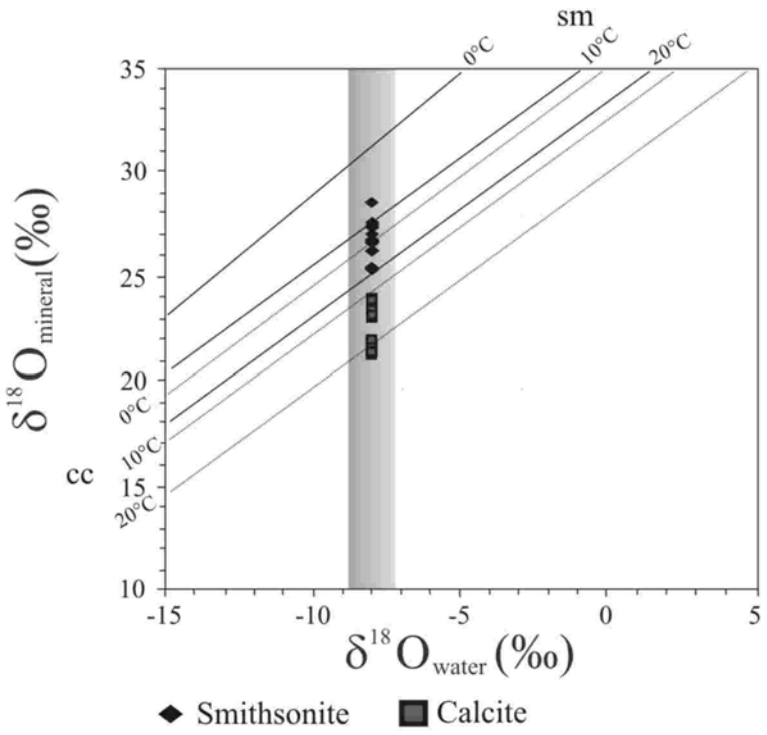

Figure 5.12: Oxygen isotope data of smithsonites (sm, rhomb), calcites (ca, square) from supergene oxidation zones of Southern Poland and estimated corresponding local paleometeoric water oxygen isotope compositions (grey strip) after the diagram of Gilg (2003).

(from -10.1 to -11.4‰ VPDB). These results are different from $\delta^{13}C_{VPDB}$ measured in other typical supergene smithsonites from Iglesiente (SW Sardinia) (Boni et al., 2003) and Liège (NW Belgium) (Coppola et al., 2007) mining districts. A similar range of values occurs in the supergene smithsonite at Villa Ruiva (Portugal) (Gilg et al., 2007a) and in high temperature smithsonite representing the carbonate stage of the base metal mineralisation in Neves Corvo deposit (Portugal) (Relvas et al., 2006). These values are very close to which shown in C3 grasses, usually present in soils where atmospheric night temperature is lower than 8°C (Cerling, 1984).

The most probable carbon sources during supergene oxidation of the sulphides are: 1) an isotopically light carbon, derived by the reduced organic matter in the soils, and 2) an isotopically heavy carbon, derived from atmospheric CO_2 and carbonate host rock. Thus, the possible explanation for the particular pattern observed in the polish *galman* could be the predominance of the first C-source, corresponding to the organic matter in the soils, with respect to the atmospheric- and host rock-derived (including OBD I and II) carbon. This aspect is relatively different from the situation from other supergene nonsulphide deposits, where a mixed (^{13}C-enriched and ^{13}C-depleted) carbon source is frequently detected in the Zn-carbonates (Boni et al., 2003; Coppola et al., 2007; Gilg et al., 2007a).

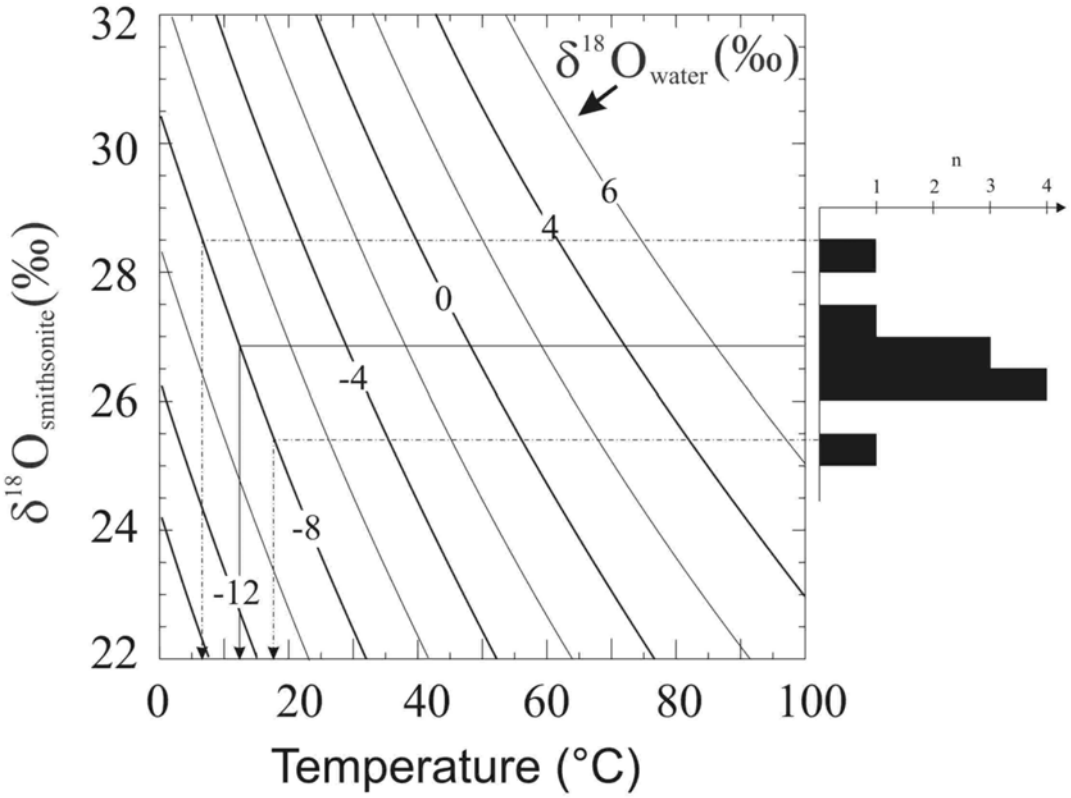

Figure 5.13: Graphical representation of oxygen isotope equilibrium curves between smithsonite (red galman) and water according to Gilg et al. (2007a), calculated for different $\delta^{18}O_{water}$ values as a function of temperature. The histogram to the right shows the oxygen isotope composition of smithsonites in *red galman* from Upper Silesia district, S Poland. Calculated temperatures for smithsonite formation are based on the $\delta^{18}O_{VSMOW}$ value of -8.0 ± 1.0‰ for the local paleometeoric water as proposed by Gilg (2003).
Note: dashed line = max and min $\delta^{18}O_{VSMOW}$ values, continue line = average $\delta^{18}O_{VSMOW}$ values.

Smithsonite carbon in *white galman* shows an ampler variability (4.5‰) than smithsonite in *red galman*. This pattern is similar to the smithsonite isotopic ratios detected in Broken Hill (Australia) or Skorpion (Namibia). Unfortunately, in our case we cannot exclude than we have not analyzed enough samples (n=3), which are not really representative for this kind of ore. However, in the *white galman* a mixed contribution of both isotopically light and heavy carbon can be considered.

Also the carbon isotope values of Zn-dolomite from the Matylda mine are in the range of isotopic composition of smithsonites in *white galman* from the same mine. This may confirms the idea of a genetic link between these two phases, which could be the result of the same continuous hydrothermal event. Therefore in the *white galman* we recognize a trend in the carbon isotope composition, which goes from heavier values in the Zn-dolomite to lighter ones in the smithsonite, where a C-reduced source became more important. This trend could further evolve with the supergene alteration of both *white galman* and sulphide ores and the relative precipitation of supergene minerals, when the C-reduced source is predominantly involved.

Also the calcites associated to *red galman* mineralisation have a very variable C-isotope composition (~6‰ VPDB), but all negative and ranging between -8.2 to -10.1‰ (VPDB). Also this range point to predominance of a ^{13}C-depleted source in the precipitation of calcite. The latter could be the usual reduced organic matter in the soils, but we cannot exclude a small contribution from the carbon from smithsonite locally replaced by calcite.

5.9.3 Origin of *white galman*

Nature, origin and distribution of *white galman* is still highly uncertain, because literature data on this subject are far from being exhaustive, and all the outcrops of what was considered *white galman* do not exist anymore.

In the old as well as current literature a hydrothermal origin for this type of deposits is commonly accepted. The *white galman* is thus considered a lateral product of the same hydrothermal event depositing the sulphide ores (Zabinski, 1958, 1986; Panek & Szuwarzynski 1974; Bak & Niec, 1978; Kucha, 2005; Kucha & Czajka, 1984). However, indisputable geochemical results (as abundant fluid inclusions and/or isotope studies) have never been mentioned in support of this theory. A short review of the different approaches to the genesis of *white galman* proposed by several authors is reported below.

According to Kucha (1984, 2005) the formation of Zn- and Fe-carbonates (metals-rich dolomite and smithsonite) occurred in a S-free reducing environment during the first stages of the primary mineralizing event, then followed by the sulphide precipitation. During this first stage, Zn, Fe and Pb were introduced in the rhombohedral structure of the carbonates. Probably this stage was responsible for the formation of the smithsonite-siderite halo around the sulphide orebodies in the Trzebionka mine (Kucha, 2003) and of the Fe-smithsonite-barite halo in the Boleslaw mine (Bak, 1993). Subsequently, under the impermeable cover of the Keuper sediments, H_2S became very abundant in the diagenetic environment, causing the conversion of the metallic carbonates into sulphides. We need to remember that this hypothesis is based on an Upper Triassic – Middle Jurassic age for the emplacement of both sulphide and associated *white galman* ores. To confirm his theory, Kucha (2005) mentioned also the fact that the *white galman* horizons in the Matylda mine are located in an equivalent stratigraphic position as the sulphide ores in the Trzebionka mine (~20km to north). Few fluid inclusions measured in the banded smithsonite- siderite overgrowths on bleached dolomite clasts and followed by sphalerite precipitation from the mineralized breccias in the Chrzanòw area have homogenisation temperatures constrained between 95 and 103°C (Kucha, 2005).

According to Zabinski (1960) a metasomatic process of the host rock (OBD) by Zn- and Fe-rich fluids was responsible for the *white galman* formation, which should have anticipated the precipitation of sulphides. In the Matylda mine, a primary origin of *white galman* instead of sulphides is confirmed by the almost total absence of sulphide minerals.

Our study has revealed a substantial difference in the mineralogy and geochemistry between the samples representing *red* and *white galman* (the latter from the Matylda mine). One of the crucial features of *white galman* from Matylda is the presence of Fe-smithsonite as well as of Zn-dolomite, which should probably have a common origin. Only in this mine-site we have detected the presence of both these phases; nevertheless they have been observed separately also in other areas of the district.

Stable isotope geochemistry may give an important contribution to solve the genetic problem of the *white galman* ore. To this aim we have to investigate from a stable isotope geochemical point of view all the carbonate phases possibly cogenetic with Fe-smithsonite. Fe-smithsonite and Zn-dolomite present in the mineralized horizon of Matylda mine have been described in literature as the main phases of this typology of nonsulphide ore (Zabinski, 1960; Kucha, 2005). Therefore, if we assume them to be the result of the same mineralizing event, the comparison of their stable isotope ratios (carbon & oxygen) may be crucial. In fact the C-isotope composition of both (Fe)-smithsonite and Zn-dolomite at Matylda mine is quite similar. These phases are both ^{13}C depleted and the values of Zn-dolomite are mostly concentrated in the higher (less negative) extreme of the range. On the whole, a difference of about 0-3‰ has been recorded between the $\delta^{13}C$ values of Fe-smithsonite and Zn-dolomite. According to Deines (2005), the carbon isotope fractionation between dolomite- and smithsonite-water, in a range of temperature between 25°C and 100°C should be about 3-4‰, with the most ^{13}C-depleted values in dolomite. The temperature up to 100°C can also be associated to a low- to moderately high-temperature hydrothermal event. The difference of the $\delta^{13}C$ values recorded in between Fe-smithsonite and Zn-dolomite at Matylda are fully in accord with the predicted fractionation (Deines, 2005) (figs. 5.10 and 5.11). This may be proof of a genetic relationship between these metal-carbonates, thus suggesting a precipitation from the same (hydrothermal?) fluid.

If we consider the *white galman* (Fe-smithsonite and Zn-dolomite) as a lateral facies formed during the primary hydrothermal event that precipitated both OBD II and sulphides, we can assume that the precipitation of *white galman* was related to a fluid with the same characteristics as those precipitating OBD II and sulphides. Therefore, on the base of the oxygen isotope composition ($0‰_{VSMOW}$) of the fluid that precipitated OBD II (Heijlen et al., 2003), we could calculate a temperature of precipitation for Fe-smithsonite and Zn-dolomite of 35-53°C (fig.

5.14) and 30-38°C respectively.

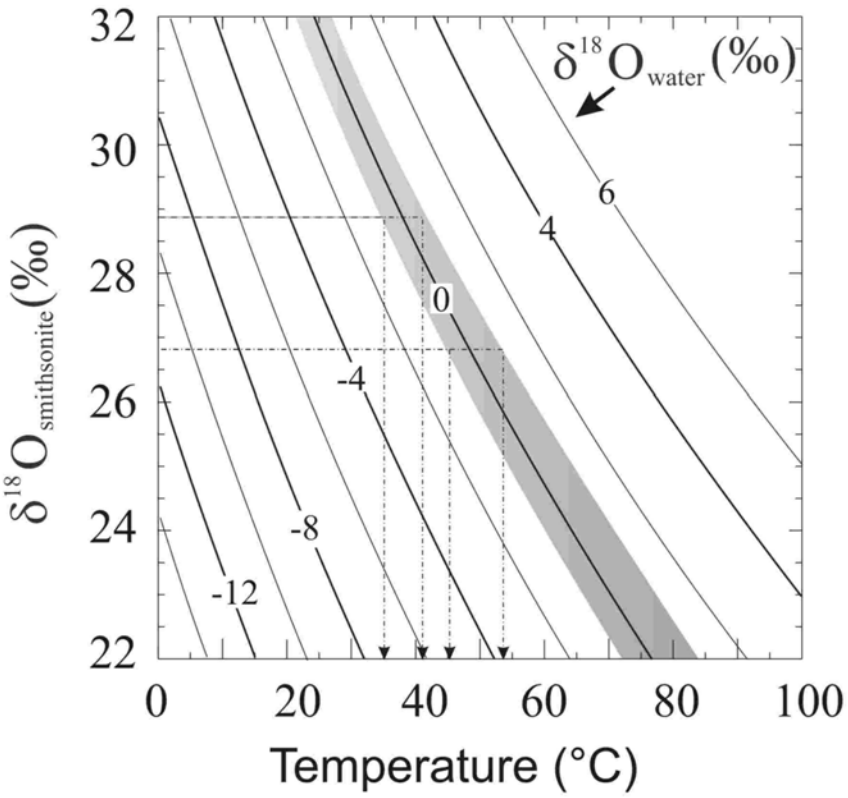

Figire 5.14: Graphical representation of oxygen isotope equilibrium curves between smithsonite (white galman) and water according to Gilg et al. (2007a), calculated for different $\delta^{18}O_{water}$ values as a function of temperature. Calculated temperatures for smithsonite formation are based on the $\delta^{18}O_{VSMOW}$ value constrained between -0.8 - 0.8‰ for the hydrothermal fluid as proposed by Heijlen et al. (2003).
Note: dashed line = max and min $\delta^{18}O_{VSMOW}$ values

These relatively low temperatures could be present in the peripheral phases of the higher temperature mineralizing events. We have to remember that (Fe-) smithsonite, siderite and Zn-Fe-dolomite form halos around the main ore-bodies and have been considered paragenetically earlier than sulphides (Bak, 1993; Kucha & Czajka, 1984). All this considerations seem to suggest that *white galman* formed during a low-temperature stage of the primary hydrothermal event from a S-free fluid as suggested by Kucha (2005). Zinc was then precipitated as carbonate instead of sulphide. Unfortunately no thermometric analysis was carried out on the *white galman* minerals, but the constant presence of monophase inclusions and of only few two-phase leaked inclusions, confirm that these carbonate phases formed under low-temperature conditions (≤50°C) (Sabouraud et al., 1980; Goldstein, 2001).

We cannot completely exclude a supergene origin for the *white galman*. If this would be the case, we can assume the isotopic composition of Tertiary paleometeoric water (Gilg, 2003) as the composition of the fluid involved in its formation. In this case we obtain a temperature of

precipitation between 5 and 12°C for (Fe-)smithsonite in *white galman.* This temperature is almost comparable with that of smithsonite in *red galman* calculated using the same value of meteoric fluid.

5.9.4 Timing of nonsulphide deposits in the Upper Silesia, S Poland

As discussed above, most of the nonsulphide ores are supergene in origin (*red galman*) and represent the product of oxidation of primary sulphides correlated to weathering and/or paleoweathering events. Only some of them, the so-called *white galman*, can be hydrothermal in origin.

Actually, both the lower and the upper temporal boundaries of nonsulphide formation in Poland are uncertain. The supergene Zn-oxides are surely younger than primary sulphide deposits, but the question about the timing of main sulphide emplacement is still open. Three different ages have been proposed for the primary mineralizing event: 1) Upper Triassic-Middle Jurassic (Sass-Gustkiewicz et al., 1982, 1998); 2) Lower Cretaceous (Hejilen et al., 2003); 3) Lower Tertiary (Leach et al., 1992, 1996a, 1996b, 1996c, 2001). In conclusion, the possible age range for the primary sulphides spans from Upper Triassic to Lower Tertiary. Presently, I am not able to pronounce myself for a sulphides emplacement age: besides, this would be beyond the objectives of this Ph.D thesis. However, considering several geological and geochemical evidences for the age of supergene nonsulphides in Upper Silesia, I am inclined to consider think that the more reliable age for the emplacement of primary ores was Lower Cretaceous as proposed by Hejilen et al., (2003) after direct dating of sphalerite. A few age-constraints to the genesis of secondary deposits will be of great importance to put at least an upper temporal limit to sulphide emplacement. These are listed below.

In the Chrzanòw area, a small concentration of oxidized minerals, together with sulphide fragments, has been discovered under a Jurassic cover, suggesting a pre-Jurassic first phase of sub-aerial exposure (Smakowski & Strzelska-Smakowska, 2005). This should imply either that the primary sulphides are even older (pre-Jurassic) or that only a smaller concentration of sulphides, result of a local mineralisation event, was oxidized during this first sub-aerial exposure. The second hypothesis is far more reliable.

It seems commonly acknowledged that the most favourable conditions for the development of the weathering processes, which could have produced most of the supergene ores in Poland, existed in Lower Tertiary. During this period an extensive sub-aerial exposure facilitated the removal of parts of the Mesozoic and Tertiary cover, thus favouring the circulation of meteoric

waters and the alteration of primary sulphides and of their host rocks. Erosion surfaces intersected by karstic channels are quite common in the region. Some of these channels are filled by Paleogene continental sediments, containing alluvial galena fragments and *galmans* (Szuwarzynski, 1978). Other karst-cavities in the Ore-bearing dolomite and underlying Gogolin limestone contain fragment of nonsulphide ores embedded within continental sandy and clayey sediments of Paleogene age. The filled cavities are then covered by Tortonian sandy clays deposited in a marine environment.

Thus seem probable that the principal paleoweathering stage, promoting the formation of most supergene Zn-(Pb-Fe) deposits, took place shortly before or during Palaeogene or Early Neogene. It was surely pre-Tortonian, as evidenced by the karst morphology filled with detrital sulphide and oxide minerals, associated to Palaeogene continental sediments (Szuwarzynski, 1978; Panek & Szuwarzynski, 1975). Block-faulting induced by the late stages of the Alpine orogeny in the Lower Tertiary, could have contributiond to accelerate the oxidation of primary sulphides before the Miocene marine ingression. However, especially in the northern-eastern part of the district where Tertiary sediment are missing, the weathering processes could have acted more or less continuously for longer periods until Recent. Indeed Upper Silesia has been characterized by a continental environment during most part of the Tertiary and Quaternary.

Other paleoweathering records detected throughout the region could be a helpful tool to age-constrain the weathering events responsible for the secondary Zn deposits. Indeed it is well known in the upland belt stretching across southeastern Poland in the front of the Carpathians, the presence of weathering remnants on altered Carboniferous, Permian and Mesozoic sedimentary rocks. These weathering evidences include de-calcified and silicified limestones, terra rossa-like clays, locally with flint nodules, clayey–sandy remnants of clastic rocks and iron-rich ochraceous sands (Pozaryski, 1951; Uberna, 1962; Alexandrowicz, 1969; Różycki, 1972; Harasimiuk, 1975; Gradziński, 1977; Kowalski, 1979; Felisiak, 1992; Liszkowski, 1996). These saprolite deposits are of various ages, but the most important of them seem to be Early Tertiary because many of these deposits occur below a cover of Miocene sediments (Alexandrowicz, 1969; Kowalski, 1979). In adjacent areas, as the Bohemian Massif and the Sudetes Upland and Foredeep, have been recognized many weathered profiles, dated from Cretaceous to Oligocene-Miocene (Migoń & Lidmar-Bergström, 2001). Many kaolinitic deposits have been recognized and described in the Lower Silesia region. At Szklary near Zabkowice Slaskie (Lower Silesia), about 200Km at NW of Krakow, a residual weathering mantle with Ni-laterite, was developed on serpentinite from the Early Palaeozoic basement. These laterites have been considered of Palaeogene age (Ostrowicki, 1965; Niskiewicz, 1967, 2000; Dubinska et al., 1986, 2000).

Kaolinitic profiles estabilished on Hercynian granite have been recognized at Zarow and Turow (Wyszomirski et al., 2003), all in the Lower Silesia, with a post Upper Cretaceous age (Gilg, 2003).

Most probably, several weathering stages affected this part of Europe from Mesozoic until Quaternary, as showed by the grus deposits of Recent age (Migoń & Lidmar-Bergström, 2001).

In conclusion, we can affirm that supergene nonsulphide ores in Upper Silesia are mainly the result of weathering processes acting mainly in the Lower Tertiary (until Miocene). However, also in Recent times sulphide oxidation may have continued, taking advantage of several distinct weathering phases; the secondary minerals were re-equilibrated with changing climate.

Timing and origin of *white galman* are actually uncertain. Assuming a Early Cretaceous age for the primary sulphides emplacement (Heijlen et al., 2003), the *white galman* was formed approximately at the same time, when the absence of Sulphur in the fluid and more oxidizing conditions hampered the precipitation of sulphides promoting instead that of the carbonates.

On the other hand, if *white galman* represents the result of supergene alteration, the different mineralogy and geochemistry recorded in this type of Zn-oxide deposit may be due to slightly different geochemical conditions and to a variable metal content in the fluid in that area where it mainly occur (Chrzanòw).

Chapter 6: Nonsulphide Zn deposits in the Irish Midlands

6.1 Introduction

The Irish Midlands represent one of the most important ore districts in Europe, known as the "Irish Orefield". Mining activity is currently concentrated mainly on sulphide ore deposits, whereas nonsulphide ores have been considered as an important source for base metals mostly in the past. The only significant nonsulphide resources in the Irish Orefield were located at Tynagh (the so-called *Residual orebody*), which was mined during the 70s, and at Silvermines, mined intermittently from the 17th century until 1953. However, in the light of the renewed interest towards Zn nonsulphide in the world, prospective projects on this type of mineralisation are currently taken into consideration also in Ireland. Recent drilling was carried out in November 2002 in the nonsulphide zone at Silvermines (Balassone et al. 2007), where a good intersection containing both primary sulphides and oxides residuum has been encountered.

Base metal (sulphide and nonsulphide) deposits, located in the Irish Midlands, are hosted in the Lower Carboniferous carbonate rocks. This orefield includes five big sulphide deposits (Navan, Tynagh, Galmoy, Silvermines and Lisheen) (fig. 6.1), and many smaller economic and sub-economic deposits all of them discovered after the 50s. Indeed, over the past 50 years, mining activity in Ireland has undergone a sensible increase. If most aspects on the nature and genesis of Irish primary sulphides have been satisfactory discussed and explained (Boyce et al., 1983; Russell, 1986; Andrew, 1986a, b, 1993; Williams & Brown, 1986; Clifford et al., 1986; Hitzman, 1995; Hitzman & Large, 1986; Hitzman & Beaty, 1996; Hitzman & Beaty, 2003; Everett et al., 1999a, 1999b; Wilkinson, 2003; Wilkinson & Earls, 2000; Wilkinson et al., 2003, 2005a, 2005b), there are still many open questions on the emplacement and timing of nonsulphide deposits. The latter are usually associated to primary sulphide Zn-Pb(-Cu) ores, in form of infill of karstic sinkholes and/or as typical *gossans*. A supergene origin related to (paleo)weathering processes, has been commonly accepted for these oxidized deposits (Balassone et al. 2007). Nevertheless, the ways in which these processes have acted, as well as the emplacement timing are actually still unclear.

Irish nonsulphide deposits have been the object of only few publications in the past. The first

descriptions of Zn nonsulphide ores in the Irish Midlands have been reported for the Tynagh deposit in Morrissey (1970), Morrissey & Whitehead (1971) and Clifford et al. (1986), and for the Silvermines deposit in Boland et al. (1992). Boni & Large (2003) quoted mainly the old literature on the subject, while a short report on nonsulphide mineralization in Galmoy is in Lowther et al. (2003). Actually, a complete mineralogical, petrographical and geochemical description of the Irish Zn-nonsulphides was lacking until the last comprehensive paper of Balassone et al. (2007), concentrated especially on Silvermines and Galmoy deposits. What is still missing, are geochronological (direct & indirect) studies that could link the formation of Irish nonsulphide ores to possible paleoweathering events.

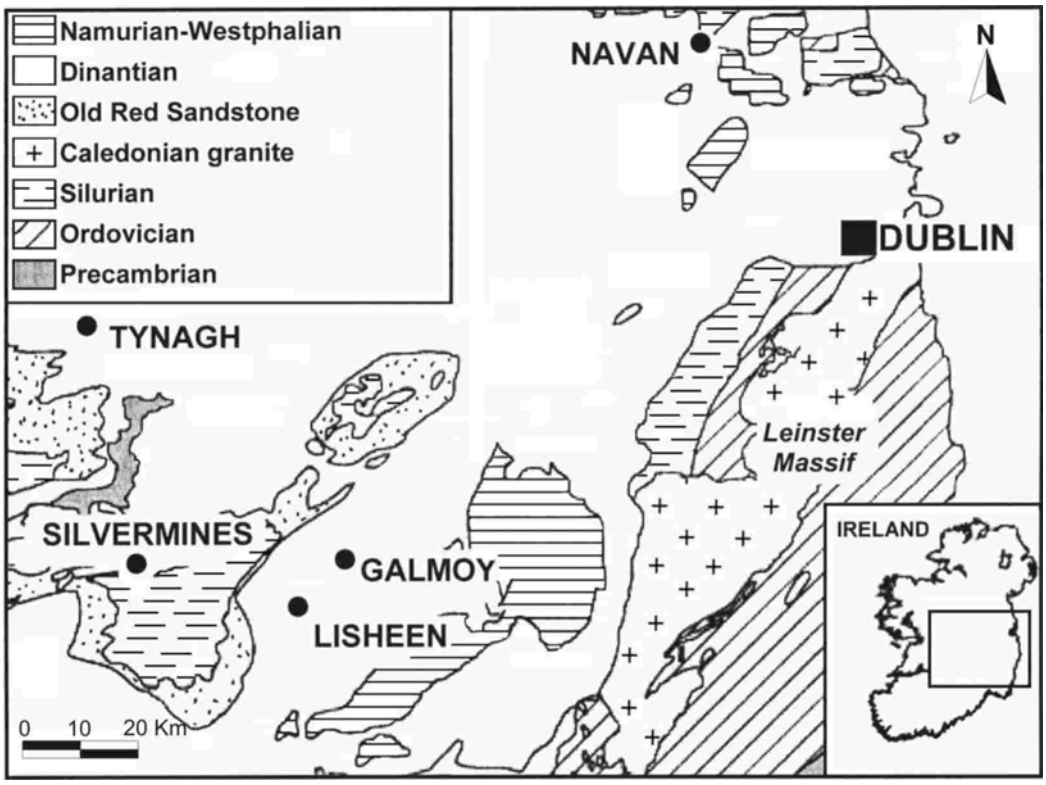

Figure 6.1: Geological sketch map of the Irish Midlands with location of most important base metal deposits (from Wilkinson & Eyre 2005, modified).

In this chapter we present a mineralogical and petrographical characterization of the three most important Zn-oxide deposits of the Irish Midlands (Silvermines, Galmoy and Tynagh), which could also explain the geochemical equilibria involved in nonsulphide genesis. Stable isotopes geochemistry (carbon and oxygen isotopes) has been also a tool for this investigation. C- and O-isotopes have been measured in Zn, Pb and Ca carbonates at Tynagh and Galmoy, in order to characterize the nature of the fluids involved in supergene alteration of primary sulphides. The obtained data have allowed us to restrain the temperature of formation of the mineral carbonates

as well as to identify the main sources of the carbon in the supergene fluid. An accurate evaluation (mostly literature-based) of the paleoweathering records linked with extensive oxidation in this part of British Isles has been also extremely useful to individuate the possible formation timing of this kind of deposits.

Most of the mineralogical and geochemical work on the nonsulphides in the Galmoy and Silvermines deposits has been carried out by other members of the Naples research group and reported in a paper recently published on Ore Geology Review (Balassone et al. 2007). I have mainly revisitated the geological setting and mineralogy of the "*Residual orebody*" of the Tynagh mine, implemented by new geochemical data, and made a general evaluation of the oxidative phenomenon in the Irish Midlands.

6.2 Geological setting of the Irish Midlands

Ireland is mainly dominated by a sedimentary sequence of Devonian-Carboniferous rocks unconformably covering a Precambrian and Lower Palaeozoic basement. The latter consists of graywackes, slates, volcanic rocks and volcanoclastic sediments of Silurian age (Hitzman & Beaty, 1996; Clifford et al., 1996). The basement was folded and faulted during the Caledonian orogeny (Silurian – Middle Devonian), which was caused by the collision between North American and European plates and the relative closure of the Iapetus Sea. The suture zone is believed to be across central Ireland, in the vicinity of Navan and Silvermines (Philips et al., 1979). The basement is affected by Late Silurian and Early Devonian intrusions related to Caledonian orogeny.

The Devonian - Carboniferous rocks represent a marine transgressive sequence whose deposition started in the Late Devonian and continued into the Lower Carboniferous. At that time, Ireland was positioned at low palaeo-latitudes, just south of the Equator (Falcon-Lang, 1999). The earliest part of the mentioned sequence is mostly confined to the Munster Basin located in the south of the country. Sediment transport was generally directed towards the south. The stratigraphical sequence begins with the Old Red Sandstone (ORS) (Late Devonian-Early Courceyan), which is widespread mainly in southern Ireland (Philips & Sevastopulo, 1986). According to Graham (1983), the Old Red Sandstone consists of detrital sediments transported from the metamorphic (Dalradian) lithologies situated far to the north.

In the Early Courceyan, the sea transgressed northwards from the southern Munster Basin in the Limerick province, producing fairly distinct depositional sequences. Based on paleogeographic

reconstructions and on lithological features, three standard successions of Courceyan age may be recognized in Ireland, which were deposited in the South Munster Basin, the Limerick Province and the Midlands Province. Tynagh and Silvermines are located in host rocks belonging to the Limerick province, while the other deposits (sulphides and nonsulphides) occur in the Midlands province.

The base of the Courceyan consists of argillaceous marine limestone, informally called Lower Limestone Shale, less argillaceous in the north of the Dublin area, covering the underlying Old Red Sandstone. In the northern Midlands, this unit passes into the Navan group deposited in a shallow marine to peritidal environment (Philox, 1984; Rizzi & Braithwaite, 1996). The Courceyan sequence continues with the Ballysteen Limestone, which is conformably covered by the Waulsortian Limestone. The Ballysteen Limestone is composed of mildly argillaceous limestone and of bioclastic/oolitic limestone with thin argillite layers deposited in shallow water carbonate platform environmnent. The overlying Waulsortian Limestone, often referred as "reef" limestone, consists of poorly stratified, massive grey micritic limestone deposited in deeper water (up to 300m). Several studies indicate that most Waulsortian Limestone, as well as the Ballysteen Limestone and Chadian and Arundian limestone, were affected by multiple dolomitisation events (Hitzman & Beaty, 1996; Somerville et al., 1997; Wright et al., 2000; Gregg, 2001; Wilkinson, 2003). After these authors two most important dolomitisation events have been distinguished: (1) extensive regional replacive dolomitisation, extended from the Hercynian front towards north, and (2) "hydrothermal" dolomitisation affecting feeder faults acting as conduits for metalliferous fluids. The timing of the dolomitisation events is still uncertain. However, the regional dolomitisation event seems to predate Zn-Pb-(Cu) mineralisation (Peace & Wallace 2000; Wright et al. 2000, Hitzman & Beaty, 2003); it should have been produced by heated marine-derived fluids (110°C and 10-13 wt% NaCl eq, Hitzman et al., 1992). The other, also hydrothermal dolomitisation, limited to the feeder zones, seems to be immediately pre- or syn-sulphide mineralisation (Wright et al., 2000; Wilkinson, 2003). Minor syn- and post-ore dolomitisation events have been also recognized by Wilkinson et al. (2005a).

In the Chadian, the sedimentation in platform carbonate environment continues and a number of basins, controlled by active faulting, developed and persisted through the whole Dinantian. Mafic volcanic rocks interlayered in Chadian-Arundian terrains, and related to this period of active tectonic, are widespread in the Irish Midlands. While during the Lower Carboniferous Ireland was undergoing a transgressive sedimentation, the collision due to Hercynian orogeny occurred further south, also influencing the tectonic regime in other areas of Ireland. The Hercynian front located in the south of the British Isles in the middle Devonian, prograded

northwards through time (Ziegler, 1988) and reached the present-day Ireland (where it coincides with the northern edge of Munster Basin, Shackleton, 1984) during the uppermost Carboniferous and Early Permian. A moderate uplift, combined with a global sea level lowering produced the regression of marine facies during Middle and Upper Carboniferous, thus leading to a change in the sedimentary environment from marine to non-marine. Middle and Upper Carboniferous terrains in Ireland consist mostly of terrestrial sediments including coal measures.

The latest phase of Hercynian orogeny (Upper Carboniferous – Permian) produced east-northeast trending upright folds, and local east and east-northeast trending thrust faults together with a pervasive cleavage (Sevastopulo, 1981). The deformation grade decreases further north, over the Munster Basin. The development of dextral, NE-trending brittle and ductile shear zones and NE-trending folds in the central Ireland is strongly controlled by basement structures, many of which are clearly reactivated Caledonian structures (Phillips & Sevastopulo, 1986).

The sedimentation of Permian and Mesozoic successions was limited to the NE of Ireland and to small grabens, while in the rest of the country, subjected to post-Hercynian uplift, the erosive processes became dominant. A numbers of fault-controlled basins were established and the sedimentation was locally limited to them. Tensional and vertical stress occurred during Upper Jurassic, probably in consequence of the opening of Atlantic sea (Ziegler, 1990). This extensional regime caused renewal uplift, subsidence and faulting in the British Isles. Later, a late Cretaceous sea flooded Ireland, which was completely submerged (Philips & Sevastopulo, 1986). From the end of Cretaceous and during Tertiary a complete emersion of the British Isles occurred, as in many other European areas, associated to several periods of strong erosion. This caused the almost complete removal of the Permian and Mesozoic covers. Weathering acted on those lithologies that were outcropping during Tertiary, as testified by many weathering profiles that can be observed mainly in Northern Ireland, spanning in age from the latest Cretaceous through Tertiary (Smith & McAlister, 1987; Migon & Lidmar-Bergström, 2001). As we will discuss later, this is the most favourable age for the development of the nonsulphide Zn deposits.

During Quaternary Ireland was covered by ice sheets whose products (moraines) still cover much of the country.

6.3 Ore deposits in the Irish Midlands

Mining activity in Ireland is mostly based on base (Zn, Pb, Ag, Cu) metals and less on Au, industrial minerals, coals and hydrocarbons. Different kinds of metal deposits, both economic

and uneconomic have been recognized in different lithologies, spanning in age from pre-Cambrian to Carboniferous. For basic information, the reader is referred to the IAEG (Irish Association of Economic Geology) volume on Irish deposits edited by Andrew et al. (1986a). The earliest evidence of metal mining in Ireland is provided by the copper exploitation during Bronze Age (http://www.minex.ie), but few other records of mining activity remain prior to a first major period of mining that started in the 19th century. After a period of prolonged depression for the Irish mining industry, which lasted since the end of Industrial Revolution until the end of II World War, the renewed increase of mining activity was due principally to the discovery of new Zn-Pb deposits hosted in Lower Carboniferous rocks of the central Irish Midlands: Tynagh in 1961, Silvermines in 1962 and Navan in 1970. This fact encouraged new prospective projects in the country and led to discover further economically valuable Zn-Pb deposits: Galmoy in 1986 and Lisheen in 1990. Actually the main focus for base metal exploration remains still the Lower Carboniferous of the Midlands. Indeed the only three still active metal mines in Ireland (Navan, Lisheen and Galmoy) produce zinc and lead concentrates from base metal deposits hosted by Lower Carboniferous rocks.

In this thesis I will deal mainly with the metal ore deposits (sulphides and nonsulphides) located in the Irish Midland province (Central Ireland). In particular, after a brief review of the primary sulphide deposits, I will report on their supergene alteration products, namely the nonsulphide ores of three important mines: Galmoy, Silvermines and Tynagh.

6.3.1 Zn-Pb(-Cu) sulphide ores

Despite a discussion on Irish primary sulphide deposits is not among the aims of this thesis, a short review on their geological setting, mineralogical assemblage and mode of emplacement, may be important to understand the genetical characteristics of the nonsulphide ores derived from them.

The Irish Midlands orefield is one of most important and productive in Europe. This mining province includes five significant deposits (Navan, Silvermines, Tynagh, Galmoy, Lisheen) and a number of smaller deposits. The total estimated tonnage of the Zn-Pb deposits is over 160 Mt with Zn and Pb grades extremely variable and constrained respectively between 3-13% and 0.5-6% (tab. 1.1) (Hitzman & Beaty, 1996 and references therein). Around 98% of the economic bodies, consisting of Zn-Pb sulphides and associated barite occur in carbonate rocks of Courceyan age, but other subeconomic sulphide mineralisations are also developed in rocks of

variable age, from Upper Devonian Old Red Sandstone to Arundian carbonates. The Waulsortian limestone (Courceyan) represents the most frequent host rock of sulphide deposits, even if smaller bodies were detected also in the Ballysteen limestone. The Navan giant mineralisation, as well as other smaller concentrations nearby, is hosted in the limestones of the Navan Group.

Sulphides occur as stratabound bodies, which show replacive, massive, brecciated, vein and void-infilling textures. Mineralised bodies are mostly developed into the hangingwall of E-NE trending normal faults, with minor bodies recorded in the footwall. The size of the single elongated bodies is extremely variable, from 30m in the vicinity of feeder faults to 1-2cm in the periphery, and shows both sharp and gradational contacts with the host rocks. Sphalerite and galena, with pyrite and marcasite in lower abundance, are the dominant mineralogical phases of the Irish Zn-Pb sulphide deposits. Tennantite and Cu-sulphides are minor phases. Barite is very common in the mineralised areas, as demonstrated by the giant barite orebody at Magcobar near Silvermines. Gangue minerals are calcite, dolomite, Fe-dolomite and minor quartz.

The timing of Zn-Pb-(Ba) mineralisations in Irish Midlands, as well as their mechanism of emplacement remains still a controversial question (Sevastopulo & Redmond, 1999; Lee & Wilkinson, 2002; Hitzman & Beaty, 2003; Symons et al., 2002; Wilkinson et al., 2005a).

Different mineralisation styles have been observed in the Irish ores. They have been related to the following genetic models: (1) ore deposition during or immediately after diagenesis of the host rock (syndiagenetic or sedimentary-exhalative model), (2) ore deposition after burial the of host rock (epigenetic or Mississippi Valley-type model).

The sedimentary-exhalative model had been presented initially by Russell (1978) and then accepted by most Irish researchers. This model envisaged the presence of a convective circulation of modified seawater in the underlying Carboniferous and Devonian sediments as well as through the basement in a extensive regime. These fluids were heated, leached a series of metals from the underlying rocks and finally ascended to near-seafloor zones along deep (feeder) faults. Metal sulphides and barite were precipitated by uprising hydrothermal metal-bearing solutions after mixing with alkaline brines or seawater on or just below seafloor (Wilkinson et al., 2003, 2005b). To agree with this model, a fluid inclusions study on sphalerite and barite reveal the presence of two distinct fluid responsible for the mineralisation at Tynagh: a metal-bearing fluid with salinity of 12% wt NaCl eq. reaching the temperature of 240°C and a sulphur-bearing fluid with 23 eq. wt% NaCl-$CaCl_2$ and temperature less than 50°C (Banks et al., 1992).

The Mississippi Valley-type model was proposed for the Irish orefield by Hitzman & Beaty (1996) and it is mainly accepted by North American scientists. In this topography-driven fluid flow model, the Hercynian Orogeny was the fundamental driving force for sulphide

mineralisation in the Irish Midlands. After the mentioned authors, the uplift of Hercynian chain further south should have provided the necessary hydrologic head for the fluids migrating towards the foreland basins in the north. Fluids were heated in the relatively deep flow paths and leached metals from the Old Red Sandstone through which they migrated. Mineralising fluids escaped through the overlying Lower Carboniferous carbonates mostly through E-NE trending normal faults (but also W-trending faults may be played an important role after Hitzman & Beaty, 1996) and mixed with saline formation seawater. Thus, a mixing of uprising metal-bearing fluids with sulphate-bearing fluids may have produced sulphides precipitation. Fluid inclusion studies suggest that the fluids involved had temperatures ranging from 100°C to 190°C and salinities of 10–23 eq. wt% NaCl (Hitzman & Beaty, 1996 and references therein). A first hydrothermal pulse may have produced a wave of pre-ore dolomitisation.

Sulphide mineralisation in the Irish Midlands has features that are akin to both Sedex- and MVT-style deposits. Features shared with Sedex deposit (syngenetic or syndiagenetic origin) are: 1) spatial relation to faults, believed to act as feeder channels; 2) relatively high temperature of the fluids (up to 240°C; Banks et al., 1992); 3) stratiform shape of the bodies; 4) presence of pyritized tubes, believed to be worm fossils (Boyce et al, 1999; 2003). This fossil fauna in Waulsortian limestone is similar to that found in ancient and modern VHMS deposits; 5) presence of chimneys (Larter et al., 1981; Russell et al., 1982; Boyce et al., 1983; Banks et al., 1985), interpreted as paleo-fluid conduits; 6) evidence of interaction of hydrothermal fluids with muddy, not lithified sediments; 7) occurrence of sedimentary breccias, which are interpreted to be developed as debris-flow, associated with synsedimentary faulting on seafloor.

On the other hand, features typical of MVT deposits are: 1) prevailing carbonate host rocks; 2) simple mineralogy; 3) hydrothermal brecciation; 4) ubiquitous dolomitisation; 5) lack of faunal change in the host rock of mineralised areas (Schultz, 1966; Sevastopulo, 1979).

All these features, common to either MVT or Sedex-type deposits, are often observed in the same individual deposit. Therefore the most probable explanation may be a multiple-stage mineralisation event, which occurred in successive steps during the diagenetic history of the host carbonates.

Due to their peculiar characteristics, the sulphide deposits in the Irish Midlands have been denominated as “Irish type” deposits.

Dating the Irish sulphides deposits is also highly problematic. Currently, only the Navan deposit has been dated with traditional methods. It is believed that here the mineralising event developed in a period constrained between Arundian and Holkerian (Peace & Wallace, 2000). According to Hitzman & Beaty (1996), the mineralisation at Navan occurred prior to and during the Arundian.

In the other deposits, the geological features seem to be in accord with a Chadian – Arundian age of mineralisation. In conclusion, it may be inferred that mineralisation was diachronous across the orefield: it initiated in the Chadian and continued until at least the early Arundian (Wilkinson et al., 2003). Recent direct Rb-Sr dating of sphalerite from Silvermines (Schneider et al., 2007) revealed an isochron age of 360 ± 5Ma, thus constraining the age of mineralisation to Early Tournaisian (Courceyan). This age is in agreement with an early, syndiagenetic-exhalative origin for the Silvermines system and is inconsistent with a gravity flow model for the mineralising fluids in the Irish orefield related to the Hercynian orogeny.

6.3.2 Nonsulphide Zn ores

Significant nonsulphide resources in the Irish Midlands have been recognized in the past only at Tynagh ("*Residual orebody*") and at Silvermines. Recent exploration programs had revealed the presence of other nonsulphide concentrations in the area of Silvermines and underground at Galmoy.

At the beginning of "modern" mining activity in Ireland (second half of the 20th century), the nonsulphide deposits were mainly neglected as zinc resource, because the focus was on the sulphide deposits, as in other European Zn-Pb mining districts. In the light of the new interest towards this kind of mineralisation throughout the world, Irish nonsulphides may represent a new exploration target.

There is at the moment only poor information on the different aspects of Irish nonsulphide deposits. This lack of extensive data encourages new studies, both from the geological than from the mineralogical-geochemical point of view.

Irish nonsulphides represent the supergene weathering products of primary sulphide ores: they occur mostly as *gossan* on the sulphide bodies, and more rarely as infilling of karstic cavities. They are generally covered by 6-10m of glacial till, composed of clayey gravels underlain by silty to sandy clays, deposited during the Midlandian Cold stage by glaciers advancing southwards across Ireland (Morrissey & Whitehead, 1971; Boni & Large, 2003).

6.3.2.1 Silvermines deposit

At Silvermines, in northern County Tipperary, Pb-Zn sulphide orebodies with associated barite, and residual supergene nonsulphides are present. This area is best known for base metal sulphide

deposits, exploited from 1968 to 1982, and barite, mined out from 1963 until 1993 (Boland et al., 1992; Department of Communications, Marine and Natural Resources, Ireland website - http://www.minex.ie: Environmental: Mine Site Rehabilitation).

Sulphide bodies occur in the Devonian and Lower Carboniferous strata on the northern downthrows side of a major east-northeast transcurrent Silvermines fault zone (fig. 6.2a, b). This main fault zone has produced a maximum northern downthrow movement of about 350m (Taylor, 1984). Northwest trending faults crosscut and dislocate the main east-northeast faults in the mineralised area. These faults are believed to have controlled the emplacement of both sulphide and nonsulphide (residual) bodies, having acted as conduits for hydrothermal and meteoric fluids (see below).

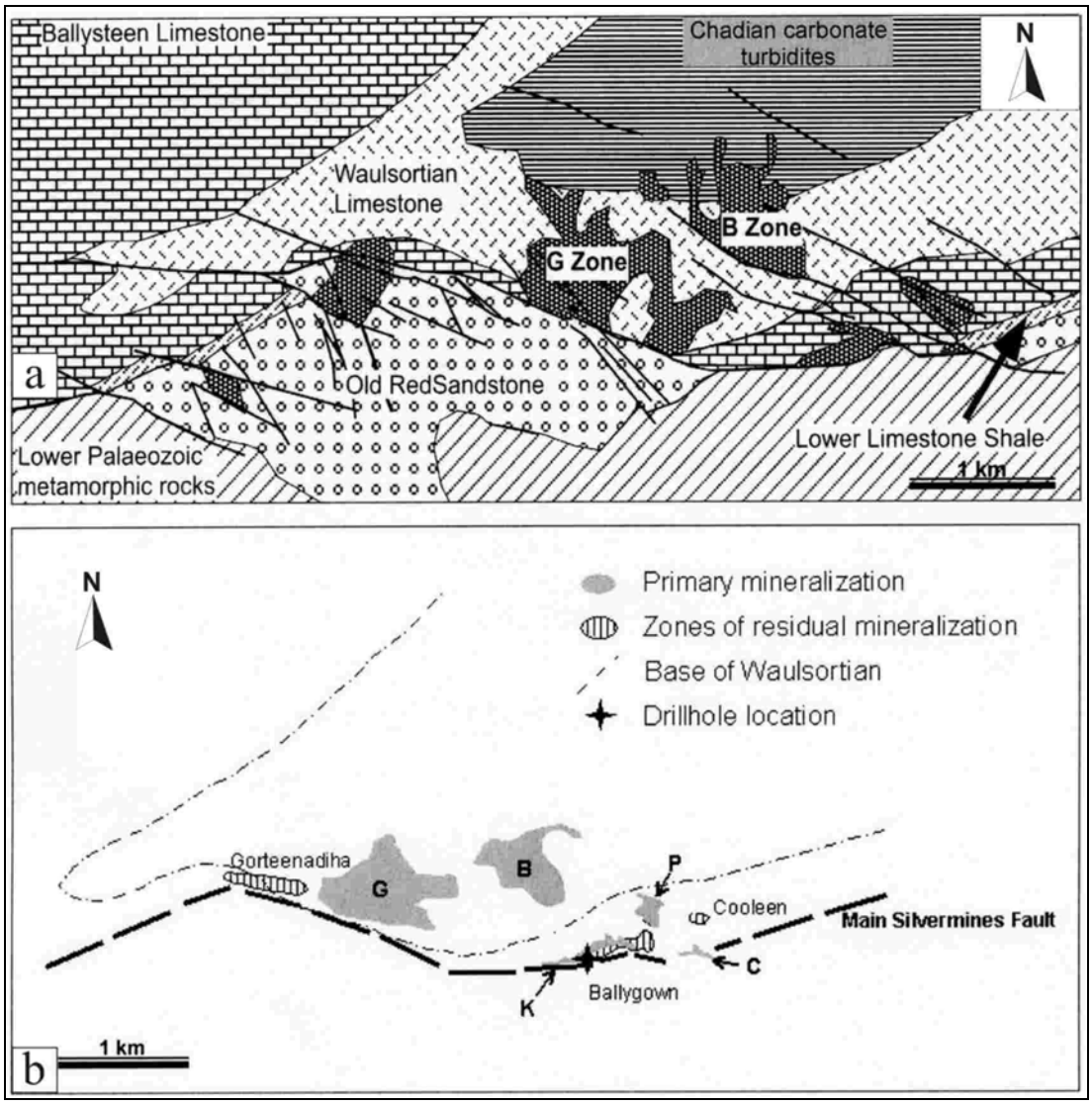

Figure 6.2: a) Geological map of Silvermines area (from Hitzman & Beaty 2003, modified); b) sketch map of the Silvermines area with location of orebodies and drillholes shown in fig. 6.5 (Knockanroe Townland) (from Boland et al., 1992).

Sulphides at Silvermines are in form of stratabound bodies occurring mainly in two different horizons of Courceyan limestone: in the overlying Waulsortian limestone and in the underlying Argillaceous Bioclastic Limestones (ABL). The mineralogy of sulphides comprises sphalerite, galena, and minor pyrite as dominant phases. Barite is often associated to primary sulphides, and becomes very abundant in the Magcobar deposit, while marcasite, chalcopyrite, sulphoarsenides and sulphosalts are minor phases.

Nonsulphide zinc ores, generally called *residual bodies*, were mined intermittently from 17th century to 1953 in the Silvermines area. At the end of 19th century nonsulphide ores were washed to eliminate the associated ochres and then the higher concentrate was treated in Wälz kilns. As a result, after processing calamine and ochre mixtures with average Zn content of 12-17% were accumulated in the dumps (Griffith, 1956). In the light of the economic revival in the world for nonsulphide ores, also these dumps may represent an effective Zn resource. A report drafted in 1933 calculated a tonnage of at least 0.5Mt of nonsulphide resources at Silvermines. This tonnage was upgraded to 1Mt with 10.79% combined Zn+Pb after a more recent evaluation made by Ennex International in the 1990s (Boland et al., 1992).

Calamine ores at Silvermines have been recognized only in four zones throughout the mine site, and exactly in the Gortheenadiha Zone, in the K zone, in the Ballygown South Zone and in the Coolen Zone (fig. 6.2b). They occur in the Lower Dolomite member of the ABL horizon. The first three zones are located in the hanging-wall of the E-trending main Silvermines fault, while the fourth zone is located at about 300m northward of the same fault. The residual bodies are better developed adjacent to faults and where Lower Dolomite horizon is nearly outcropping and weathered. The fault control on the emplacement of primary and specially of secondary mineralisation is particularly evident in the Ballygown North Zone, where the secondary mineralisation is developed in weathered host rocks and follows a north-east trending fault (Boland et al., 1992). In consequence of the current climatic conditions in Ireland, the top of the water table at Silvermines before mineral exploitation would have been quite near the today's surface.

Residual material, unconsolidated or semi-consolidated is developed on top of the bedrock or form layers within its most superficial parts. Zn-oxide deposits have been recognized both in form of *gossan* in situ, and as physically transported material; before exploitation they were completely buried by glacial sediments. Zn-oxide ores were mainly concentrated in steep-sided trough, partially karstified, overlying or connected with subcropping lenses of primary mineralisation. Residual material also fills vertical and sub-vertical fractures, 3m wide, in the vicinity of the main sulphide bodies (Boland et al., 1992). Replacement of primary sulphides also

occurs (Griffith, 1956).

In order to determine the real distribution of secondary Zn and Pb-bearing minerals, the Geological Survey of Ireland carried out additional drilling at Silvermines in November 2002. The aim was to obtain a good intersection containing both primary sulphides and oxides-residuum. These drill cores have been exhaustively studied, both from the mineralogical and geochemical point of view by Balassone et al. (2007). Therefore, most concepts discussed in the present work are based on the data published in the mentioned paper.

Mineralogy of nonsulphide ore at Silvermines seems to be dominated by smithsonite and hemimorphite, nevertheless several variations on the distribution of these mineralogical phases have been observed. Hemimorphite is the dominant Zn phase in the Coolen body, and also in the upper level of other deposits while smithsonite becomes the most important Zn phase in the lower levels of oxidized bodies (Boland et al., 1992). The preferential precipitation of Zn-silicate with respect to Zn-carbonate could be related to silica activity, derived from the host marly limestones reacting with acidic ground water. Also supergene siderite in association with smithsonite has been recorded in the lower levels of the oxidized bodies (Rhoden, 1960). In this respect, Boland et al. (1992) concluded that the distribution of "supergene" minerals (in particular hemimorphite and smithsonite) reflects the depth of the oxidation level: hemimorphite and associated iron oxides appear to be concentrated in the upper levels of the oxidation zone and smithsonite in the lower levels. A possible cause for this change of mineralogy with depth, which could be observed in all residual orebodies in the Silvermines area, is the progressive alteration of smithsonite to hemimorphite by silica-bearing waters percolating from the surface (Boland et al., 1992). I can anticipate that these features have been not detected in the samples from drill-holes 302/3 and 303/3, located in Knockanroe Townland at the periphery of the main orebody (Balassone et al., 2007). In fact, in the 302/03 drillcore both hemimorphite and smithsonite are equally distributed, whilst in 303/03 smithsonite is more abundant than hemimorphite and prevails in near-surface environment. In Balassone et al. (2007) it has been also reported that clear evidences of oxidation can be traced down to a maximum depth of 40-50m, as evidenced by the presence of supergene minerals in the deeper parts of the cores.

6.3.2.2 Galmoy deposit

In the Galmoy area, north Co. Kilkenny, four Zn-Pb ore bodies (G, CW, K, R Orebody) have been recognized. They represent, with the Lisheen deposits, the more southern evidences of mineralization in the Irish Midlands. The G and CW bodies were individuated in the 1986 as

result of drill testing and geophysical anomaly, and mined since 1997. The K and R bodies have been discovered more recently, in 1995 and 2002 respectively.

As of mid-2004, reserves at Galmoy stood at 4.18Mt, grading 14.2% zinc, 4.4% lead and 46.4g/t silver. Of this, 2.1Mt of ore were contained in the recently (2002) discovered R zone orebody (ARCON Mines Ltd – now Galmoy Mines Ltd – web site).

The deposits occur within the basal part of the brecciated Waulsortian Limestone, which lie on the Argillaceous Bioclastic Limestone (ABL). The host rock in the mineralised area is dolomitised in its entire thickness up to 1Km NW of the mine, where an approximately SW-NE trending dolomitisation front occurs. Despite of this, looking in detail, the limit between dolomitised and undolomitised limestone is not sharp.

The mineralised bodies at Galmoy occur on the northern (down-thrown) side of an E-W trending normal fault, called G Fault (fig. 6.3). G and R bodies are spatially, and probably genetically, related to this fault. The CW bodies occurs 400-500m to the north of main G Fault, and its location seem to be controlled by a NW-SE reverse fault zone and an undulating NE-SW anticline. However, it is accepted that these faults may have acted as pathways for hydrothermal uprising hydrothermal fluids.

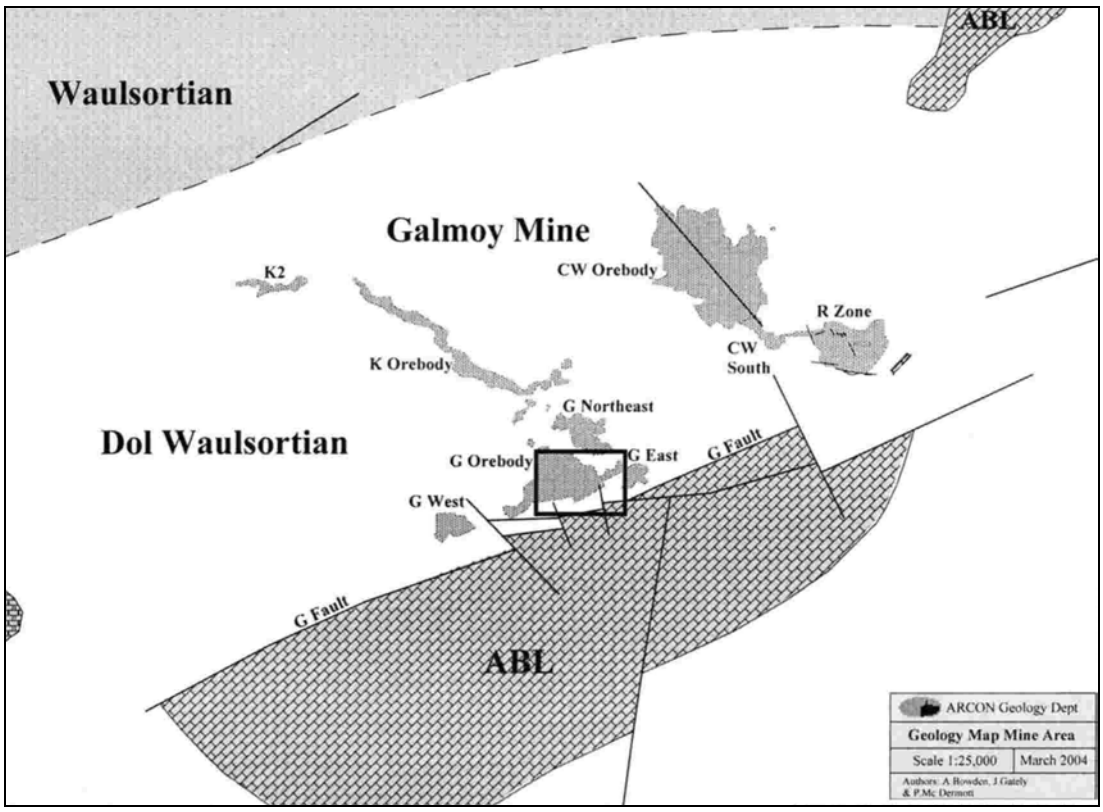

Figure 6.3: Geological map of the Galmoy area with the location of the orebodies (from Balassone et al., 2007)

Mineralisation formed tabular, massive and semi-massive bodies, with an average thickness of 4-5m. The G body dips gently to the north and CW body to southwest. They are located at depth between 50 and 150m below today's surface. The ore deposits and bedrock are buried under about 5m thick of a sandy till, whose thickness is minor beneath small hills. The mineralogical assemblage is simple, nevertheless substantial differences have been observed among individual bodies. Sphalerite, galena and pyrite-marcasite are the main sulphide minerals. The K and CW body are rich in sphalerite, R body is rich in sphalerite and galena and in the G body sphalerite, galena and pyrite/marcasite are present. Significant amounts of Cu-Ag sulphides have been identified in the footwall of the R orebody and trace amounts at depth in drill holes in the southern part of the G orebody (Doyle et al. 1992). Barite occurs as primary or detrital phase. No evidences of supergene sulphides, as previously reported (Lowther et al., 2003) exist (Balassone et al., 2007). Traces of secondary minerals (smithsonite, hemimorphite, cerussite and iron oxides) have been found in the weathered zone (Lowther et al., 2003). Prior to the commencement of mining in 1995, the top of the water table in the Galmoy area would have typically ranged from 1 to 30m in depth below surface.

6.3.2.3 Tynagh deposit

The Tynagh Zn-Pb deposit (Co. Galway) is one of the earlier (1961) orebodies discovered in the Lower Carboniferous rocks of the Irish Midlands, as a result of conventional shallow soil geochemistry and geophysics (EM and IP), followed by intensive drilling. Three distinct mineralised zones (I, II and III) with primary (sulphides) and residual (supergene sulphides and nonsulphides) orebodies were found. The initial ore reserves were 3.76Mt with 4.27% Zn and 4.76% Pb of sulphides with economic grades of copper and silver and 1.20Mt with 4.66% Zn, 9.92% Pb, 1.32% Cu and 104g/t Ag (Clifford et al., 1986). After a further evaluation, the final total resources were estimated at approximately 10Mt grading 8% Pb and 4% Zn, and economic concentrations of copper and silver (Department of Communications, Marine and Natural Resources, Ireland website – http://www.minex.ie/: Mineral Potential : Base Metals). Additional barite ores were recovered from the tailings. The mine commenced production in 1965 in the residual orebody, which was exploited until 1974, whilst exploitation of primary sulphides continued until 1980, when the mining activity in this area was definitely terminated.

The Tynagh primary deposit occurs on the northerly hanging-wall of an approximately east-west striking and 50-60° N dipping normal fault (North Tynagh Fault) (fig. 6.4). This ores hosted by the dolomitised Waulsortian Limestone of Courceyan age striking almost parallel to North

Tynagh Fault. This fault, with a maximum throw of about 600m, represents the northern boundary of Old Red Sandstone. It was active during hypogene mineralisation (Moore, 1975) and it is believed to be the feeder zone of the Tynagh deposit. Adjacent to the fault, a series of northerly striking folds (fig. 6.4) could have played a secondary role in the movement of mineralising fluids during primary and secondary mineralisation.

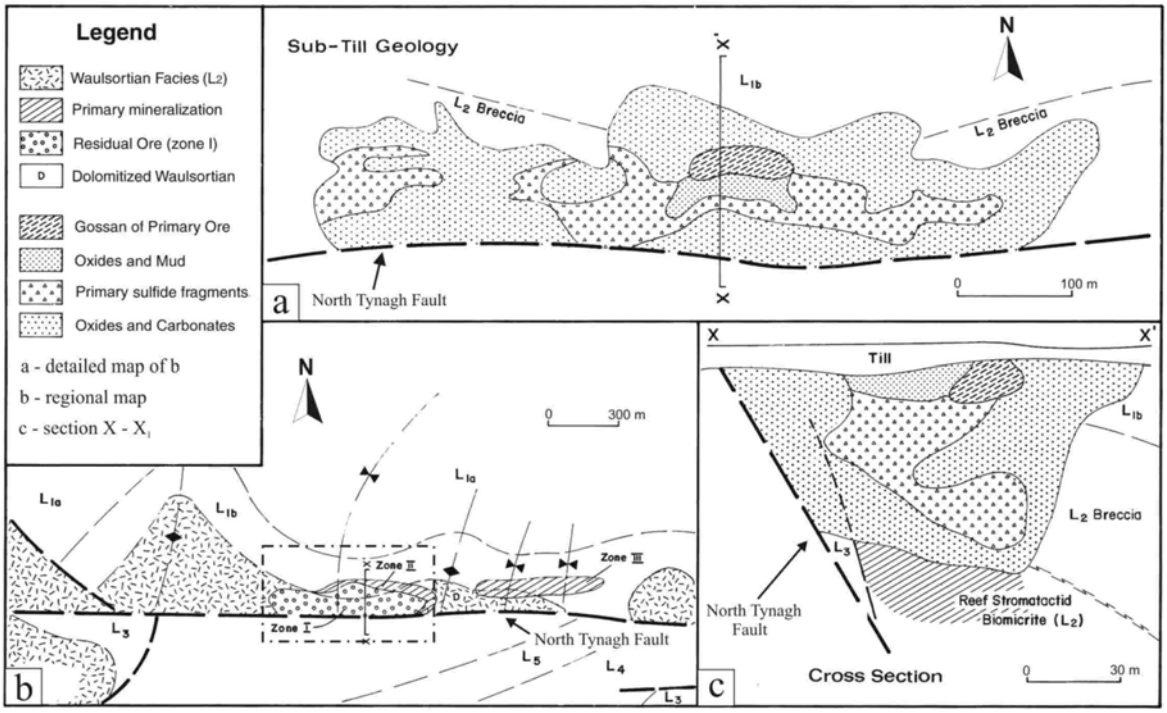

Figure 6.4: a) *Residual orebody* at Tynagh; b) the *Residual orebody* is shown in the general framework of the primary ore deposit; c) section X -X' across the deposit (L1, L2, etc.) refers to Carboniferous stratigraphy and facies (from Clifford et al., 1986, modified)

The mineralisation was mainly concentrated in the Waulsortian micrite and only a small part in other lithologies, as the Lower Muddy Limestone and the overlying Calp (Chadian-Holkerian) (Clifford et al., 1996). The primary sulphides form two orebodies (zone II and III) separated by barren dolomite and occur also in the lower levels of zone I, whose top part corresponds to the *residual orebody*. The sulphide bodies are stratabound and elongated parallely to the North Tynagh Fault. More in the south the mineralisation occurs in form of steeply dipping lenses. The sulphide ores show textures replacive of the host rock and of cavity infill. They occur also in veins related to a last mineralising stage.

The mineralogy of the sulphide ores consists predominantly of galena, sphalerite and minor pyrite (and As-pyrite), chalcopyrite, tennantite, tetrahedrite, bornite and barite (Boast et al., 1981; Clifford et al., 1986; Banks et al., 2002). Calcite is the main gangue mineral, but dolomite is also common. Different dolomitisation events occurred pre-, syn- and post-mineralisation,

causing the precipitation of several stages of hydrothermal dolomite and Fe-dolomite. A late dolomitising event, occurring after the main sulphide phase, was followed by precipitation of calcite and chalcopyrite in vein and cavities (Boast et al., 1981).

Although the majority of the ore was clearly epigenetic, some mineralisations have been considered as syn-sedimentary (Boast et al., 1981).

Nonsulphide ore occurred only in the upper part of zone I, in the so-called *residual orebody*, consisting of unconsolidated material filling a karstic sinkhole. The sinkhole occurs as an elongated cavity in the hanging-wall of the North Tynagh Fault, parallel to the fault strike. It occurs between the Waulsortian Limestone and the overlying Calp Formation (Clifford et al., 1986). The estimated size of the deposit was approximately 700m in the east-west direction and less than 100m in the north-south one. As the karstic depression progressively deepened and developed into a trough, the sidewalls became steeper so that boulders and fragments of decalcified host rocks and primary ores collapsed into black mud of karst infill sediment. The initial ore resources in the *residual ore body* were 4Mt, subdivided in 2.80Mt with 8.55% Pb and 7.36% Zn in sulphide ore and 1.20Mt with 9.92% Pb and 4.66% Zn in nonsulphide ore (Clifford et al., 1986).

The *Residual Body* includes fragments of primary sulphides and host rock, as well as supergene sulphides and nonsulphide minerals. Some supergene sulphides have been observed to replace fossil wood of different ages (Eocene/Oligocene? – last interglacial?) (Morrissey & Whitehead, 1971). The fragments of primary sulphides have the same composition as the stratabound carbonate-hosted Zn-Pb ores, whilst nonsulphide minerals include smithsonite, hemimorphite, cerussite, malachite and azurite. Fe-(hydr)oxides, mainly limonite and goethite, and sulphates are also common. Smithsonite is the main supergene Zn-mineral at Tynagh. It is ubiquitous and the most important phase in the lower part of the oxidized bodies, where is often associated to "limonite" (Morrissey, 1970). The oxidation of sulphides produced the precipitation of smithsonite and cerussite in the cavity infills, while the Cu-carbonates are locally very abundant at the periphery of the oxidized zone. Secondary minerals precipitated also in the surrounding host lithologies, where migrating metal-bearing fluids produced extensive replacement of the wallrock. Smithsonite was produced mainly in the western, sphalerite-rich part of zone I, whereas cerussite and malachite are enriched in the eastern parts which contained originally much more galena than sphalerite and locally Cu-sulphides/sulphosalts. Hemimorphite formed where the host limestones had a strong clay content (Morrissey & Whitehead, 1971).

Supergene ores in the Tynagh area, as well as in the other investiged deposits, are covered by glacial till.

6.4 Mineralogy of the nonsulphide ores

In this chapter will be discussed the mineralogy of the nonsulphides from Silvermines, Galmoy and Tynagh deposits. The data on the first two deposits are mostly derived from the recently published paper of Balassone et al. (2007).

6.4.1 Silvermines deposit

The general mineralogy of nonsulphides at Silvermines (Boland et al., 1992) has been already reported in previous paragraphs. Here we report on the results from the drillholes 302/02 and 303/03. The samples from the 302/03 and 303/03 cores at the periphery of main orebody mostly consist of incoherent material with variable granulometry and an abundant clay fraction. Frequently, small concretions and crystalline aggregates have been observed in voids and fractures, whilst a massive structure occurs rarely.

The mineralogy of the secondary ores and its variation with depth is systematically shown in figure (6.5a, b). Ore mineralogy is quite simple, with smithsonite and hemimorphite being dominant. More rarely hydrozincite was detected, mainly in the holes drilled at the periphery of the main body (Balassone et al., 2007).

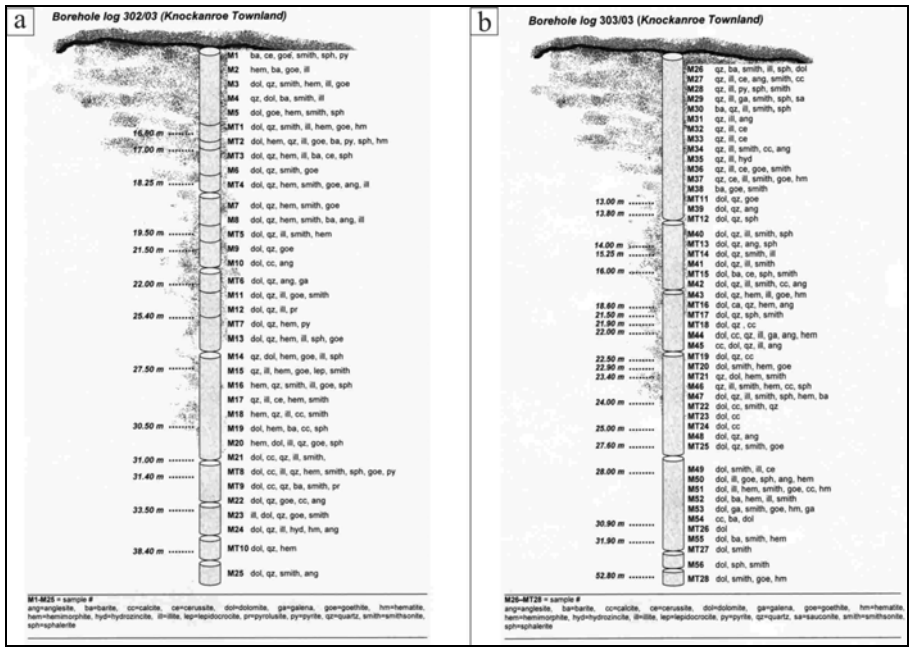

Figure 6.5: a) Silvermines drillhole 302/3, with location of the analysed samples and the corresponding mineral associations (minerals in order of decreasing abundance). The drillhole ends at a depth of 69.34 m (from Balassone et al. 2007); b) Silvermines drillhole 303/3, with location of the analysed samples and the corresponding mineral associations (minerals in order of decreasing abundance). The drillhole terminates at a depth of 69.12 m (from Balassone et al., 2007).

In both drillholes, these nonsulphide minerals can occur together; nevertheless the local prevalence of one over the others is also possible. In 302/03 smithsonite and hemimorphite are distributed equally throughout the entire section, whilst in drillcore 303/03, smithsonite is more common than hemimorphite. The latter is more common in the lowermost levels of the drillcore. Cerussite and in minor abundance hydrocerussite and anglesite are the most important Pb-minerals present (Griffith, 1956; Boland et al., 1992, Balassone et al., 2007). Iron hydroxides and oxides (mainly goethite and hematite), derived from the oxidation of pyrite, are commonly present in "limonitic" boxworks and in small concretions with amorphous manganese minerals. Relicts of sulphides (sphalerite, galena and pyrite/marcasite) and barite are sporadically present. No clear evidence of supergene sulphides has been found in the Silvermines samples, as was the case of the Tynagh "*Residual Orebody*" (Morrissey and Whitehead, 1971). Dolomite and Fe-dolomite (affected by strong oxidation) are the principal gangue minerals. Detrital and diagenetic quartz is widespread, whilst calcite has been found only rarely. Illite is often associated to the supergene minerals. In the clayey fraction the latter clay type is dominant, but Zn-bearing clays (probably sauconite) have been detected by XRPD analyses in many samples.

After OM and SEM observation, different morphologies of smithsonite have been detected and consequently compared with those described in Sardinia (Boni et al., 2003) and Belgium (Coppola et al., 2007). Three most important morphological types of smithsonite have been observed in the samples from both drillcores. Smithsonite consisting of subhedral tiny crystals (Type II, after Boni et al. 2003), with a mean size of 20-50μm and with slightly rounded faces, is fairly abundant at Silvermines. This type coats irregular voids and fractures and sometimes may replace the dolomite host rock (fig. 6.6a). A typical "*rice grain*" morphology of smithsonite (also recorded in Sardinia) is very common. The single whitish *grains* can reach a maximum dimension of 1mm in length. This distinct morphology has been observed encrusting the surfaces of earthy, deeply red to brown calamine samples (fig. 6.6b) and is often in paragenetic association with euhedral hemimorphite (fig. 6.6f). This type of smithsonite occurs in the upper parts of the drill cores and appears to be always the final phase to be precipitated. Its chemical composition corresponds to rather pure Zn carbonate.

Two important varieties of type IV smithsonite (Boni et al. 2003) are frequently present in the smithsonite-rich samples from Silvermines: these are tiny rounded aggregates (fig. 6.6c) and clusters of thin platelets, distinctly stacked-up in one direction (commonly 40×40×150mm in size). This morphology is very common also in the Belgian nonsulphides (Coppola et al., 2007). The latter type has been mostly observed in the Fe-rich varieties (fig. 6.7d), which also partly replace the dolomitic host rock (fig. 6.6e). The aggregates show well-developed rhomboedral

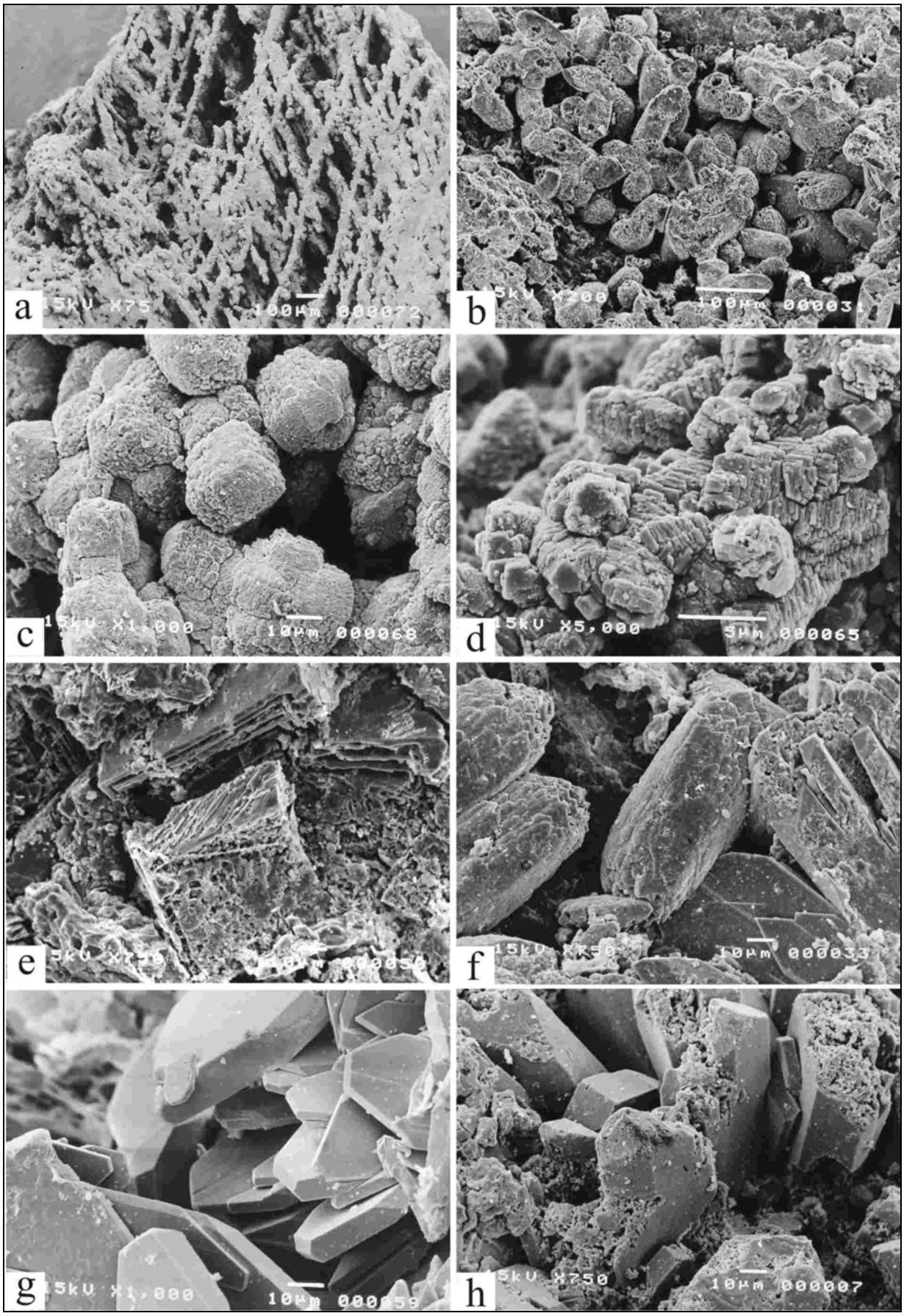
a
15kV X75 100µm 000072
b
5kV X200 100µm 000031
c
15kV X1,000 10µm 000068
d
15kV X5,000 5µm 000065
e
5kV X750
f
15kV X750 10µm 000033
g
15kV X1,000 10µm 000059
h
15kV X750 10µm 000007

faces. Type IV occurs as cavity- and fracture-filling. Unaltered idiomorphic hemimorphite crystals occur in cavity-lining aggregates (fig. 6.6g), while partly corroded crystals are associated to minute crystals of clay minerals and Fe-oxides (fig. 6.6h). Type II and the two varieties of Type IV, equally distributed in both drillcores are earlier generations in the nonsulphide ore paragenesis. Only the ferroan variety of Type IV is less frequent at Silvermines. The Fe-rich varieties, e.g. ferroan Type IV (up to 10.5 wt% FeO) and Type II (up to 4.0 wt% FeO) are the result of dolomite host rock replacement. Cerussite, coexisting with Ag, Mn and Fe(hydr-) oxides, has been detected in the uppermost oxidation zone of both drillcores down to 10-15m below surface. In conclusion, Type II and IV represent earlier morphologies compared to Type III in the smithsonite paragenesis.

6.4.2 Galmoy deposit

A mainly compact structure has been observed in the samples from the G orebody in the Galmoy deposit. The mineralogical study on these samples has revealed the virtually absence of hemimorphite, in contrast to the hemimorphite reported in the CW orebody at Galmoy and to both Silvermines and Tynagh. Also at Galmoy smithsonite represent the more abundant economic nonsulphide mineral and forms different types of aggregates with variable colours. The complete mineralogical assemblage includes also cerussite, Fe-oxides and hydroxides (goethite, hematite and lepidocrocite), anglesite and traces of hydrozincite. The presence of willemite was mentioned in an unpublished mine report by Strongman (2003), but has not been confirmed in our study. Relicts of primary sulphides are mainly represented by pyrite, sphalerite and galena, while no evidence of supergene sulphides. Locally barite also occurs as a primary or detrital phase. Calcite and clay minerals, including illite and traces of nontronite are the main gangue minerals.

SEM and OM observations revealed the presence of three important morphological types of smithsonite in the analysed samples. Type V smithsonite is the dominant morphological type (fig. 6.7a) in this deposit. It forms globular crusts exhibiting variable colours. The globular variety of type V smithsonite is dominant at Galmoy. It appears to replace sulphide minerals and to be the first deposited smithsonite generation. Type IV smithsonite is also common but recognizable only by SEM-EDS; it can occur as a Fe-enriched variety (fig. 6.7b), as well as in Fe-poor aggregates (fig. 6.7c).

Figure 6.6: Secondary electron images of various smithsonites (classified as in Sardinia and Belgium nonsulphide ores), and hemimorphite occurrences at Silvermines: a) Type II smithsonite; b) Type III smithsonite; c) Type IV smithsonite; d) Type IV, Fe-rich smithsonite; e) dolomite partially replaced by Fe-bearing Type IV smithsonite; f) idiomorphic hemimorphite with Type III smithsonite; g) euhedral hemimorphite aggregates, h) hemimorphite with clay minerals and Fe (oxyhydr)oxides (from Balassone et al., 2007).

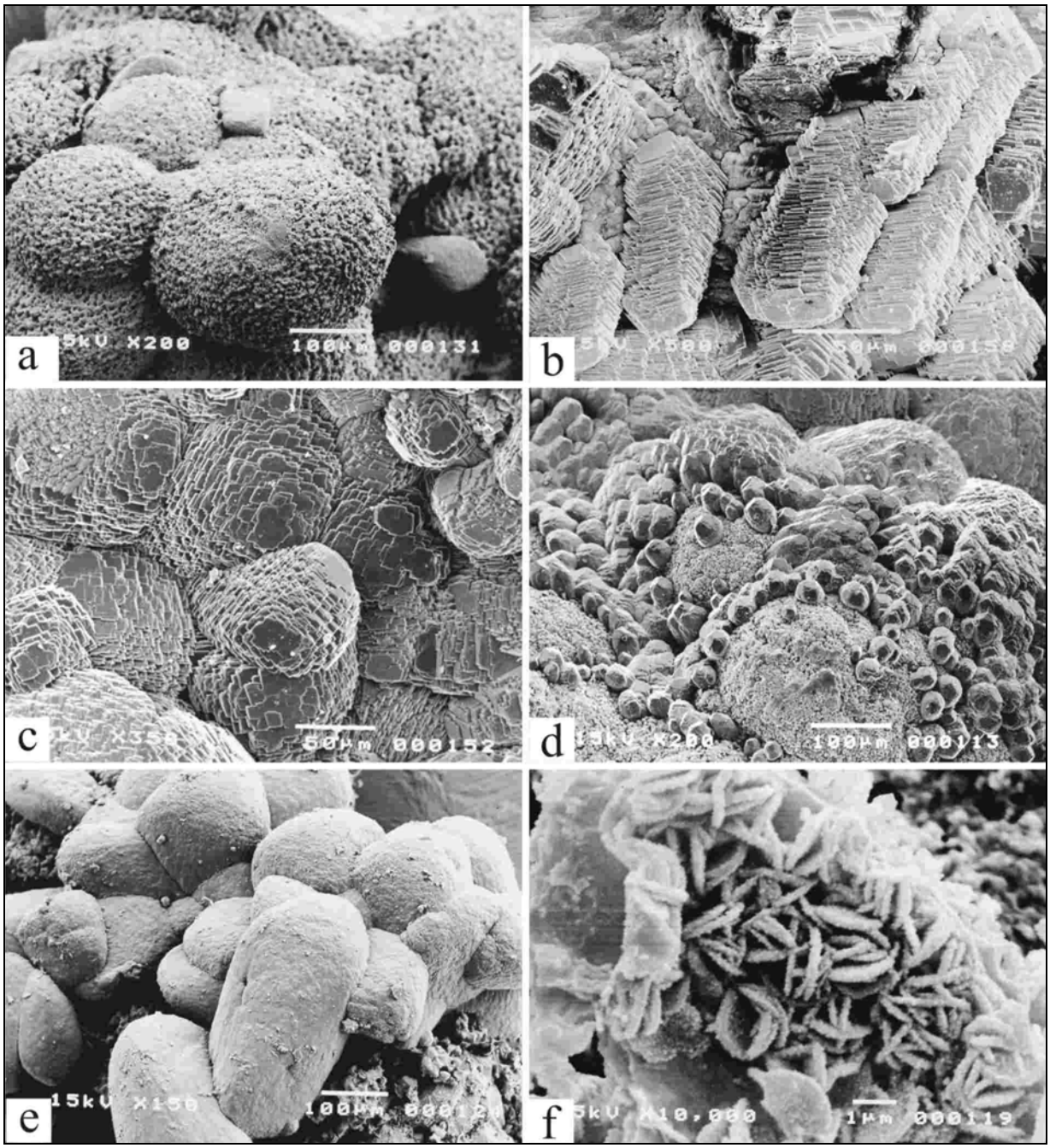

Figure 6.7: Secondary electron images of different smithsonite morphologies and sulphates from Galmoy mine: a) Type V globular smithsonite; b) Type IV (ferroan variety) smithsonite; c) Type IV smithsonite, a variety with well defined rhombohedral faces; d) Type IV smithsonite growing on Type V; e)) Type III smithsonite; f) jarosite coating Fe (oxyhydr)oxides and clay minerals (from Balassone et al., 2007).

In some of the examined samples, Type IV smithsonite is growing on globular Type V (fig. 6.7d). The last paragenetical smithsonite type observed at Galmoy, as at Silvermines, is the "*rice grain*"-shaped Type III occurring as whitish encrustations in cavities (fig. 6.7e) and/or coating earlier smithsonite types. Observations at SEM revealed the presence of pyrite crystals coated and/or partially replaced by both Type IV and Type V smithsonite followed by type III in voids. Despite the fact that the paragenetical relationships among the distinct morphological types are complex, a likely paragenesis at Galmoy could be Type V→Type IV→Type III.

Other minerals detected at Galmoy are sulphates, mainly gypsum, boyleite, rozenite, jarosite and copiapite in well-formed crystals. Boyleite crystals coating primary sulphides have been detected by SEM, as well as white jarosite encrusting a Fe oxide- and clay minerals-rich matrix (fig. 6.7f). The sulphates formed clearly later than most secondary Zn carbonates.

6.4.3 Tynagh deposit

The most important mineralogical and petrographical aspects of the *residual body* at Tynagh, have been studied and presented in a few papers during the last thirty years. Above all, we should cite Morrissey's (1970) unpublished Ph.D thesis and Morrissey & Whitehead (1971). Other data on the paragenetic assemblage of nonsulphide ores that could be applied to a genetic interpretation did not exist so far.

The Tynagh samples we have investigated are erratic and originate from the Morrissey collection at the Imperial College of London. For this reason, a study on the spatial distribution of the secondary phases in the weathered profile and their relations with primary sulphides was not possible in Tynagh. In the samples from the Imperial College collection, however, we could carry out interesting mineralogical and petrographical observations on the general texture and paragenesis of the nonsulphides.

The secondary deposits at Tynagh are in form of consolidated and semi-consolidated earthy material, with limited crystalline zones. The nonsulphide minerals show a very ample range of textures and structures. They occur as well-crystallized replacements of the host rock, and as late aggregates of crystals and globular concretions in cavities and voids. Moreover, the supergene minerals can replace the primary sulphides and and precipitate as late cement phases.

Smithsonite, cerussite and hemimorphite are the most common minerals in the oxidized samples from Tynagh; azurite and malachite are less common. Zn-rich clay minerals agglomerates, probably consisting of sauconite, occur generally as residual materials transported and deposited in cavities. Sulphide remnants, consisting mainly of sphalerite and galena, with signs of alteration and/or partially replaced by nonsulphides, have been also identified. Detrital fragments of barite in cavities have been observed, which are subsequently cemented by secondary phases. Calcite is the principal gangue mineral associated to secondary ores, but also Fe-Mn-(hydr)oxides have been commonly observed (tab. 6.1).

Table 6.1: XRD analyses of the samples from Tynagh deposit (Irish Midlands); mineral symbols are in order of abundance.

	Sample	Mineral(s)
Tynagh	Ty2	te, qz, Ba-rich ort
	Ty3	ba, az, mim, hyce, ce
	Ty4	az, mal, ba, ce, ort
	Ty5	cc, qz, py, Cu-py, ga, sph
	Ty6	az, ce, hem, bar, ort, sm, pseudo-mal
	Ty7	cc, qz, hem, bar
	Ty8	bar, az, mim, go
	Ty9	bar
	Ty10	sph
	Ty11	sm
	Ty12	sm, cc, go
	Ty13	sm, ga, py, hem, qz
	Ty14	hem, cer, sau
	Ty15	mal, ce, bay
	Ty16	ce
	Ty17	bar, go
	Ty18	sm, sa
	Ty20	cc, sm
	Ty21	sm, qz, sa
	Ty22	ce

*Abbreviations: az = azurite, ba = barite, cc = calcite, ce = cerussite, ga = galena, go = goethite, hem = hemimorphite, hyce = hydrocerussite, mal = malachite, mim = mimetite, ort = orthoclase, py = pyrite, qz = quartz, sa = sauconite, sm = smithsonite, sph = sphalerite, te = tetrahedrite.

6.4.3.1 Smithsonite

Smithsonite ($ZnCO_3$) has been detected by XRD and microprobe analyses in almost all investigated specimens. This study has revealed the presence of two types of smithsonite micromorphologies that can be compared with the micromorphologies recorded at Silvermines and Galmoy (Balassone et al., 2007), as well as with those of Sardinian (Boni et al., 2003) and Belgian (Coppola et al., 2007) smithsonites. Only Type I and Type VI have been observed in the samples from Tynagh. Type I smithsonite, corresponding to rhombohedral, distinctly idiomorphic crystals with maximum dimensions less than 50μm (sample TY 12), is not very common, and occurs as isolated crystals in voids, or coats the inner part of a few cavities, forming tiny encrustations. Type VI smithsonite, consisting of big scalenohedral crystals oriented along the crystallographic *c* axes, with sizes constrained between 100 and 500μm and usually curved crystal faces, represents the more common morphology observed in the Tynagh deposit. Type VI forms polycrystalline aggregates assembled in yellow and green globular or mammillary concretions on the inner wall of cavities or as infilling of veins (fig. 6.8a, b). This

morphology seems to be a late generation, as was the case in Belgian calamine ores (Coppola et al., 2007). Coarse crystalline smithsonite with pseudo-idiomorphic crystals replaces the inner sediments of late cavities or the carbonate host rock. It is often associated to Fe(-Mn)-oxides and more rarely to smectite (sauconite?). In this case, smithsonite and oxides form zoned rounded crystalline aggregates, 30-50μm in diameter, with alternated Fe-rich (oxides) and Zn-rich (smithsonite) bands. An earlier generation of microcrystalline smithsonite also accompanied by disseminated Fe-oxides, has been observed only in sample TY18. It pre-dates the precipitation of younger Zn-carbonate phases.

6.4.3.2 Hemimorphite

Hemimorphite, though less widespread than smithsonite in the Tynagh nonsulphide assemblage, has been detected by XRD analysis in a few investigated samples. It seems to be a late phase, even if its relationships with the other supergene phases are not clear. At Tynagh, as well as at Silvermines and Galmoy, hemimorphite-rich samples are virtually smithsonite-free. This Zn-hydrosilicate occurs as tabular crystals, elongated along the *b* axis and assembled in radial concretions. In the core of the spherical concretions, hemimorphite is impregnated with Fe(hydr)oxides (fig. 6.8c, d). Similar aggregates have been observed in Belgian nonsulphides (Coppola et al., 2007; chapter 3 of present Ph.D thesis). The dimensions of hemimorphite aggregates are constrained between 100 and 500μm. Hemimorphite has been quoted previously from the *residual body* of Tynagh (Morrissey, 1970; Morrissey & Whitehead, 1971). The presence of hemimorphite in nonsulphide deposits suggests a strong SiO_2 activity (Moore, 1972) and a lower buffering capacity of the host carbonates (Hitzman et al., 2003).

6.4.3.3 Cerussite

Cerussite is also one of the main constituents of the nonsulphide mineralogical association in Tynagh *residual body*, which I could also detect in many samples. This carbonate represents one of the typical products of supergene alteration of galena. It has been mainly observed in brecciated sediments where the single cerussite crystals are cemented by Fe-oxides, malachite and azurite (fig. 6.8e). The cerussite crystals present evident signs of physical alteration probably owing to mechanical transport. A thin oxide blanket coats the single crystals. Tabular crystals elongated along the *b* axes have dimensions extremely variable, up to 1.5mm. In few cases, a late cerussite generation occurs in the cement of the brecciated samples. This generation precipitated

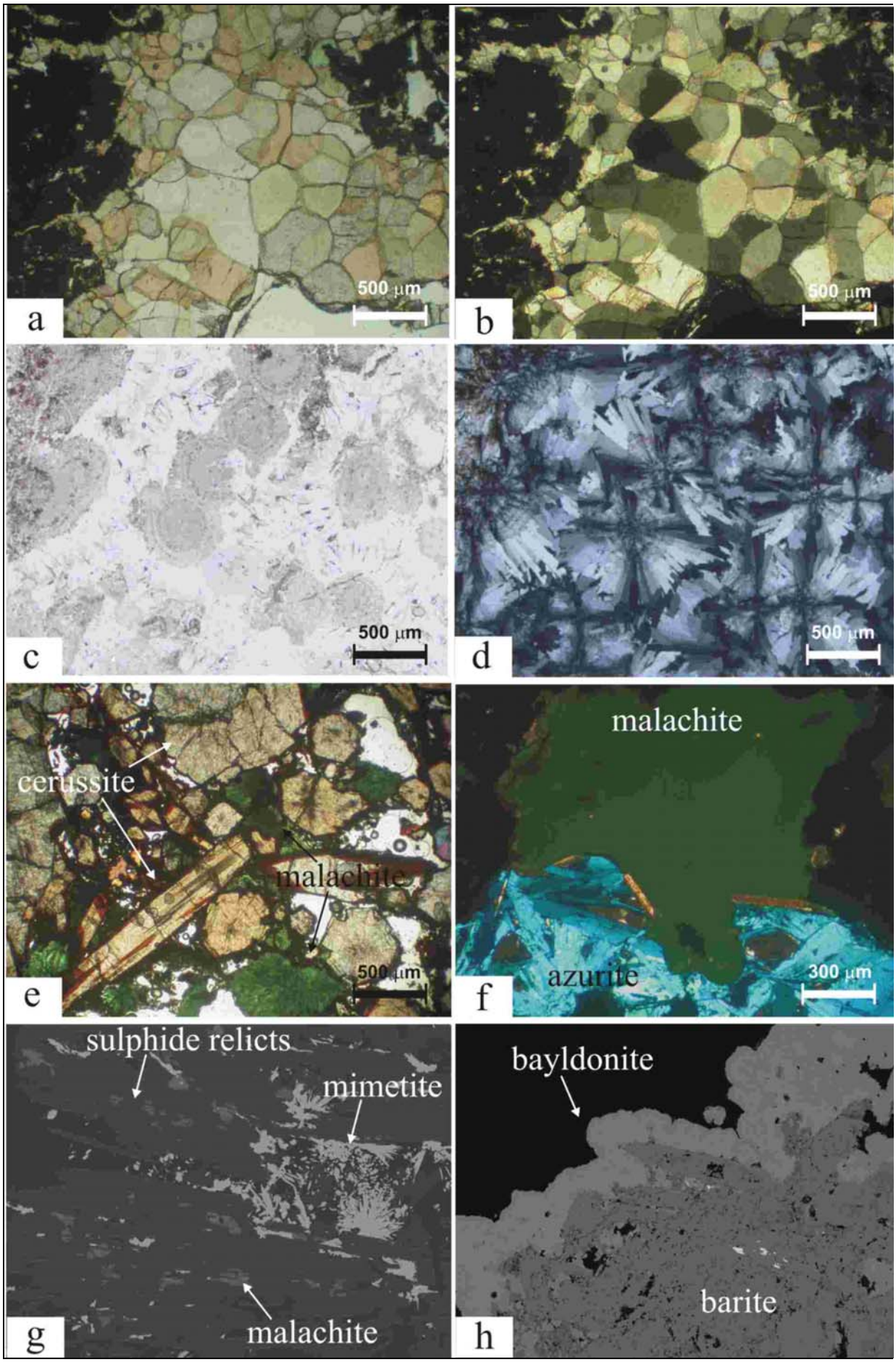
a
500 µm
b
500 µm
c
500 µm
d
500 µm
cerussite
malachite
e
500 µm
malachite
azurite
f
300 µm
sulphide relicts
mimetite
malachite
g
bayldonite
barite
h

surely later than Fe(hydr)oxides, and probably replaces pieces of galena. Cerussite has been also detected in association with barite crystals.

6.4.3.4 Cu-carbonates

Azurite and malachite are typical secondary phases of the supergene ores at Tynagh, as previously cited by Morrissey (1970), Morrissey & Whitehead (1971) and Clifford et al. (1986). Their occurrence, not recorded in other investigated European nonsulphide deposits, is principally due to the high content of Cu-sulphosalts in the Irish primary mineralisation. Only traces of these hydrated carbonates have been recorded in other Irish nonsulphide deposits. Balassone et al. (2007) did not detect any Cu-minerals in the investigated samples from the Silvermines (periphery of main body) and Galmoy (G orebody) deposits. Malachite at Tynagh forms green botryoidal-shaped radial aggregates with acicular crystals up to 2mm in length (6.9e), and globular concretions 1mm thick (fig. 6.8f). Malachite grows on barite and cerussite fragments in brecciated samples. Azurite shows pale blue acicular crystals growing in voids (fig. 6.8f), whose dimensions are constrained between 0.1 and 2mm. Also some small, mechanically transported azurite fragments have been observed in breccia samples.

Azurite and malachite represent accessory phases in the nonsulphide mineralogical assemblage. They surely post-date the main oxidation event that caused the precipitations of smithsonite, hemimorphite and cerussite.

6.4.3.5 Other minerals

Other minerals at Tynagh include remnants of primary sulphides, arsenate (as mimetite $Pb_5[Cl(AsO_4)_3]$ and bayldonite $Cu_3Pb[OH(AsO_4)]_2$), pseudo-malachite $Cu_5[(OH)_2PO_4]_2$, para-alumohydrocalcite $CaAl_2(CO_3)_2(OH)_4 \cdot 6H_2O$ and sulphates. Additionally, several types of Fe-(hydr)oxides, mainly goethite, have been detected.

Figure 6.8: a) thin section image (NII) of late smithsonite in cavity with remnants of partially oxidised sulphide minerals, Tynagh (TY18); b) thin section image (N+) of (a); c) thin section image ((NII) of spherical aggregates of acicular crystals of hemimorphite, Tynagh (TY14); d) thin section image (N+) of (c); e) fragments of derital cerussite crystals coated by a thin oxide blanket and fibrous aggregates of malachite, Tynagh (TY15); f) thin section image (NII) of paragenetically associated malachite and azurite, Tynagh (TY4); g) backscattered electron image of partially oxidised sulphide minerals with mimetite and malachite in voids, Tynagh (TY15); h) backscattered electron image of barite crystals coated by bayldonite, Tynagh (TY6).

6.5 Petrography and paragenesis of nonsulphide ores

Optical microscopy (OM) is a helpful tool to understand the relationships among the secondary phases and of them with the host rock. It is also important to detect the mineral paragenesis of the single deposits, as well as the timing of deposition. I have applied this technique only to the samples from the *Residual body* of Tynagh, relying on the paper of Balassone et al. (2007) for the petrography of Silvermines and Galmoy.

Smithsonite is the most abundant phase among nonsulphide minerals in the Tynagh deposit, followed by hemimorphite, cerussite, malachite and azurite. Fe-(hydr)oxides and calcite, as gangue minerals, are likewise present. All smithsonite generations are characterized by low-order interference colours ranging from white to grey when observed under crossed nichols. OM combined with cathodoluminescence observation has revealed the presence of different generations of smithsonite as crystalline aggregates with variable forms. A first generation of microcrystalline, fine-grained smithsonite, coexisting with Fe-(hydr)oxides, detected only in sample TY12, replaces the dolomite host rock. It shows a red dull luminescence becoming non-luminescent where Fe-(hydr)oxides prevail. In few cases, the nuclei of the smithsonite crystals show a red luminescence. Coarser crystalline smithsonite (with a strong red luminescence) forming globular concretions contains oxidised pieces of altered sulphides. Late smithsonite, showing a luminescence variable from bright red to pink, grows in fractures and/or cavities on the smithsonite generation derived from host rock replacement. In few cases only the crystal rims present a red-pink luminescence. It is generally known that smithsonite luminescence, as in other carbonates, is directly correlated to Mn^{+2} (as activator) and Fe^{+2} content (as quencher) (Götte & Richter, 2004). In particular, the luminescence is higher for a Mn content in smithsonite <1000ppm, while at concentrations exceeding ~1000ppm, the observed intensity is lower than expected from the calculated linear equation due to quenching effects of Mn^{+2} in high concentration.

Hemimorphite, consisting of very small, radiated crystals with low-order interference colours, is often associated to Fe-Mn-(hydr-)oxides, while its relationship with smithsonite and Cu-carbonates is not yet clear.

A first generation of cerussite with crystalline aggregates, precedes the precipitation of Cu-carbonates (azurite and malachite) and Fe-(hydr)oxides, whereas a second generation fills the fractures and it is associated to late smithsonite. Mimetite, bayldonite, malachite, azurite and Fe-Mn-(hydr)oxides represent late phases in the paragenetic sequence of secondary ores at Tynagh. Malchite and azurite form crystalline aggregates as well as globular concretions growing on

cerussite and barite fragments. More rarely, fragments of azurite aggregates have been observed in breccia samples. Fe-(hydr)oxides with inclusions of malachite occur as breccia cement or coat the external faces of cerussite crystals. Mimetite has been observed also associated with Fe-oxides and relicts of sulphides. It usually occurs as spherical aggregates of pale white acicular crystals in voids (fig. 6.8g). SEM observations have revealed that a first generation of mimetite replaces the big crystals of cerussite. Bayldonite is especially present around barite crystals (fig. 6.8h).

In conclusion, I could observe that in most Tynagh samples Pb and Cu minerals are coexisting, while the Zn minerals are often isolated and in direct contact with the weathered host rock.

6.6 Major and trace element geochemistry of nonsulphide ores

SEM combined with microprobe analyses was carried out on the secondary ores from Tynagh, Silvermines and Galmoy mines, in order to establish the chemical compositions of the most important nonsulphide phases. I have mainly worked on the samples from Tynagh: the results will be compared with the data set on "oxidized" phases from Silvermines and Galmoy published by Balassone et al. (2007).

6.6.1 Silvermines deposit

Whole rock analyses on the samples from both cores drilled at Silvermines (Balassone et al., 2007) show a highly variable Zn content. In 302/03 Zn ranges from about 0.4 to 20.0 wt%; Fe, Pb and Mn reach their maximum values in the top of profile, with 30.9 wt% Fe, 8.9 wt% Pb, and 2.8 wt% Mn. The high Ca and Mg content is due to the presence of dolomite recorded in Zn-free samples. Cd and As concentrations are generally below detection limit, while Ag content varies from 0 to 32 ppm. Pb has been detected in the uppermost oxidation zone of drillcore 302/03, this being in relation to the presence of cerussite. With depth, Zn (in form of smithsonite and hemimorphite) partly correlates with Ag. Both Ag and As decrease with depth. In drillcore 303/03, Zn ranges from 0.9 to 23.6 wt%. Fe ranges between 3.5 and 25.3wt% with the higher concentrations occurring in the upper levels of the core. Mn and Pb mimic the same trend. Locally high Pb values are related to the occurrence of cerussite (fig. 6.5). Ca and Mg behave sympathetically as in drillcore 302/03. In both 302/03 and 303/03 cores, Zn shows an inverse correlation with Ca and Mg: this might be due to the replacement of dolomite host rock first by primary and then by secondary Zn minerals.

In table 6.2 WDS microprobe analyses of representative smithsonites and hemimorphites from Silvermines are reported (Balassone et al., 2007). Type III and IV smithsonites show a composition quite close to ideal smithsonite, with low contents of FeO (up to 0.42 wt% in Type III and 0.68 wt% in Type IV), CaO (up to 0.59 wt% in Type III and 0.57 wt% in Type IV) and minor and/or trace amounts of MgO, MnO, and PbO. Type II and the ferroan variety of Type IV show high FeO contents, in the range 2.7 to 4.0 wt% for Type II and of 8.1 to 10.5 wt% for Type IV. MnO can reach up to 2.0 wt%in Type IV. Hemimorphite displays a stoichiometric chemical composition, with SiO2 varying between 24.8 and 25.0 wt% and ZnO ranging between 65.3 and 65.2 wt%, with only traces of Fe, Ca and Mg.

Table 6.2: Microprobe analyses of selected smithsonites and hemimorphites from 302/03 and 303/03 Silvermines drill cores (Ireland) pointing to compositional variations (from Balassone et al., 2007)

	Smithsonite									
sample	**MT1**				**MT5**				**MT8**	
	Type III		Type IV		Type III		Type IV		Type IV	
ZnO	63.55	63.48	63.99	63.54	63.7	63.61	64.15	64.01	63.52	63.42
FeO	0.38	0.42	0.13	0.23			0.45	0.54	0.34	0.68
MnO	0.05	0.08					0.09			0.54
CaO	0.34	0.26	0.36	0.57	0.58	0.57	0.36	0.21	0.53	0.08
MgO	0.33	0.29	0.23	0.18	0.31	0.18			0.23	
PbO	0.06	0.04								
CO_2*	35.41	35.32	35.37	35.3	35.4	35.2	35.46	35.27	35.38	35.27
Total	100.12	99.89	100.08	99.82	99.99	99.56	100.51	100.03	100.00	99.99

	Fe-smithsonite					Hemimorphite			
sample	**MT20**		**MT28**			**MT1**		**MT20**	
	Type IV		Type II						
ZnO	52.82	50.87	60.57	59.88	**SiO_2**	24.76	24.94	24.51	24.69
FeO	8.07	10.49	2.68	3.99	**ZnO**	67.25	66.73	66.25	67.38
MnO	2.02	1.79	0.20	0.13	**FeO**	0.10	0.21	0.22	0.31
CaO	0.40	0.59	0.87	0.67	**CaO**				0.35
MgO	0.97	0.24			**MgO**		0.18		
PbO					**H_2O***	7.21	7.24	7.68	7.36
CO_2*	36.27	35.90	35.35	35.58					
Total	100.55	99.88	99.67	100.25	**Total**	99.32	99.30	98.66	100.09

* calculated from stoichiometry

6.6.2 Galmoy deposit

WDS analyses have been carried out on smithsonite and cerussite from G orebody in the Galmoy deposit (tab. 6.3). Metal content variations have been observed in the analysed samples.

"*Rice grain*" smithsonite generally displays low Fe content, in the range 0.12 to 0.35wt% FeO

Table 6.3: Microprobe analyses of selected smithsonites and cerussites from the Galmoy Mine — G orebody (Ireland) (from Balassone et al., 2007).

	Smithsonite										Cerussite				
sample	**MG2**		**MG13**		**MG16**		**MG17**					**MG3**		**MG8**	
	Type V		Type III		Type IV		Type V		Type IV						
ZnO	59.72	60.50	61.65	61.89	63.52	63.43	60.73	60.68	61.06	61.31	**PbO**	83.24	82.70	82.91	84.16
FeO	0.98	0.85	0.29	0.35	0.04	0.09	0.86	0.75	1.16	1.13	**ZnO**	0.03		0.02	
MnO	0.07	0.10						0.03		0.07	**FeO**	0.02	0.06	0.02	
CaO	0.94	0.84	0.99	0.84	0.63	0.53	1.25	1.27	1.14	1.11	**CdO**	0.13	0.05	0.16	0.15
MgO	0.34	0.31	0.22	0.39	0.16	0.22	0.23	0.19	0.38	0.42	**CO_2***	16.52	16.40	16.46	16.68
PbO	1.99	1.91	1.02	1.05	0.67	0.62	1.36	1.39	0.78	0.85					
CO_2*	34.59	34.82	34.89	35.13	35.33	35.29	35.02	34.92	35.38	35.54					
Total	98.63	99.33	99.06	99.65	100.35	100.18	99.45	99.23	99.90	100.43	**Total**	99.94	99.21	99.57	100.99

	Smithsonite									
sample	**MG18**		**MG19**				**MG24**			
	Type III		Type III		Type V		Type III		Type V**	
ZnO	61.05	60.84	61.58	60.84	62.88	62.61	62.69	62.50	61.99	62.04
FeO	1.02	0.99	0.65	0.29	0.34	0.44	0.17	0.12	0.46	0.36
MnO	0.05	0.06		0.06	0.10	0.12	0.03	0.05	0.10	0.07
CaO	1.10	0.98	0.92	0.98	0.55	0.61	0.60	0.70	0.85	0.80
MgO	0.23	0.28	0.39	0.28	0.23	0.67	0.62	0.52	0.42	0.30
PbO	1.15	1.12	0.88	1.12	0.94	0.80	0.58	0.82	1.00	1.10
CO_2*	35.16	34.99	35.17	34.56	35.30	35.72	35.44	35.34	35.34	35.14
Total	99.76	99.26	99.59	98.13	100.34	100.97	100.13	100.05	100.16	99.81

* calculated from stoichiometry

** NiO up to 0.25 wt%, CoO up to 0.22 wt%.

with the exception of sample MG18 (1.0 wt% FeO). Lead and Ca reach up to ~1.0 wt% each, while Mg and Mn contents are low. Both Fe-rich and Fe-poor varieties of Type IV smithsonite are found at Galmoy as in Silvermines and Tynagh. However, the ferroan variety has a maximum FeO content of only 1.16 wt%, much lower than at Silvermines and Tynagh. Type V smithsonite shows a high content of PbO (up to ~2.0 wt%) and CaO can reach up to ~1.3 wt%. Traces of Mn, Mg, Ni and Co have also been detected. Cerussite composition does not show enrichment in any particular element, except for the presence of small traces of Cd, Zn and Fe.

6.6.3 Tynagh deposit

At Tynagh, Zn is mainly contained in smithsonite and, in minor abundance, in hemimorphite, but also in hydrated sulphates (mainly boyleite) and Zn-clays. Pb occurs in cerussite, anglesite and, in minor abundance in arsenates (i.e. mimetite, bayldonite). This nonsulphide deposit is characterized by a higher content of Cu with respect to other investigated nonsulphide deposits in Ireland and Europe. Cu is mainly concentrated in azurite and malachite. Iron occurs as sulphates (jarosite, rozenite) and (hydr)oxides (goethite, hematite). In the secondary deposits there are still fragments and remnants of primary sulphides.

Several chemical analyses on the Tynagh samples (Tab. 6.4) showed: 1) a variable Zn content in smithsonite, constrained between 57.80 and 63.33 wt% ZnO, and 2) a content of other metals in the Zn-carbonate up to few points per cent. In particular, CaO concentration is constrained between 0.03 and 1.67 wt%. and MnO between 0 and 1.84 wt%. Traces of CdO and PbO (< 1 wt%) have been also detected in smithsonite. An extraordinary high CuO concentration (0.47 – 3.97 wt%) has been found in Tynagh smithsonite. Fe-rich variety of smithsonite (so called "monheimite") with FeO up to 13.06 wt% has been detected also by WDS in sample TY12. This smithsonite type has also high contents of MnO (1.94 - 3.62 wt%), CaO (0.60 - 1.30 wt%), CdO (0.17 - 1.57 wt%) and PbO (0.66 - 1.59 wt%).

Tynagh hemimorphite has an almost stoichiometric composition, with SiO_2 ranging between 23.48 and 27.93 wt%, and ZnO varying between 60.33 and 69.4 wt%. Only traces of Al and Fe (less than 0.1 wt%) have been detected in this hemimorphite.

Cerussite is very homogeneous and almost stoichiometric in its composition. Traces of Zn and Ca (less than 0.1% wt) have been detected. The copper carbonates (azurite and malachite) show an average CuO content of 65.5 wt% and 63.46 wt% respectively. ZnO content in these carbonates can reach 1.9 wt%, while only traces of Cd, Ca, Mn, Fe and Co have been detected.

Table 6.4: Microprobe analyses of selected smithsonites, hemimorphites and cerussites from Tynagh deposit (Ireland).

	smithsonite and Fe-smithsonite							
sample	**TY12**				**TY18**			
ZnO	56.98	50.59	46.99	41.29	58.63	61.77	59.63	63.33
FeO	0.69	4.00	6.72	13.06	0.08	0.08	0.16	0.04
MnO	1.94	3.26	3.62	3.36	0.25	0.03	0.00	0.05
CaO	1.30	1.04	0.76	0.61	0.35	1.67	0.60	0.06
CuO	0.04	0.16	0.12	0.03	3.83	0.47	2.82	1.16
CdO	0.17	0.57	0.64	0.82	0.62	0.36	0.91	0.55
PbO	1.19	1.33	1.37	1.44	0.44	0.28	0.50	0.22
CO_2*	34.32	35.03	38.26	37.29	34.68	35.32	34.86	35.31
total	97.11	97.39	102.28	100.72	98.95	100.07	99.55	100.82

	cerussite					hemimorphite		
sample	**TY22**					**TY14**		
ZnO	82.81	82.23	83.7	83.97	**SiO_2**	27.93	26.58	24.61
FeO					**ZnO**	60.33	67.08	69.4
MnO					**FeO**	0.8		
CaO	0.17				**CaO**			
PbO	0.05				**Al_2O_3**	2.33		
CO_2*	16.64	16.21	16.5	16.66	**H_2O***	7.66	7.54	7.38
total	99.83	98.44	100.2	0	**total**	99.05	101.2	101.4

* calculated from stoichiometry

6.7 C and O isotopes geochemistry

I have already discussed the principles of stable isotopes geochemistry and their possible applications to the study of supergene carbonates in a previous chapter of this thesis work.

This technique has been applied to smithsonite, cerussite and azurite from the Tynagh and Galmoy deposits. No carbonates from Silvermines have been analyzed yet, due to the difficulty to obtain pure carbonate phases from the drillcore samples of the latter mine. The results of the isotopic analyses are shown in table 6.5 and figure 6.9.

6.7.1 Smithsonite

Carbon- and oxygen-isotopic ratios of 5 smithsonites from Tynagh and 11 smithsonites from Galmoy have been measured.

The $\delta^{18}O_{VSMOW}$ values of smithsonite from Tynagh are constrained between 29.5 and 30.5‰, with an average value of 30.1 ± 0.3‰ (1σ, n = 5). $\delta^{18}O$ values of smithsonite from Galmoy are

Table 6.5: Carbon and oxygen isotope data of Zn and Pb carbonates from the Irish Midlands orefield (Ireland).

Sample	Mineral*	Description	Location	$\delta^{13}C_{V\text{-}PDB}$ (‰)	$\delta^{18}O_{V\text{-}SMOW}$ (‰)	*Ave.*	$\pm\sigma$
MG2	sm	massive smithsonite	Galmoy	-7.1	30.7		
MG2a	sm	orange crust	Galmoy	-7.5	29.6		
MG13	sm	earthy smithsonite in cavity	Galmoy	-8.2	29.7		
MG16	sm	massive smithsonite	Galmoy	-8.4	29.2		
MG17	sm	massive smithsonite	Galmoy	-7.0	30.0		
MG18	sm	massive smithsonite	Galmoy	-5.7	30.7		
MG18a	sm	white crystals	Galmoy	-7.8	29.8		
MG18b	sm	spherical aggregates	Galmoy	-8.6	29.5		
MG19	sm	white crust	Galmoy	-7.9	29.5		
MG24a	sm	crust in cavity	Galmoy	-7.6	29.2		
MG24b	sm	crust in cavity	Galmoy	-6.2	31.1	29.9	0.7
TY 21a	sm	green globular concretion	Tynagh	-9.2	29.5		
TY 18C	sm	white globular concretion	Tynagh	-10.4	29.4		
TY 18A	sm	crystalline smithsonite (inner part)	Tynagh	1.3	30.5		
TY 18B	sm	green globular concretion	Tynagh	-10.9	29.5		
TY 12A	sm	concretional smithsonite	Tynagh	-9.7	30.1	29.8	0.5
MG8-2	ce	crust on massive sulfides in cavity	Galmoy	-8.6	17.9		
MGM-1	ce	acicular crystals in cavity	Galmoy	-0.1	16.6	17.2	0.9
TY 3D	ce	white crystals	Tynagh	-13.8	17.5		
TY 16A	ce	crystalline aggregate	Tynagh	-15.8	18.5		
TY 22A	ce	crystalline aggregate	Tynagh	-16.4	18.4	18.1	0.5
TY 8B	az	blue concretion	Tynagh	-11.4	30.7		

Abbreviations: az = azurite, ce = cerussite, sm = smithsonite

constrained between 28.3 and 31.5‰ VSMOW, with average values of 30.0 ± 1.0‰ (1σ, n=11). We can observe that Irish Zn-carbonates, from both Tynagh and Galmoy, have a similar oxygen isotopic composition. Nevertheless in Galmoy a slightly broader range of isotopic ratios has been detected. A possible explanation could be the limited number of measurements performed on Tynagh smithsonite. The $\delta^{18}O$ values of Irish smithsonite are generally higher than those measured in other smithsonites from carbonate-hosted supergene nonsulphide deposits in Europe, e.g., SW Sardinia (27.4 ± 0.9‰, Boni et al., 2003) E-Belgium (28.4 ± 0.8‰, Coppola et

al., 2007), Upper Silesia (26.8 ± 0.3‰, this Ph.D thesis), and elsewhere in the world, e.g., Broken Hill-NSW (27.6 ± 1.1‰; Gilg et al., 2007a).

Differences with other supergene nonsulphide deposits have been evidenced also in the carbon isotopic composition of smithsonite. The $\delta^{13}C_{VPDB}$ values in Irish smithsonites range mainly from -5.7 to -10.9‰, showing more negative values in respect to other nonsulphide deposits (Gilg et al. (2007a). Similar values (-10.9 ± 0.9‰) have been observed only in the *red galman* smithsonite from Upper Silesia mining district (this work). An individual outlier values (+1.3‰) has been measured in the specimen TY18a from Tynagh. Generally, carbon isotopic compositions of smithsonite from Tynagh have values lighter than those measured in the smithsonite from Galmoy.

The prevalence of negative $\delta^{13}C_{VPDB}$ values in the Irish smithsonite suggests the dominance of a ^{13}C-poor source/s, especially in Tynagh deposits, while in Galmoy a more important contribution of a ^{13}C-rich source has been detected.

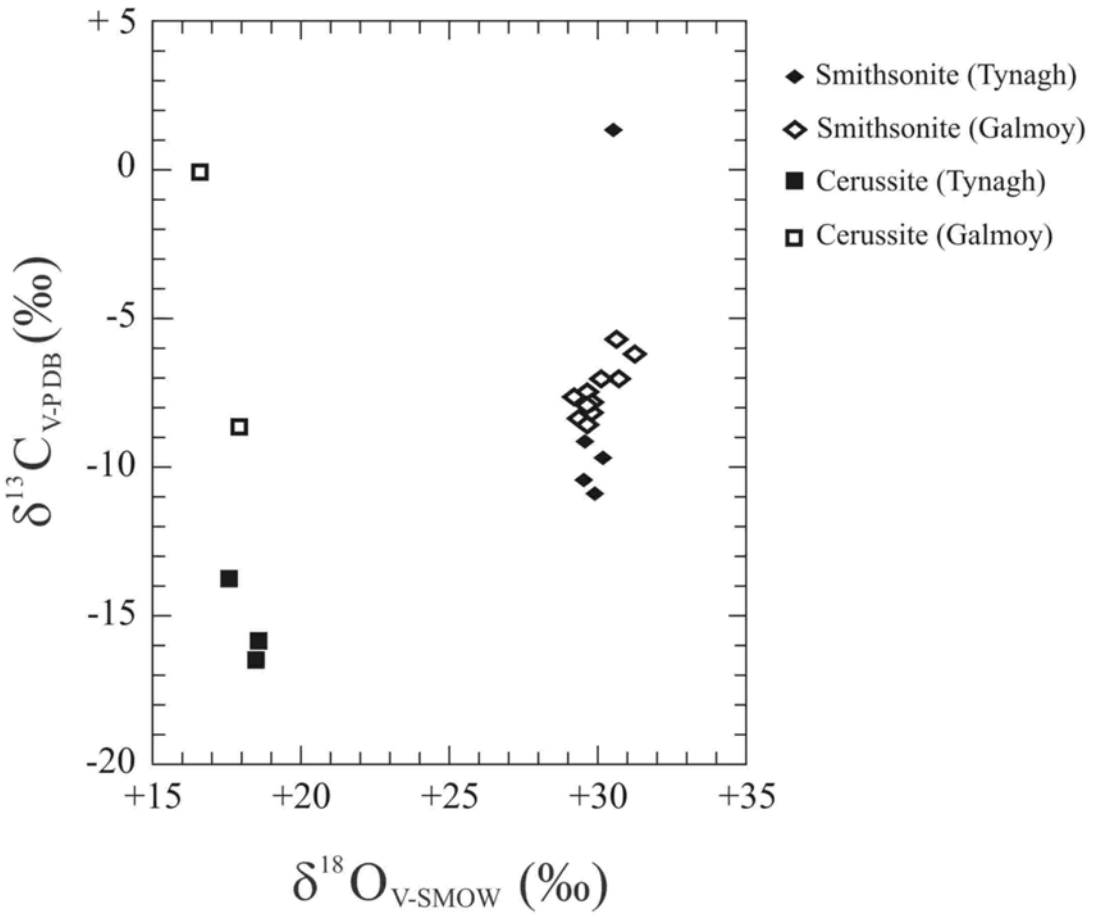

Figure 6.9: Plot of $\delta^{13}C$ *vs*. $\delta^{18}O$ for various Zn, and Pb carbonates (smithsonite and cerussite) from Tynagh and Galmoy deposits, Irish Midlands.

6.7.2 Pb- and Cu-carbonates

Cerussite from Tynagh (n=3) and Galmoy (n=2) and a single azurite from Tynagh have been also investigated from a stable isotope point of view. The oxygen isotope composition of cerussite in both deposits has values similar between the two mines (Tynagh: 18.2 ± 0.6‰; Galmoy: 17.9 ± 1.7‰). However, as well as for smithsonite, the specimens from Galmoy show a broader range of values. A different situation has been detected for the carbon isotopic composition of Pb-carbonates. In particular, the $\delta^{13}C_{VPDB}$ values of cerussite from Tynagh (-13.9 to -16.4‰) are more negative than $\delta^{13}C_{VPDB}$ values of cerussite from Galmoy (-8.6 and -0.1‰). Thus, if the carbon isotopic composition of cerussite from Tynagh is similar to those recorded in other supergene deposits, Pb-carbonates from Galmoy are relatively ^{13}C-depleted.
An individual azurite specimen from Tynagh shows carbon and oxygen isotopic composition comparable to other supergene carbonate minerals: $\delta^{18}O_{VSMOW}$ is 30.7‰ and $\delta^{13}C_{VPDB}$ is -11.4‰.

6.8 Thermometric analysis of fluid inclusions

A fluid inclusions (FIs) study has been carried out on transparent minerals from nonsulphide samples of Tynagh deposit. Unfortunately, the observations have been possible only in few cerussite crystals of crystalline appearance. In the other phases, neither a description of the FIA, or microthermometric measurements could be carried out because of the low number of inclusions, their small size and the frequent presence of oxides, which have hampered a good observation. At least 2 FIA can be recognized. The first FIA includes rounded, lobate and frequently negative crystal shaped inclusions 2-15μm in length. The maximum dimension of these supposed primary inclusions is parallel to the crystal boundaries. Most of these inclusions (95%) are liquid monophase and the rest (5%) are liquid-rich two-phase inclusions. Less commonly secondary and pseudosecondary fluid inclusions are aligned along trails. Their lengths are less than 1μm, but bigger inclusions (4-5μm) are also common. Almost exclusively liquid monophase inclusions are included in this FIA.
All liquid inclusions of the different FIAs could not be analysed microthermometrically because they did not nucleate a bubble after freezing down to -80°C. Neither a phase change with formation of an ice-like phase has been observed. Other kinds of reliable data, however, have been obtained on primary inclusions.

During the cooling experiments leakage was produced and easily detected in many inclusions, which were those avoided during microthermometry or discarded after measurement. Homogenisation temperature (T_h) measured in few primary two-phase inclusions show a very ample range, constrained between 70 and 160°C. Melting temperatures (T_m) of these inclusions range between 0 and -4.9°C. Primary FIs frequently displayed metastability phenomena in the nucleation of vapour bubbles during cooling; indeed T_m up to 7.5°C have been measured. These phenomena are frequent in aqueous solution with low salinity (Roedder, 1984). Following the T_h measurements, the samples were stretched by heating them above 150°C, in order to generate a gas phase in the monophase inclusions, so that subsequent cryogenic measurements could be made. In most cases no bubble was observed. Other fluid inclusions were too small and the visibility was too poor to allow a reliable estimate of the eutectic temperature after freezing. Thus, no reliable information on the composition of the fluids is available.

6.9 Discussion

6.9.1 Geological factors controlling the emplacement of Irish nonsulphide deposits

Nonsulphide deposits in Irish Midlands have the typical characteristics of supergene ores formed through weathering of primary sulphides. Thus, sub-aerial exposure combined with action of meteoric water, are directly involved into the oxidation of primary sulphides and relative formation of secondary nonsulphide deposits in the Irish Midlands as in other typical supergene deposits. As it has be done for the other supergene deposits, I will consider all the processes (tectonic uplift, karst dissolution, subaerial exposure and climate), which were active in this area after the emplacement of primary sulphides (Upper Carboniferous) and could have contributed to the emplacement of the nonsulphide ores.

A continental environment was established in most parts of Ireland during Permian and Mesozoic, after the post-Hercynian generalized uplift and strong erosion. This long period of subaerial exposure was followed by marine sedimentation during Cretaceous (Chalks deposits). A renewed evidence of uplift with displacement of several hundreds of meters, post-Early Eocene in age, is known to have occurred in southeastern Ireland (Cunningham et al., 2003). Badley (2001) also reports strong Tertiary fault-related uplifts in the southern Co. Mayo, north of the Galway region where Tynagh is located. However, clear-cut evidence whether and how these events have involved also the mineralised areas, is still lacking. All the primary and secondary base metal deposits in Ireland are entirely covered by glacial till whose thickness ranges about

few meters. This geological setting can be used as a proof for a pre-Midlandian age for the main oxidation event/s. However, due to the limited thickness of the glacial cover on the oxidized ores, one cannot exclude that weathering processes continued to act on the sulphide deposits also after deposition of the glacial sediments, especially during the Quaternary inter-glacial periods.
A well-developed karstic network seems to be absent in the carbonate-hosting secondary deposits in Irish Midlands. This aspect was evidenced firstly at Tynagh by Morrissey (1970) and Morrissey & Whitehead (1971), who described the *residual orebody* as a concentration of transported secondary minerals and clays in a shallow sinkhole. Also Balassone et al. (2007) discussed the lack of a proper network at Galmoy and Silvermines, this fact being backed by the absence of Type I smithsonite, usually occurring in the phreatic zone (Boni et al. 2003). The limited abundance of this smithsonite type also at Tynagh would confirm the immaturity of the weathered profile and the absence of strong karst dissolution of the host rocks. The lack of strong karstic features has certainly hampered the drainage of the meteoric waters, which should have facilitated the supergene alteration of primary sulphides. The faults network in the mineralised areas, which acted as conduits for the hydrothermal fluids depositing the primary sulphides, could have been thus the preferential paths for descending meteoric waters during oxidation events. Extensive fracturation of the host rock probably contributed to the migration of oxidizing fluid.

6.9.2 Stable isotopes

6.9.2.1 Paleoclimate indications

The investigated supergene Zn, Pb, Cu carbonates from the weathered zone of sulphide deposits show a very common pattern of relatively constant oxygen and often highly variable carbon isotope compositions, as well as in other supergene nonsulphide deposits. The variation of oxygen isotopic composition is limited within the deposit for both smithsonite (29.6 ± 0.6‰ VSMOW) and cerussite (17.8 ± 0.8‰ VSMOW). This fact evidences two aspects: 1) the temperature and oxygen isotopic composition of the supergene fluid were constant (~3‰ variation of oxygen isotopic composition of water), and 2) an isotopic fractionation exists between Zn and Pb carbonates, as predicted in the literature (Golyshew et al., 1981; Gilg et al., 2007a). Cerussite (av. 17.8‰ VSMOW) shows $\delta^{18}O$ values about 12‰ lower than cogenetic smithsonite (av. 29.9‰ VSMOW) and azurite (30.7‰ VSMOW), perfectly comparable with the value of 11.0 ± 1.0‰ predicted by Gilg et al. (2007a). Unfortunately we have no data on the

calcite associated with the secondary metal carbonates in this mining district, to compare their isotopic compositions.

$^{18}O/^{16}O$ could be used as a geothermometer, if we know exactly two of the three following variables: 1) the oxygen isotopic composition of carbonate, 2) the water and temperature of formation, 3) the relative isotopic fractionation equations between carbonate and water. In the case of Irish nonsulphides, only the oxygen isotopic ratios of smithsonite and cerussite have been measured. Therefore, the oxygen isotope data are not conclusive with respect to the timing of oxidation and can be interpreted in two ways. The first one considers the carbonates to be in equilibrium with a fluid (meteoric water) whose $\delta^{18}O_{VSMOW}$ is -6.5 ± 0.5 ‰, a signature similar to that of the present-day meteoric waters (Diefendorf & Patterson, 2005). In this case, on the base of the fractionation equations smithsonite-water and cerussite-water (Gilg et al., 2007a) and azurite-water (Melchiorre et al., 2000), the calculated temperature of precipitation are respectively 7°C ± 5 for smithsonite (figs. 6.10 and 6.11), 14°C ± 7.5 for cerussite (fig. 6.10) and 16°C for azurite. Thus, a substantial difference among temperature of precipitation of the Zn Pb and Cu carbonates arises, with the lowermost temperatures recorded in smithsonite with respect to cerussite. This trend has been noted also in the other supergene nonsulphide ores investigated in this work. The calculated temperatures are comparable with those recorded now in Ireland, with an annual mean air temperature of 9°C (IAEA, 2001). However, these temperatures are indeed too low when compared with those of other supergene nonsulphide deposits (tab. 9.1).

On the contrary, if the main weathering occurred in the Early Tertiary under an estimated temperature of 15-20°C, in accord with the majority of temperatures recorded in other supergene deposits, the oxygen isotope composition of paleometeoric waters producing the Irish nonsulphides would be calculated at about -5‰ using the fractionation factors of Gilg et al. (2007a) for smithsonite and cerussite. This isotopically heavy water could be expected in a hot and humid climate at low altitude and latitude. A stable carbon isotope study on goethite, gibbsite, and organic matter in the late Palaeocene laterites (~60Ma) of Antrim (Northern Ireland), also suggests an interval of hot and humid climate, associated to elevated atmospheric CO_2 concentration (Tabor & Yapp, 2005), which could be responsible for the oxidation of sulphides deposits in Irish Midlands.

6.9.2.2 Carbon sources

The carbon isotope compositions of supergene carbonates are highly variable with smithsonite recording values between -5.7 and -10.9‰, with the exception of one single value of +1.3‰, and

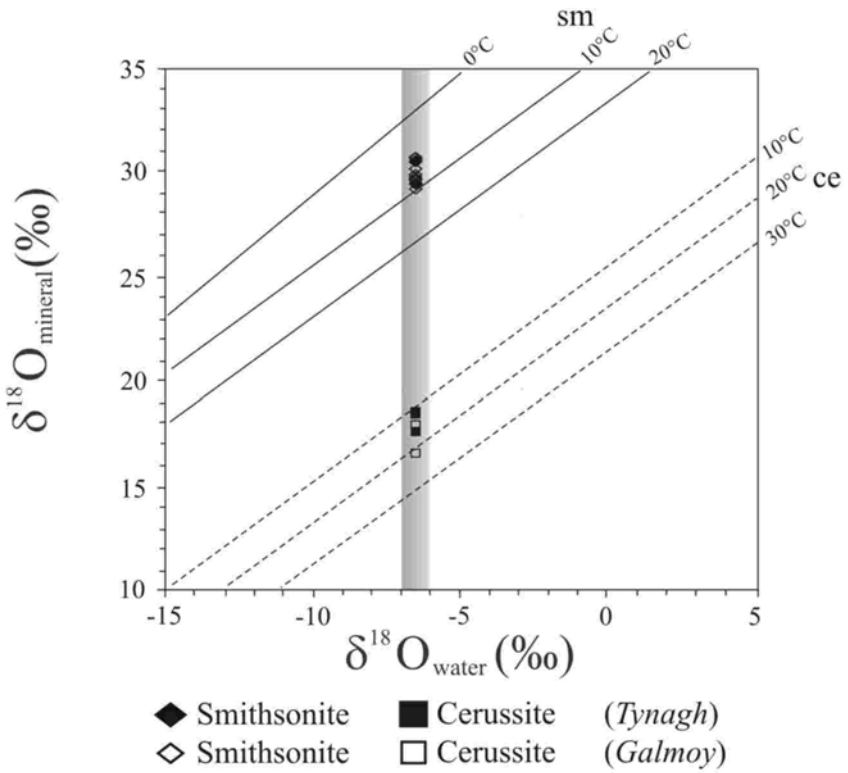

Figure 6.10: Oxygen isotope data of smithsonites (sm, rhomb) and cerussite (cc, square) from supergene oxidation zones of the Irish Midlands (Ireland) and estimated corresponding oxygen isotope compositions (grey strip) of local meteoric water, as proposed by Diefendorf & Patterson (2005).

cerussite between -16.4 to -0.1‰. These data evidence two aspects. There is a clear indication for the existence of multiple carbon sources as well as of a substantial carbon isotope fractionation between Pb and Zn carbonates. The predominance of ^{13}C-depleted values indicates a major contribution of a C-reduced source/s. The possible ^{13}C-enriched sources in supergene carbonate-hosted environment are principally three, all of them with $\delta^{13}C_{VPDB}$ values around 0‰: atmospheric CO_2, soil CO_2 from the decomposition of C4 plants (Cerling, 1984) and marine carbonate host-rock. The soil CO_2 from decomposition of C3 plants might be the most probable C-reduced source. However, Melchiorre et al. (2001) and Melchiorre & Enders (2003) suggested that also the oxidation of sulphide-oxidizing bacteria within sulphides ores as consequence of a dropping water table might be an alternative source for ^{13}C-depleted carbon in supergene carbonates.

Mineralised limestones and carbonates syn- and post primary ores at Tynagh have oxygen isotope composition around 0 ± 4‰ (VSMOW) (Boast, 1981): they might represent an additional ^{13}C-enriched source in this deposit. The latter source may be more important when direct replacement of host rock or of carbonate-stage of primary mineralising event occurs. In this case newly formed carbonate could inherited the carbon isotopic composition of replaced

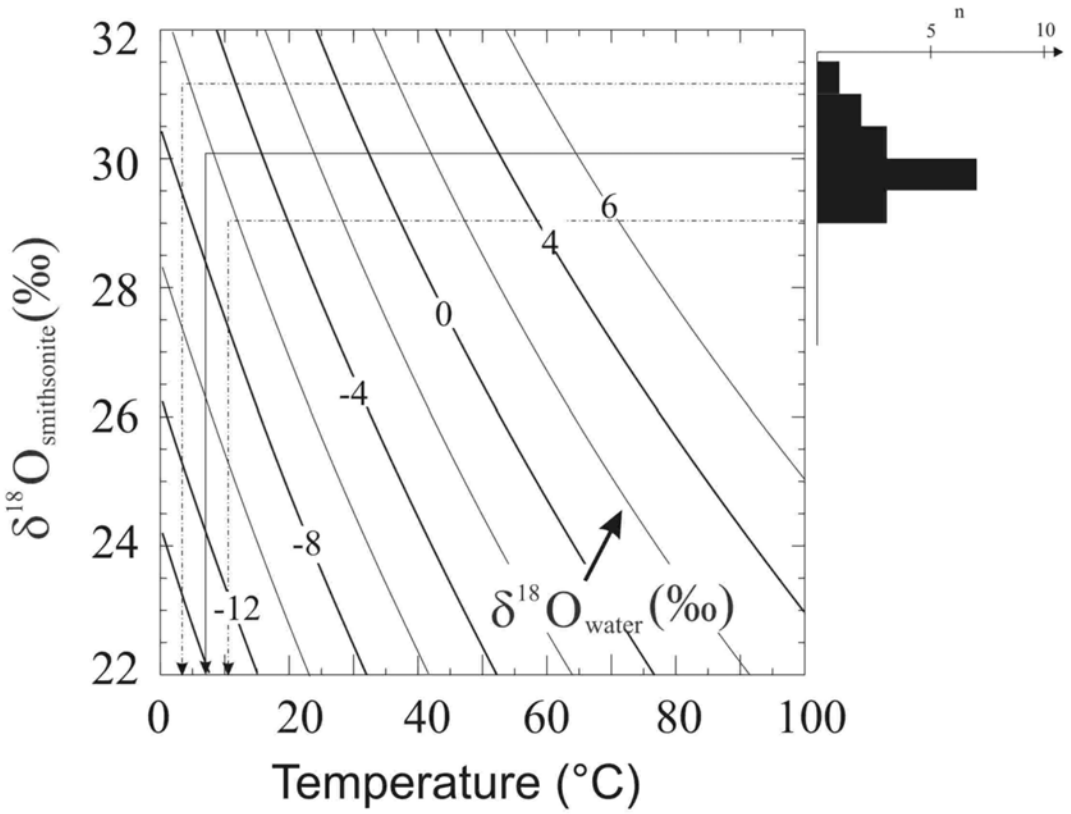

Figure 6.11: Graphical representation of oxygen isotope equilibrium curves between smithsonite and water according to Gilg et al. (2007a), calculated for different $\delta^{18}O_{water}$ values as a function of temperature. The histogram to the right shows the oxygen isotope composition of smithsonites from Galmoy and Tynagh deposits, Ireland. Calculated temperatures for smithsonite formation are based on the $\delta^{18}O_{VSMOW}$ value of -6.5 ± 1.0‰ for the local meteoric water as proposed by Diefendorf & Patterson (2005).
Note: dashed line = max and min $\delta^{18}O_{VSMOW}$ values, continue line = average $\delta^{18}O_{VSMOW}$ value

phases.

In the Teenage supervene no sulphide deposit as in other supergene nonsulphide deposits in the world (e.g. Belgium, Gig et al., 2007a) a substantial difference of $\delta^{13}C_{VPDB}$ = 9‰ between smithsonite and crosstie from the same deposit is recorded. According to previous calculations, at temperature of 15-20°C, cerussite and smithsonite should show a difference of carbon isotopic composition of ~5‰ (Deines, 2004). This difference has not been detected in the Galmoy deposit where the carbon isotope values of cerussite are unusually high and perfectly comparable with those of smithsonite. A possible explanation might be the precipitation of cerussite in isolated cavities, sealed from the remaining fluids in a local closed system. Thus, according to the law of mass conservation, if there is not a new fluid that arrives in the sealed cavity, the newly formed minerals, cerussite in this case, will inherit the isotopic composition of the mother fluid and then the isotopic fractionation becomes less important. This situation is completely different from what is usually occurring in the oxidation zone, where a new supply of organic carbon from oxidized soils and from soluted wall rocks continuously arrives and the minerals

have to isotopically re-equilibrate with it.

6.9.3 Timing of supergene nonsulphide deposits in the Irish Midlands

As discussed in the previous paragraphs, a supergene origin for the Irish nonsulphide deposits is universally accepted. These secondary deposits surely formed during a period of uplift combined with favourable drainage conditions. Nevertheless, some aspects on their origin and timing are still uncertain.

At the moment, unambiguous proofs to age-constrain the (paleo)weathering events acting in the genesis of nonsulphide deposits are lacking for Tynagh, Silvermines and Galmoy, as well as for other small deposits of the Irish Orefield (Balassone et al., 2007). Therefore, only indirect proofs on the age and environment constraints of sulphide oxidation in Ireland will be discussed here.

Nonsulphide ores in the Irish Midlands occur well below today's water table. This fact evidences two important aspects: a) they are genetically related to paleoweathering processes (when the water table was deeper), which acted under climatic conditions different (drier?) from the current ones; b) the limited depth of the nonsulphides occurrence may possibly suggest an incomplete evolution of the weathering profile. On the other hand, it may be possible that a renewed uplift and erosion of the upper parts of the weathered profile occurred earlier than deposition of glacial till.

Despite the fact that both Permian and lower Mesozoic in Ireland were characterized by uplifts and strong erosive processes, which caused the disappearance of part of the lithologies overlying the primary sulphides and their host rocks, most probably the genesis of the supergene ores should not be associated with those ages. This assumption seems to be confirmed by the absence of well detectable paleo-weathering records of that time in Irish Midlands.

During Cretaceous and the lower Tertiary great part of continental Europe was characterized by subaerial exposure, caused by tensional tectonics and differential uplifts. This was an ideal setting for extensive and prolonged weathering, resulting in several horizons of ferricrete, thick paleosoils and kaolinitic clay deposits. Especially during Tertiary particular climatic conditions (hot & humid, with dry intervals), which increase and favour weathering in continental environment, occurred in this part of Europe. These processes might have been present throughout continental Ireland and played a role in the formation of the nonsulphide Zn deposits.

Several paleoweathering records affecting various lithologies have been recognized in Northern Ireland, as well as in central and northern Scotland and in southwestern England (Migon & Lidmar-Bergström, 2001). It is often difficult to assign an age to these records, because of the

absence of a well-dated cover on the residual deposits. However, in many cases dating is precise enough to affirm that these deposits formed in several time spans during the Tertiary (Smith & McAlister, 1987). *Terra rossa*-like paleosoils, saprolite passing to bauxite and saprolite grus have been found in between the Early Tertiary basalts in the Antrim region (Northern Ireland). The paleosoils occur on the top of Cretaceous chalky limestones, while the ferralitic saprolite and bauxite occur as interbasaltic horizons on the Antrim plateau. Grus deposits are developed mostly on granite masses of the Mourne Mountains and their surroundings (Smith & McAlister, 1987; Power & Smith, 1994). The ages of these three different types of residual deposits are variable. In particular the *Terra Rossa*-like residual deposits are surely pre-basaltic (65Ma), while the ferralitic horizons are linked to early Paleocene weathering processes (65-62Ma) (Migon & Lidmar-Bergström, 2001). The laterite and bauxite deposits probably formed under hot and humid, tropical and sub-tropical monsoonal climate (Grubb, 1963; Bardossy & Aleva, 1990; Oliviera & Campos, 1991; Price et al., 1997). Warm and humid climate was present at high latitudes, including the British Isles, in the Early Tertiary (Bardossy & Aleva, 1990; Frakes, 1979). Tabor & Yapp (2005) on the base of stable isotope measurements on goethite, gibbsite, and organic matter in the Antrim laterites, consider the deposition of these supergene minerals as an effect of a hot and humid climate at high paleo- latitude, with a contribution of elevated atmospheric CO_2.

In southwestern England (Cornwall and Devon) a multitude of (paleo)weathering records exist, wich affect different lithologies. These records are: 1) kaolinite deposits on the Hercynian granites (China Clay type), whose thickness varies between few and hundreds meters, 2) residual laterites on Mesozoic sedimentary rocks and 3) grus derived from the weathering of granites (called *growan*) (Migon & Lidmar-Bergström, 2001). The weathering processes, which caused the formation of these residual deposits probably developed in different periods during Tertiary and Quaternary. In particular, kaolinite deposits and laterites have been dated as Early Tertiary (Issac, 1981, 1983; Green, 1985). A first kaolinisation stage during Late Cretaceous has been also considered (Green, 1985). Lidmar-Bergström (1986) considers the existence of a first weathering stage on the Hercynian granites during Jurassic-Cretaceous. The weathering products were subsequently buried by marine sediments during the Cretaceous transgression and again sub-merged during Palaeogene.

In conclusion, despite the paucity of direct evidences to constrain the age of the nonsulphide Zn deposits in Ireland, we can attribute their deposition to the weathering events, which were active in this part of Europe during early Tertiary. However, we cannot exclude that sulphide oxidation processes might have continued through time until Present time.

Chapter 7: Other nonsulphide Zn deposits in Europe

7.1 Introduction

Many other nonsulphide occurrences are present in Europe (Iglesias district - Sardinia, Reocin and Cartagena – Spain, Lavrion and Thassos – Greece, Alpine district – Italy, Austria and Slovenia), but only in some of them considerable tonnage of oxidised Zn minerals have been the object of exploitation in the past. In fact, in some of these deposits only uneconomic concentrations of oxidised Zn minerals have been discovered. For this reason, nopt very much has been published in the current literature (Boni & Large, 2003).

All the non sulphide Zn deposits are thought to be of supergene origin and therefore to be the result of the same geological factors that controlled the main districts: uplift, oxidation of primary sulphide orebodies by percolating meteoric water and subsequent fossilization of the weathered profiles, under particular climatic conditions (warm and humid with dry periods).

In this thesis, the minor European nonsulphide deposits have not been object of detailed investigation, but they will be considered only as a whole from timing point of view.

The general features (mineralogy, geochemistry of primary and secondary deposits, type of host rock, and probable age of weathering producing nonsulphides) of mentioned Zn-oxides deposits will be separately discussed in the next paragraphs.

7.2 Nonsulphide ore deposits in the Iglesias district, SW Sardinia (Italy)

The mining district of southwest Sardinia is one of the classical area where primary carbonate-hosted Zn-Pb sulphides ores are associated to a relatively thick secondary oxidation zone containing Zn carbonates and silicates.

The nonsulphide ore deposits in the Iglesias district, SW Sardinia (Italy) have been recently reviewed and subjected to new analytical work by Boni et al. (2003).

Mining activity in SW Sardinia is now completely finished, as in many other part of Europe, for both sulphide and nonsulphide ores, but until 1970, when the exploitation definitely stopped, about 150Mt of mixed sulphide and nonsulphide ores, with variable content of Zn and Pb (tab.

1.1) had been extracted from several mines. Additional resources in mine dumps, flotation tailings, and smelter residues are actually present in the area.

The setting of primary and secondary ores, the mineralogy of secondary Zn ores and their relationship with primary sulphides, as well as the geological evidences and timing of the weathering events in this area, will be briefly discussed.

Two most important group of primary ores occur in the Iglesias district. The first group is represented by stratabound lead-zinc sulphide deposits (sedimentary exhalative and Mississippi Valley-type) hosted by Cambrian carbonates. Their emplacement age is surely pre-Hercynian, nevertheless the exact timing is unknown (Boni et al., 1996).

A second group of primary metal deposits include base metals-Ba-F veins and paleokarst ores precipitated by relative low-temperature and high salinity fluids (Boni et al., 1996). Their mineralogy is quite simple, including Ag-rich galena and barite. Also these deposits are hosted in Palaeozoic carbonate lithologies. Their possible timing is age-constrained between Hercynian and Alpine orogeny (possibly Jurassic).

Both Pre-Hercynian sulphides and Lower Paleozoic host rock in SW Sardinia have been strongly deformed, sheared and tilted during Hercynian orogeny. Later on this area was also subjected to Alpine orogeny (Tertiary), which produced block-faulting and further dislocated the sulphide bodies. These processes caused the deep circulation of meteoric water, which promoted oxidation of primary orebodies extending down to several hundred of meters below surface. The alteration front of the weathering profiles over the whole area, is highly variable. It shows no geometric correspondence with present water table: it is most probably related to past geomorphologic conditions (Boni et al., 2003). Several styles of secondary mineralisation occur in this district such as partial replacement of the host carbonates and strata-bound primary sulphides and concentrations of ferruginous, “earthy” smithsonite and hemimorphite-rich clays. The latter occurr as irregular fillings in a maze of interconnecting karst cavities and open conduits in the upper levels of the mines. The mineralogical assemblage is extremely complex, with smithsonite, hydrozincite and hemimorphite as the principal zinc-bearing minerals. Cerussite, anglesite and phosgenite are locally present as well as other “exotic” mineralogical phases (Billows, 1941; Moore, 1972; Stara et al., 1996). Calcite and subordinated quartz are the principal gangue minerals.

Stable isotope geochemical studies on smithsonite from the oxidation zone in the Iglesias mining district revealed variable $\delta^{13}C$ values, ranging from -10.4 to -0.6‰ (VPDB) and constant $\delta^{18}O$ values (25.7 – 28.9‰ VSMOW, av. 27.6 ± 0.9‰) (Boni et al., 2003; Gilg et al., 2007a). The same pattern has been observed in cerussite from this district (Gilg et al., 2007a) with $\delta^{18}O_{VSMOW}$

constrained between 16.7 and 18.0‰ (av. 17.4 ± 0.9‰) and $\delta^{13}C_{PDB}$ ranging from -21.0 to -6.5‰. These data evidence a mixed source of Carbon during the oxidation of sulphides (C-depleted and C-enriched) and a constant temperature and oxygen composition of the meteoric fluid. Considering the oxygen isotope composition of the local paleometeoric water (DeVivo et al., 1997), Gilg et al. (2007a) have calculated new temperature of precipitation for the metals carbonates in the Iglesias district, ranging between 11-23°C (smithsonite) and 16.7 and 18°C (cerussite).

Nonsulphide ores in Sardinia are surely supergene in origin.They are considered as the result of in situ oxidation, during weathering event/s, and replacement, locally with limited transport, of the primary sulphide phases, brought about by meteoric fluids circulating in a deep karstic network in Cambrian carbonate rocks (Boni et al., 2003). The geological period when the main weathering stage promoted the oxidation of the primary sulphides is actually uncertain, owing to multiple oxidation events through time.

Moore (1972), considered that initial oxidation of primary sulphide deposits may have taken place during the Mesozoic. According to Boni et al. (2003), the most reliable time span in which both tectonic and climatic conditions were favourable to the formation of most of the nonsulphides range from middle Eocene - which was the emersion phase in most of Sardinia, followed by lateritisation of the Palaeozoic lithotypes, deep karstification, and deposition of the continental Cixerri Formation - to Plio-Pleistocene - when a tensional tectonic phase was responsible for the differentiated uplift of distinct sectors of the Palaeozoic basement. Nevertheless a reactivation of these processes might have occurred up to early Pleistocene, when extension was capable of causing further differentiated uplifts of the Palaeozoic fault blocks.

7.3 Nonsulphide ore deposits in the Alpine district (Italy, Austria and Slovenia)

The Alpine Zn-Pb mining district, which contains more than 200 carbonate-hosted Zn-Pb deposits, encompassed over both sides of the Periadriatic suture zone, between Northern and Southern Alps. It includes southern Austria, northeastern Italy and northwestern Slovenia. The mineralised stratabound sulphide ores are mainly hosted in Upper Triassic carbonate rocks and are associated with local dolomitisation. Primary sulphide ores have historically been referred as Alpine-type lead-zinc district, Alpine metallogenic province or, less frequently, Bleiberg-type deposits (e.g., Sangster, 1976; Brigo et al., 1977). However, the geological and geochemical

features of the Alpine lead-zinc ores are consistent with other Mississippi Valley type deposits in the world (Leach & Sangster, 1993). The economically most important deposits were located in southern Austria (Bleiberg), northwestern Slovenia (Mezica), and northern Italy (Raibl, Gorno, and Salafossa). Sphalerite was quantitatively more important than galena, but the relative abundance of both sulphide minerals varies extensively along the ore district (Cerny et al., 1982). Iron sulphides are also present. This sphalerite-dominated phase of the ore mineralisation appears to have been deposited during Late Triassic to Early Jurassic (Kuhlemann, 1995; Zeeh et al., 1997), while a less important mineralising event, galena-dominated, occurred during the Tertiary, mainly in Miocene (Kuhlemann, 1995; Zeeh et al., 1997; Kappler & Zeeh, 2000). Nonsulphide ores have been never dated.

Mining activity in this area is now exhausted and the remaining nonsulphide zinc resources are not important under an economic point of view, even though significant resources of high-grade Zn nonsulphide ores (30-50% Zn) have been exploited in the past. In the Italian side of the district nonsulphide exploitation was mostly concentrated in the Gorno district, with ca 780,000 t of Zn and at the Raibl mine, with 188,000 t of Zn (Di Colbertaldo, 1967).

Based on the Hitzman's classification, both wall-rock replacement and karst filling nonsulphide types occur. Supergene minerals concentrations are present in the upper levels of the Raibl mine, where the thickness of completely oxidised ores can reach ca 550m, and in the Bleiberg deposit where they extended below the current water table (Boni & Large, 2003). The mineralogical assemblage of secondary ores includes smithsonite and hydrozincite with anglesite and cerussite in minor abundance. Wulfenite ($PbMnO_4$) is a common mineral in these ores.

The timing of nonsulphide deposits emplacement in the Alpine mining district is very difficult for two important reasons: 1) a cover of nonsulphide deposits is absent and 2) other age-constrained weathering records are generally absent in this and adjacent areas. In conclusion only a lower temporal limit is deducible, and it consists in the age of emplacement of the main sulphide ores (Late Triassic – Early Jurassic). However we should consider that the Alpine orogeny in this part of Europe has surely promoted the formation of a fault network in the Mesozoic carbonates, thus dislocating primary sulphide orebodies up to a surface environment where they were more vulnerable to action of meteoric fluids. These factors most probably enhanced the oxidative processes on sulphides and the relative formation of secondary ores.

7.4 Nonsulphide ore deposits in Greece

Economically important nonsulphide resources in Greece were present at the Lavrion mines, near Athens, and on the Thassos Island. Their importance is exclusively historical, because suitable nonsulphide deposits are now absent. In particular at Lavrion, any remaining resources have now been rendered unavailable by urban development.

About 1.1Mt of calcined calamine from wastes of ancient mining and from the exploited raw material were used to produce high-grade zinc oxides in the Lavrion area at the beginning of the 19th century. The mine then closed in 1978. No published data on the tonnage of secondary ores at Thassos exists. Also Greek nonsulphide deposits are derived from supergene alteration of primary sulphide orebodies.

Primary sulphides at Lavrion consist in manto-type Pb-Ag-Zn marble hosted ore deposits with a massive structure (Skarpelis, 2005). The mineralogical assemblage includes sulphide minerals, Fe-rich sphalerite, galena, pyrite, chalcopyrite, arsenopyrite, and sulphosalts, as tetrahedrite, polybasite, proustite, boulangerite, bournonite, enargite, pyrargyrite, pearseite. The proposed age for the sulphide emplacement is the latest Miocene (Skarpelis, 2005, 2007).

The sulphide mineralization was subjected to intense supergene oxidation which lead to formation of secondary Zn-rich deposits. The thickness of the oxidation zone visible today may exceed 270m. The oxidation of primary bodies and the subsequent emplacement of secondary ores was controlled by hydrogeological features. Usually, the oxidised bodies occur in the vicinity of primary ones.

The most important supergene minerals are smithsonite, hydrozincite, hemimorphite with zincian dolomite, calcite, aragonite and Fe-hydroxides as gangue. Smithsonite predates the precipitation of hemimorphite and hydrozincite.

Secondary ores have been recognized in different settings: a) botryoidal concretions filling vertical to subvertical spaces along joint planes in the marble and as marble replacement along joints and bedding planes; b) botryoidal or globular aggregates coating the walls of karstic cavities; c) filling voids in secondary iron-ore bodies, where they are associated mainly with hematite and goethite and other secondary minerals (Skarpelis, 2005). The major factors controlling nonsulphide emplacement were the formation of open spaces in the marble due to interaction of acidic water with host rock, where secondary minerals precipitated, and the presence of a well developed karst network.

Also in this region the timing of secondary Zn deposit is uncertain, but it is clear that their emplacement is later than the primary ores (latest Miocene, Skarpelis, 2007). Therefore it is

probable that nonsulphide ores are not older than Pliocene. Thus the presence of other paleoweathering records in this part of Europe postdating latest Miocene may be important to age-constrain Greek nonsulphide ores.

7.5 Nonsulphide ore deposits in Spain

Nonsulphide deposits have been discovered in several regions of Spain: Cantabria, Pyrenees, Basque country, and the Santander Province, but only some of them were economically important and therefore exploited in the past. Nonsulphide deposits in Spain are principally associated to two style of primary mineralisation: 1) stratabound lead-zinc ores hosted by hydrothermally dolomitised limestones of the Cretaceous carbonate platform in the northern and central Spain (Reocin type), interpreted as Mississippi Valley type (Velasco et al., 1994); 2) manto and epithermal mineralisation in the Betic Cordillera of southeast Spain related to Neogene volcanism and hosted primarily by Palaeozoic to Triassic carbonates and volcanic rocks (Arribas & Tosdal, 1994).

In the first group of sulphide mineralisation (stratabound deposits) have been recognized different structures and textures, including replacement, cavity infilling, stratiform massive and vein-type mineralisation. Examples of secondary nonsulphide ores associated to them have been discovered at Reocin and Lanestosa (Basque country), and at Mercadel and Novales-Udias. The latter deposits are comparatively less important from an economic point of view. The age of the secondary deposits emplacement in the northern Spain is actually uncertain. Neverthelesswe mention that the Mesozoic carbonate platform in northern Spain was subjected to several phases of vertical tectonism and differential uplift that resulted in the development of an extensive karst morphology. Several fluctuations of the water table through the primary sulphide deposits have also been recorded (Boni & Large, 2003). As we know, these processes may have contributed to the development of weathered profiles on sulphide bodies leading to precipitation of supergene minerals.

Other nonsulphide occurrences, in the Betic Cordillera, include above all the deposit of Las Cruces. The latter deposit has been discovered in 1994 after drilling, in the Palaeozoic sequences covered by about 150m of Miocene sediments. The mineralogy of sulphide mineralisation was dominated by pyrite with varying amount of base metal sulphide minerals. The primary ores were folded and faulted during Hercynian orogeny, then uplifted and exposed to pre-Miocene atmospheric weathering (Doyle et al., 2003). During this weathering phase also mechanical

transport of the weathering product occurred. Subsequently, the sediments of a shallow sea buried both the primary deposits and their weathered profiles. Further the secondary enrichment zone is mostly developed in the first 50m under old pre-Miocene paleosurfaces, but it can locally reach 120m of depth. The weathering profiles show a sensible vertical zonation from a mineralogical point of view, with a Fe-*gossan* in the upper part, which formed above the water table, underlain by an unusual Cu-rich zone formed after leaching and re-precipitation of Cu-ions below water table (Doyle et al., 2003). The mineralogy of secondary ores is dominated by Cu minerals, both sulphides and carbonates (Knight, 2000).

In this deposit secondary ores are age-constrained, due to the presence of a well conserved Miocene cover overlying them. The oxidation of primary sulphides at Las Cruces most probably occurred in the Early Tertiary, this in agreement with previous work referring to paleweathering and paleosurfaces in other part of Spain and Western Europe (Grandin & Thiry, 1983; Blanc-Valleron & Thiry, 1993). Almost all the Iberian peninsula contains also other paleoweathering records whose age spans in the entire Tertiary (Borger, 1997; Gutierrez-Elorza & Gracia, 1997; Molina-Ballesteros et al., 1997).

Chapter 8: Discussion and conclusions

8.1 Foreword

In the previous chapters the mineralogical, geochemical and petrographic aspects of three important European Zn nonsulphide mining districts investigated in this Thesis (Liège, Upper Silesia and Irish Midlands) have been shown. Many differences and affinities have been observed between the nonsulphide deposits contained in the various districts. Moreover, the isotopic ratios of metal carbonates, an helpful tool to characterize the mineralising fluids (Gilg et al. 2007a), show in many cases a certain similitude, even though local differences may be observed, as in the case of the *red galmans* of the Polish nonsulphide ores.

The possible timing of the single districts has been dealt separately, considering the existing paleoweathering records in each area and in the areas adjacent to those hosting the nonsulphide ores. In this chapter we will try to frame this discussion in a broader picture, where the possible correlations between the main periods of paleoweathering in Europe and the formation of supergene nonsulphide ores will be taken into account. In this picture we will consider most of the paleoweathering records present in Europe after Hercynian orogeny, their possible timing, and last but not least, also the climatic conditions to which they were associated.

8.2 Mineralogical, petrographic and geochemical comparison between the investigated European nonsulphide ore deposits: affinities and differences

Investigated nonsulphide Zn deposits in Europe are generally hosted by carbonate lithologies (limestones and dolomites), as many other supergene Zn deposits in the world. This seems to be a common characteristic of this type of secondary supergene deposits. The presence of carbonate host rock is fundamental to buffer the metal-bearing acidic fluids and to promote the precipitation of supergene Zn minerals. In some cases the presence of siliceous rocks may be important to provide a SiO_2 source for the formation of hemimorphite and willemite. For example the Namurian-Tournasian shales, hosting part of the primary and secondary

mineralisation in the Liège district, may represent such SiO_2-source and therefore justify the presence of abundant willemite. Another case is the Silvermines deposit (Irish Midlands district), where part of the primary mineralisation is hosted in the Lower Limestone Shale level of Courceyan age, directly covering the siliciclastic rocks of the Old Red Sandstone Fm. In this mine, hemimorphite is the most important nonsulphide Zn mineral in the secondary ore, with no trace of willemite.

The selected European Zn-nonsulphide deposits occur in different settings, which in accord with the Hitzman's classification are:

1) Zn-rich *gossans* in the upper oxidised zone of primary sulphide orebodies;
2) Concentrations of secondary Zn-minerals as partial replacement of carbonate host rocks in the neighbourhood of primary orebodies;
3) Detrital concentrations of both types 1) and 2) as infilling of karstic cavities.

In each mining district each of these settings occurs. The presence of secondary ores in a well-developed karst network has been observed in all investigated areas, this representing the most abundant typology of nonsulphide deposit in each district.

Mineralogical investigation has revealed that in all selected deposits the typical ore minerals of the supergene nonsulphide assemblage occur comprising, in order of abundance, smithsonite, hemimorphite, hydrozincite (as Zn-minerals), and cerussite (as Pb-mineral). Fe-Mn(hydr)oxides, containing varying amounts of economic metals (Zn, Pb and Cu) are usually associated to the main supergene phases. Secondary Cu-minerals (malachite and azurite) have been detected only in the Irish deposits, where their presence is related to the high Cu-content of the primary mineralisation. Zn-sulphates occur in minor abundance with respect to the above-mentioned minerals. Among the relicts of primary sulphide minerals still present in the oxidised bodies, galena is definitely more abundant than sphalerite and Fe-sulphides (pyrite, marcasite), thus confirming the high resistance to supergene weathering of Pb-sulphides with respect to Zn- and Fe-sulphides. An exception to the typical supergene mineralogical assemblage is represented by the abundant willemite in the Liège district. Another peculiar case is the association of Fe-smithsonite and Zn-dolomite in the Polish *white galman*, which occurs as a lateral phase of the sulphide ores. However, as previously discussed in the paragraphs 4.9.3 and 5.9.3 respectively, willemite and *white galman* may have an origin (hydrothermal?) different from the generally acknowledged supergene genesis of nonsulphide ores. In both cases we could not record the presence of Fe(hydr)oxides, which are particularly abundant in the nonsulphide ores of indubitable supergene origin (smithsonite-hemimorphite dominated assemblage).

The exact paragenetic sequences of secondary ores are not always ascertained. The relationships between Zn and Pb supergene minerals are also often unclear. On the whole, we could establish that smithsonite (some generations) is the first and more abundant supergene mineral to be segregated: it can replace primary sulphides, host rock carbonates and/or precipitate in voids. It is generally followed by hemimorphite, (less) hydrozincite and by other "exotic" minerals. In all the districts examined, late calcite (meteoric) is associated to the Zn and Pb secondary minerals; it represents the latest mineral phase to precipitate in fractures and cavities.

Smithsonite occurs in different morphological types and habits. Some of them have been recognized in all the mining districts, while others are characteristic of few single deposits. For this reason, it has been not always possible to effectuate a correlation between the smithsonite morphologies in the investigated districts. This type of comparisons has been carried out only on smithsonite samples from the Liège and Irish Midlands districts, which have been compared with the morphological types of Sardinian smithsonites, published in Boni et al. (2003). Smithsonite from Polish nonsulphides has very different characteristics that can hardly be compared with those from the other deposits.

As previously mentioned, hemimorphite generally postdates smithsonite in the supergene ores, but an exception is surely represented by the Belgian deposits, where a first generation of this Zn hydrated silicate seems to replace directly the anhydrous silicate willemite.

Also the geochemical analyses have revealed both differences and affinities between the investigated deposits in the various districts. As shown in tables 4.5, 5.3, 6.2, 6.3 and 6.4, smithsonite can contain variable amounts of elements other than Zn in the crystalline lattice (Mn, Ca, Pb, Mg). High amounts of Cd are present in smithsonite from Belgium, the Irish Midlands and especially from the Upper Silesia district, whereas other non-economic, polluting metals (the so-called "*nasties*") are practically absent in the crystalline lattice of the analysed smithsonites. A peculiar characteristic of the Zn-carbonate is the high amount of Fe (up to 15 wt.% FeO) recorded in several smithsonite generations from all the three districts. In the Belgian deposits Fe-smithsonite represents a late phase in the supergene paragenetic sequence, while in the Irish ores, especially in Tynagh and Silvermines, Fe-smithsonite is one of the earlier smithsonite types to precipitate. The Fe-rich smithsonite variety has been detected also in the Polish deposits where this phase is commonly associated only to *white galmans* (hydrothermal?) ores. No evidence of Fe-smithsonite has been detected in the polish supergene ore type (*red galman*).

Hemimorphite shows similar mineralogical and geochemical characteristics among the investigated European nonsulphide deposits. It generally occurs as crystalline aggregates, with the typical radiated structure of single tabular crystals elongated along the *b* crystallographic

axis. Chemical analyses carried out on this Zn silicate show a stoichiometric chemical composition with only few amounts of Al, Ca, Fe and occasionally Pb. Also several analysed cerussites throughout the different districts reveal an almost stoichiometric composition, with only occasional traces of Zn.

Averaging values of C and O isotopic data are reported in table 8.1. Belgian smithsonites present a constant $\delta^{18}O$ and a more variable $\delta^{13}C$. These C-O patterns are almost identical to those of smithsonite from the Iglesiente district (SW Sardinia) (Boni et al., 2003). The relatively uniform values of oxygen ratios recorded in Belgian smithsonites imply a constant temperature and isotopic composition of fluids during weathering and precipitation of oxidized phases. Uniform values of $\delta^{18}O$ are also recorded in Pb-carbonates and calcites associated. The broad range of $\delta^{13}C$ measured in Zn and Pb carbonates in the same district (a fact also recorded in SW Sardinia), indicates the presence of at least two carbon sources available during oxidation process: a ^{13}C-enriched source derived from the organic matter of the overlying soils and a ^{13}C-enriched marine carbon, originated from dissolution of the carbonate host rocks.

Smithsonite from the *red galman* in Lower Silesia shows a limited range of $\delta^{13}C_{VPDB}$ values and lightly variable $\delta^{18}O_{VSMOW}$ values. The uniform values of $\delta^{13}C_{VPDB}$ detected in supergene *red galman* are quite unusual for supergene carbonate-hosted deposits (Boni et al., 2003; Coppola et al., 2007; Gilg et al., 2007a). This could mean a predominance of the reduced soil-derived carbon source during *red galman* formation. Smithsonites from *white galman* have more variable and positive carbon isotope values, but broadly similar oxygen isotope compositions. The C-isotope variation of *white galman* smithsonites indicates a mixed contribution between carbon derived from OBD host rock and organic carbon from the soils.

In the Irish Midlands the Zn, Pb and Cu carbonates show a very common pattern of relatively constant oxygen and often highly variable carbon isotope compositions, as well as in other supergene nonsulphide deposits. The variation of oxygen isotopic composition is limited within the deposit for both smithsonite and cerussite. Cerussite shows $\delta^{18}O_{VSMOW}$ values about 12‰ lower than cogenetic smithsonite. Also in the Irish nonsulphides there is a clear indication for the existence of multiple carbon sources as well as of a substantial carbon isotope fractionation between Pb and Zn carbonates. However, the predominance of ^{13}C-depleted values indicates a major contribution of a C-reduced source/s.

In all the supergene nonsulphide deposits considered, the C-isotopic composition of metal carbonates with more negative values is similar to the composition of pedogenetic calcites formed in soils with predominant C3 plants (Gilg et al., 2007a).

Table 8.1: C and O isotopic data of Zn, Pb, Ca, and Cu carbonates from investigated mining districts and from Iglesias mining district (SW Sardinia)

Localization	mineral	number of analyses	$\delta^{13}C_{VPDB}$ Ave. (min/max)	$\delta^{18}O_{VSMOW}$ Ave. (min/max)	references
Iglesiante (SW Sardinia)	smithsonite	25	(-10.4/-0.6)	27.6 (25.7/28.9)	Boni et al., (2003)
	cerussite	10	(-21/-11.3)	17.4 (16.7 / 18.0)	Boni et al., (2003); Gilg et al., (2007)
	hydrozincite	2	(-2.4/-7.1)	26.8 (26.6/27.0)	Boni et al., (2003)
	phosgenite	6	(-9.8/-4.2)	20.6 (20.1/21.2)	Boni et al., (2003); Gilg et al., (2007)
	calcite	5	(-10.3/-9.2)	25.1 (24.7/25.6)	Boni et al., (2003)
Liege (NE Belgium)	smithsonite	23	(-11.6/-1.6)	28.4 (27.1 / 30.2)	Coppola et al., (2007); this study
	cerussite	5	(-18.4/-14.7)	17.8 (16.8 / 19.3)	Coppola et al., (2007); this study
	calcite	5	(-10.4/-6.1)	25.4 (24.7/25.7)	Coppola et al., (2007); this study
Irish Midland					
Tynagh	smithsonite	5	(-10.3/1.3)	30.1 (29.5/30.5)	this study
	cerussite	3	(-16.4/-13.9)	18.2 (17.6/18.6)	this study
	azurrite	1	-11.4	30.7	this study
Galmoy	smithsonite	14	(-8.6/-5.7)	30.0 (28.3/31.5)	this study
	cerussite	2	(-8.6/-0.1)	17.9 (16.6/19.6)	this study
Upper Silesia (S Poland)	smithsonite (*red galman*)	11	(-11.4/-10.1)	26.8 (25.3/28.5)	this study
	smithsonite (*white galman*)	3	(-7.4/-2.9)	27.8 (26.8/28.9)	this study
	cerussite	1	(-12.8)	13.8	this study
	calcite	12	(-10.1/-4.4)	22.8 (21.3/23.9)	this study

8.3 Paleoweathering in Europe during Mesozoic and Tertiary and timing of nonsulphide Zn deposits

Paleoweathering studies have contributed to paleogeographic and paleoclimatic reconstructions during the geological history of the Earth. They are based on the evaluation of the records of past weathering events, based on the altered profiles of different mineralogical composition and origin, combined with age dating of detected paleosurfaces and paleosoils. Also the karst systems with their infillings are among the possible records of paleoweathering, which can be investigated. However, this type of study generally presents some difficulties, due to the scarcity or absence of good geological records of ancient terrestrial deposits and/or datable erosion surfaces.

Especially on the European continent, only a scanty testimony of non-marine evolution is preserved, which occurs as a patchwork of landforms and weathering horizons of different ages and origin, discontinuous in the space and time. Moreover, some of these profiles have a polygenetic evolution. Only part of the weathering profiles have been dated either with isotopic methods, by paleomagnetism or more directly, following the stratigraphic principle of superposition of well-dated sediments on top of the residual deposits. Nevertheless, all existing evidence shows that continental evolution and relative weathering on the exposed lithologies has undergone a sensible increase during particular periods of geological history, while an almost complete quiescence was present in other periods.

In this Thesis we have reviewed the most important paleoweathering records present on the European continent with their geo-tectonic and climatic significance, which can have a relationship with nonsulphide deposits from a timing point of view. The result is be the individuation of:

a) a number of periods during which supergene alteration was stronger in Europe,

b) favourable climate conditions leading to the formation of most European nonsulphide zinc-lead deposits.

In the current literature many papers on the geology and mineralogy of the paleoweathering records in Europe exist. In fewer cases, with the aid of stable isotope geochemistry, also climate indications on these records have been given. This type of study has a remarkable importance, because weathering is a major ore-forming process traditionally accepted for commodities such as Al, Fe and Ni (bauxites and laterites), but also for other supergene deposits derived from the alteration of Cu and Zn sulphides. In the first case the process of metal enrichment consists in profound mineralogical changes of the bulk rock and possibly mass transport, whilst in the

formation of secondary Cu and Zn deposits dissolution processes of both primary sulphides and part of the host rock, metal transport and re-precipitation are involved (Hitzman et al. 2003; Sillitoe 2005).

Many recurring records of weathering events and erosion phases have been individuated and related to major sea level changes, tectonic activity and paleoclimate in Europe. In some cases several weathered profiles of different origin and ages are spatially associated.

Previous studies seem to demonstrate that the main bulk of weathering records (kaolinites, Ni-laterites, bauxites) were produced in Europe during two distinct periods: Cretaceous-Early Eocene and Oligocene-Miocene (Herrington et al., 2007). Weathering has been a continuous process through time, but general and local geological conditions have resulted in preserved mantles of different ages. Migon & Lidmar-Bergström (2002) pointed out that in Europe "an apparent trend from an earlier kaolinitic/ferrallitic style of weathering in the Mesozoic and Early Tertiary, towards a grussic style by the end of the Cainozoic, does not only reflect climate change, but it is also broadly consistent with tectonic/geomorphic history and related changes in land surface stability. Miocene and Plio-Pleistocene saprolites, in particular, show that in different geomorphological and lithological circumstances different types of weathering mantles could have evolved" (fig. 8.1).

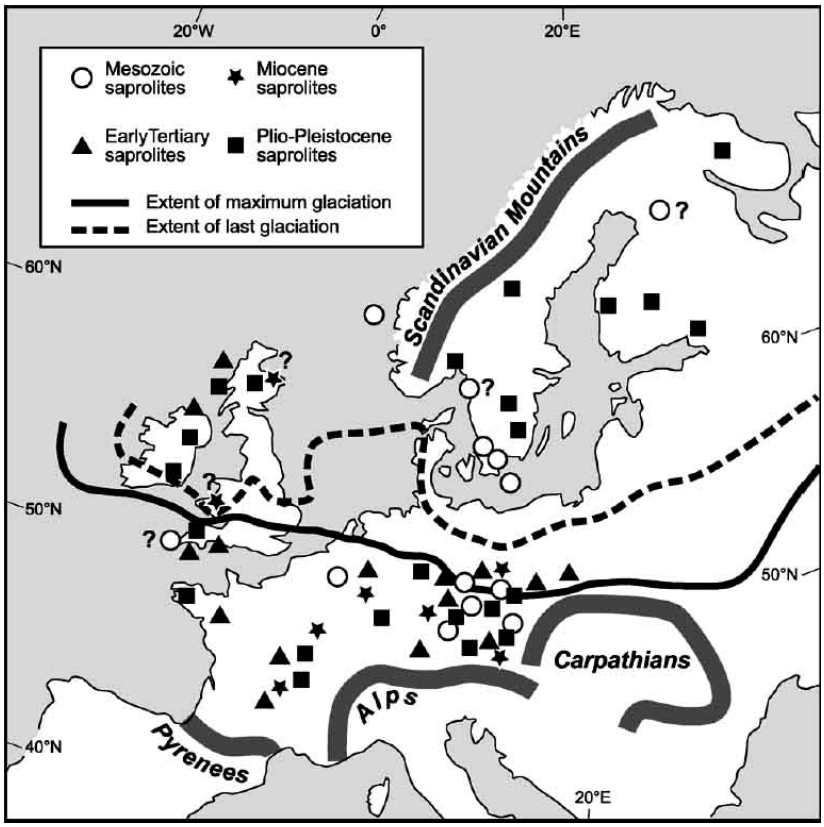

Figure 8.1: Location map indicating most important saprolite deposits in central and north Europe. V-Vogelsberg, F-Fichtelgebirge (from Migoń & Karna Lidmar-Bergström, 2002).

The bulk of European bauxite deposits have been deposited from Lower Cretaceous up to Lower Eocene. They occur mainly in Southern and Eastern Europe (southern Italy, southern France, Sardinia, Greece, former Jugoslavia, Hungary). French deposits are present in Provence (Thiry et al., 2006), on the border of the Paris Basin (Thiry et al., 2005, 2006; Simon-Coinçon et al., 2005), in the Pyrenees chain (Thiry et al., 2006; Combes et al., 1998; Combes & Peybernes, 1996) and also in the southern side of the Massif Central (Thiry et al., 2006; Simon-Coinçon et al., 2005). They represent the filling of karsts cavities deepened in Jurassic and Lower Cretaceous carbonates (karst bauxite) as well as paleosoils intercalated in the Upper Jurassic - Lower Cretaceous carbonate sequences. In the latter case, the bauxite deposits mirror brief periods of local emersion. In most cases the bauxite bodies are covered by Late Cretaceous trasgressive sediments, which provide an upper time limit for this weathering phase. A marine ingression takes place diachronously in this part of Europe from Aptian to Maastrichtian covering the weathered profiles and signalizing the end of a main period of surface alteration.

Also Fe-laterites and Ni-laterites are present in southern Europe, especially in the Balkan peninsula (Albania, Greece and Kosovo). They occur in different setting. Usually Ni-laterites represent authochtonous weathered profiles posted on Jurassic peridotites, or reworked allochthonous laterites deposited on unweathered ultrabasic rocks. Occasionally laterites were re-deposited on Mesozoic carbonate sediments, or formed intercalations in Miocene sedimentary sequences (Herrington et al., 2005). The age of the weathering phases producing the lateritic bauxites and Ni-laterites in the Balkan peninsula has not been always cleared, due to the absence of well dated cover rocks. As an example, Skarpelis et al. (1996) proposed a Tertiary age for the bauxite emplacement in SE Albania, whereas a Cretaceous age for the weathering event leading to the main bauxite generation in Greece is commonly accepted.

Lateritic deposits have been recognized also in northern and central Europe. In the Bohemian Massifs a few lateritic horizons, stratigraphically associated to kaolinitic saprolites, occur under Cenomanian sediments (Grygar at al., 1997) or even under Eocene to Miocene deposits (Migoń, 2003). At Szklary, NW of Krakow (Lower Silesia), a Ni-laterite weathering mantle considered of Palaeogene age (Dubinska et al., 1986; Niskiewicz, 2000), was developed on serpentinites belonging to the Early Palaeozoic basement. In the Rhenish Slate mountains (Vogelsberg Massif, central Germany), a bauxitic horizon with a ferralitic imprint was developed on basalts of Middle Miocene age (Schwarz, 1997). Other ferralitic profiles occur in the Antrim Plateau in NE Ireland, where they are dated as Paleocene (Hill et al., 2000).

The commercial kaolinite deposits represent another distinct type of weathering record in Europe, which testify strong supergene alteration processes on exposed rocks. These deposits

occur as weathered profiles *in situ* or as reworked matter deposited in depressions and/or cavities. Generally it is accepted that kaolinitic saprolite formed under less extreme climate conditions (humid to temperate climate) compared with those responsible for the formation of bauxite and laterite deposits. In fact, a minor drainage is needed to avoid leaching and total dispersion of silica: a typical process occurring in bauxites. Kaolinite deposits are widespread in Europe, but they are mostly concentrated in the central and northern part of continent (Migoń & Lidmar-Bergström, 2001). On the Fennoscandian shield many kaolinitic saprolites have been individuated in different stratigraphic settings (Elvhage & Lidmar-Bergström, 1987; Lidmar-Bergström, 1995; Lidmar- Bergström et al., 1997). In this part of Europe the most suitable time span for deep kaolinitic weathering was Mesozoic, from late Triassic onwards. However, for the main bulk of kaolinitic saprolites in central Europe an age spanning from Lower Cretaceous to Paleogene has been proposed; some minor kaolinite deposits record also a Miocene age (Migon & Lidmar-Bergström, 2001; Yans, 2003).

Iron-rich kaolinitic saprolites, classically named as "Siderolithic", are present in the Massif Central in France and Lorraine in Belgium. These formations, previously ascribed to Tertiary, after paleomagnetic (Théveniaut et al., 2002; Ricordel et al., 2005) and isotopic dating (Yans, 2003), have been re-interpreted as being formed during Lower Cretaceous. However, the formation of the "Siderolithic" continued also until Lower Tertiary.

Several types of saprolites developed on bedrocks of different nature and origin are known from the northwest of the Bohemian Massif, the area constrained between Czech Republic to the east and Bavaria (Germany) to the west. In this region several kaolinitic saprolites and ferricretes are present in different stratigraphical settings. Some kaolinites occur under Cenomanian sediments (Upper Cretaceous), and are associated to a pre-Upper Cretaceous erosion surface established in the northern part of Bohemian Massif (Demek, 1982; Kral, 1985). Other kaolinite-rich saprolites were established on granites in the Sudetes. These secondary kaolinitic horizons and relative denudational surfaces are mantled by clastic deposits of Miocene and Pliocene age (Sadowska, 1977; Ciuk & Piwocki, 1979; Dyjor, 1986; Migoń, 1997a) or by basalts aged 28–2 Ma (Neogene to Recent). Therefore, the above-mentioned deep weathering mantles must be at least of Palaeogene age (Migoń, 1997a).

Other well-known kaolinite deposits are present on the German side of the Bohemian Massif (Gilg, 2000). These deposits are derived from the weathering of the crystalline basement and of the Triassic sandstone derived from its degradation. On the basis of geological evidence and stable isotope geochemistry Gilg (2000) considered the kaolinite deposits in this region to have been formed during two main weathering periods: late Early Cretaceous and Late Oligocene to

Mid-Miocene. To the kaolinite deposits of Lower Silesia in Poland, derived from the alteration of the Hercynian granites and Upper Cretaceous arkoses, was assigned from Gilg (2003) a post Upper Cretaceous age, like many other kaolinite deposits in Europe.

The best known of all saprolites in southwest England are again kaolinite concentrations developed on Hercynian granites (Bristow, 1969, 1977; Bristow & Exley, 1994; Sheppard & Gilg, 1996). Deep weathering and advanced alteration are not restricted to the granite massifs, but have also been reported from the metamorphic rocks in Cornwall (Walsh et al., 1987) and from the tablelands of West Dorset and East Devon (Waters, 1960; Isaac, 1981, 1983). The latter include also laterite-like profiles. These kaolinitic and lateritic weathered profiles are usually considered of Early Tertiary age (Isaac, 1981, 1983; Green, 1985), but the possibility of the onset of kaolinisation in Late Cretaceous cannot be excluded (Green, 1985). In the the Armorican Massif NW France (Brittany), the formation of kaolinite in surficial conditions is demonstrated by the existence of alteration profiles enriched in kaolinite at the top of metamorphic and sedimentary formations, but also on Hercynian granites (Boulvais et al., 2000). The different stages of large-scale supergene kaolinization events in Brittany are older than Oligocene, with the most important weathering period identified during the upper Cretaceous-lower Eocene.

Grus is a particular type of saprolite, composed of particles of sand and gravel fractions, with very little silt and clay. Its texture evidences an immature alteration stage. *Grus* is most common on granitoid rocks, but other rock types may also produce a *grus* weathering. It is generally accepted that the immaturity of *grus* saprolite may be related to young, still ongoing saprolitisation process, or it would point to a much less aggressive environment, warm to cool (Migoń, 2003) with respect to climate favouring the development of kaolinite horizons. This type of weathering record is quite abundant mainly in northern Europe (Fennoscandian peninsula, British Isles). Occasionally it has been individuated at lower latitudes (central France, Bohemian Massif and Sudetes mountains). Precise dating of European examples is usually difficult because of scarcity of overlying, well dated deposits. *Grus* saprolites are quite abundant in northern Ireland (Mourne Mountains; Smith & McAllister, 1987), eastern Ireland (Wicklow mountains; Power & Smith, 1994) and also in the Donegal in the extreme northwest of country (Migoń & Lidmar-Bergström, 2001). They are usually superimposed on granites and gneisses. Age determination of the *grus* saprolites is difficult, nevertheless capping by glacial deposits is usually taken as evidence for a pre-glacial age of these weathering profiles. Many grus occurrences are known from the Buchan area in NE Scotland (Hall, 1985, 1986,1987; Hall et al., 1989; Migoń & Lidmar-Bergström, 2001). Precise dating of saprolites in NE Scotland is difficult because of scarcity of overlying, well-dated deposits, but in most cases dating is precise enough

to infer their pre-Quaternary ages. In the majority of cases, the grus profiles are covered only by Devensian tillites. Slightly decomposed granites, ascribed to grus saprolites, are present on the granite upland in the Dartmoor area, SW England (Eden & Green, 1971). Also in this case, the dating of *grus* profiles is difficult, but Eden and Green (1971) on the base of climatological data, argued that this type of weathering probably occurred during Pliocene and early Pleistocene. *Grus* saprolites are quite abundant also in the Bohemian Massif (Korber & Zech, 1984; Kubiniok, 1988; Borger, 1992), as well as in the NE side of the same Massif, notably in the Karkonosze Mountains and in the Jelenia Gora Basin in the West Sudetes (Jahn, 1962; Borkowska & Czerwinski, 1973; Migoń, 1997b). Also in this case, they are considered as pre-Quaternary in age, on the base of a cover of glaciogenic deposits. Where the glaciogenic cover is absent, grusification could also be of Quaternary age. *Grus* type saprolites abound in southern Sweden (Lidmar-Bergström et al., 1997) but are also known from other areas of the same country, including the western coast (Hillefors, 1985), north-central Sweden (Lundqvist, 1985) and many other scattered sites (Elvhage & Lidmar-Bergström, 1987). Also in this case the presence of a cover of Weichselian tillites suggests a Pliocene to Early Pleistocene age for these weathering mantles. *Grus* saprolites in Finland and Norway are much likely pre-Pleistocene in age (Migoń & Lidmar-Bergström, 2001). However, *grus* saprolites are locally present also in the Massif Central and Normandy (Migoń & Lidmar-Bergström, 2001) and seem to be associated to the main lower Tertiary weathering events.

Although dating of weathering mantles is often circumstantial, and is usually also deducted by local geological features instead of absolute age data, it is ascertained that the majority of the post-Paleozoic paleoweathering records in Europe (laterite, kaolinite and *grus*) point to well-distinct periods. Most of the lateritic profiles seem to predate the Upper Cretaceous transgression, with some exceptions as the ferralitic laterite on the Miocene basalts of the Vogelsberg Massif (Germany) or the Paleocene lateritic bauxites at Antrim (N Ireland). Also several kaolinitic profiles in central Europe are pre-Late Cretaceous in age even though Early Tertiary and Miocene kaolinitic saprolites are also widely diffused. In the Iberian Pirite Belt are recorded several weathering profiles on the primary ores, which have produced an enrichment of secondary sulphides and thick ferralitic crusts (Las Cruces, Doyle et al. 2003). These profiles are covered by Miocene marine sediments.

During the first weathering phase (pre-Upper Cretaceous) mainly bauxite and few Ni-laterites were formed in southern Europe (in prevalence on the African side of the Thethys), whereas kaolinite-rich saprolites prevailed in the European continent. But other kaolinite deposits in central Europe have been also ascribed to Tertiary, mainly pre-Miocene weathering, whilst *grus*

deposits, especially occurring in northern Europe, seem to be much more recent (Pliocene-Pleistocene).

It is so far accepted that climate is one of most important controlling factors on the development of weathered profiles, together with the bulk mineralogy of protore. Thus, a tropical climate, with rainfalls in excess of 1.2m during 9-11 wet months per year with an annual mean temperature in excess of 22°C, is needed for the silica leaching and concomitant upgrade of Al and the final formation of bauxites (Bàrdossy & Aleva, 1990). Similar climate conditions have been taken into account also for the formation of Ni-laterites (Budel, 1982). But apparently, more recently this thesis needs to be reviewed. In fact, there is growing evidence that in many circumstances alternating wet-dry conditions, more common in savannah-type settings, are more favourable to the formation of laterites, including Ni-laterites, rather than a truly humid-tropical environment. Slightly less extreme climate conditions are needed for the formation of kaolinite deposits, because a less pronounced drainage would avoid the complete leaching of silica in these environments. As discussed above, *grus* saprolites may represent only an immature stage of protore weathering and therefore they could originate in the same climate that favoured the formation of kaolinite deposits.

Climatic conditions for the formation of supergene zones over weathered Cu and Zn-Pb sulphide bodies are possibly less restricted than those requested for laterites and bauxites (Herrington et al., 2007). The region best known for supergene enrichment of Cu sulphide ores in the world is Chile, where warm temperatures in semi-arid to pluvial conditions imposed on pedeplain topography were ideal environments to form this kind of deposits (Sillitoe, 2005). Similar conditions would appear to favour locally also the formation of secondary Zn deposits (Reichert & Borg, 2007): the presence of a well-distinct dry season may be important to promote Zn precipitation in form of carbonates and silicates, and avoid a complete dispersion of metal. However, for the replacement and cavity filling process of the newly formed minerals in carbonate rocks, the necessity for an available carbonate trap subjected to strong karstic dissolution is self-evident. In this respect, it may be no coincidence that during much of the Mesozoic, entire regions of Europe consisted largely of large areas of exhumed and eroded carbonates (many of them mineralised with Pb-Zn sulphides), forming a suitable scenery for karstic weathering.

In the paleogeographic maps corredated with climate data derived from the web-based publications of Scotese and Boucot are reported the ‘peak’ periods of supergene deposit formation. It is apparent that in many cases there are broad correlations between climatic data and deposit types. There are many anomalies in the data though, which need clarification. As

mentioned before, bauxites and Ni-laterites do not seem to be restricted to tropical zones since in the Mid Cretaceous the southern European bauxites and Ni-laterites are clearly developed in what are depicted as temperate zones. Bauxite and Ni-laterite deposits formed in the Miocene fit the tropical climate zones much better, although again many examples of Ni-laterite are found in more temperate climatic zones. An interpretation of these data may indicate that there is a much broader range of climate conditions suitable for the formation of supergene deposit types than currently proposed. Another possibile interpretation of the broad ranges of ages assigned to similar deposit types, may indicate that features such as tectonic evolution and erosion rates, as well as local hydrological conditions may actually be more important than climate. Therefore, periods characterised by progressive uplift with only moderate erosion would be favourable to the formation of most deposit types.

Referring to tectonic evolution, it is noted that in Europe, the Cretaceous marked one distinctive period of closure of part of the Tethys ocean accompanied by collision, uplift, exhumation of ophiolites, arc volcanics and carbonate successions. The exhumation of carbonate rocks may have led to the development of a well developed karstic network, which may have represented both a physical and possibly a chemical trap for many supergene deposits, including Zn-Pb nonsulphide ores. The Miocene marked the final closure of the Tethys with the formation of the Alpine-Balkan and Pyrenean chains, a tectonic event that has been also followed by strong uplifts.

The central European nonsulphide Zn(-Pb) deposit may be related to the pre-Upper Cretaceous and Paleogene-Miocene main weathering events. Unfortunately climatic conditions for the formation of supergene zones over weathered sulphide bodies of Zn are possibly even less proscriptive than those accepted for lateritic deposits and leave several possibilities still open. However, according to the recent assumptions of Reichert & Borg (2007), a temperate climate with dry periods would appear to be the most favourable for the precipitation of secondary Zn deposits.

Our stable isotopic studies evidence that supergene minerals in the nonsulphide Zn deposits (smithsonite and cerussite) formed at temperatures constrained between 10 and 20°C (tab. 8.2). These data are perfectly in agreement with published temperatures of precipitation of Zn- and Pb-carbonates from other classical types of supergene nonsulphide Zn deposits worldwide (fig. 8.2) (Gilg et al., 2007a). Only in the Irish deposits lower temperatures (3-13°C) have been calculated for smithsonite (this considering today meteoric waters as mother fluid of the supergene ores). On the whole, these temperatures point to depositional conditions typical of temperate zones, like those actually occurring at mid-latitudes, where the possibility of a distinct

Table 8.2: Calculated temperature of formation of Pb, Zn and Ca carbonates using corresponding estimated isotopic composition of local paleometeoric and hydrothermal water (see the text)

Localization	mineral	number of analyses	$\delta^{18}O_{VSMOW}$ Ave. (min/max)	$\delta^{18}O_{VSMOW}$ water	references	T(°C) Ave. (min/max)
Iglesiente (SW Sardinia)	smithsonite	25	27.6 (25.7/28.9)	-6.5	1[a]	15(11/23)
	cerussite	10	17.4 (16.7 / 18.0)	-6.5	1[a]	16(13/20)
	hydrozincite	2	26.8 (26.6/27.0)	-6.5	1[a]	
	phosgenite	6	20.6 (20.1/21.2)	-6.5	1[a]	16(14/19)
	calcite	5	25.1 (24.7/25.6)	-6.5	1[a]	
Liege (NE Belgium)	smithsonite	23	28.4 (27.1 / 30.2)	-6.1	2[a]	14(7/19)
	cerussite	5	17.8 (16.8 / 19.3)	-6.1	2[a]	16(9/22)
	calcite	5	25.4 (24.7/25.7)	-6.1	2[a]	12(11/15)
Irish Midland						
Tynagh	smithsonite	5	30.0 (29.5/30.5)	-6.5	5[a]	7(3/13)
	cerussite	3	18.2 (17.6/18.6)	-6.5	5[a]	14(6/21)
	azurrite	1	30.7	-6.5	5[a]	
Galmoy	smithsonite	14	30.0 (28.3/31.5)	-6.5	5[a]	7(3/13)
	cerussite	4	17.9 (16.6/19.6)	-6.5	5[a]	14(6/21)
Upper Silesia (S Poland)	smithsonite (*red galman*)	11	26.8 (25.3/28.5)	-8	3[a]	12(7/18)
	Fe-smithsonite (*white galman*)	3	27.8 (26.8/28.9)	(-0.8/0.8)	4[b]	(34/53)
	Fe-smithsonite (*white galman*)	3	27.8 (26.8/28.9)	-8	3[a]	(5/12)
	cerussite	1	13.8	-8	3[a]	28
	calcite	12	22.8 (21.3/23.9)	-8	3[a]	15(11/22)

1. Boni et al. (2003), De Vivo et al. (1987); 2. Yans (2003); 3. Gilg (2003); 4. Heijlen et al., (2003); 5. Diefendorf & Patterson, 2005.

a: meteoric water; b: hydrothermal fluid.

dry season also exists. However, if we consider that the deposition of nonsulphide deposits usually occur as infilling of deep karst cavities, then we might affirm that these temperature probably established in these environments also under a more extreme, tropical climate.

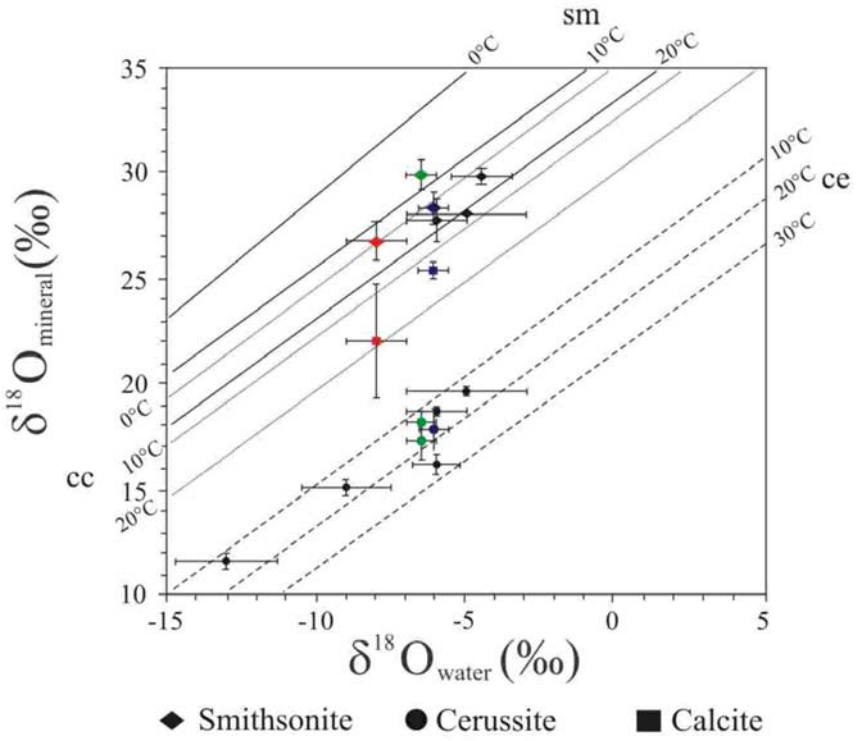

Figure 8.2: Oxygen isotope data of cerussite (ce, circles), calcites (ca, square), and smithsonites (sm, rhomb) from supergene oxidation zones of investigated ore deposits including other classical supergene nonsulphide deposits in the world (Gilg et al., 2007a), and estimated isotopic composition of local paleometeoric water (for references see table 8.2. Note: red = Upper Silesia district, green = Irish Midlands district, blue = Liège district; supergene deposits in the figure: Broken Hill – Australia, Preguiça - Portugal, Skorpion – Namibia, Tui – New Zeland, Milos – Greece, Garpenberg – Sweden, Freihung – Germany.

The geological constraints on the ages of the nonsulphide Zn ores in the three mining districts are:

1) Liège: some parts of the ore bodies (the willemite-rich ones) are covered by the continental sandstone of the Aachen Fm (Upper Cretaceous). These parts of the supergene ores are therefore pre-Upper Cretaceous and their timing could be comparable with the main weathering phase, which produced many commercial kaolinite deposits, as well as the oldest "Sidérolithique" in Europe. However, due to the reduced thickness and high permeability of the sandstone cover, oxidation the primary sulphides may have continued in depth also after the Upper Cretaceous transgression and throughout Tertiary.
2) Upper Silesia: part of the ore bodies are covered by Miocene marine sediments. If we assume a Middle Cretaceous age for the deposition of primary sulphides (Heijlen et al., 2003), the bulk of nonsulphides may have started to form during the Tertiary weathering

phases, which have been also responsible for the genesis of the kaolinite and Ni-laterite deposits in the Lower Silesia district.

3) Irish Midlands: Tynagh and Silvermines "*residual bodies*" are covered by Quaternary glacial sediments and the weathered profiles below them, developed on the primary sulphides are quite immature. Actually, the presence of many *grus* saprolites in several areas of the British Isles is in accord with a young and immature weathering process in this part of Europe. If we assume that the Irish nonsulphide Zn deposits started to develop during Early Tertiary, in concomitance with climatic conditions causing the lateritization of the Antrim basalts in the north of the country, we cannot exclude that oxidation process acting on the Irish primary sulphides may have been repeatedly rejouvenated under less extreme climates and may be still ongoing.

References

Albers, H.J., 1978. Die Sande von Aachen und Hauset (Äquivalente der Haltener Sande Westfalens). Sedimentologie, Faziesanalyse und hydrogeologische Bedeutung. Nachrichten der Deutschen Geologischen Gesellschaft 19: 2-3.

Alexandre, J. and Thorez, J., 1995. Au Secondaire et au Tertiaire, l'Ardenne tropicale. L'altération des roches et les climats anciens. In: Demoulin, A., [eds.], L'Ardenne. Essai de Géographie physique. Hommage au Professeur Pissart, Département de Géographie physique et du Quaternaire, Université de Liège: 53-67.

Alexandrowicz, S.W., 1969. Utwory paleogenu w poludniowej części Wyżyny Krakowskiej (Couches de Paléogéne de la partie méridionale du Plateau de Cracovie). Rocznik Polskiego Towarzystwa Geologicznego (Annales Societatis Geologorum Poloniae), 39(4): 681-694.

Andrew, C.J., Crowe, R.W.A., Finlay, S., Pennell, W.M., and Pyne, J.F., [eds.], 1986a. Geology and genesis of mineral deposits in Ireland, Irish Association for Economic Geology, Dublin: 709p.

Andrew, C.J., 1986b. The tectono-stratigraphic controls to mineralization in the Silvermines area, county Tipperary, Ireland, In: Andrew, C.J., Crowe, R.W.A., Finlay, S., Pennell, W.M., and Pyne, J.F., [eds.], Geology and Genesis of Mineral Deposits in Ireland, Irish Association for Economic Geology, Dublin: 377-418.

Andrew, C.J., 1993. Mineralization in the Irish Midlands, In: Patrick, R.A.D. and Polya, D.A., [eds.], Mineralization in the British Isles, London, Chapman and Hall: 208–269.

Arribas, A. Jr. and Tosdal, R.M. 1994. Isotopic composition of Pb in ore deposits of the Betic Cordillera, Spain: Origin and relationship to other European deposits. Economic Geology, 89: 1074-1093.

Badley, M. E., 2001. Tertiary faulting, footwall uplift and topography in western Ireland. In: Shannon, P.M., Haugthon, P.D.W. and Corcoran, D.V. [eds.], The petroleum exploration of the Ireland's offshore basin, Geological Society, London, Special Publications, 188: 201-207.

Bak, B., 1986. Węglanowa mineralizacja Zn, Pb i Fe w śląsko-krakowskich złożach rud cynku i olowiu. Unpublished report in Archives of the Academy of Mining and Metallurgy, Krakow, Poland.

Bak, B., 1993. Ferroan dolomites and ankerites from the Silesian-Krakow deposits of zinc and lead ores. Geological Quarterly, 37(2): 279-290.

Bak, B. and Niec, M., 1978. The occurrence of monheimite in the Boleslaw Zn-Pb ore deposits near Olkusz. Mineralogica Polonica, 9: 123-128.

Bak, B. and Zabinski, W., 1981. On the continuity of the solid solution series smithsonite-siderite. Mineralogica Polonica, 12: 75-80.

Balassone, G., Rossi, M., Boni, M., Stanley, G. and McDermott, P., 2005. Supergene nonsulfide Zn-Pb ores at Silvermines and Galmoy (Ireland). ESF Workshop on Nonsulfide Zn-Pb Deposits, 21th - 23th April, 2005, Iglesias, Italy, Abstract: 5-6.

Balassone, G., Rossi, M., Boni, M., Stanley, G., and McDermott, P., 2007. Mineralogical and geochemical characterization of nonsulfide Zn–Pb mineralization at Silvermines and Galmoy (Irish Midlands), Ore Geology Reviews (2007), doi:10.1016/j.oregeorev.2006.06.001.

Balcon, J., 1981. Quelques idées sur les minéralisations plombo-zincifères dans les formations carbonatées de Belgique. Bulletin de la Société Belge de Géologie, 90: 9-61.

Banks, D.A., 1985. A fossil hydrothermal worm assemblage from the Tynagh lead-zinc deposit in Ireland. Nature, 313: 128-131.

Banks, D.A., and Russell, M.J., 1992. Fluid mixing during ore deposition at the Tynagh lead-zinc deposit in Ireland. European Journal of Mineralogy, 4: 921-931.

Banks, D.A., Boyce, A. J., Samson, I. M., 2002. Constraints on the origins of fluids forming Irish Zn-Pb-Ba deposits: evidence from the composition of fluid inclusions. Economic Geology, 97: 471–480.

Bàrdossy G. and Aleva, G.J.J., 1990. Lateritic bauxites. Amsterdam, Elsevier, 624p.

Bartholomé, P. and Gérard, E., 1976. Les gisements plombo-zincifères de la région d'Engis, province de Liège, Belgique. Annales des Mines de Belgique, 2: 901-917.

Beyer, F., 1995. Isotopen-Hydrogeologie der Aachener Thermalquellen. Geological Institute of the University of Cologne, Special Publication, 105: 1-123.

Billows, E., 1941. I minerali della Sardegna ed i loro giacimenti. Rendiconti Università di Cagliari: 331-335.

Bladh, K.W., 1982, The formation of goethite, jarosite, and alunite during the weathering of sulfide-bearing felsic rocks. Economic Geology, 77: 176-184.

Blanc-Valleton, M.M. and Thiry, M., 1983. Mineraux argilleux, paléoalterations, palèopaysages et sequences climatique. Exemple du Paléogène continental de France. In: Paquet, H. and Clauer, N. [eds.]. Sédimentologie et Géochimie de la Surface. Colloque a la memoire de George Millot, Acad. des Sciences, Paris: 199-216.

Boast, A.M., Coleman, M.L., and Halls, C., 1981. Textural and stable isotopic evidence for the genesis of the Tynagh base metal deposit, Ireland. Economic Geology, 76: 27-55.

Bodnar, R.J., 1993. Revised equation and table for determining the freezing point depression of H_2O-NaCl solutions. Geochimica et Cosmochimica Acta, 57: 683-684.

Bodnar, R.J. and Sterner, M.S., 1987. Synthetic fluid inclusions. In: Ulmer, G.C. and Barnes, H.L. [eds.], Hydrothermal Experimental Techniques, John Wiley & Sons, New York, NY, (USA): 423-457.

Bogacz, K., Dzulynski, S. and Haranczyk, C., 1970. Ore-filled hydrothermal karst features in the Triassic rocks of the Krakow-Silesian region. Acta Geologica Polonica, 20(2): 247-267.

Bogacz, K., Dzulynski, S., Haranczyk, C. and Sobczynski, P., 1972. Contact relations of the ore-bearing dolomite in the Triassic of the Krakow-Silesian region. Annales de la Societe Géologique de Pologne, 42(4): 347-372.

Bogacz, K., Dzulynski, S., Haranczyk, C. and Sobczynski, P., 1975. Origin of the ore-bearing dolomite in the Triassic of the Krakow-Silesian Pb-Zn ore district. Annales de la Societe Géologique de Pologne, 45(2): 139-155.

Boland, M.B., Clifford, J.A., Meldrum, A.H. and Poustie, A., 1992. Residual base metal and barite mineralization at Silvermines, Co. Tipperary, Ireland. In: Bowden, A.A., Earls, G., O'Connor, P.G., Pyne, J.F., [eds.], The Irish Minerals Industry 1980-1990. Irish Association for Economic Geology, Dublin: 247-260.

Boland, M.B., Kelly, J.G. and Schaffalitzky, C. 2003. The Shaimerden supergene zinc deposit, Kazakhstan: a preliminary examination. Economic Geology, 98(4): 787-795.

Boni, M., 2003. Non-sulfide zinc deposits: a new-(old) type of economic mineralization. In: M. Chiaradia [eds.]. SGA News Nr. 15, August 2003: 1 and 6-11.

Boni, M. and Large, D.E., 2003. Non-sulfide Zinc mineralization in Europe: an overview. Economic Geology, 98: 715-729.

Boni, M. and Large, D.E, 2005. Paleoweathering in Europe and nonsulfide Zn-ores: a neglected link. ESF Workshop on Nonsulfide Zn-Pb Deposits, 21th – 23th April, 2005, Iglesias, Italy, Abstract: 9-10.

Boni, M., Iannace, A., and Balassone, G., 1996. Base metal ores in the lower Palaeozoic of south-western Sardinia. In: Sangster, D.F., [eds.], Carbonate-hosted lead-zinc deposits, Society of Economic Geologists, 75th Anniversary Volume, Special Publication, 4: 18-28.

Boni, M., Gilg, H.A., Aversa, G. and Balassone, G., 2003. The "Calamine" of SW Sardinia (Italy): geology, mineralogy and stable isotope geochemistry of a supergene Zn-mineralization. Economic Geology, 98: 731-748.

Boni, M., Coppola, V., Dejonghe, L. and Fedele, L., 2005a. Willemite in the Belgian nonsulfide zinc deposits: a fluid inclusion study. Periodico di Mineralogia, 74: 87-100.

Boni M., Dinarès-Turell J. and Sagnotti, L., 2005b. A first attempt to paleomagnetic dating of non-sulfide Zn ores in SW Sardinia (Italy). Annals of Geophysics, 48

(2): 1-12.

Borg, G., Kärner, K., Buxton, M., Armstrong, R. and Merwe, Schalk W. v. d. M., 2003. Geology of the Skorpion supergene zinc deposit, southern Namibia. Economic Geology, 98: 749-771.

Borger, H., 1992. Paleotropical weathering on different rocks in Southern Germany. Zeitschrift fuer Geomorphologie, N.F., Supplementband, 91: 95-108.

Borger, H., 1997. Environmental changes during the Tertiary: the example of palaeoweathering residues in central Spain. In: Widdowson, M. [eds.], Palaeosurfaces: Recognition, Reconstruction and Palaeoenvironmental Interpretation, Geological Society, London, Special Publications, 120: 159 - 173.

Borkowska, I. and Czerwinski, J., 1973. On some mineralogical and textural features of granite regolith in the Karkonosze Mts. Studia Geographica, 33. 43-52.

Boulvais, P., Vallet, J-M., Esteoule-Choux, J., Fourcade, S. and Marineau, F., 2000. Origin of kaolinization in Brittany (NW France) with emphasis on deposits over granite: stable isotopes O, H constraints. Chemical Geology, 168: 211-223.

Boyce, A.J., Coleman, M.L. and Russell, M.J., 1983. Formation of fossil hydrothermal chimneys and mounds from Silvermines, Ireland. Nature, 306: 545-550.

Boyce, A.J., Fallick, A.E., Little, C.T.S., Wilkinson, J.J., and Everett, C.E., 1999. A hydrothermal vent tube worm in the Ballynoe baryte deposit, Silvermines, Ireland: Implications for timing and ore genesis. In: Stanley, C.J., et al. [eds.], Mineral deposits: Processes to processing, 5th Biennial SGA Meeting, 22th –25th August, London, Proceedings: 825-827.

Boyce, A.J., Little, C.T.S. and Russell, M.J., 2003. A new fossil vent biota in the ballynoe barite deposit, silvermines, Ireland evidence for intracratonic sea-floor hydrothermal activity about 352Ma. Economic Geology, 98(3): 649-656.

Boyle, D.R., 1994, Oxidation of massive sulfide deposits in the Bathurst mining camp, New Brunswick: Natural analogues for acid drainage in temperate climates. In: Alpers, C.N., and Blowes, D.W. [eds.], Environmental geochemistry of sulfide oxidation, American Chemical Society Symposium, Series 550: 535-550.

Breddin, H., 1932. Über die tiefsten Schichten der Aachener Kreide sowie eine Senone Einebnungsfläche und Verwitterungsrinde am Nordabfall des Hohen Venn. Zentralblatt für Mineralogie Abt. B, 12: 593-613.

Breddin, H. Brühl, H. and Dieler, H., 1963. Das Blatt Aachen-Nordwest der praktisch-geologischen Grundkarte 1:5000 des Aachen Stadtgebietes. Geologische Mitteilungen, 1: 251-428.

Brewster, D., 1822. New mineral from Aachen, near Altenberg. Edinburgh,

Philosophical Journal, 6: 184.

Brewster, D., 1824. Description of hopeite, a new mineral, from Altenberg, near Aix-la-Chapelle. Transactions of the Royal Society of Edinburgh, 10: 107.

Brigo, L., Kostelka, L., Omenetto, P., Schneider, H.J., Schroll, E., Schulz, O. and Strucl, I., 1977. Comparative reflections on four alpine Pb-Zn deposits. In: Klemm, D.D. and Schneider, H.J. [eds.], Time and strata-bound ore deposits, Berlin, Springer: 273-293.

Bristow, C.R., 1969. Kaolin deposits of the United Kingdom of Great Britain and Northern Ireland. Kaolin Deposits of the World. Europe XXIII International Geological Congress, 15: 275-288.

Bristow, C.R., 1977. A review of the evidence for the origin of the kaolin deposits in SW England. 8th International Kaolin Symposium and Meeting on Alunite, Madrid and Rome, Proceedings, 2: 1-19.

Bristow, C.R. and Exley, C.S., 1994. Historical and geological aspects of the China Clay industry of South-West England. Transactions of the Royal Geological Society of Cornwall, 21: 247-314.

Brochwicz-Lewinski W., Pozaryski W. and Tomczyk H., 1983. Ruchy przesuwcze w poludniowej Polsce w paleozoiku. Przeglad Geologiczny, 31(12): 651-658.

Brugger, J., McPhail, D.C., Wallace, M. and Waters, J., 2003. Formation of willemite in hydrothermal environments. Economic Geology 8: 919-935.

Budel J., 1982. Climatic geomorphology. [Fischer, L. and Busch, D., trans.] Princeton, NJ, Princeton University Press, 443p.

Bukowy, S., 1984. Struktury waryscyjskie regionu śląsko-krakowskiego. Geologia Prace Naukowe Uniwersytetu Slaskiego: 691p.

Bultynck, P., Geukens, F. and Smolderen, A., 2001. Permian lithostratigraphic units, the Malmédy graben (Belgium). In: Bultynck, P. and Dejonghe, P. [eds.], Guide to a Revised Lithostratigraphic Scale of Belgium. Geologica Belgica, 4: 105-106.

Burzewski, W., 1969. Strukturalne warunki jury olkusko-wolbromskiej jako brzegowe dla hydrodynamiki zloz naftowych niecki nidzianskiej. Polska. Akademia. Naukowe, Oddzial. Krakowie, Kom. Nauk Mineral., Prace Geologiczne: 61p.

Cairncross, B., 1997. The Otavi Mountain Land Cu-Pb-Zn-V deposits. Mineralogical Record, 28: 109-130 .

Carvalhosa, A.B., 1965. Contribução para o conhecimento geológica da região entra Portel and Ficalho (Alentejo). Serviços Geológicos de Portugal Memória, 11: 1-138.

Cauet, S., Weis, D., 1983. Lead isotope study of lead-zinc mineralization and its host sediments, Heure, Belgium: basis for a genetic model. Economic Geology, 78: 1011-1016.

Çerny, I., Scherer, J., and Schroll, E., 1982. Blei-Zink-Verteilungsmodell in stilliegenden Blei-Zink-Revieren der Karawanken. Archiv für Lagerstättenforschung der Geologischen Bundesanstalt, 2: 15–22.

Cesàro, G., 1886. Note sur une nouvelle face de la calamine. Bulletin de la Société Française de Minéralogie, 19: 242.

Cesàro, G., 1887. Note sur quelques minéraux (dont la willémite fibroradiée de Moresnet). Annales de la Société Géologique de Belgique, 14: 142-143.

Cesàro, G. 1898. Description des minéraux phosphatés, sulfatés et carbonatés du sol belge. Mémoires de l'Académie Royale des Sciences, des Lettres et des Beaux-Arts de Belgique, 53(4): 1-136.

Cesàro, G., 1908. Biréfringence de l'Adulaire, de la Sanidine, de la Thomsonite, de la Willémite, de la Microsommite et de la Thomsénolite. Académie Royale de Belgique, Bulletin de la Classe des Sciences, 7: 619-650.

Chang, L.L.J., Howie, R.A. and Zussmann, J., 1996. Rock-Forming Minerals. Non-Silicates: vol. 5B, Longman, London, 392p.

Church, S.E., Vaughn, R.B., Gent, C.A., and Hopkins, R.T., 1996. Lead-isotopic, sulphur isotopic, and trace-element studies of galena from the Silesia-Krakow Zn-Pb ores, polymetallic veins from Góry Świętokrzyskie Mts. and Mysków porphyry copper deposit, Poland. Prace Instytutu Geologicznego, 154: 139-155.

Ciuk, E. and Piwocki, M., 1979. Trzeciorzed w rejonie Zabkowic Slaskich. Biuletyn Instytutu Geologicznego, 320: 27-56.

Clauer, N. and Chaudhuri, S., 1992. Isotopic signatures of sedimentary rocks. Lecture Notes in Earth Sciences 43, Springer, Berlin: 529.

Clifford, J.A., Ryan, P. and Kucha, H., 1986. A review of the geological setting of the Tynagh orebody, Co. Galway. In: Andrew, C.J., Crowe, R.W.A., Finlay, S., Pennell, W.M. and Pyne, J.F. [eds.], Geology and Genesis of Mineral Deposits in Ireland, Irish Association for Economic Geology: 419-439.

Combes, P.J. and Peybernes, B., 1996. Succession des facies, mise en place des bauxites et structuration des Pyrenees au Cretace inferieur. Comptes Rendus, Academie des-Sciences, Serie II: Sciences de la Terre et des Planetes, 322(8) : 669-676.

Combes, P.J., Peybernes, B. and Leyreloup, A.F., 1998. Alterites and bauxites as indicators of the European and Iberian margins of western Pyrenees during Upper Jurassic-Lower Cretaceous, west of the Ossau valley (Pyrenees-Atlantiques, France). Comptes Rendus de l' Academie de Sciences, Serie IIa: Sciences de la Terre et des Planetes, 327(4): 271-278.

Cooper, B.J., Gibbs, G.V. and Ross, F.K., 1981. The effects of heating and dehydration on the crystal structure of

hemimorphite up to 600°C. Zeitschrift für Kristallographie, 156: 305-321.

Coppola, V., Boni, M., Gilg, H.A., Balassone, G. and Dejonghe, L. 2007. The "calamine" nonsulfide Zn–Pb deposits of Belgium: Petrographical, mineralogical and geochemical characterization. Ore Geology Reviews (2007), doi:10.1016/j.oregeorev.2006.03.005.

Cunningham, M.J.M., Densmore, A.L., Allen, P.A., Phillips, W.E.A., Bennett, S.D., Gallangher, K. and Carter, A., 2003. Evidences for post-early Eocene tectonic activity in southern Ireland. Geological Magazine, 140: 101-118.

Czajka, K., 1991. Geochemia złóż rud Zn-Pb w niece bytomskiej. Rudy i Metale, 36(3): 107-112.

Dejonghe, L., 1990. Présence de gersdorffite et de nickeline dans le filon plombo-zincifère de Bleiberg (Belgique). Bulletin de la Société Belge de Géologie, 99: 93-96.

Dejonghe, L., 1998. Zinc-lead deposits of Belgium. Ore Geology Reviews, 12: 329-354.

Dejonghe, L. and Jans, D., 1983. Les gisements plombo-zincifères de l'Est de la Belgique. Chronique de la Recherche Minière, 470: 3-24.

Dejonghe, L. and Boni, M., 2005. The "Calamine-type" zinc-lead deposits in Belgium and West Germany: a product of Mesozoic palaeoweathering processes. Geologica Belgica, 8(3): 3-14.

Dejonghe, L., Ladeuze, F. and Jans, D., 1993. Atlas des gisements plombo-zincifères du Synclinorim de Verviers (Est de la Belgique). Mémoires pour servir à l'Explication des Cartes Géologiques et Miniére de Belgique, 33: 1-483.

de Launay, L., 1913. Traité de Métallogenie, Béranger, vol 3: 934p.

de Magnée, I., 1967. Contribution à l'étude génétique des gisements belges de plomb, zinc et barytine. Economic Geology, Monograph, 3: 255-266.

Demek, J., 1982. Zarovnane povrchy Ceske vysociny. Geomorfologicka konference, Univerzita Karlova, Praha: 37-46.

Demoulin, A., 1995. L'Ardenne bouge toujours. Néotectonique du massif ardennais. In: Demoulin, A. [eds.], L'Ardenne: Essai de Géographie Physique. Hommage au Professeur Pissart, Département de Géographie Physique et du Quaternaire, Université de Liège: 110-135.

Demoulin, A., 2003. Paleosurfaces and residual deposits in Ardenne-Eifel: historical overview and perspectives. Géologie de la France, 1: 17-21.

De Vivo, B., Maiorani, A., Perna, G., and Turi, B., 1987. Fluid inclusion and stable isotope studies of calcite, quartz and barite from karstic caves in the Masua mine, south-western Sardinia, Italy. Chemie der Erde, 46: 259-273.

De Wijkerslooth, P., 1949. Die Blei-Zink-Formation Süd-Limburgs (Holland) und ihr

mikroskopisches Bild. Mededelingen Geol. Stichting, 3 (nieuwe serie): 83-102.

Di Colbertaldo, D., 1967. Il giacimento piombo-zincifero di Raibl in Friuli (Italia). International Geology Congress, 18th, London, 1948, Proceedings: 125.

Doyle, M., Morrissey, C. & Sharp, G., 2003. The Las Cruces orebody, Seville Province, Andalucia, Spain. In: Kelly, J.C., Andrew, C.J., Ashton, J.H., Boland, M.B., Earls, G., Fusciardi, L. & Stanley, G. [eds.]. Europe's Major Base Metal Deposits, Irish Association for Economic Geology: 381-389.

Dubinska, E., 1986. Nickel-bearing ferric analogue of montmorillonite from weathering crust at Szklary near Zabkowice Slaskie (Lower Silesia). Archiwum Mineralogoczne, 41(2): 35-47.

Dubinska, E., Sakharov, B.A., Kapron, G., Bylina, P. and Kozubowski, J.A., 2000. Layer silicates from Szklary (Lower Silesia): from ocean floor metamorphism to continental chemical weathering. Geologica Sudetica, 33(2): 85-106.

Duchesne, J.C., Rouhart, A., Schoumaker, C. and Dillen, H., 1983. Thallium, nickel, cobalt, and other trace elements in iron sulfides from Belgian lead-zinc vein deposits. Mineralium Deposita, 18: 303-313.

Dupuis, C., 1992. Mesozoic kaolinized giant regoliths and Neogene halloysitic cryptokarsts: two stricking paleoweathering types in Belgium. In: Schmitt, J.M. and Gall Q. [eds.], Mineralogical and Geochemical Records of Paleoweathering. École des Mines de Paris (ENSMP), Mémoire des Sciences de la Terre. 18 : 61-68.

Dupuis, C., Charlet, J.M., Dejonghe, L. and Thorez, J., 1996. Reconnaissance par carottage des paléoaltérations kaolinisées mésozoiques de la Haute Ardenne (Belgique). Le sondage de Transinne (1894E-495): premiers résultats. Annales de la Société Géologique de Belgique, 119: 91-109.

Dupuis, C., Nicaise, D., De Putter, T., Perruchot, A., Demaret, M. and Roche, E., 2003. Miocene cryptokarsts of Entre-Sambre-et-Meuse and Condroz plateaus. Paleoenvironment, evolution and weathering processes. Géologie de la France, 1: 27-31.

Dyjor, S., 1986. Evolution of sedimentation and paleogeography of nearfrontiers areas of the Silesian part of the Parathethys and the Tertiary Polish-German Basin. Geologia, 12(3): 7-23.

Eden, M.J. and Green, C.P., 1971. Some aspects of granite weathering and tor formation. Geografiska Annaler, Series A: Physical Geography, 53(2): 92-99.

Effenberger, H., Mereiter, K. and Zemann, J., 1981. Crystal structure refinement of magnesite, calcite, rhodochrosite, siderite, smithsonite and dolomite, with discussion of some aspects of the stereochemistry of calcite-type carbonates. Zeitschrift für

Kristallographie, 156: 223-243.

Eikert, F. 1971. Budowa geologiczna podpermskiego podloza pólnocno-wschodnim obrežezenia Górnośląkiego Zaglębia Węglowego. Prace Instytutu Geologicznego, 66: 77.

El Samani, Y., Touray, J.C., Pouit, G. and Guyot, G., 1986. La minéralisation en Zn-Cu-Mn-Ba d'Abu Samar et les indices de la plaine d'Allaikabeib (Soudan): des accumulations métallifères métamorphisées d'origine exhalative- sédimentaire. Chroniques Reserches Minières, 483: 3-18.

Elvhage, C. and Lidmar-Bergström, K., 1987. Some working hypotheses on the geomorphology of Sweden in the light of a new relief map. Geografiska Annaler, Series A, Physical Geography, 69: 343-358.

Ertus, R., Dupuis, C. and Trauth, N., 1989. Un nouveau type d'accumulation minérale de surface par épigénie d'altération météorique: halloysitisation sous couverture dans un karst sur calcaire silicifié (Belgique). Comptes Rendus de l'Académie des Sciences (Paris), 309: 595-601.

Esquevin, J., 1957. Sur la composition minéralogique des moresnétites et l'existence probable d'une novelle phyllite zincifère. Comptes Rendus de l'Académie des Sciences (Paris), A/3150, 4022.

Everett C.E., Wilkinson, J.J., and Rye, D.M., 1999a. Fracture-controlled fluid flow in the lower Palaeozoic basement rocks of Ireland: implications for the genesis of Irish-type Zn-Pb deposits. In: McCaffrey, K.G.W., Lonergan, L. and Wilkinson, J.J. [eds.], Fractures, fluid flow and mineralization. Geological Society, London, Special Publications, 155: 247-276.

Everett, C.E., Wilkinson, J.J., Boyce, A.J., Ellam, R.M., Fallick, A.E., and Gleeson, S.A., 1999b. The genesis of Irish-type Zn-Pb deposits: characterisation and origin of the principal ore fluid. In: Stanley, C.J. [eds.], Mineral deposits: Processes to processing, 5th Biennial SGA Meeting, 22th –25th August, London, Proceedings: 845-848.

Falcon-Lang, H.J., 1999. The Early Carboniferous (Courceyan–Arundian) monsoonal climate of the British Isles: evidence from growth rings in fossil woods. Geological Magazine, 136(2): 177-187.

Faure, G., 1986. Principles of Isotope Geology, 2nd Ed., John Wiley and Sons [eds.], New York: 589p.

Felder, W.M., 1975. Lithostratigrafie van het Boven-Krijt en het Dano-Montien in Zuid-Limburg en het aangrenzende gebied. In: W.H. Zagwijn and C.J. Van Staalduinen [eds.], Toelichting bij de geologische overzichtskaarten van Nederland. Rijksgeologische Dienst Haarlem: 63-75.

Ferreira, A. B., 1951. Gisement de calamine et smithsonite du Sud du Portugal. In: Agard, J., et al [eds.], International Geological Congress: report of the 18th Session, Great Britain, London, 1948 – Part

VII: Symposium and Proceedings of section E: The geology, paragenesis and reserves of the ores of lead and zinc: 249-250.

Field, C.W., Fifarek, R.H., 1985. Light stable isotope systematics in the epithermal environment. Reviews in Economic Geology, 2: 99–128.

Fransolet, A.M. and Bourguignon, P., 1975. Données nouvelles sur la Fraipontite de Moresnet (Belgique). Bulletin de la Société Française de Minéralogie, 98: 235-244.

Frondel, C., 1972. The minerals of Franklin and Sterling Hill - a checklist. Wiley Interscience, New York: 94p.

Frondel, C. and Baum, J.L., 1974. Structure and mineralogy of the Franklin zinc-iron-manganese deposit, New Jersey. Economic Geology, 69: 157-180.

Ghysel, P., Geukens, F., Laloux, M. and Hance, L., 2000. Carte géologique de Wallonie à 1:25000, Gemmenich-Botzelaar, Henri Chapelle-Raeren, Petergensfeld-Lammersdorf.

Gilg, H.A., 2000. D-H evidence for the timing of kaolinization in Northeast Bavaria, Germany. Chemical Geology, 170: 5-18.

Gilg, H.A., 2003. Ein Beitrag zur Isotopen-geochemie von Tonmineralien und Tonen. Habilitationschrift. Fakultät Chemie, Technische Universität München.

Gilg, H.A. and Boni, M., 2004. Stable isotope studies on Zn and Pb carbonates: their role in mineral exploration of non-sulphide deposits. SEG Conference, Perth WA, 27th September – 1st October, 2004, Proceedings: 361-365.

Gilg, H.A., Struck, U., Vennemann, T. and Boni, M., 2003. Phosphoric acid fractionation for smithsonite and cerussite between 25 and 72 °C. Geochimica et Cosmochimica Acta, 67: 4049-4055.

Gilg, H.A., Boni, M., Hocleitner, R. and Struck, U., 2007a. Stable isotope geochemistry of carbonate minerals in supergene oxidation zones of Zn–Pb deposits. Ore Geology Reviews: doi:10.1016/j.oregeorev.2007.02.005

Gilg, H. A., Krüger, Y., Stoller, P., Frenz, M., Boni, M. and Ziemann, M., 2007b. Temperatures in sulfide oxidation zones: microthermometry of monophase aqueous fluid inclusions and stable isotope systematics. European Current Research on Fluid Inclusions (ECROFI-XIX) University of Bern, Switzerland, 17th -20th July, 2007: 130.

Głazek J., 1989. Paleokarst of Poland. In: Paleokarst, a systematic and regional review, Elsevier, Amsterdam: 77-105.

Goldstein, R.H., 2001, Fluid inclusions in sedimentary and diagenetic systems: Lithos, 55: 159-193.

Goldstein, R.H. and Reynolds, T.J., 1994. Systematics of fluid inclusions in diagenetic minerals. Society for Sedimentary Geology, Short Course, 31: 87-121.

Gorecka, E., 1993. Geological setting of the Silesian-Krakow Zn-Pb deposits.

Geological Quarterly, 37(2): 127-146.

Götte, T. and Richter, D.K., 2004. Quantitative high-resolution cathodoluminescence spectroscopy of smithsonite. Mineralogical Magazine 68: 199-207.

Graham, J.R., 1983. Analysis of the Upper Devonian Munster Basin, an example of a fluvial distributary system. In: Collinson, J. D. & Lewin, J. [eds.], Modern and Ancient Fluvial Systems, International Association of Sedimentologists, Special Publication, 6: 473-483.

Grandin, G. and Thiry, M., 1983. Les grandes surfaces continentales tertiaires des régions chaudes. Succession des types d'alterations. Cahiers ORSTOM. Series Géologie, 13: 3-18.

Graulich, J.M., 1983. L'hydrologie thermale de Chaudefontaine. Bulletin de la Société Belge de Géologie, 92: 195-212.

Graulich, J.M., Dejonghe, L. and Cnudde, C., 1984. La définition du Synclinorium de Verviers. Bulletin de la Société Belge de Géologie, 93: 79-82.

Green, C.P., 1985. Pre-Quaternary weathering residuals, sediments and landform development: examples from southern Britain. In: Richards, K.S., Arnett, R.R., Ellis, S. [eds.], Geomorphology and Soils, London: 58-77.

Gregg, J.M., Johnson, A.W., Shelton, K.L., Somerville, I.D. and Wright, W., 2001. Dolomitization of the Waulsortian Limestone (Lower Carboniferous) in the Irish Midlands. Sedimentology, 48: 745-766.

Griffith, S.V., 1956. The Silvermines operation, Co. Tipperary, Ireland. Mining Magazine serialized March 1955 to January 1956: 137-150; 206-215; 277-282; 332-337.

Groves, I., Carman, C.E. and Dunlap, J.W., 2003. Geology of the Beltana willemite deposit, Flinders Ranges, South Australia: Economic Geology, 98: 797-818.

Gruszczyk, M., 1956. O wyksztalceniu i genezie slasko-krakowskich zloz cynkowo-olowianych. Biuletyn Instytutu Geologicznego, 90: 5-186.

Gruszczyk, H. and Wielgomas, L., 1990. Zinc and lead ores in the Silesia-Krakow Triassic. In: Osika, R. [eds.], Geology of Poland, Volume VI: Mineral Deposits, Publishing House Wydawnictwa Geologiczne, Warsaw: 172-183.

Grygar, T., Kral, R., Nekovarık, C. and Zelenka, P., 1997. Relics of laterites on the Letovice Crystalline Complex, Moravia. Journal of the Czech Geological Society, 42: 121-127.

Gussone, R., 1964. Untersuchungen und Betrachtungen zur Paragenese der Blei-Zink-Erzlagerstätten im Raume Aachen-Stollberg. Dissertation RWTH Aachen, Germany: 130p.

Gutiérrez-Elorza, M. and Gracia, F. J., 1997. Environmental interpretation and evolution of the Tertiary erosion surfaces in the

Iberian Range (Spain). In: Widdowson, M. [eds.], Paleosurfaces: recognition, reconstruction and paleoenvironmental interpretation, Geological Society, London, Special Publications, 120: 147-158.

Hall, A.M., 1985. Cenozoic weathering covers in Buchan, Scotland, and their significance. Nature, 315. 392-395.

Hall, A.M., 1986. Deep weathering patterns in north-east Scotland and their geomorphological significance. Zeitschrift fuer Geomorphologie, 30(4): 407-422.

Hall, A.M., 1987. Weathering and relief development in Buchan, Scotland. In: Gardiner, V. [eds.], International Geomorphology 1986 Part II. Wiley, Chichester: 991-1005.

Hall, A.M., Mellor, A. and Wilson, M.J., 1989. The clay mineralogy and age of deeply weathered rock in north-east Scotland. Zeitschrift fuer Geomorphologie, N.F., Supplementband, 72: 97-108.

Hance, L., Dejonghe, L., Ghysel, P., Laloux, M. and Mansy, J.L., 1999. Influence of heterogenous lithostructural layering in orogenic deformation in the Variscan Front Zone (eastern Belgium). Tectonophysics, 309: 161-177.

Harańczyk, F., 1981. Ontogeneza dolomitow kruszconosnych; Przeglad Geologiczny, 29(10): 513-518.

Harańczyk, F., Szostek, L., 1969. Remarks on some opinions dealing with features of "Trzebionka" zinc-lead ore deposits and the genesis of the Ore-bearing dolomite. Rudt Metale Nieżel, 14: 218-225.

Heijlen, W., Muchez, P., Banks, D.A. and Nielsen, P., 2000. Origin and evolution of synsedimentary, syn- and posttectonic high salinity fluid at the Variscan thrust front Belgium. Journal of Geochemical Exploration, 69-70, 149-152.

Heijlen, W., Muchez, P. and Banks, D.A., 2001. Origin and evolution of high-salinity, Zn-Pb mineralising fluids in the Variscides of Belgium. Mineralium Deposita, 36: 165-176.

Heijlen, W., Muchez, Ph., Banks, D.A., Schneider, J., Kucka, H. and Keppens. E., 2003. Carbonate-hosted Zn-Pb deposits in Upper Silesia, Poland: origin and evolution of mineralizing fluids and constraints on genetic models. Economic Geology, 98: 911-932.

Herch, A., 2000. The thermal springs of Aachen/Germany - what Charlemagne did not know. Environmental Geology, 39: 437-447.

Herrington R.J., Zaykov, V.V., Maslennikov, V.V., Brown, D. and Puchkov, V.N., 2005. Mineral Deposits of the Urals and Links to Geodynamic Evolution. In: Hedenquist, J.W., Thompson, J.F.H., Goldfarb, R.J. and Richards, J.P. [eds.], Earth environments and processes, Society of Economic Geologists, 100th Anniversary Volume, Special Publication: 1069-1095.

Herrington, R., Boni, M., Skarpelis, N. and Large, D.E, 2007. Paleoclimate, weathering and ore deposits – a European perspective. In: Andrew, C.J. et al. [eds.], Mineral deposits at the beginning of the 21st century, 9th Biennial SGA Meeting, 20th - 23th August, Dublin, Ireland, Proceedings: 1373-1376.

Hill, I.G., Worden, R.H. and Meighan, I.G., 2000. Geochemical evolution of a palaeolaterite: the Interbasaltic Formation, Northern Ireland. Chemical Geology, 166: 65-84.

Hillefors, A., 1985. Deep-weathered rock in western Sweden. Fennia, 163. 293-301.

Hitzman, M.W., 1995. Mineralization in the Irish Zn-Pb-(Ba-Ag) orefield. In: Anderson, K., Ashton, J., Earls, G., Hitzman, M., and Tear, S. [eds.], Irish Carbonate-hosted Zn-Pb Deposits, Guidebook Series, Society of Economic Geologists, 21: 25-61.

Hitzman, M. W. and Large, D.E., 1986. A review and classification of the Irish carbonate-hosted base metal deposits. In: Andrew, C.J., Crowe, R.W.A., Finlay, S., Pennell, W.M., and Pyne, J.F., [eds.], Geology and Genesis of Mineral Deposits in Ireland, Irish Association for Economic Geology, Dublin: 217-238.

Hitzman, M.W. and Beaty, D.W., 1996. The Irish Zn-Pb-(Ba) Orefield. In: Sangster, D.F. [eds.], Carbonate-hosted Lead-Zinc Deposits, Society of Economic Geologists, 75th Anniversary Volume, Special Publication, 4: 112-143.

Hitzman, M.W. and Beaty, D.W., 2003. The Irish Zn-Pb-(Ba-Ag) Orefield. In: Kelly, J., Andrew, C.J., Ashton, J., Boland, M., Earls, G., Fusciardi, L. and Stanley, G. [eds.], Europe's Major Base Metal Deposits, Irish Association for Economic Geology, Dublin: 499-531.

Hitzman, M.W., O'Connor, P., Shearley, E., Schaffalitzky, C., Beaty, D.W., Allan, J.R., and Thompson, T., 1992. Discovery and geology of the Lisheen Zn-Pb-Ag prospect, Rathdowney Trend, Ireland. In: Bowden, A., Earls, G., O'Connor, P., Pyne, J., [eds.], The Irish Minerals Industry 1980-1990, Irish Association for Economic Geology, Dublin: 227-246.

Hitzman, M.W., Reynolds, N.A., Sangster, D.F., Allen, C.R. and Carman, C., 2003. Classification, genesis, and exploration guides for non-sulfide zinc deposits. Economic Geology, 98: 685-714.

Hoefs, J., 1987. Stable Isotope Geochemistry, third edition, Springer-Verlag, Berlin: 241p.

Hughes, M., 1987, The Tsumeb orebody, Namibia, and related dolostone-hosted base metal ore deposits of central Africa. Unpublished Ph.D. thesis, Johannesburg, South Africa, University of Witswatersrand: 448p.

Hurlbut, C. S. Jr., 1957. Zincian and plumbian dolomite from Tsumeb, South-West Africa. American Mineralogist, 42: 798-803.

Ingwersen, G., 1990. Die sekundären

Mineralbildungen der Pb-Zn-Cu-Lagerstätte Tsumeb Namibia (Physikalisch -chemische Modelle). Dissertation Thesis, Universität Stuttgart: 233p.

Isaac, K.P., 1981. Tertiary weathering profiles in the plateau deposits of East Devon. Proceedings of the Geologists' Association, 92: 152-168.

Isaac, K.P., 1983. Tertiary lateritic weathering in Devon, England, and the Palaeogene continental environment of South-west England. Proceedings of the Geologists' Association, 94: 105-114.

Jahn, A., 1962. Geneza skałek granitowych. Czas. Geogr., 33: 19-44.

Jasienska, S., and Zabinski, W., 1972. Electron microprobe investigation of unusual zincian dolomite from the Warynski mine (Upper Silesia). Mineralogia Polonica, 3: 67-70.

Johnson, C.A., Rye, D.M. and Skinner, B.J., 1990. Petrology and stable isotope geochemistry of the metamorphosed zinc-iron-manganese deposit at Sterling Hill, New Jersey: Economic Geology, 85: 1133-1161.

Kamona, F., 1993, The carbonate hosted Kabwe Pb-Zn deposit, central Zambia: Unpublished Ph.D. dissertation, Aachen, Germany, Rheinisch-Westfalischen Technischen Hoschschule: 207p.

Kappler, P. and Zeeh, S. 2000. Relationship between fluid flow and faulting in the Alpine realm (Austria, Germany, Italy). Sedimentary Geology, 131: 147-162.

Kiersnowski, H. and Maliszewska, A., 1985. Coarse-clastic Rotliegendes sediments of the Siewierz -Olkusz region in the light of new data [Eng. Sum.]. Przeglad Geologiczny, 33 (4): 181-192.

Klaska, K.H., Eck, J.C. and Pohl, D., 1978. New investigation of willemite. Acta Crystallographica, 34: 3324-3325.

Klau, W. and Mostler, H.J., 1983. Alpine Middle and Upper Triassic Pb–Zn deposits. In: Kisvarsanyi, G., Grant, S.K., Pratt, W.P., Koenig, J.W. [eds.], International Conference on Mississippi Valley Type Lead-Zinc Deposits, University of Missouri-Rolla, Rolla, Missouri, Proceedings: 113-128.

Knight, F., 2000. The mineralogy, geochemistry and genesis of th secondary sulphide mineralisation of the Las Cruces deposit, Spain. Ph.D. Thesis, Univeristy of Wales, Cardiff.

Korber, E. and Zech, W., 1984. Zur Kenntniss tertiärer Verwitterungsreste und Sedimente in der Oberpfalz un ihrer Umgebung. Relief, Boden, Paläoklima, 3: 67-150.

Kotas A., 1982. Zarys budowy geologicznej Górnośląskiego Zagłębia Węglowego. Przew. LIV Zjazdu PTG Sosnowiec: 45-72.

Kozłowski A., 1994. A preliminary fluid inclusion model of the Silesian-Krakow Zn-Pb ores origin in Southern Poland. Berichte der Deutschen Mineraloschiscen Gesellschaft (Beiheft zur European Journal

of Mineralogy), 6(1): 153p.

Kozlowski A., 1995. Origin of Zn-Pb ores in the Olkusz and Chrzanów districts: a model based on fluid inclusions. Acta Geologica Polonica, 45(2): 83-141.

Kozlowski A., 2001. Fluid inclusions in ore-bearing dolomite, Silesian-Krakow area, Poland. In: Piestrzyński, A. [eds.], Mineral Deposits at the beginning of the 21st century, Joint 6th Biennial SGA-SEG Meeting, 26th - 29th August, Kraków, Poland, Proceedings: 141-144.

Kozlowski, A., Leach, D.L., and Viets, J.G., 1996. Genetic characteristics of fluid inclusions in sphalerite from the Silesian-Krakow ores, Poland. Prace Instytutu Geologicznego, 154: 73-83.

Kral, V., 1985. Zarovnane povrchy Ceske vysociny. Studie CSAV, 10.

Krokowski, J., 1984. Mesoskopowe studia strukturalne wosadach permsko-mezozzoicznych poludniowo-wschodniej czseci Wyzyny Slasko-Krakowskiej: Rocz. Pol. Tow. Geol., 54: 79-121.

Krzyczkowska-Everest, A., 1990. Petrographic characteristics of the Ore-bearing dolomites of the Goradzdza beds, from Olkusz-Boleslaw Region (South Poland). Prace Mineralogiczne, 81: 7-49.

Kubiniok, J., 1988. Kristallinvergrusung an Beispielen aus Südostaustralien und deutschen Mittelgebirgen. Kölner geographische Arbeiten, 48: 1-178.

Kucha, H., 2003. Mississippi Valley Type Zn – Pb deposits of Upper Silesia, Poland. In: Kelly, J.G., Andrew, C.J., Ashton, J.H., Boland, M.B., Earls, G., Fusciardi, L., Stanley, G. [eds.], Europe's Major Base Metal Deposits, Irish Association for Economic Geology, Dublin: 253-271.

Kucha, H., 2005. Oxysulfides, smithsonite-siderite and Fe-free smithsonite as indicators of conditions of formation of primary and supergene non-sulfide Zn-Pb deposits, Upper Silesia, Poland. ESF Workshop on Nonsulfide Zn-Pb Deposits, 21th - 23th April, 2005, Iglesias, Italy, Abstract: 24-25.

Kucha, H. and Czajka, K., 1984. Sulphide-carbonate relationships in Upper Silesian Zn-Pb deposits (Mississippi Valley type), Poland, and their genesis. Transactions of the Institution of Mining and Metallurgy, 93: B12-B19.

Kuhlemann, J., 1995. Zur Diagenese des Karawanken-Nordstammes (Österreich/ Slowenien): Spättriassische, epigenetische Blei-Zink-Vererzung und mitteltertiäre, hydrothermale Karbonat-zementation. Archiv für Lagerstättenforschung der Geologischen Bundesanstalt, 18: 57-116.

Kurek, S., 1988. Regularities in occurrence of Zn-Pb mineralization in sediments of the Upper Paleozoic, northeastern margin of USCB (abs.). Prace Instytutu Geologicznego, 7: 396-401.

Kutek, J. and Glazek, J., 1972. The Holy Cross area, central Poland, in the Alpine

Cycle. Acta Geologica Polonica, 22: 603-652.

Laloux, M., Geukens, F., Ghysel, P. and Hance, L., 2000. Carte et notice explicative de la carte géologique de Wallonie à 1:25.000. Feuilles Gemmenich-Botzelaar 35/5-6; Henri-Chapelle-Raeren 43/1-2; Petergensfeld-Lammersdorf 43/3-4. Ministère de la Région wallonne.

Land, L.S., 1983. The application of stable isotopes to studies of the origin of dolomite and to problems of diagenesis of clastic sediments. In: M.A. Arthur [eds.], Stable isotopes in sedimentary geology, Society for Sedimentary Geology, Short Course, 10: 1-22.

Large, D.E, 2001. The geology of non-sulphide zinc deposits - an overview. Erzmetall, 54: 264-276.

Large, D.E., Schaeffer, R. and Hohndorf, A., 1983. Lead-isotopes data from selected galena occurrences in the north Eifel and north Sauerland, Germany. Mineralium Deposita, 18: 235-243.

Larter, R.C.L., Boyce, A.J. and Russell, M.J., 1981. Hydrothermal pyrite chimneys from the Ballynoe baryte deposit, Silvermines, County Tipperary, Ireland. Mineralium Deposita, 16: 309-318.

Leach, D.L. and Viets, J.G., 1992. Comparison of the Krakow-Silesian Mississippi Valley-type district, southern Poland, with Mississippi Valley-type districts in North America. USGS, Open-File Report OF/92-704: 72p.

Leach, D.L., and Sangster, D.F. 1993. Mississippi Valley-type lead-zinc deposits. In: Kirkham, R.V., Sinclair, W.D., Thorpe, R.I. and Duke, J.M. [eds.], Mineral deposit modelling, Geological Association of Canada, Special Paper, 40: 289-314.

Leach, D.L., Viets, J.G., and Gent, C.A., 1996a. Sulphur isotope geochemistry of ore and gangue minerals from the Silesian-Krakow Mississippi Valley-type oreore district, Poland: Prace Instytutu Geologicznego, 154: 123-137.

Leach, D.L., Viets, J.G., and Powell, J.W., 1996b. Textures of ores from the Silesian-Krakow zinc-lead deposits, Poland: Clues to the ore-forming environment. Prace Instytutu Geologicznego, 154: 37-50.

Leach, D.L., Viets, J.G., Kozlowski, A. and Kibitlewski, S., 1996c. Geology, geochemistry, and genesis of the Silesia-Krakow zinc-lead district, southern Poland. In: Sangster, D. F., [eds.], Carbonate-hosted lead-zinc deposits, Society of Economic Geologists, 75th Anniversary Volume, Special Publication, 4: 144-170.

Leach, D.L., Bradley, D., Lewchuk, M.T., Symons, D.T., de Marsily, G. and Brannon, J., 2001. Mississippi Valley-type lead-zinc deposits through geological time: implications from recent age-dating research. Mineralium Deposita, 36: 711-740.

Leach, D., Bechstädt, T., Boni, M. and Zeeh,

S., 2003. Triassic-hosted MVT Zn–Pb ores of Poland, Austria, Slovenia and Italy. In: Kelly, J.G., Andrew, C.J., Ashton, J.H., Boland, M.B., Earls, G., Fusciardi, L., Stanley, G. [eds.], Europe's Major Base Metal Deposits, Irish Association for Economic Geology, Dublin: 169-213.

Leavens, P.B., and Patton, J.D., 2000. The Desert View mine, San Bernardino Mountains, California: A possible intermediate between Långban, Sweden and Franklin, New Jersey. San Bernardino County Museum Association Quarterly, 47: 17-21.

Lee, M.J., and Wilkinson, J.J., 2002. Cementation, hydrothermal alteration, and Zn-Pb mineralization of carbonate breccias in the Irish Midlands: Textural evidence from the Cooleen zone, near Silvermines, County Tipperary. Economic Geology, 97: 653-662.

Legrand, R., 1968. Le Massif du Brabant. Mémoires pour servir à l'Explication des Cartes géologiques et minières de la Belgique, 9: 148.

Lespineux, G., 1905. Etude génésique des Gisements miniers des bords de la Meuse et de l'Est de la province de Liège. Congrès International Mines, Métallurgie, Mécanique et Géologie Appliquée, Liège 1905, Vaillant-Carmanne: 1-27.

Levy, M., 1843. Description de plusieurs espèces minérales appartenant à la famille du zinc. Annales des Mines, Paris, 4ème série/4: 507-520.

Libowitzky, E., Kohler, T., Armbruster, T. and Rossman, G.R., 1997. Proton disorder in dehydrated hemimorphite; IR spectroscopy and X-ray structure refinement at low and ambient temperatures. European Journal of Mineralogy, 9: 803-810.

Lidmar-Bergström, K., 1995. Relief and saprolites through time on the Baltic Shield. Geomorphology, 12: 45–61.

Lidmar-Bergström, K., Olsson, S. and Olvmo, M., 1997. Palaeosurfaces and associated saprolites in southern Sweden. In: Widdowson, M. [eds.], Palaeosurfaces: Recognition, Reconstruction and Palaeoenvironmental Interpretation, Geological Society, Special Publication, 120: 95-124.

Lombaard, A.F., Günzel, A., Innes, J., and Krüger, T.L., 1986. The Tsumeb lead-copper-zinc-silver deposit, south west Africa/Namibia. In: Anhaeusser, C.R., and Maske, S., [eds.], Mineral deposits of southern Africa, Geological Society of South Africa, 2: 1761-1787.

Lundqvist, J., 1985. Deep-weathering in Sweden. Fennia, 163: 287-292.

Machel, H.G., Mason, R.A., Mariano, A.N. and Mucci, A., 1991. Causes and emission of luminescence in calcite and dolomite. In: Baker, C.E. and Kopp, O.C. [eds.], Luminescence Microscopy and Spectroscopy – Qualitative and Quantitative applications. Society for Sedimentary

Geology, Short Course, 25: 9-25.

Markham, N.L., 1960. The willemite-hemimorphite relationship. Economic Geology, 55: 844-847.

Marumo, F. and Syono, Y., 1971. The crystal structure of Zn_2SiO_4-II, a high-pressure phase of Willemite. Acta Cristallographica, section B27, part 10: 1868-1870.

McDonald, W.S. and Cruickshank, D. W.J., 1967. Refinement of the structure of the hemimorphite. Zeitschrift für Kristallographie, 124: 180-191.

McMurdie, H.F., Morris, M.C., Evans, E.H., Paretzkin, B., Wong-Ng, W. and Hubbard C.R., 1986. Standard X-ray diffraction powder patterns from the JCPDS Research Associationship Powder Diffraction, 1(3): 265-275.

McPhail, D.C., Summerhayes, E., Welch S. and Brugger J., 2004. The geochemistry and mobility of zinc in the regolith. In: Roach, I.C. et al. [eds.], Advances in Regolith, CRC LEME, Canberra: 287-291.

Melchiorre, E.B. and Williams, P.A., 2001. Stable isotope characterization of the thermal profile and subsurface biological activity during oxidation of the Great Australia deposit, Cloncurry, Queensland, Australia. Economic Geology, 96: 1685-1693.

Melchiorre, E.B. and Enders, M.S., 2003. Stable isotope geochemistry of copper carbonates at the Northwest Extension deposit, Morenci district, Arizona: implications for conditions of supergene oxidation and related mineralization. Economic Geology, 98: 607-621.

Melchiorre E.B., Criss R.E., and Rose T.P., 1999. Oxygen and carbon isotope study of natural and synthetic malachite. Economic Geology, 94**:** 245-259.

Melchiorre E.B., Criss R.E., and Rose T.P., 2000. Oxygen and carbon isotope study of natural and synthetic azurite. Economic Geology, 95: 623-630.

Melon, J., Bourguignon, P. and Fransolet, A.M., 1976. Les Minéraux de Belgique. Lelotte, Dison: 280p.

Michael, R., 1913. Die Geologie des ober-schlesischen Steinkohlebezirkes. Festschrift XII Allgemeinen Deutschen Bergmannstage in Breslau, Berlin, 1: 1-415.

Migoń, P., 1997a. Tertiary etchsurfaces in the Suedetes Mountains, SW Poland: a contribution to the pre-Quaternary morphology of Central Europe In: Widdowson, M. [eds.], Palaeosurfaces: Recognition, Reconstruction and Palaeoenvironmental Interpretation. Geological Society, Special Publication, 120: 187-202.

Migoń, P., 1997b. Palaeoenvironmental significance of grus weathering profiles: a review with special reference to northern and central Europe. Proceedings of Geological Association, 108: 57-70.

Migoń, P., 2003. Paleoweathering record and paleosurfacesin the Bohemian Massif,

Central Europe and Fennoscandian Shield, Northern Europe. A basis for East-West comparisons. Géologie de la France, 1: 53-56.

Migoń, P. and Lidmar-Bergström, K., 2001. Weathering mantles and their significance for geomorphological evolution of central and northern Europe since the Mesozoic. Earth Science Reviews, 56: 285-324.

Migon, P. and Lidmar-Bergström, K., 2002. Deep weathering through time in central and northwestern Europe: problems of dating and interpretation of geological record. Catena, 49: 25-40.

Mochnacka, K. and Sass-Gustkiewicz, M., 1981. The metasomatic zinc deposits of the Pomorzany Mine (Krakow-Silesian ore district, Poland). Annales de la Societe Geologique de Pologne, 51(1-2): 133-151.

Molina-Ballesteros, E., García Talegón, J. and Vicente Hernández M.A., 1997. Palaeoweathering profiles developed on the Iberian Hercynian Basement and their relationship to the oldest Tertiary surface in central and western Spain. In: Widdowson, M. [eds.], Palaeosurfaces: Recognition, Reconstruction and Palaeoenvironmental Interpretation, Geological Society, London, Special Publication, 120: 175-185.

Monteiro, L.V.S, Bettencourt, J.S., Spiro, B., Graça, R., de Oliveira, T.L., 1999. The Vazante zinc mine, Minas Gerais, Brazil: Constraints on willemitic mineralization and fluid evolution. Exploration Mining Geology, 8: 21-42.

Monteiro, L.V.S., Bettencourt, J.S., Spiro, B., Graça, R. and de Olivera, T.F., 2000. The Vazante zinc mine, Minas Gerais, Brazil: constraints on willemitic mineralization and fluid evolution. Exploration and Mining Geology, 8: 21-42.

Monteiro, L.V.S., Bettencourt, J.S., Juliani, C. and de Oliveira, T.F., 2006. Geology, petrography, and mineral chemistry of the Vazante non-sulfide and Ambrósia and Fagundes sulfide-rich carbonate-hosted Zn–(Pb) deposits, Minas Gerais, Brazil. Ore Geology Reviews, 28(2): 201-234.

Moore, J.M., 1972. Supergene mineral deposits and physiographic development in southwest Sardinia, Italy. Transactions Institution Mining and Metallurgy, Section B, Applied Earth Science, 71: B59–B66.

Moore, J.M., 1975. Fault tectonics at Tynagh mine, Ireland. Transactions Institution of Mining and Metallurgy, Section B, Applied Earth Science, 84: B141-145.

Morrissey, C.J., 1970. The mineralogy, structure and origin of the lead-zinc-copper residual orebody at Tynagh Co. Galway, Ireland. Unpublished Ph.D Thesis, London University.

Morrissey, C.J. and Whitehead, D., 1971. Origin of the Tynagh residual orebody. 9th Commonwealth Mining and Metallurgical Congress 1969, Institution of Mining and Metallurgy, Proceedings: 1-15.

Moryc, W., 1971. The Triassic of the foreland

of central Carpathians. Annales Societatis Geologorum Poloniae, 67: 429-437.

Motyka, J., Pulido-Bosch, A., Borczak, S. and Gisbert, J., 1998. Matrix hydrogeological properties of Devonian carbonate rocks of Olkusz (Southern Poland). Journal of Hydrology, 211: 140-150.

Muchez, P., Slobodnik, M., Viaene, W. and Keppens, E., 1994. Mississippi Valley-type Pb-Zn mineralization in Eastern Belgium: indications for gravity-driven flow. Geology, 22: 1011-1014.

Narkiewicz, M., 1993. Cathodoluminescence study of the ore-bearing and related dolostones in the Triassic of the Silesian-Krakow district. Geological Quarterly, 37(2): 265-278

Nieć M., 1980. Model of formation of Cracovian-Silesian type zinc-lead deposit at Boleslaw near Olkusz, Poland. In: Ridge, J.D. [eds.], 5th quadrennial IAGOD symposium on the genesis of ore deposits, Snowbird, Utah, 17th August 1978, Proceedings: 445-457.

Nieć, M., Blanda, B., and Niedzielski, B., 1993. Zinc-lead ore deposit in Lower Triassic (Roethian) dolomites at Bolesław (Olkusz region, Poland). Geological Quarterly, 37(2): 157-174.

Nielsen, P., Swennen, R. and Keppens, E., 1994. Multiplestep recrystallization within massive ancient dolomite units: an example from the Dinantian of Belgium. Sedimentology, 41: 567-584.

Niskiewicz, J., 1967. Geological structure of the Szkalry Massif (Lower Silesia). Rocznik PTG, 37: 387-416.

Niskiewicz, J. 2000. The Szklary Massif nickel-bearing weathering cover. Geologica Sudetica, 33(2): 107-130.

Ohmoto, H., Rye, R.O., 1979. Isotopes of sulfur and carbon. In: Barnes, H.L. [eds.] Geochemistry of Hydrothermal Ore Deposits, 2nd edition, Wiley, New York: 509-567.

O'Neil J.R., Clayton R.N., and Mayedak, T.K., 1969. Oxygen fractionation in divalent metal carbonates. Journal of Chemistry Physics, 51: 5547-5558.

Osman, A.E.M., 1989. Smithsonite in the oxidation zone of the Upper Silesia Zn-Pb ore deposits (Orzel Bialy Mine, Bytom Area), Poland. Mineralogia Polonica, 20: 57-68.

Ostrowicki, B. 1965. Nickel minerals of the weathering zone of serpentinites at Szklary (Lower Silesia). Prace Mineralogiczne, Polska Akademia Naukowe, 1: 1-92.

Palache, C., Berman, H. and Frondel, C., 1951. The System of Mineralogy of James Dwight Dana and Edward Salisbury Dana. Yale University, Volume II: 539p.

Panek, S. and Szuwarzynski, M., 1975. Fossil sinkholes with galena mineralization in the vivinity of Chrzanow (Krakow-Silesian region). Rocznik PTG, 45: 177-189.

Panek, S. and Szuwarzynski, M., 1976. O przedtortonskiej dolonie erozyjnej

wypelnionej osadami trzeciorzedowymi w okolicach Chrzanowa (translated title: *A pre-Tortonian valley with Tertiary fill near Chrzanow*). Annales de la Societé Géologique de Pologne, 46(4): 503-523.

Peace, W.M. and Wallace, M.W., 2000. Timing of mineralization at the Navan Zn-Pb deposit: a post-Arundian age for Irish mineralization. Geology, 287: 711-714.

Petrascheck, W., 1918. Das Alter der polnischen Erze: Kaiser Kgl. Geol. Reichs-Anst. Verh.: 11p.

Philips, W.E. and Sevastopulo, G.D., 1986. The structural and stratigraphic setting of Irish mineral deposits. In: Andrew, C.J., Crowe, R.W.A., Finlay, S., Pennell, W.M., and Pyne J.F. [eds.], Geology and genesis of Mineral Deposits in Ireland. Irish Association for Economic Geology, Dublin: 1-30.

Philips, W.E.A., Flegg, A.M. and Anderson, T.B., 1979. Strain adjacent to the Iapetus suture in Ireland. In: Harris, A.L., Holland, C.H. and Leake, B.E. [eds.], The Caledonian of British Isles - reviewed. Geological Society, London, Special Pubblication, 8: 257-262.

Philox, M.E., 1984. Lower Carboniferous litho- stratigraphy of the Irish Midlands. Irish Association for Economic Geology, Dublin: 89p.

Piekarski, K., 1965. Wplyw wietrzenia dolnojurajskiego na zloza rud Zn i Pb w triasie slasko-krakowskim. Przeglad Geologiczny, 2: 54-59.

Pouchou, J.L. and Pichoir, F., 1991. Quantitative analysis of homogeneous or stratified micro-volumes applying the model "PAP". In: Heinrich, K.F.J. and Newbury, D.E. [eds.], Electron Probe Quantification, Plenum Press, New York: 31-75.

Pough, F.H., 1941. Occurrence of willemite. American Mineralogist, 26: 92-102.

Power, E.T. and Smith, B.J., 1994. A comparative study of deep weathering and weathering products: case studies from Ireland, Corsica and Southeast Brazil. In: Robinson, D.A., Williams, R.B.G. [eds.], Rock Weathering and Landform Evolution, Wiley, Chichester: 21-40.

Przenioslo, S., 1974. Cynk i olow w utworach weglanowych triasu rejonu zawierciańskiego (translated title: *Zinc and lead in Triassic carbonate rocks of the Zawiercie area*). Biuletyn Instytutu Geologiczny, 278: 115-199.

Przenioslo, S., 1976. An outline of the metallogeny of zinc and lead ores in the Silesian-Cracovian region, In: Fedak, J., [eds.], The current metallogenic problems of central Europe, Warsaw, Wydawnictwa Geologiczne: 367-384.

Quesnel, F., 2003. Paleoweathering and paleosurfaces from northern and eastern France to Belgium and Luxembourg: geometry, dating and geodynamic implications. Géologie de la France, 1: 95-104.

Quinif, Y. and Vandycke, S., 2001. Karstic phenomena in the Han-sur-Lesse region, Rochefort, Belgium. Bulletin d'information des Géologues du Bassin de Paris, 38: 6-19.

Radwanek-Bak, B., 1982. Zasieg glebokosciowy strefy utlenienia w zlozu rud Zn-Pb Boleslaw. Rudy i Metale Niezelazne, 27: 220-225.

Radwanek-Bak, B., 1983. Charakterystyka petrograficzna utlenionych rud cynku ze zloz obszaru Boleslawia i Olkusza. Rocznik Polskie Towarzystwo Geologiczne, 53: 235-254.

Radwanski, A., 1968. Transgresja dolnego tortonu na obszarze wyzyny Miechowskiej i Krakowskiej (translated title: *Lower Tortonian transgression in the Miechow and Kracow uplands*). Acta Geologica Polonica, 18(2): 387-440.

Reichert, J. And Borg, G., 2007. Numerical simulation and a geochemical model of supergene carbonate-hosted nonsulphide zinc deposits. Ore Geology Reviews (2007), doi: 10.1016/j.oregeorev.2007.02.006.

Relvas, J.M.R.S., Barriga, F.J.A.S. and Longstaffe, F.J., 2006. Hydrothermal alteration and mineralization in the Neves-Corvo volcanic-hosted massive sulfide deposit, Portugal II. Oxygen, hydrogen and carbon isotopes. Economic Geology, 101(4): 791-804.

Reynolds, N.A., Chisnall, T.W., Kaewsang, K., Keesaneyabutr, C. and Taksavasu, T., 2003. The Padaeng supergene nonsulfide zinc deposit, Mae Sod, Thailand. Economic Geology, 98(4): 773-785.

Rhoden, H.N., 1960. Mineralogy of the Silvermines district, Co. Tippery, Ireland. Mining Magazine, 32: 128-139.

Ricordel, C., Thiry, M., Moreau, M.G. and Théveniaut, H., 2005. Paleomagnetic dating on "Siderolithic" paleoweathering profiles along French Massif Central. 2nd General Assembly, European Geosciences Union, Vienna, Austria, 24th-29th April 2005, Geophysical Research, Abstract, 7, 06631.

Rizzi, G., and Braithwaite, C.J.R., 1996. Cyclic emersion surfaces and channels within Dinantian limestones hosting the giant Navan Zn-Pb deposit, Ireland. In: Peter, S., Somerville, I. D., Gareth, J.L. [eds.], Recent advances in Lower Carboniferous geology, Geological Society, London, Special Publications, 107: 207-219.

Roedder, E., 1984. Fluid inclusions. Reviews in Mineralogy, 12: 646p.

Rosenbaum, J. and Sheppard, S.M.F., 1986. An isotope study of siderites, dolomites and ankerites at high temperature. Geochimica et Cosmochimica Acta, 50: 1147-1150.

Rosenberg, P.E., and Foit, F.F. Jr., 1979. The stability of transition metal dolomites in carbonate systems: A discussion. Geochimica et Cosmochimica Acta, 43: 951-955.

Rozanski, K., Araguás-Araguás, L. and Gonfiantini, R., 1993. Isotopic patterns in

modern global precipitation. In: Swart, P.K., Lohmann, K.C., McKenzie, J. and Savin, S. [eds.], Climate Change in Continental Isotopic Records, Geophysical Monograph, American Geophysical Union, Washington DC, 78: 1-36.

Russell, M.J., 1978. Downward-excavating hydrothermal cells and Irish-type ore deposits: importance of an underlying thick Caledonian prism. Transactions Institution Mining and Metallurgy, Section B, Applied Earth Science, 87: B167–B171.

Russell, M.J., 1986. Extension and convection; a genetic model for the Irish Carboniferous base metal and barite deposits. In: Andrew, C.J., Crowe, R.W.A., Finlay, S., Pennell, W.M., and Pyne J.F. [eds.], Geology and genesis of Mineral Deposits in Ireland, Irish Association for Economic Geology, Dublin: 545-554.

Russell, M.J., Boyce, A.J., Larter, R.C.L. and Samson, I.M., 1982. The significance of hydrothermal pyrite chimneys in the Silvermines deposit. In: Brown, A.G. and Pyne, J.F. [eds.], Mineral exploration in Ireland: Progress and development 1971-1981, Irish association for Economic Geology, Dublin: 171-172.

Sabouraud, C., Macquar, J.-Cl., and Rouvier, H., 1980. Les inclusions fluides, témoins, et faux-témoins des conditions de depot: quelques exemples pris dans les minéralisations de Pb, Zn, Ba, F du sud du Massif Central Français. Mineralium Deposita, 15 : 211-230.

Sadowska, A., 1977. Roślinnośé i stratygrafia górnomioceńskich pokladów wegla Polski poludniowo-zachpdniej. Acta Paleobotanica, 18(1): 87-122.

Sangster, D.F., 1976. Carbonate-hosted lead-zinc deposits. In: Wolf, K.H., [eds.], Handbook of stratabound and stratiform ore deposits, Amsterdam, Elsevier, 6: 447-456.

Sass-Gustkiewicz, M., Dzulyński, M., and Ridge, J.D., 1982. The emplacement of zinc-lead sulfide ores in the Upper Silesian district - a contribution to the understanding of Mississippi Valley-type deposits. Economic Geology, 77: 392-412.

Sass-Gustkiewicz, M., 1996. Internal sediments as a key to understanding the hydrothermal karst origin of the Upper Silesian Zn-Pb ore deposits. In: Sangster, D. F., [eds.], Carbonate-hosted lead-zinc deposits, Society of Economic Geologists, Special Publication, 4: 171-181.

Sass-Gustkiewicz, M. and Dzulyński, M., 1998. Comments on the origin of strata-bound Zn–Pb ores in the Upper Silesia, Poland. Annales Societatis Geologorum Poloniae, 68: 267-278.

Schneider, J., Haack, U., Hein, U.F. and Germann, A., 1999. Direct Rb-Sr dating of sandstone-hosted sphalerites from stratabound Pb-Zn deposits in the northern Eifel, NW Rhenish Massif, Germany. In: Stanley, C.J. et al. [eds.], Mineral Deposits: Processes to Processing, 5th Biennial SGA

Meeting, 22th – 25th August, London, Proceedings: 1287-1290.

Schneider, J., von Quadt, A., Wilkinson, J. and Boyce, A.J., 2007. Age of the Silvermines Irish-type Zn-Pb deposit from direct Rb-Sr dating of sphalerite. In: Andrew, C.J, et al. [eds.], Mineral deposits at the beginning of the 21st century, 9th Biennal SGA Meeting, Dublin, Ireland 20th – 23rd August, Proceedings: 377-380.

Schriel, W., 1954. Der Briloner Galmei-Distrikt. Zeitschrift der geologische Gesellschaft, 106: 308-349.

Schultz, R.W., 1966. The Lower Carboniferous cherty iron-formation at Tynagh, County Galway, Ireland - a discussion. Economic Geology, 61: 1443-1449.

Schwarz, T., 1997. Lateritic bauxite in central Germany and implications for Miocene palaeoclimate. Palaeogeography, Palaeoclimatology, Palaeoecology, 129: 37-50.

Schwinn, G., Wagner, T., Baatartsogt, B. and Markl, G., 2006. Quantification of mixing processes in hydrothermal systems by combination of stable isotope and fluid inclusion analyses. Geochimica et Cosmochimica Acta, 70: 965-982.

Scotese, C. R., Atlas of phanerozoic plate tectonic reconstructions, *PALEOMAP Prog. Rep. 01-1090*, 1990. Department of Geology, University of Texas, Arlington, Texas: 57p.

Servigne, M., 1943. La photo-luminescence des willémites. Bulletin de la Société Française de Minéralogie, 66: 452-478.

Sevastopulo, G.D., 1979. The stratigraphical setting of base-metal deposits in Ireland. In: Prospecting in areas of glaciated terrain, Istitution of Mining and Metallurgy: 8-15.

Sevastopulo, G.D., 1981, Hercynian structures. In: Holland, C.H., [eds.], A Geology of Ireland, Edinburgh, Scottish Academic Press: 147-172.

Sevastopulo, G.D. and Redmond, P., 1999. Age of mineralisation of carbonate-hosted, base metal deposits in the Rathdowney Trend, Ireland. In: McCaffrey, K.J.W., Lonergan, L. and Wilkinson, J.J. [eds.], Fractures, Fluid Flow and Mineralisation, Geological Society, London, Special Publications, 155, 303-311.

Shackleton, R.M., 1984. Thin-skinned tectonics, basement control and the Variscan front. In: Hutton, D.H.W, and Sanderson-David, J. [eds.], Variscan tectonics of the North Atlantic region, Geological Society, London, Special Publications, 14: 125-129.

Sheppard, S.M.F. and Gilg, H.A., 1996. Stable isotope geochemistry of clay minerals. Clay Mineralogy, 31: 1-24.

Sibley, D.F., and Gregg, J.M., 1987. Classification of dolomite rock textures. Journal of Sedimentary Petrology, 57: 967-975.

Sillitoe, R.H., 2005. Supergene oxidized and

enriched porphyry copper and related deposits. In: Hedenquist, J.W., Thompson, J.F.H., Goldfarb, R.J. and Richards, J.P. [eds.], Earth environments and processes, Society of Economic Geologists, 100th Anniversary Volume, Special Publication: 723-768.

Simon-Coinçon, R., Bruxelles, L., Ricordel, C. and Thiry, M., 2005. The continental French Massif Central during Late Jurassic and Early Cretaceous: paleoweathering and paleolandforms. 2nd European Geosciences Union General Assembly, Vienna, Austria, 24th-29th April 2005, Geophysical Research Abstract, 7, 07929.

Simonov, M.A. and Belov, N.V., 1970. Crystal structures of willemite Zn_2SiO_4 and its germanium analog Zn_2GeO_4. Soviet Physics and Crystallography, 15: 387-390.

Sitzia, R., 1965. Osservazioni su alcune ferrosmithsoniti di Montevecchio. Symposium Problemi Geo-Minerari Sardi. Associazione Mineraria Sarda, Cagliari-Iglesias, Proceedings: 434-437.

Skarpelis, N., 2005a. Non-sulfide zinc ores in Lavrion, Greece). ESF Exploratory Workshop Nonsulfide Zn-Pb ores, 21th – 23th April, 2005, Iglesias, Italy, Abstract: 25.

Skarpelis, N., 2007. The lavrion deposit (SE Attica, Greece): geology, mineralogy and minor element chemistry. Neues Jahrbuch fur Mineralogie, Abhandlungen, 183: 227-249.

Skarpelis, N., Grazhdania A. and Burri, S., 1996. Tertiary nickel laterites of S.E. Albania. Eurolat '96 Conference, University of Aveiro, Aveiro, Portugal, 18th 21th July, Abstract.

Sliwinski, S., 1966. Dolomityzacja morskich utworów triasu krakowsko-śląskiego. Rudy i Metale Niezelazne, 11(3): 122-132.

Sliwinski, S., 1969. The development of ore-bearing dolomite in the Krakow-Silesian area. Prace Geologiczne Polska Akademia Naukowe, 57: 124.

Smakowski, T. and Strzelska-Smakowska, B., 2005. The calamine ores from the Silesia-Krakow ore province (Poland). ESF Exploratory Workshop Nonsulfide Zn-Pb ores, 21th – 23th April, 2005, Iglesias, Italy, Abstract: 35-36.

Smith, B.J. and McAlister, J.J., 1987. Tertiary weathering environments and products in northeast Ireland. In: Gardiner, V. [eds.], International Geomorphology, Part II. Wiley, Chichester: 1007-1031.

Smolarska, I., 1968. Charakterystyka mineralogiczna dolomitów ruszconośnych wschodneiej części slasko-krakowskiego zaglębia kruszcowego. Prace Mineralogie Kom. Nauk. Miner, Polska Akademia Naukowe, Oddz. W Krakowie: 13.

Sobczynski, P., Szuwarzynski, M., and Wojnar, E., 1978. Formy wystepowania mineralizacji w niecce Chrzanowskiej. Prace Instytutu Geologicznego, 83: 185-192.

Somerville, I.D., Strogen, P., Gregg, J.M., and

Shelton, K.L., 1997. Fluid flow, dolomitization, and mineralization in Lower Carboniferous carbonate rocks, southern Irish Midlands: a preliminary report. Geofluids II, Second International Conference on Fluid Evolution, Migration and Interaction in Sedimentary Basins and Orogenic Belts, Belfast, UK, Abstract: 209-212.

Stara, P., Rizzo, R., and Tanca, G.A., 1996. Iglesiente-Arburese, miniere e minerali. Ente Minerario Sardo, 1: 238p.

Steinfink, H. and Sans, F.J., 1959. Refinement of the crystal structure of dolomite. American Mineralogist, 44: 679-682.

Swart, P.K., Burns, S.J. and Leder, J.J., 1991. Fractionation of the stable isotopes of oxygen and carbon during reaction of calcite with phosphoric acid as a function of temperature and methods. Chemical Geology, 86: 89-96.

Sweeney, M.A., Patrick, R.A.D. and Vaughan, D.J., 1991. The nature and genesis of willemite deposits of Zambia. In: Pagel, M. and Leroy, J. [eds.], Source, transport, and ore deposition of metals, 1st Biennial SGA Meeting, 30th August – 3rd September, Nancy, France, Proceedings: 139-142.

Symons, D.T.A., Sangster, D.F., and Leach, D.L., 1995. A Tertiary age from paleomagnetism for Mississipi Valley-type zinc-lead mineralisation in Upper Silesia, Poland. Economic Geology, 90: 782-794.

Symons, D.T.A., Smethurst, M.T. and Ashton, J.H., 2002. Paleomagnetism of the Navan Zn-Pb deposit, Ireland. Economic Geology, 97: 997-1012.

Szuwarzynski, M., 1978. Eluwialne i supergeniczne kruszce w utworach trzeciorzedowych z okolic Chrzanowa. Rudy i Metale Niezelazne, 23(7): 345-349.

Szuwarynski, M., 1993. The lead and zinc ore deposits in the vicinity of Chrzanów. Geological Quarterly, 37(2): 209-228.

Szuwarynski, M., 1996. Ore bodies in the Silesia-Krakow Zn-Pb ore district, Poland. Prace Instytutu Geologicznego, 154: 9-24.

Takahashi, T., 1960. Supergene alteration of zinc and lead deposits in limestone. Economic Geology, 55: 1083-1115.

Taylor, S., 1984. Structural and palaeotopographic controls of lead and zinc mineralisation in Silvermines orebodies, Republic of Ireland. Economic Geology, 79: 529-548.

Théveniaut, H., Wyns, R. and Quesnel, F., 2002. Etude paléomagnétique de la Borne de fer. Journée du Partenariat de Recherche et Développement entre le BRGM et l'ANDRA, 5 mars 2002, Orléans, France, Programme et résumés: 63-65.

Thiry, M., Simon-Coinçon, R., Quesnel, F. and Wyns, R., 2005. Altération bauxitique associée aux argiles à chailles sur la bordure sud-est du basin de Paris. Bulletin de la Société Géologique de France, 176(2): 199-214.

Thiry, M., Quesnel, F., Yans, J., Wyns, R.,

Vergari, A., Theveniaut, H., Simon-Coinçon, R., Ricordel, C., Moreau, M.G., Giot, D., Dupuis, C., Bruxelles, L., Barbarand, J. and Baele, J.M., 2006. Continental France and Belgium during the early Cretaceous: paleoweatherings and paleolandforms. Bulletin de la Société Géologique de France, 177(3): 155-175.

Timmerhans, C., 1905. Les gites métallifères de la région de Moresnet. Congrès International Mines, Métallurgie, Mécanique et Géologie Appliquée, Liège, Vaillant-Carmanne: 297- 324.

Tucker, M.E. and Wright, V.P., 1990. Carbonate sedimentology. Blackwell, Oxford: 482p.

Unrug, R. and Dembowski, Z., 1971. Diastrophic and sedimentary evolution of the Moravia–Silesia basin. Rocznik Polskie Towarzystwo Geologiczne, 41: 119-168.

Unrug, R., Harańczyk, C. and Chocyk-Jamińska, M., 1999. Easternmost Avalonian and Armorican-Cadomian terranes of central Europe and Caledonian-Variscan evolution of the polydeformed Kraków mobile belt: Geologic constraints. Tectonophysics, 302: 133–157.

Vairinho, M.M. and Fonseca, E.C., 1989. Distribução do Fe, Mn, Zn, Pb e Cu na zona de oxidação supergénica do jazigo Preguiça (Alto Alentejo, Portugal). Determinação das fases-su-porte do Zn, Pb e Cu por extracção química selectiva sequêncial. Revista da Universidade de Aveiro, Geociências, 4: 97–110.

Velasco, F., Herrero, J.M., Gil, P.P., Alvarez, L. and Yusta, I., 1994. Mississippi Valley type, Sedex and iron deposits in Lower Cretaceous rocks of the Basque-Cantabrian basin, northern Spain. In: Fontboté, L., and Boni, M., [eds.], Sediment-hosted Zn-Pb ores, Society of Geology Applied to Mineral Deposits, Berlin-Heidelberg, Special Publication, 10: 246-270.

Vercautere, C. and Van den Haute, P., 1993. Post-Palaeozoic cooling and uplift of the Brabant Massif as revealed by apatite fission track analysis. Geological Magazine, 130: 639-646.

Viets, J.G., Hofstra, A.H. and Emsbo, P., 1996. The composition of fluid inclusions in ore and gangue minerals from Mississippi Valley-type Zn-Pb deposits of the Krakow-Silesian region of southern Poland: Genetic and environmental implications; In: Gorecka, E., Leach, D.L., Kozlowski, A., [eds.], Carbonate hosted zinc-lead deposits in the Silesian-Krakow area, Poland, Prace Instytutu Geologicznego, Warsaw: 166-181.

Walsh, P.T., Atkinson, K., Boulter, M.C. and Shakesby, R.A., 1987. The Oligocene and Miocene outliers of West Cornwall and their bearing on the geomorphological evolution of Oldland Britain. Philosophical Transactions of the Royal Society of London, Series A, Mathematical and Physical Sciences, 323: 211-245.

Walther, H.W., 1984. La métallogénie de la

République Fédérale d'Allemagne. In: Explanatory memoir of the metallogenic map of Europe and neighbouring countries, UNESCO, Earth Sciences, 17: 187-235.

Walther, H.W., 1986. Federal Republic of Germany. In: Dunning, F.W. and Evans, A.M. [eds.]. Mineral Deposits of Europe, Volume 3: Central Europe. The Institution of Mining and Metallurgy, The Mineralogical Society, London: 175-301.

Waters, R.S., 1960. The bearing of superficial deposits on the age and origin of the upland plain of East Devon, West Dorset and South Somerset. Transactions of Institute of British Geographers, 28: 89-97.

Wazewska-Riesenkampf, W., 1959. Dolomity cynkowe w strefach utleniena slasko-krakowskich zloz cynkowo-olowianych. Prace Instytutu Hutn.: 11.

Whittaker, E.J.W. and Zabinski, W., 1981. X-Ray diffraction by Zincian Dolomite. Mineralogia Polonica, 12(2): 15-24.

Wickman, F.E., Blix, R. and von Ubisch, H., 1951. On the variations in the relative abundances of the carbon isotopes in carbonate minerals. Journal of Geology, 59: 142-50.

Wilk, Z., 1989. Hydrogeological problems of the Krakow-Silesia Zn-Pb ore deposits. In: Bosak, P., Ford, D.C., Glazek, J. and Horacek, I. [eds.], Paleokarst, a systematic and regional review, Developments in Earth Surface Processes, 1: 513-531.

Wilkinson, J.J, 2003. On diagenesis, dolomitisation and mineralisation in the Irish Zn-Pb orefield. Mineralium Deposita, 38: 968-983.

Wilkinson, J.J. and Earls, G., 2000. A high temperature hydrothermal origin for black dolomite matrix breccias in the Irish Zn-Pb orefield. Mineralogical Magazine, 64: 1077-1096.

Wilkinson, J.J., Boyce, A.J., Everett, C.E., and Lee, M.J., 2003. Timing and depth of mineralization in the Irish Zn-Pb ore field. In: Kelly, J.G., Andrew, C.J., Ashton, J.H., Boland, M.B., Earls, G., Fusciardi, L., and Stanley, G. [eds.], Europe's major base metal deposits, Irish Association for Economic Geology, Dublin: 483-497.

Wilkinson, J.J., Eyre, S.L. and Boyce, A.J., 2005a. Ore-forming processes in Irish-type carbonate-hosted Zn-Pb deposits: Evidence from mineralogy, chemistry, and isotopic composition of sulfides at the Lisheen mine. Economic Geology, 100: 63-86.

Wilkinson, J.J., Everett, C.E. and Boyce, A.J., 2005b. Intracratonic crustal seawater circulation and the genesis of subseafloor zinc-lead mineralization in the Irish orefield. Geology, 33: 805-808.

Williams, P. A. (1990) Oxide Zone Geochemistry. Ellis-Horwood, New York.: 286p.

Wodzicki, A., 1987. Origin of the Cracovian-Silesian Zn-Pb deposits. Annales Societatis Geologorum Poloniae, 57: 3-36.

Wright, W.R., Johnson, A.W., Shelton, K.L.,

and Gregg, J.M., 2000. Fluid migration and rock interactions during dolomitisation of the Dinantian Irish Midlands and Dublin basin. Journal of Geochemical Exploration, 69-70: 159-164.

Wyczolkowski, J., 1982. Transgresja morza triasowego na obszarze polnocno-wschodniego obrzezenia Gornoslaskiego Zaglebia Weglowego (translated title: *Transgression of the Triassic sea at the northeastern border of the Upper Silesia coal field*). Biuletyn Instytutu Geologicznego, 342: 39-77.

Wyszomirski, P., Lukasik, W. and Cieslikiewicz, I. 2003. Kaolinitic clays of Turow open pit as a raw material for the production of ceramic tiles by means of fast firing. Gospodarka Surowcami Mineralnymi, 19(4): 5-13.

Yans, J., 2003. An overview of the saprolites of Belgium and their potential kaolinite supplies to Mesozoic and Cainozoic sediments. Géologie de la France, 1: 33-37.

Yapp C.J., 1997. An assessment of isotopic equilibrium in goethites from a bog iron deposit and a lateritic regolith. Chemical Geology, 135: 159-171.

Zabinski, W., 1958. Ferrogalmei (monheimite-galmei) from Katy near Chrzanow. Bulletin of the Academy of Polish Science, Series Science Chemistry, Geology, Geography 6(6): 389-393.

Zabinski, W., 1959. Zincian dolomite from Warynski mine, Upper Silesia. Bulletin of the Academy of Polish Science, Series Science Chemistry, Geology, Geography, 7: 355-358.

Zabinski, W., 1960. Charakterystyka mineralogiczna strefy utlenienia slasko-krakowskich zloz kruszcow cynku i olowiu. Prace Geologiczne, 1: 7-99.

Zabinski, W., 1980. Zincian dolomite: The present state of knowledge. Mineralogia Polonica, 2: 9-31.

Zabinski, W., 1986. Zincian dolomite: The present state of knowledge. A supplement to Mineralogia Polonica, 17(2): 69-71.

Zawislak, L., 1970. Brunkit z kopalni Olkusz. Rudy i Metale Niezelazne, 15(6): 419-422.

Zawislak, 1971, Dolomity cynkowe w slasko-krakowskich zlozach rud cynku i olowiu. Z. Prace Naukowe Uniwersytetu Slaskiego: 397p.

Zeeh, S., Walter, U., Kuhlemann, J., Herlec, U., Keppens, E. and Bechstädt, T., 1997. Carbonate cements as a tool for fluid flow reconstruction: a study in parts of the eastern Alps (Austria, Germany, Slovenia). In: Isabel P., Montañez J. M. G. and Shelton, K. L. [eds.], Basin-Wide diagenetic patterns: integrated petrologic, geochemical, and hydrologic considerations, Society for Sedimentary Geology, Special Publication, 57: 167-181.

Zeeh, S., Kuhlemann, J. and Bechstädt, T., 1998. The classical Pb-Zn-deposits of the Eastern Alps (Austria/Slovenia) revisited: MVT deoposits resulting from gravity

driven fluid flow in the Alpine realm. Geologija, 41: 257-273.

Zheng, Y.F., 1999. Oxygen isotope fractionation in carbonate and sulfate minerals. Geochemical Journal, 33: 109-126.

Zheng, Y.F. and Hoefs, J., 1993. Carbon and oxygen isotopic covariations in hydrothermal calcites. Mineralium Deposita, 28: 79-89.

Ziegler, P.A., 1988. Evolution of the Arctic-North Atlantic and the western Tethys: American Association of Petroleum Geologist Memoir: 43p.

Ziegler, P.A., 1990. Geological atlas of Western and Central Europe. Shell International Petroleum Co. and the Geological Society of London: 239p.

Appendix 1: List of abbreviation

α = isotope fractionation coefficient

N = North **E** = East **S** = South **W** = West

a, b, c = crystallographic axes

d = lattice spacing

°C = degree Celsius

CL = cathodoluminescence

EG = glycolation

EDS = energy dispersive spectrometer

WDS = wavelength dispersive spectrometer

FI = fluid inclusion

FIA = fluid inclusion assemblage

Fm. = formation

ICP-ES = Inductively Coupled Plasma Atomic Emission Spectroscopy

k = element distribution coefficient

Ma = million years

Mt = million tonnes

OM = optical microscopy

ppm = part per million

SEM = scanning electron microscope

$\mathbf{T_h}$ = homogenisation temperature

$\mathbf{T_e}$ = first melting or eutectic temperature

$\mathbf{T_m}$**final** = final melting temperature

$\mathbf{T_m}$**ice** = ice melting temperature

$\mathbf{T_m}$**hy** = salt hydrate melting temperature

XRPD = X-ray powder diffraction

VPDB = Vienna Pee Dee Belemnite

VSMOW = Vienna Standard Mean Oceanic Water

wt% = weight percentage

eq. wt% = equivalent weight percentage.

OBD = Ore Bearing Dolomite

Acknowledgements

Thanks:

to Prof. **Maria Boni** of the University of Naples (Italy) for introducing me to the world of ore deposits and for giving me the chance to carry out this scientific project. I'd like to thanks her especially for her helpful suggestions during this work and for her critical review of the thesis. I also appreciated her ability to providing connections essential for the development of this project, as well as to providing funding for fieldtrip and participation at congresses. I never will forget her humoristic comments which made up less boring these three years of work.

to Prof. **Bożena Strzelska-Smakowska** of AGH University of Science and Technology of Krakow for organization of my visit in Krakow. I also would to thank her for the "beautiful" outcrops of nonsulphide deposits and for the connections with mining companies in Poland;

to Prof. **W. Zabinski**, who opened all the mineral collections of AGH University of Science and Technology of Krakow to show and give to me nice samples of Polish calamines;

to dr. **Hans Albert Gilg** for the isotopic measurements and for the data interpretations;

to **Richard Herrington** for him hospitality during my stay at the Natural History Museum of London;

to **the staff** of EMMA division at Natural History Museum of London for their continue assistance during analytical work;

to Prof. dr. **Thilo Bechstädt** of University of Heidelberg for him hospitality and for the possibility to use laboratories, and also the guest room in the department;

to Prof. **Benedetto De Vivo** for the possibility to carry out thermometric analyses of fluid inclusions;

to dr. **Luca Fedele** who helped me with measurements and interpretation of the thermometric analyses of fluid inclusions and who readily answered to my frequent e-mails, also during his stay in USA. Moreover, I want to thank him, with his computer skill, who has been of great helpful to resolve many problem with my computer; To dr. **Stefano Albanese** for his helpful for the good suggestion in the page layout of this thesis. It was nice to have him at the next door to help me in every moment;

to **Krzak Mariusz** who come with me in the Polish land in search of nonsulphide ore deposits and for his continue assistance with Polish people and their language;

to my (ex-)colleague and friend **Rosario Terracciano** for the long helpful discussions on the nonsulphide ore deposits which were of inestimable help for me and for the development of this thesis. I want to thank him the continue support during the last three years, it was fundamental for me;

to the **miner** who helped me to go out from Earth's meanders (Trzebionka mine) when my hope, to see again the sun, were completely finished.